NGNP-PLD-GEN-RPT-N-00007 OCTOBER 06, 2009
Revision 0

Next Generation Nuclear Plant: Plant Level Assessments Leading to Fission Product Retention Allocations

APPROVALS

Function	Printed Name and Signature	Date
Authors	Name: Diana Naidoo Company: Pebble Bed Modular Reactor (Pty) Ltd. Name: Karl Fleming Company: Technology Insights	October 06, 2009 October 06, 2009
Reviewer	Name: Roger Young Company: Pebble Bed Modular Reactor (Pty) Ltd.	October 06, 2009
Reviewer	Name: Fred Silady Company: Technology Insights	October 06, 2009
Approval	Name: Edward Brabazon Company: Shaw Environmental & Infrastructure	October 06, 2009

Westinghouse Electric Company LLC
Nuclear Power Plants
Post Office Box 355
Pittsburgh, PA 15230-0355

LIST OF CONTRIBUTORS

Name and Organization	Date
Wilma Van Eck Pebble Bed Modular Reactor (Pty) Ltd.	September 21, 2009
Bernard Muller Pebble Bed Modular Reactor (Pty) Ltd.	September 21, 2009
Johan Straus Pebble Bed Modular Reactor (Pty) Ltd.	September 21, 2009
Lori Mascaro Technology Insights	September 21, 2009
Hanno vd Merwe Pebble Bed Modular Reactor (Pty) Ltd.	September 21, 2009
Gerhard Strydom Pebble Bed Modular Reactor (Pty) Ltd.	September 21, 2009
Fred Torri Technology Insights	September 21, 2009
Alastair Ramlakan Pebble Bed Modular Reactor (Pty) Ltd.	September 21, 2009
Nilen.Naidu Pebble Bed Modular Reactor (Pty) Ltd.	September 21, 2009
Pieter Swanepoel Pebble Bed Modular Reactor (Pty) Ltd.	September 21, 2009
Henriette van Graan Pebble Bed Modular Reactor (Pty) Ltd.	September 21, 2009
Tsvetana Mateva Pebble Bed Modular Reactor (Pty) Ltd.	September 21, 2009
Scott Penfield Technology Insights	September 21, 2009

BACKGROUND INTELLECTUAL PROPERTY

Section	Title	Description

REVISION HISTORY

RECORD OF CHANGES

Revision No.	Revision Made by	Description	Date
F	Diana Naidoo / Karl Fleming	1st Release for client comment	09/21/2009
0	Roger M Young	Incorporation of client comments	10/06/2009

DOCUMENT TRACEABILITY

Created to support the following Document(s)	Document Number	Revision
N/A		

TABLE OF CONTENTS

LIST OF TABLES

LIST OF FIGURES

ACRONYMS

Acronym	Definition
ASTEC	Accident Source Term Evaluation Code
AVR	Arbeitsgemeinschaft Versuchs-Reaktor
BDBE	Beyond Design Basis Event
BE	Best Estimate
CB	Core Barrel
CBCS	Core Barrel Conditioning System
CCS	Core Conditioning System
CEDE	Committed Effective Dose Equivalent
CFD	Computational Fluid Dynamics
CFR	Code of Federal Regulations
CIP	Core Inlet Pipe
CMIV	CCS Main Isolation Control Valve
COP	Core Outlet Pipe
CPA	Containment Part of ASTEC
CR	Control Rod
DBA	Design Basis Accident
DBE	Design Basis Event
DCFs	Dose Conversion Factors
DDNs	Design Data Needs
DEGB	Double Ended Guillotine Break
DLOFC	Depressurized Loss of Forced Cooling
dP	Pressure Difference
DPP	Demonstration Power Plant
DR	Delayed Release
DVS	Depressurization Vent Shaft
DVSE	Depressurization Vent Shaft East
DVSW	Depressurization Vent Shaft West
EAB	Exclusion Area Boundary
EBS	Equivalent Break Size
eDCF	effective Dose Conversion Factor
EDE	Effective Dose Equivalent
ENV.	Environment
EPA	Environmental Protection Agency
FHL	Filter House Level
FHSS	Fuel Handling and Storage System
FIP	Filter Inlet Plenum
FPY	Full Power Years

Acronym	Definition
FR	Fraction Open
GRS	Gesellschaft für Anlagen und Reaktorsicherheit mbH
He	Helium
HPB	Helium Pressure Boundary
HPS	Helium Purification System
HTGR	High Temperature Gas-cooled Reactor
HVAC	Heating, Ventilation, Air Conditioning
ICDS	In-core Distribution System
IFI	Initial Fuel Inventory
IHX	Intermediate Heat Exchanger
IR	Initial Release(from fuel)
IRSN	L'Institut de Radioprotection et de Sûreté Nucléaire
LB	Lower Bound
LBEs	Licensing Based Events
LWR	Light Water Reactor
MFT	Maximum Fuel Temperature
MHTGR	Modular High Temperature Gas-Cooled Reactor
NGNP	Next Generation Nuclear Plant
NHSS	Nuclear Heat Supply System
NRC	Nuclear Regulatory Commission
PAG	Protective Action Guides
PBMR	Pebble Bed Modular Reactor
PCS	Power Conversion System
PHTS	Primary Heat Transport System
PRA	Probabilistic Risk Assessment
PRS	Pressure Relief System
PSID	Preliminary Safety Information Document
RB	Reactor Building
RBVV	Reactor Building Vent Volume
RCCS	Reactor Cavity Cooling System
RCS	Reactivity Control System
RIT	Reactor Inlet Temperature
RLC	Reactor Lower Cavity
RN	Radionuclide
ROT	Reactor Outlet Temperature
RPV	Reactor Pressure Vessel
RRB	Remainder of Reactor Building
RTC	Reactor Top Cavity
SAS	Small Absorber Sphere

Acronym	Definition
SEGB	Single Ended Guillotine Break
SFR	Shear Force Ratio
SG	Steam Generator
SHTS	Secondary Heat Transport System
SIP	Stack Inlet Plenum
SSCs	Systems, Structures and Components
TEDE	Total Effective Dose Equivalent
TII	Total Initial Inventory
TRISO	Triple Coated Isotropic
UB	Upper Bound
X/Q	Weather Dispersion Factor

Note: SI units and radionuclide identifiers have been excluded from this list. Acronyms or abbreviations used in figures which have legends are not necessarily included in this list.

PLANT LEVEL ASSESSMENTS LEADING TO FISSION PRODUCT ALLOCATIONS

SUMMARY AND CONCLUSIONS

SUMMARY

The work documented in this report includes studies to determine the steady-state plant conditions and plant response during expected transients for the Next Generation Nuclear Plant (NGNP) (Section 1), studies to evaluate the radionuclide (RN) releases from a spectrum of leaks and breaks in the Helium Pressure Boundary (HPB) of the Primary Heat Transport System (PHTS) (Section 2) and the development of design targets for radionuclide barrier retention capabilities to guide the next phase of the design (Section 3). The design basis for the work is the 500 MWt PBMR NGNP at 750°C ROT and 280°C RIT, powering a steam cycle through a Secondary Heat Transport System (SHTS) helium loop.

In the normal operation steady-state and expected transient evaluations, it is shown that all steady-state operating conditions and transients postulated are in principal achievable with careful design of the plant control strategies and the Core Conditioning System (CCS). Notable in the steady-state cases is the trade-off in size requirements for the CCS between the pressurized and depressurized shutdown states. In the pressurized case, the CCS should ideally be smaller to prevent over-cooling of the core. However in the depressurized state, a larger CCS may be required to ensure sufficient cooling of the core and to prevent buoyancy effects in the reactor. Engineering solutions will have to be applied to balance these two requirements. For the normal operation start-up and shutdown transients, the main concerns are maintaining the SHTS pressure above that of the PHTS and ensuring that the pressure difference between the primary and secondary sides of the Intermediate Heat Exchanger (IHX) remains within its limits. Control strategies to address these concerns are outlined in this document.

The evaluation of RN releases and offsite doses from HPB breaks refines the previous reactor building (RB) study of 2008 [1] in terms of the analysis performed. In the previous study, it was shown that a small break depressurized loss of forced cooling (DLOFC) resulted in greater RN releases from the PHTS to the reactor building (RB), greater RN releases from the RB to the environment and correspondingly greater offsite doses than a medium sized break. This is due to the fact that the majority of the delayed RN releases from the fuel occurs after the blowdown is complete for the medium break at which time only a minimal driving force exists to transport the radionuclides (RNs) from the PHTS to the RB. In the case of the small break, the blowdown is still in progress when the majority of the delayed RN releases from the fuel occurs, providing an enhanced transport mechanism for RNs from the PHTS to the RB. The current work has confirmed this RN PHTS release behavior for small and medium break depressurized loss of forced cooling (DLOFC) events. In addition, the current work includes the effect of convection cooling in the core during the depressurization for the small breaks, which was previously not modeled and leads to lower DLOFC temperatures and hence lower delayed RN releases from the fuel. This, coupled with the lower Reactor Outlet Temperature (ROT) in the

current design leads to much lower RN releases from the fuel than in the 2008 RB study [1]. As a result, where the previous study indicated that a RB would be necessary for RN retention, the current study shows offsite doses below the required limits even without taking RB retention into account based on the best estimate release and dose analysis performed in this study. Inclusion of RB retention provides additional margin to the dose limits.

Modeling of the helium and air gas exchange between the PHTS and RB showed that PHTS air-ingress post-blowdown for a medium size break is minimal. It also indicated that the volume of the compartment in which the break occurs has a major effect on the air ingress amount. Corrosion sensitivity studies indicated that the corrosion expected for these ingress scenarios is minor compared to the total graphite in the core. It is noted, that the helium/air gas exchange and corrosion results are only a first approximation and that verification of these results is required using detailed computational fluid dynamics (CFD) analyses which was not part of the scope of this work.

Detailed multi-compartment modeling of the Reactor Building (RB) including leakage paths showed much higher RN retention factors than were expected from the previous study. It was however shown that the form of the RNs in terms of dust, vapor and aerosol is of major importance for this retention. This is an area that requires further investigation. The modeling of a detailed RB also allowed this study to better investigate the effects of RB leakage pathways on the final offsite doses. Some counter-intuitive behavior was observed in that closing of the Depressurization Vent Shaft (DVS) damper after the blowdown phase actually increased the total offsite doses even though the total RN releases from the RB were reduced relative to the case when the DVS damper remained open. This behavior is attributable to the differences in the effective dose conversion factors for elevated DVS releases compared to ground level releases which differ by an order of magnitude.

The barrier retention capability targets were developed for the fuel, PHTS HPB, and RB barriers, as well as a target for composite retention capability of all three barriers. These allocations are presented in Table 1. Based on the offsite dose uncertainty analyses, the degree of confidence in which the barrier retention capability targets are achievable and the margin to offsite dose requirements is also identified.

Table 1 RN Retention Barrier Design Target Allocations for NGNP Conceptual Design

Parameter	Mean	5%tile	50%tile	95%tile
Fuel Release Fraction	2.05E-05	2.68E-07	4.10E-06	7.87E-05
PHTS HPB Release Fraction	4.40E-01	1.47E-01	4.19E-01	8.00E-01
Reactor Building Release Fraction	1.73E-02	1.34E-03	1.31E-02	4.68E-02
Composite Three Barrier Release Fraction	1.64E-07	4.73E-10	1.86E-08	6.00E-07
I-131 Release to Environment - Curies	2.12E+00	6.05E-03	2.39E-01	7.81E+00
Margin Factor to 5rem Thyroid CEDE PAG Limit [Note 1]	1.85E+02	7.77E+04	1.67E+03	4.99E+01
Margin Factor to 25rem TEDE DBA Dose Limit [Note 1]	1.16E+04	4.99E+06	1.06E+05	3.14E+03
Note 1: These values are obtained by dividing the dose limit by the corresponding percentile of the dose uncertainty distribution; hence the higher doses have lower margins to the limit				

Barrier retention factors are design targets to guide the next phase of the NGNP design and are not to be confused with regulatory requirements. Demonstration that regulatory requirements can be met is outside the scope of the current study and will require more detailed definition of the design and a comprehensive probabilistic and deterministic safety analysis planned for future NGNP design phases.

The evaluation of barrier performance and barrier allocations should be updated for each future design stage to maintain adequate margins against dose limits.

CONCLUSIONS

Conclusions from Section 1; Plant Level Analyses for Normal Operation and Anticipated Transients

In general, the analysis has indicated two important factors that must be considered in the design. Firstly, it indicates that very careful design of the control strategies is necessary to ensure that the pressure of the SHTS remains higher than the pressure of the PHTS and that the pressure difference between the primary and secondary side of the IHX remains within limits. Secondly, the CCS has to be sized carefully to ensure it can supply the flow needed for the depressurized shutdown while not exceeding the maximum flow for the pressurized case.

- Additional conclusions from the steady state results are:
  - Normal operating condition: The desired operating point is achievable with the current plant layout.
  - Lower operating condition: In order to prevent the necessity of inventory control, the pressure bias on the IHX can be maintained by lowering the hot gas temperature in the NHSS and maintaining the cold gas temperature. Alternatively, additional preheating of the feedwater can be applied. The recommended and simpler option is the lowering of the hot gas temperature.
  - Shutdown (PCS heat sink): The ROT can be maintained at the required level by adjusting the water flow through the SG. It must be verified that the SG can be operated with this low water flow (about 3% of the flow at full power) under these conditions. The low water flow rate is not expected to be a problem, since no boiling is required at this stage.
  - Shutdown (CCS heat sink): To prevent the RIT and ROT from dropping below acceptable limits, either the CCS mass flow can be throttled further by using a fine control valve in parallel with the CMIV, or a bypass for the CCS heat exchanger can be implemented. The fine control is recommended because a CCS cooler bypass valve will receive gas in excess of 700°C and would therefore be classified as a hot valve. The CCS heat exchanger size cannot be reduced as it must be sized for the depressurized condition.

  - Depressurized condition: Although the ROT obtained is higher than the original requirement, a bigger problem may be the very small mass flow rate through the reactor. The minimum mass flow rate needed to prevent buoyancy effects in the reactor must be determined and, if required, the CCS circulator size can be increased. It must be kept in mind, however, that the pressurized shutdown condition would also be affected by this.
- The conclusions and recommendations from the start-up transition analysis are:
  - The main concern during the start-up is the sudden change in pressure on the secondary side of the IHX the moment the SG water flow is started (which furthermore causes the pressure in the SHTS to drop below that of the PHTS). This is due to the fact that the preheating of the feedwater was not activated at this stage (feedwater temperature is still 35°C). The dip can be lessened by starting to heat the feedwater before the water flow is started.
  - The pressurization of the start-up takes about 11 hours (almost half of the total start-up time) at the assumed injection rates of 0.1kg/s into the PHTS and 0.15kg/s into the SHTS. The exact injection rates that can be achieved must still be verified, which will impact the start-up time.
  - It is recommended that the injection rate ratio of the PHTS and SHTS be chosen such as to ensure that the pressure of the SHTS stays above that of the PHTS during pressurization.
  - With the start-up strategy used in this analysis, the PHTS and SHTS circulators are only started once full inventory is reached. The total start-up time can possibly be reduced by starting up the circulators whilst pressurizing, thus starting to heat up the system whilst pressurizing.
- The conclusions and recommendations for the shutdown transition are:
  - The SG helium outlet temperature dropped quickly the moment the SHTS circulator was switched off, causing the pressure in the SHTS to also drop sharply to below that of the PHTS. This drop in temperature and pressure can possibly be reduced by ramping down the SHTS circulator speed at a slower rate.
  - The temperature of the RIT did drop slightly below 50°C (minimum reached was about 44°C), but due to the pressure being quite low at this stage, it is not expected to be a problem. Depressurization can however be started sooner (whilst the temperatures are still relatively high) to increase this minimum temperature reached.
  - The assumed extraction rates of 0.1kg/s for the PHTS and 0.15kg/s for the SHTS must still be verified and the impact of faster or slower rates on the minimum temperatures reached must be investigated.

Conclusions from Section 2; Plant Level Analyses for PHTS Helium Pressure Boundary Leaks and Breaks

- From the PHTS and RB analysis it was shown that:
  - The longer blowdown time for the small break results in a significantly greater percentage of the delayed RN release from the fuel being transported to the RB.
  - Significant retention of dust and fission products occurs in the RB especially in the RTC and IHX compartments.
  - Air intake to the RB through the leakage paths provides an additional driving force for release through the stack.
  - Closure of the stack damper significantly reduces the stack release and increases the leakage release for the 4mm break. The reduction in stack release is less for the 100mm break because the contribution of the initial release that is attached to dust is more significant and unaffected by the damper closing.
  - Releases from the RB are very sensitive to assumptions made regarding the form of the RNs entering the RB (aerosol or gas).
  - The helium fraction in the RTC and IHX compartments increases to dominant levels reducing the density and thereby affecting the pressure difference between compartments.
  - The surface areas of the compartments within the RB play a significant role in the cooling of the gas which also influences the pressure in the compartments.
  - It was observed that temperature and density effects are important in the evolution of the flows in the reactor building. Counter intuitive behavior can occur due to the pressure and density effects induced by the lower density helium gas.
  - Note should also be taken in the design that a multi compartment RBVV will retain more RNs than a single compartment RBVV.
  - Further nodalization of the IHX and RRB compartments would be useful to investigate buoyancy effects that were not included in this study but may contribute to the RN releases.
- The key conclusions of the dose evaluation include the following:
  - Minimum ratios of the PAG thyroid CEDE limit to calculated dose:
    - 2.5 for the 4mm no RB retention cases, Case 1a(4)
    - 47 for the 4mm RB retention cases, Case 3a(4)
  - Minimum ratios of the NRC TEDE limit to dose:
    - 180 for the 4mm no RB retention cases, Case 1a(4)
    - 3500 for the 4mm RB retention cases, Case 3a(4)
  - No RB retention is required to meet dose limits based on realistic assumptions used in this study.

  - The RB retention cases included in this study reduce the offsite doses by 1 – 6 orders of magnitude relative to the no RB case providing additional margin to limits
  - Assumptions made about the RB response and characteristics of the source term greatly influence the offsite doses.
    - Cases in which the DVS damper recloses have higher doses than when it remains open due to the increase in ground level releases for these cases.
    - Cases with DVS filtration result in the same (for the 4mm vapor cases) or lower doses (for all other cases) especially for cases in which the non-dust RNs are assumed to be in aerosol form.
    - Cases in which the non-dust RNs are assumed to be in vapor form as opposed to aerosol form have higher doses. Significant RB deposition occurs for RNs assumed to be in aerosol form.
  - Dose is more sensitive to ground level releases than DVS stack releases due to the 50m stack influence on X/Q.
  - For each comparable case, the 100mm break dose is one to four orders of magnitude less than the 4mm break dose. Results confirm 2008 RB study results that longer blowdown time for the small break results in a significantly greater percentage of the delayed RN release from the fuel being transported to the RB and accordingly greater doses.
  - Differences in trends for the 4mm and 100mm cases are a result of the larger contribution of the initial release that is attached to dust to the total dose in the 100mm cases. The RNs that are attached to dust do deposit in the RB and are filterable when released through the vent shaft
    - For the 100mm vapor case when the damper remains open, filtration reduces the doses, 20% for the thyroid CEDE and by a factor of 5 for the TEDE. For the 4mm vapor cases, filtration has no effect on the overall doses.
    - The reduction in doses is significantly larger between the RB vapor case with open damper and the no RB retention case for the 100mm case than for the 4 mm case.
    - The opposite is true for the reduction in doses for the RB aerosol case with open damper. The 4mm shows a greater reduction in doses relative to the no RB retention case.
- It is obvious from the results that the forms of the RNs in the RB play an important part in the retention and filtration. Experimental investigation into the form of the RNs (vapor / aerosol) as well as the adsorption to dust is therefore important.

Conclusions from Section 3; Radionuclide Barrier Retention Allocations

The following conclusions and insights from the Barrier Allocation task will shape future design phases of the NGNP:

- Barrier retention factors are design targets to guide next phase of NGNP design; not to be confused with regulatory requirements.

- There is an expectation that barrier retention capabilities will be evaluated in the next design phase and changes are expected due to:
  - Design changes and greater level of detail in design
  - Improvements in state of knowledge due to improved and more detailed models and data
  - More complete evaluation of HPB break sizes, locations, and plant response scenarios; treatment of more radio-nuclides; limiting scenarios to set allocations likely to change
- Barrier retention allocations may change as design is optimized to maintain margins against limits
- Margins to limits may be reduced if warranted by reduced uncertainties in performance
- Barrier allocations completed are based on HPB break size and location expected to be limiting for design basis events for an assumed set of boundary conditions defined in this section
- RN retention allocation for reactor building, a factor of 10 reduction in source terms for I-131 and Cs-137, have been enhanced in this study by factor of more than 5 relative to that specified in the 2008 RB study [1]
- RN retention allocation for the HPB is rather limited for small breaks but it is important to include to demonstrate barrier defense-in-depth capability; HPB barrier retention is more significant for larger breaks due to lack of pressure driving force during delayed fuel release based on the 2008 and 2009 study results
- RN retention allocation targets for the fuel augments the fuel performance specification
- Thyroid PAG dose dominated by delayed fuel releases at ground level from RB that occur post-blowdown after DVS damper is closed
- Methodology for evaluating barrier performance and barrier allocations should be updated for each future design stage to maintain adequate margins against dose limits

It is rather noteworthy that the potential releases during the post-blowdown phase of the 4-mm DLOFC were found to dominate the results and provide the limiting conditions for determining the barrier allocations. This is noteworthy because in the point estimate evaluations provided with the computer models in Section 2, there is no release predicted from the HPB into the RB following blowdown for the 4mm break because the core temperatures are decreasing and the PHTS helium is contracting during this period. It is noted however that in the point estimate analysis, RN transport from the RB to the environment continues post-blowdown and makes a significant contribution to the dose. In the uncertainty analysis, based on engineering judgment, some RN transport into the RB was postulated due to phenomena such as diffusion and natural convection that were not modeled in the computer programs. These RNs had been released from the fuel in the computer simulations but were retained in the PHTS due to lack of a modeled transport mechanism. This insight points to the importance of future work to resolve the uncertainties associated with gas-exchange phenomena.

INTRODUCTION

The work detailed in this report is aimed at providing a refined analysis of source term and fission product transport for a reference PBMR NGNP plant design. The study contributes to the ultimate goal of the development of radionuclide (RN) design criteria for Licensing Based Events (LBEs) that will assure compliance with top-level regulatory requirements.

The work is divided into three sections:

Section 1 (Plant Level Analysis for Normal Operation and Anticipated Transients) covers analysis of initial plant conditions and expected transients in normal operation of the NGNP. The primary objective is to describe the development of an integrated plant model of the Nuclear Heat Supply System (NHSS) and the application of this model to establish operating conditions, modes and states, and plant transient conditions during expected frequent start-up and shutdown transients and mode transitions.

Section 2 (Plant Level Analysis for PHTS Helium Pressure Boundary Leaks and Breaks) evaluates the radionuclide releases from a spectrum of leaks and breaks in the Primary Heat Transport System (PHTS) Helium Pressure Boundary (HPB). The primary objective of this section is to make significant progress toward the capability to calculate mechanistic source terms for release of radioactive material from the reactor building for a representative small (1mm to 10mm Equivalent Break Size (EBS)) and medium size (100mm EBS) HPB break accounting for the relevant phenomena expected to be significant for the PBMR NGNP design. A secondary objective is to revisit the conclusions of the 2008 RB study [1] based on an improved capability to predict mechanistic source terms than was possible previously. Where possible analysis is performed using more realistic models than were used in the 2008 study. Greater realism is expected in the current study related to the following source terms aspects:

- Modeling the feedback on core thermal responses and resulting delayed fuel releases created from the partially pressurized conditions for small breaks. The 2008 RB study [1] ignored this effect and thus over-predicted the magnitude of the delayed release from the fuel into the PHTS circuit.
- More realistic model of the coupled thermo-fluid behavior of the depressurization of the PHTS into the RB and from the RB to the environment over the full range of HPB break sizes in the CIP.

In Section 3 (Radionuclide Barrier Retention Allocations), design targets for radionuclide retention capabilities of the barriers to radionuclide release are developed for the next phase of the NGNP design. These barrier retention capability targets are developed for the fuel, PHTS, and RB barriers. These design targets are derived from a quantitative uncertainty analysis of the mechanistic source terms and radiological doses whose best estimate analysis is covered in Section 2. The uncertainty analysis provides a basis for identifying key sources of uncertainty that are candidates for future Design Data Needs (DDNs).

1. PLANT LEVEL ANALYSES FOR NORMAL OPERATION AND ANTICIPATED TRANSIENTS

This section describes the development of an integrated plant model of the NHSS. The integrated model was used to develop steady state conditions and to analyze plant transitions as part of normal operation, as well as to test the plant control and operating philosophy. This model was also used to model the effect of a series of pipe breaks on the NHSS and the reactor building, which served as a starting point for the fission product release calculation chain. The pipe breaks are described in Section 2.

In the sections that follow, the thermal hydraulic analysis code, the model development and integration are described. Steady state operation is then summarized followed by definitions of the assessed transitions.

1.1 DESCRIPTION OF THE INTEGRATED NHSS MODEL

The thermal hydraulic code Flownex [3] was used to develop an overall integrated model of the NHSS. Flownex is a thermal fluid network analysis code that uses the basic principles of mass, momentum and energy conservation to numerically solve a network of interconnected elements. The code can solve steady state equilibrium, as well as transient conditions. The Flownex code was also used to model the PBMR Demonstration Power Plant (DPP) Main Power System.

The purpose of a plant level model of the NHSS is to capture the integrated system dynamic response based on plant control and component interaction. This is necessary to assess the plant behavior and control philosophy. A representation of the NHSS configuration modeled in Flownex is shown in Figure 1-1.

The integrated model contains a detailed component model of the Intermediate Heat Exchanger (IHX), based on the results of the Intermediate Heat Exchanger Development and Trade Studies task [2]. In addition to the IHX, the model includes the reactor, circulators, check valve, piping, Steam Generator (SG), Core Conditioning System and all interconnecting pipes. All components were modeled to second order level, which implies performance characteristics that allow for off-design conditions, realistic thermal capacitances, heat losses and gas inventories. The steam cycle was not modeled explicitly; realistic boundary conditions were assumed for the feedwater and steam conditions. Since the plant transitions analyzed are slow controlled transients, the assumption that these boundary conditions are controlled perfectly to their required set points are valid.

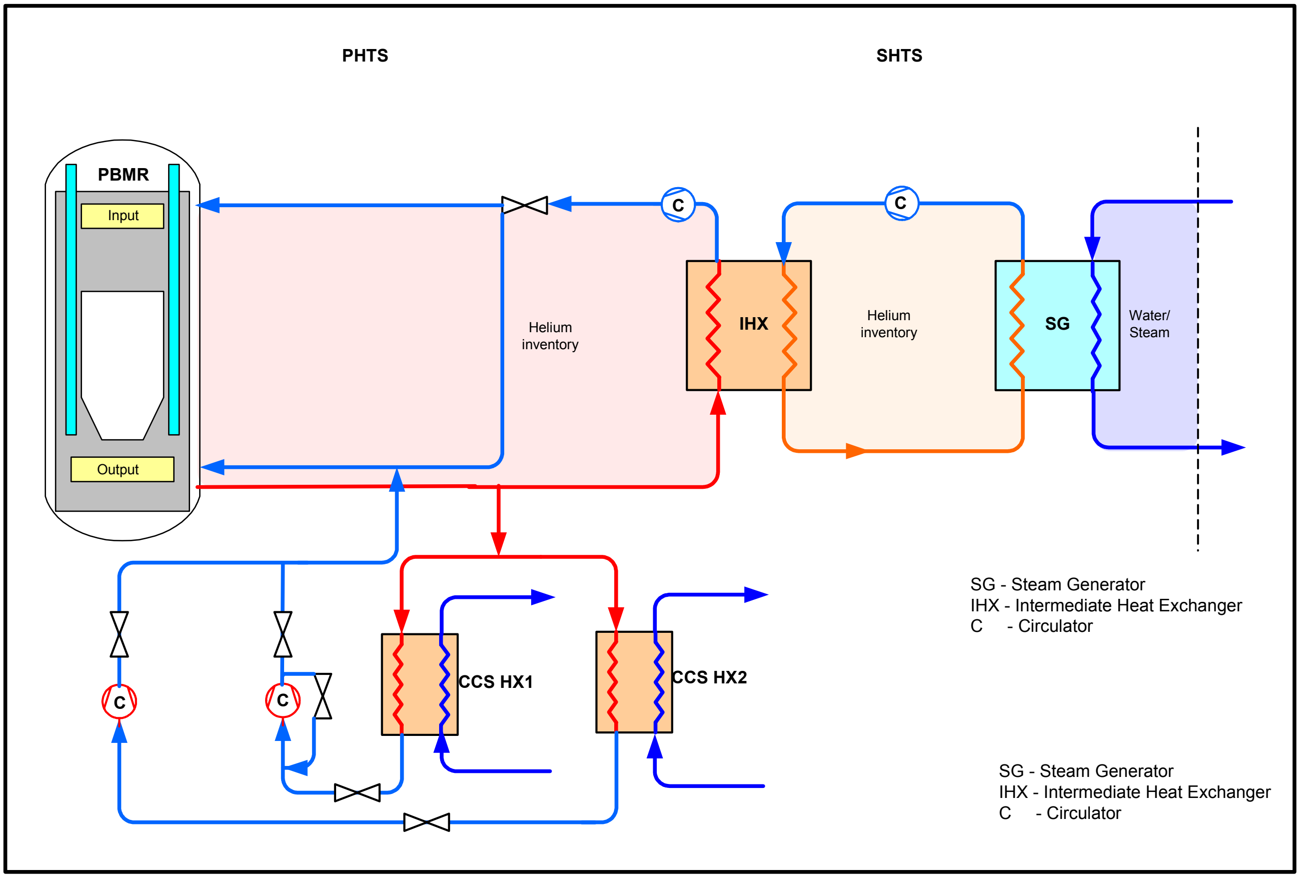

Figure 1-1 NGNP plant configuration analyzed in Flownex

It is important to note that the model has some limitations. Although the thermal capacitance of the IHX and SG active heat transport area is included, the thermal capacitance of the vessel internals is not included. This will, in reality, slow down the very fast temperature response of the gas inside the vessel. Not taking these factors into account results in the prediction of higher temperature spikes and increased gradients, which is conservative for most cases. Furthermore, Flownex was not developed to solve networks at very low flows where natural convection takes precedence. It will, however, induce flow due to buoyancy differences. Heat transfer correlations suitable for very low flow conditions must be used to ensure that the calculated heat transfer coefficients are in the right order of magnitude.

To perform the plant transitions described in the next section, plant controller models were also developed. This ensured realistic transitions between the plant states.

1.2 PLANT LEVEL ANALYSIS

The following plant-level analyses were performed:

- Steady-state heat balances for the upper, nominal and lower operating conditions, as well as for the shutdown and depressurized maintenance conditions.
- Transitions between the following states:
    - Start-up from depressurized maintenance conditions to full power operation.
    - Shutdown from full power operation to depressurized maintenance conditions.
- Analysis of a spectrum of pipe breaks (presented in Section 2 of this report).

1.2.1 Operational States and Transitions/Transients

In order to proceed with the plant-level analysis task, a conceptual states and transitions diagram was proposed. This is shown in Figure 1-2. The plant can be taken from one state to another by following various paths indicated on this figure. The details and results of the states and transitions analyzed will be described in the next few sections.

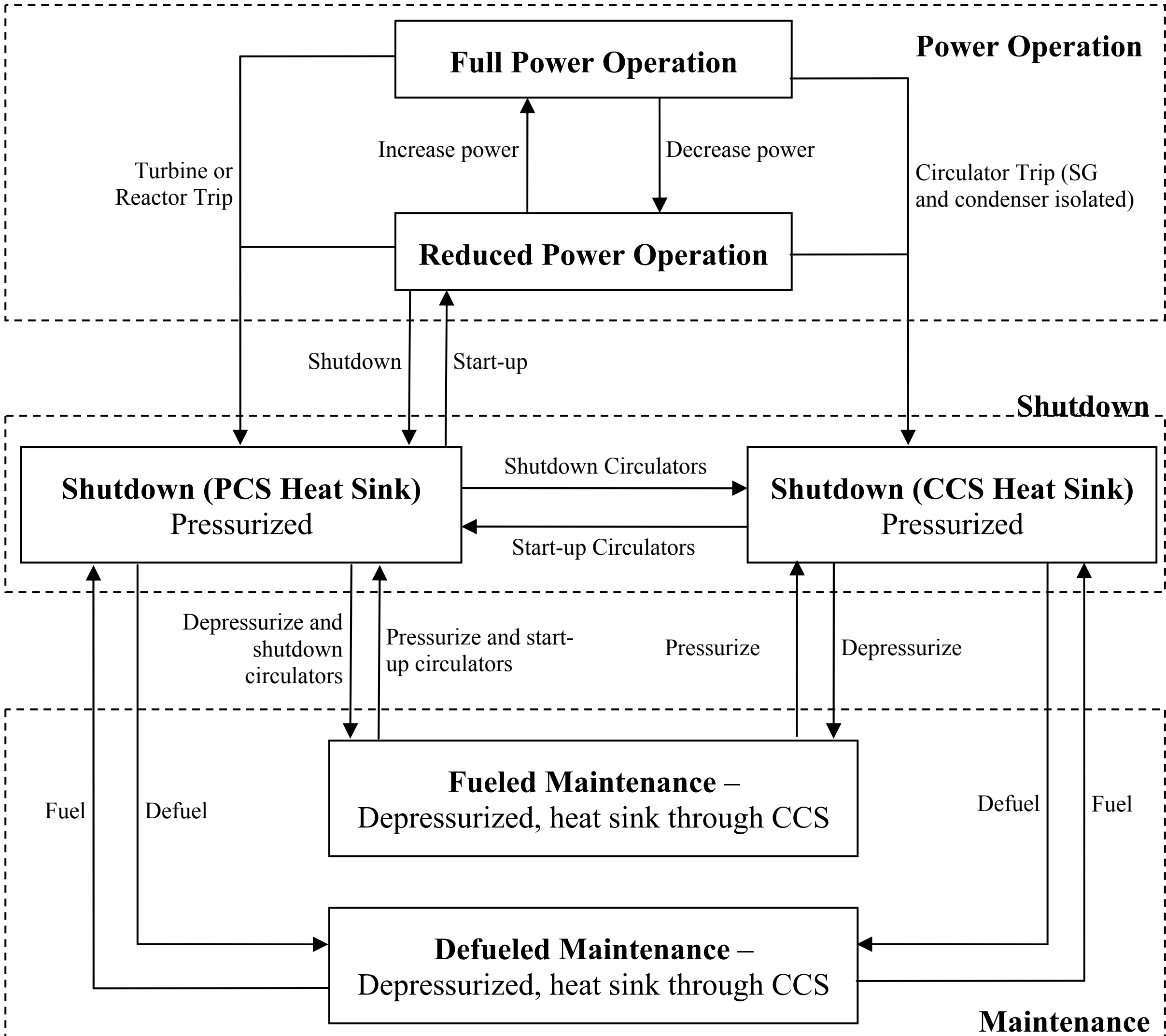

Figure 1-2: Operational States Diagram

1.3 STEADY-STATE CONDITIONS

The steady-state conditions that were analyzed with the Flownex model included the following:

- Power Operation
  - Full Power Operation - Nominal operating point (reactor at 100% power, full inventory)
  - Full Power Operation - Upper operating point (currently defined the same as the nominal operating point)
  - Reduced Power Operation - Lower operating point (reactor at 40% power, full inventory)

- Shutdown (Pressurized)
  - Pressurized maintenance (heat sink through Power Conversion System)
  - Pressurized maintenance (heat sink through Core Conditioning System)
- Fueled Maintenance (Depressurized)

1.3.1 Full Power Operation (Nominal Operating Condition)

This condition defines the reference case for all the analyses. The operating conditions are defined as follows:

- 500 MW Reactor Thermal Power
- 750°C Reactor Outlet Temperature (ROT)
- 280°C Reactor Inlet Temperature (RIT)
- 9MPa helium pressure at the exit of the PHTS circulator
- 9.1MPa helium pressure at the exit of the Secondary Heat Transport System (SHTS) circulator
- Steam conditions: 567°C, 16.9MPa.
- SG feedwater conditions: 163.7°C, 17.9MPa.
  - SG water flow rate must be calculated to obtain the required steam conditions.
- 10% of the flow through the primary circulator must be diverted through the core outlet pipe annulus to cool the core outlet pipe.

Further details are provided in Figure 1-3. For the purpose of this analysis, the upper operating condition is defined as being identical to the nominal steady-state.

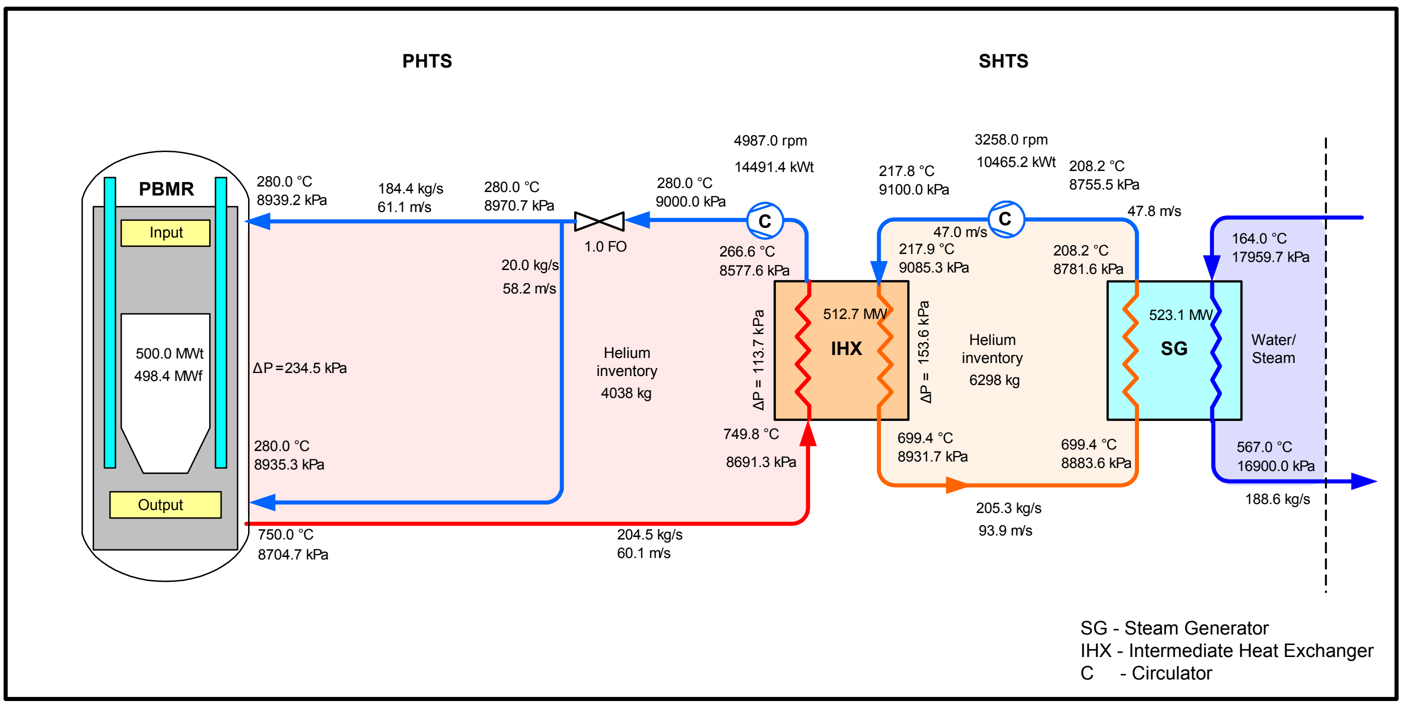

Figure 1-3: Full Power Operation (Nominal/Upper Operating Point)

The Flownex normal operation steady-state analysis indicates that the desired operating point is achievable with the defined plant layout.

1.3.2 Reduced Power Operation (Lower Operating Condition)

This operating condition is defined as the lowest power operating condition at which steam can be produced at its nominal conditions (although at a lower mass flow rate). When operating at a reduced reactor power level, care should be taken that the pressure in the PHTS does not increase above the pressure in the SHTS. Because the cold leg of the PHTS and SHTS represents the largest portion of the helium volume in the system, the pressure in the two systems are mostly determined by the temperature of the cold legs (provided the inventory remains unchanged). At lower power levels, the SHTS can thus be maintained at a higher pressure using one of the following methods:

- Lower the ROT to keep the RIT constant (preferred)
- Increase the feedwater temperature
- Active inventory control

Various permutations for the above were investigated. After evaluating the various options, it is recommended to use the option where the ROT is decreased when the reactor power is reduced. The proposed operating conditions for the reduced power condition are therefore as follows (see Figure 1-4):

- 200 MW Reactor Thermal Power (40% of normal operation power)
- ~ 600°C ROT
- 280°C RIT
- Steam conditions: 567°C, 16.9MPa.
- Feedwater temperature is assumed to drop to 120 °C at 40% power; inlet pressure is an outcome of the steady-state analysis
- The feedwater mass flow rate must be adjusted to obtain the required steam conditions
- 8.74MPa in PHTS
- 8.76MPa in SHTS
    - For these conditions, the SHTS pressure is only marginally higher than PHTS. To increase this margin, it is recommended that the ROT be increased slightly (which will increase the RIT and thus the SHTS pressure).
- Full inventory

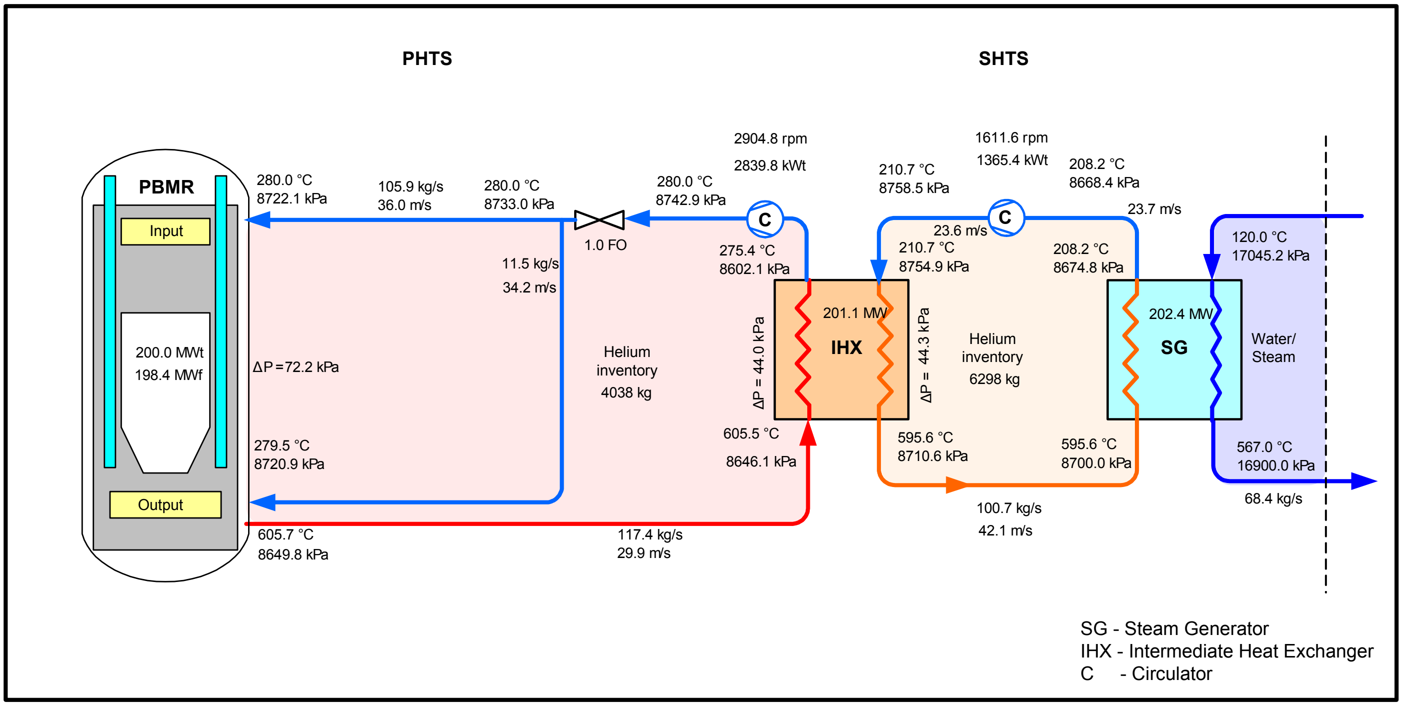

Figure 1-4: Lower Operating Point

1.3.3 Shutdown (Pressurized)

This condition is defined by the method of decay heat removal. The decay heat from the reactor is taken 12 hours after the onset of shutdown. This value was calculated to be 2.581 MW. The plant will be operating at the same helium inventory in the PHTS and SHTS as for the nominal case. Heat removal can occur in one of two ways:

- Using the main loop (Power Conversion System (PCS)): The circulators will be at a low speed (10%) and the feedwater mass flow rate will be at 20 – 25% of its nominal flow rate. The feedwater inlet conditions will be at 35 °C (the Rankine circuit was not simulated, thus an assumed value slightly higher than room temperature was used).
- Using the Core Conditioning System (CCS): The CCS circulator will remove all decay heat from the reactor. The main loop circulators are off and the non-return valve at the primary circulator outlet is closed. There is no water flow through the steam generator.

The conditions for the shutdown state with heat removal through the PCS are given below and on Figure 1-5:

- 150°C ROT
- ~ 130°C RIT
- Circulators at 10% speed.
- Feedwater temperature 35°C.
- Feedwater flow rate is reduced to remove only the required heat.

- 6.3MPa in PHTS
- 6.6MPa in SHTS
- Full inventory

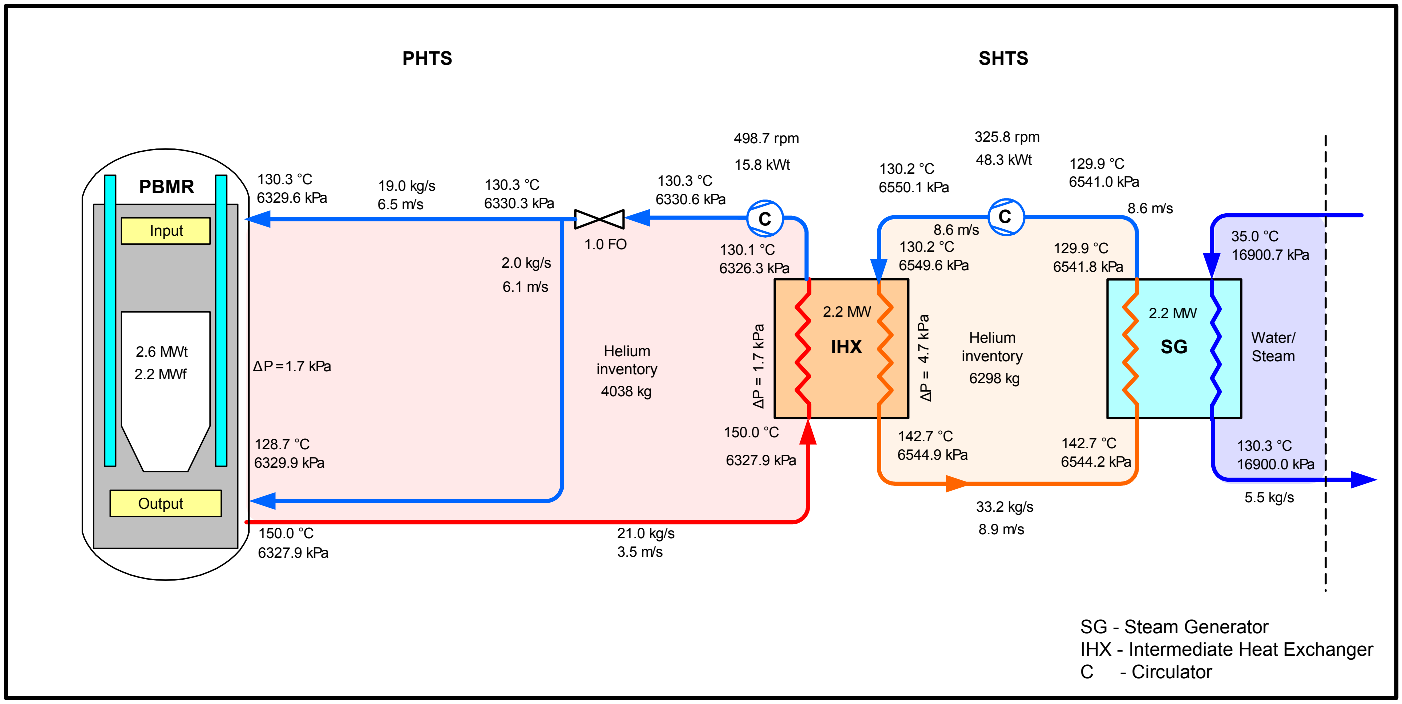

Figure 1-5: Shutdown (PCS Heat Sink)

It can be seen in Figure 1-5 that the feedwater flow rate required is very low (only approximately 3% of the normal operations flow). This is expected to be acceptable considering that boiling is not required at this stage. It should however be verified that the SG can operate under these conditions.

The conditions for the shutdown state with heat removal through the CCS are given below and on Figure 1-6:

- ~ 120°C ROT
- ~ 50°C RIT
- PHTS and SHTS circulators stopped
- CCS circulator at 10% speed
- 5.5MPa in PHTS
- Full inventory

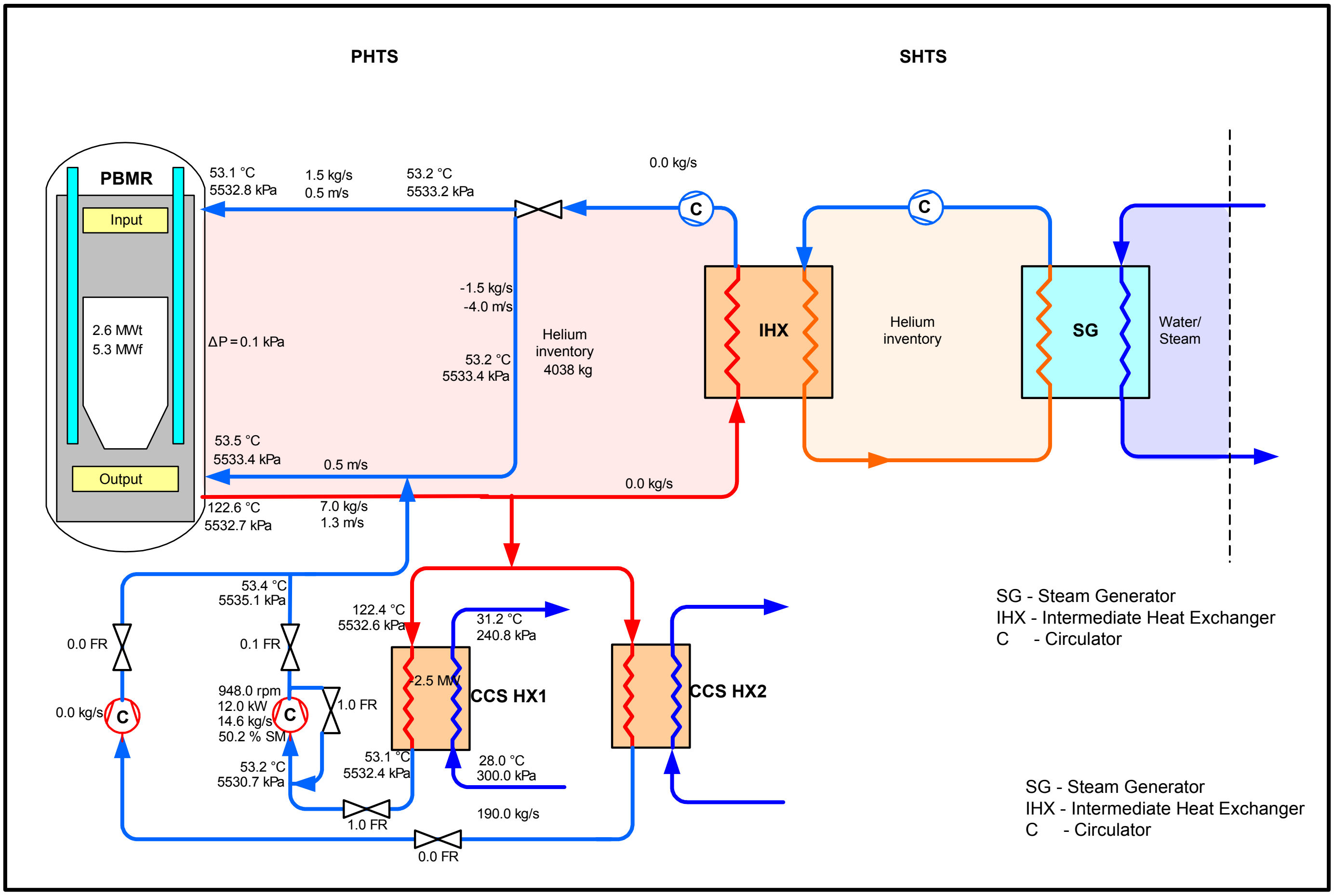

Figure 1-6: Shutdown (CCS Heat Sink)

It is important to note that for this state the RIT is very close to its minimum limit of 50°C. This requirement originates from the reactor pressure vessel (RPV), to prevent radiation embrittlement. To prevent the RIT from dropping below this limit, either the CCS mass flow can be throttled further by using a fine control valve in parallel with the CCS main isolation control valve (CMIV), or a bypass for the CCS heat exchanger can be implemented. The fine control is recommended as a CCS cooler bypass valve will receive gas in excess of 700°C and would therefore be classified as a hot valve. The CCS heat exchanger size cannot be reduced as it must be sized for the depressurized condition.

1.3.4 Fueled Maintenance (Depressurized)

For this state the pressure of the PHTS and SHTS is set to atmospheric pressure. Decay heat removal is facilitated by the core conditioning system (CCS) as illustrated in Figure 1-7. The proposed operating conditions are:

- The CCS circulator will be set at its maximum speed to keep the ROT below 300°C
- The CCS main isolation valve will be fully open and the CCS circulator bypass valve will be fully closed to provide maximum flow through the reactor

- The primary circulator outlet valve is closed and the PHTS and SHTS circulators are not in operation
- The decay heat from the reactor was taken one day (24 hours) after the onset of shutdown. This was calculated to be 2.11 MW.
- ~ 250°C ROT
- ~ 60°C RIT

It must be noted that for these conditions, the ROT could not be reduced further than 250°C using the CCS. The reactor mass flow rate is also very small (2 kg/s) which might cause unpredictable flow patterns in the reactor and non-uniform temperature distributions. To obtain a lower ROT and higher mass flow rates, the CCS circulator would have to be resized.

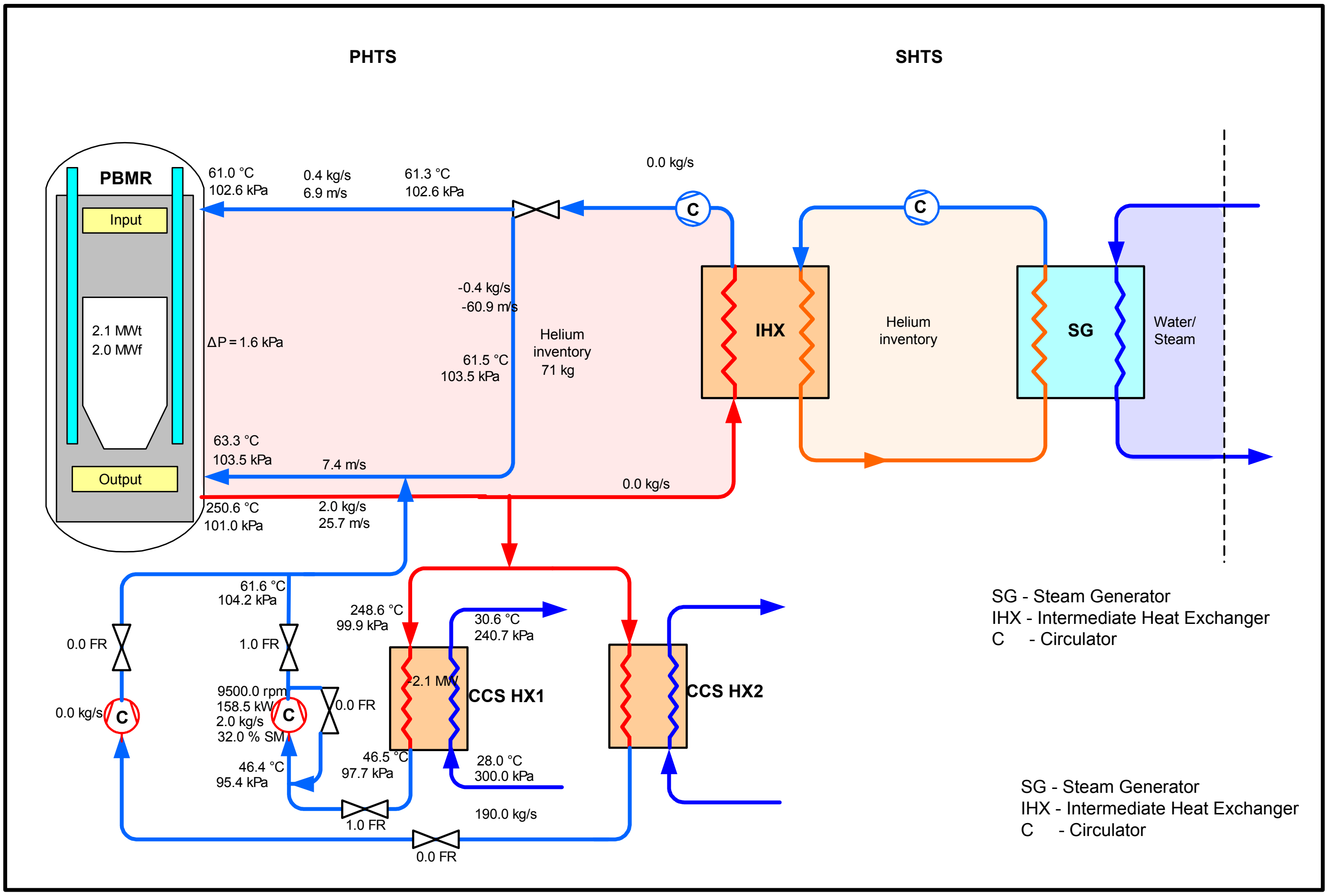

Figure 1-7: Depressurized Maintenance Condition

1.4 STATE TRANSITIONS

The following two transitions were modeled:

- Start-up (from 'Fueled Maintenance' to 'Full Power Operation').
- Shutdown (from 'Full Power Operation' to 'Fueled Maintenance').

It is assumed that there is decay heat present during start-up, i.e. that the reactor has previously run in power operation.

1.4.1 Start-up Transition

The full start-up transition (from 'Fueled Maintenance' to 'Full Power Operation') is shown in red on the states diagram in Figure 1-8. It must be noted that there are more than one start-up path that can be followed – the transition illustrated in Figure 1-8 is merely a proposal that was analyzed.

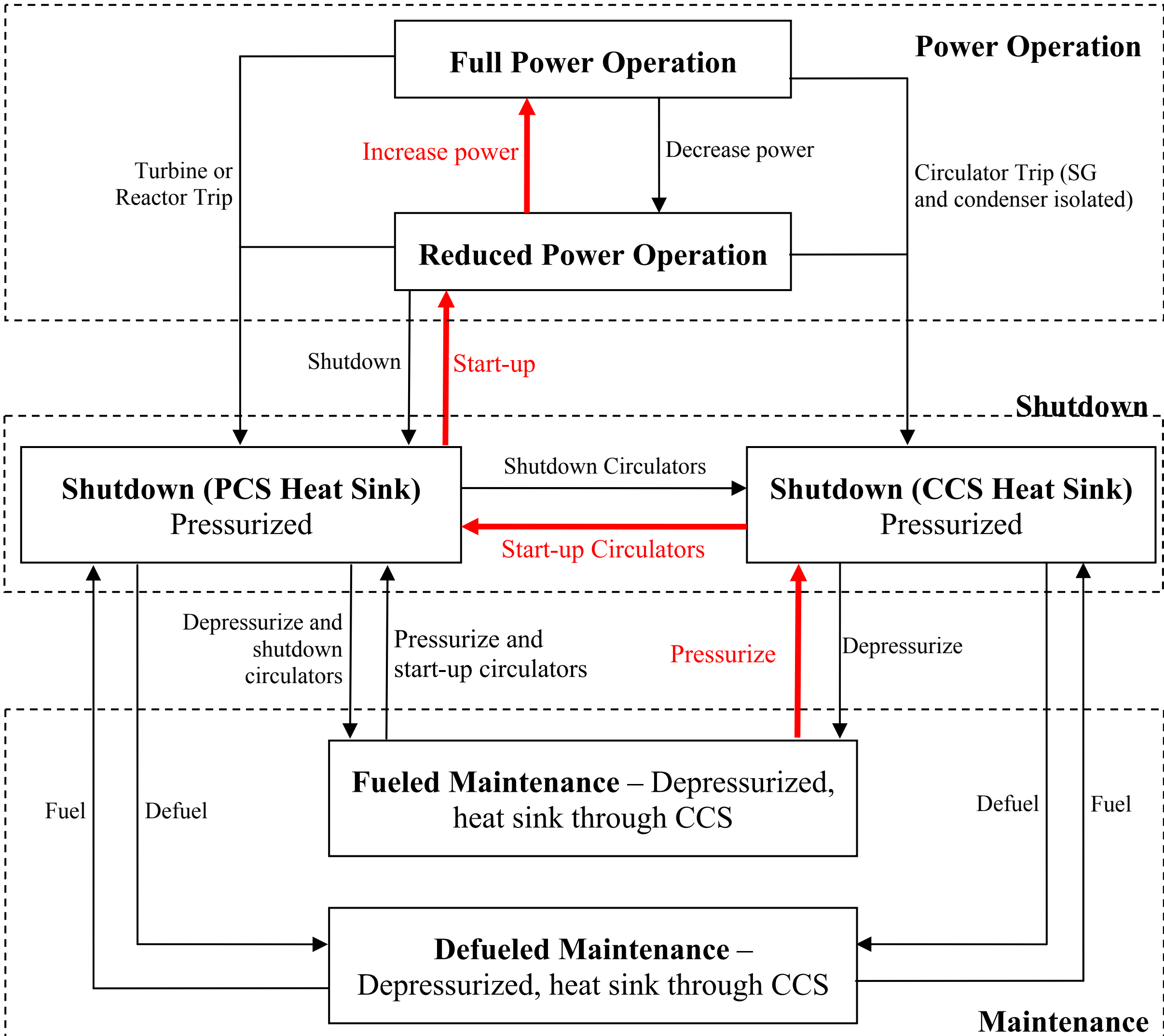

Figure 1-8: Start-up Path on States Diagram

The different phases that were analyzed for the start-up are listed below:

- PHASE 1 (Pressurize)
  - The PHTS and SHTS are pressurized to full inventory (helium was injected at an assumed rate of 0.1kg/s into the PHTS and 0.15kg/s into the SHTS).
  - The CCS removes the decay heat.
- PHASE 2 (Start-up circulators):
  - The main circulators are ramped up to full speed to heat up the reactor.
  - The CCS circulator reverts to idling mode.
  - The SG is closed off (no water flow), thus the water pressure builds up to 16.9MPa as the water heats up.
- PHASE 3 (Start-up: 0 to 40% power):
  - When the SG helium outlet temperature increase above 208°C (normal operating point), the SG water flow is started and used to control SG helium outlet temperature at 208°C.

    - The reactor is made critical at this stage and the reactor power is ramped up to 40% power. The reactor power is ramped up at such a rate the ROT will increase at approximately 100°C/hr.
    - The primary circulator speed is fixed at 40%.
    - The RIT is controlled at 280°C using the secondary circulator speed.
- PHASE 4 (Increase power):
    - The reactor power is ramped up from 40% to 100% power (again at a rate that the ROT will increase at approximately 100°C/hr).
    - The SG feedwater temperature is increased from 125°C at 40% power to 164°C at 100% power.
    - The RIT is controlled at 280°C using the primary circulator speed.
    - The SG helium outlet temperature is controlled at 208°C using the secondary circulator speed.
    - The steam temperature is controlled at 567°C using the water mass flow through the SG.
    - The steam pressure is maintained at 16.9MPa.
    - The inventory is topped up to full pressure (the PHTS up to 9MPa and the SHTS up to 9.1MPa) towards the end of this phase.

Some of the major results of the start-up simulation are presented in Figure 1-9 to Figure 1-11. As can be seen from Figure 1-11, whilst pressurizing, the pressure of the SHTS is lower than that of the PHTS. This can easily be rectified by pressurizing the SHTS at a slightly faster rate. The pressure in the SHTS furthermore sharply drops by more than 1 000kPa the moment the SG water mass flow rate controller is switched on (this controller is used to control the SG helium outlet temperature at 208°C). This is due to the fact that the SG feedwater temperature is still cold (35°C), since the preheating had not been activated in the simulation. This dip in pressure can probably be reduced by starting the feedwater heating sooner. From Figure 1-11 it can also be seen that the SHTS pressure returns to above the PHTS pressure the moment the feedwater temperature is increased to 120°C at the end of Phase 3 (thus the moment the feedwater heating was started).

According to the analysis the whole start-up procedure takes about 24 hours to complete. The majority of the time (11 hours) is used to pressurize the two circuits due to the low chosen injection rate. If this injection rate is increased, the start-up time can be reduced significantly.

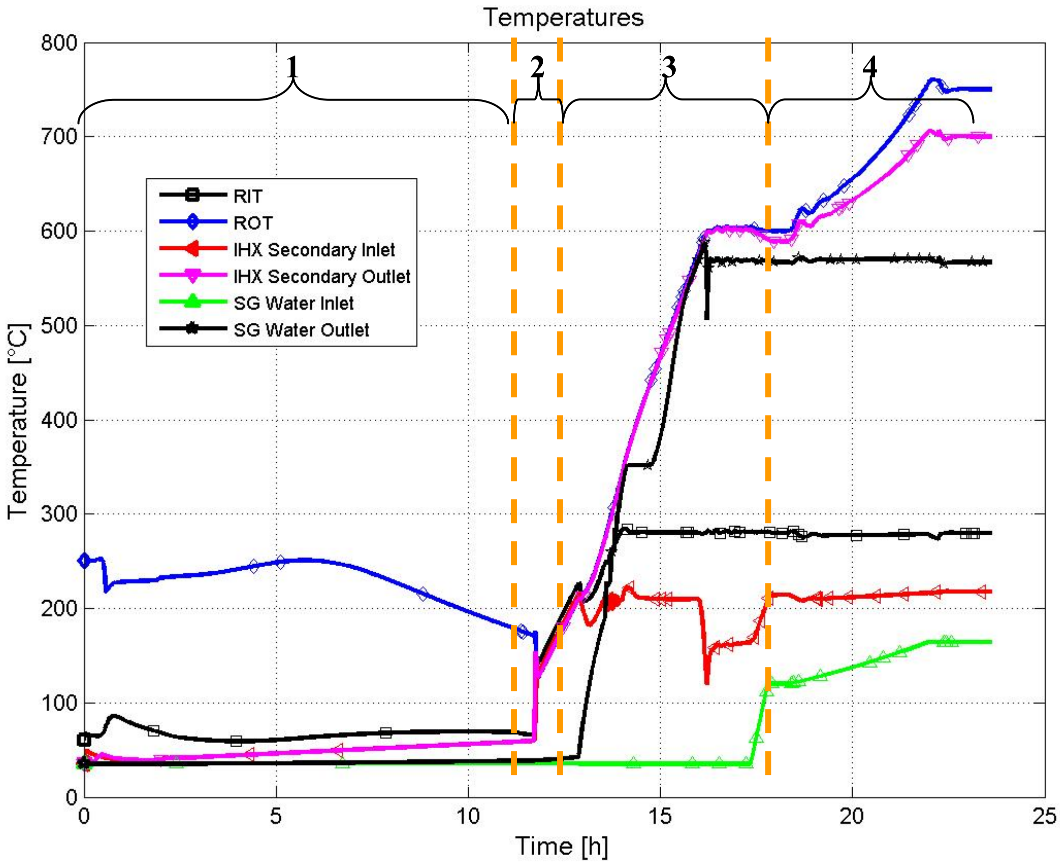

Figure 1-9: Helium and Water Temperatures (Start-up)

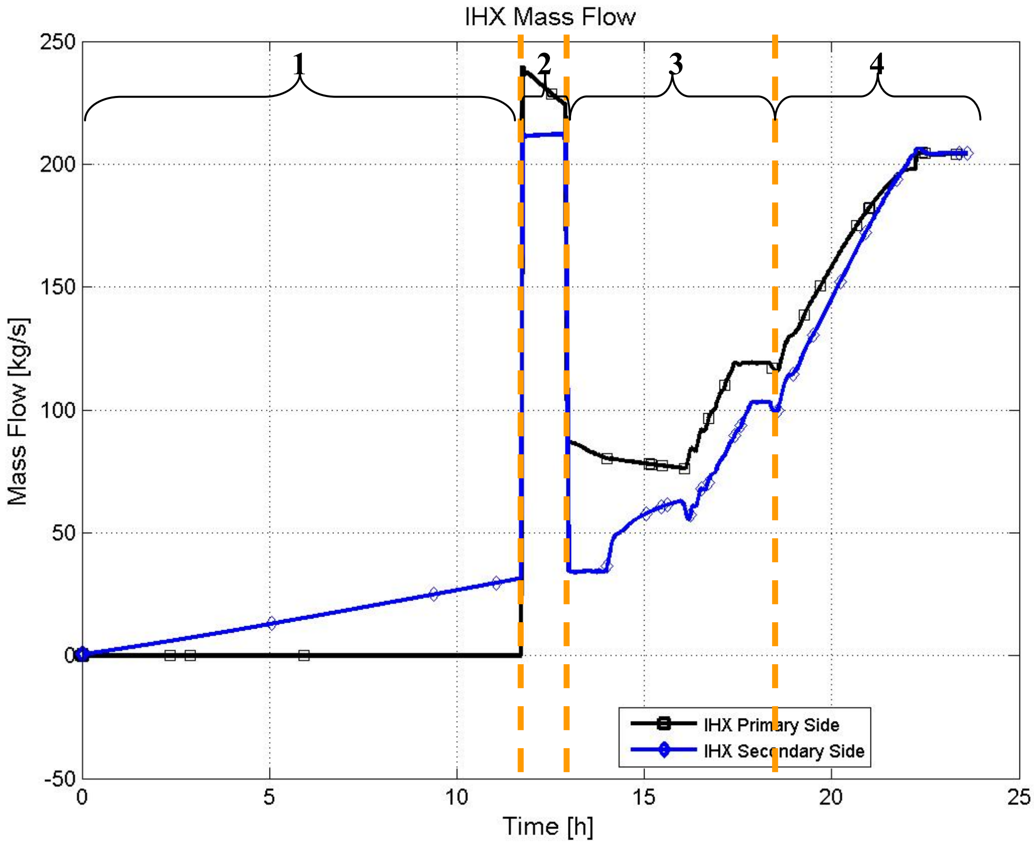

Figure 1-10: IHX Mass Flow (Start-up)

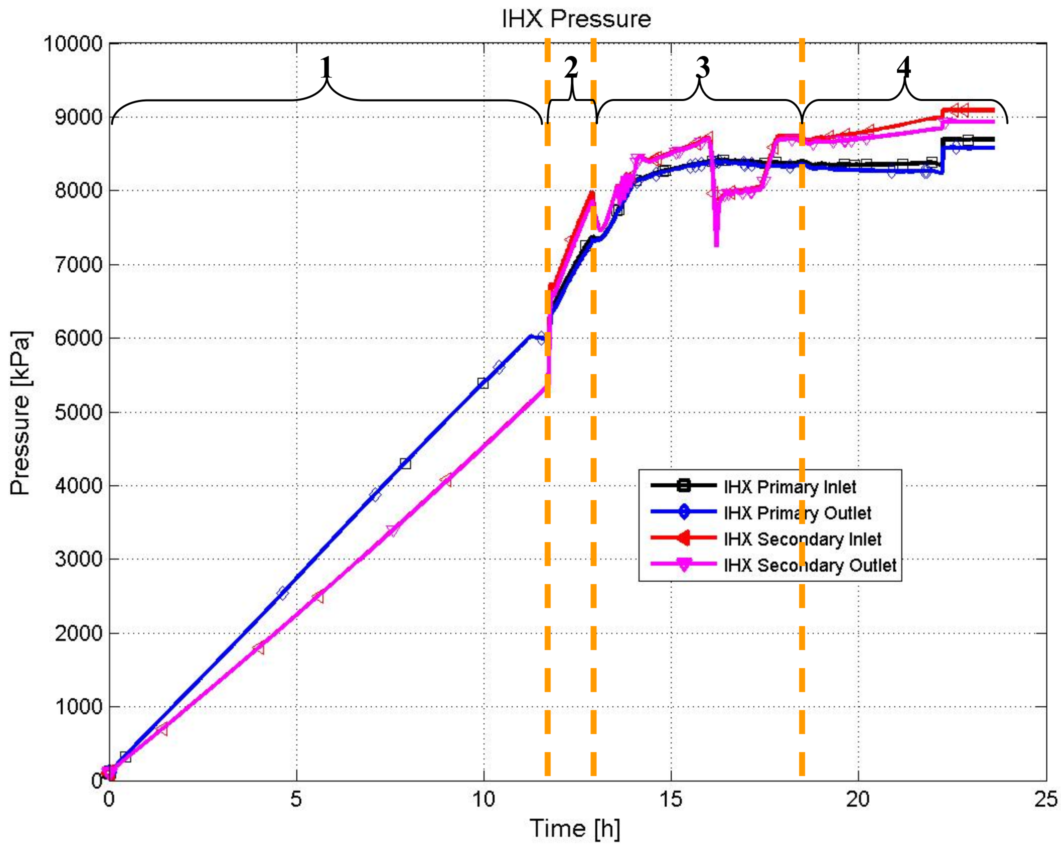

Figure 1-11: IHX Pressure (Start-up)

1.4.2 Shutdown Transition

The full shutdown transition (from ‘Full Power Operation’ to ‘Fueled Maintenance’) is shown in red on the states diagram in Figure 1-12.

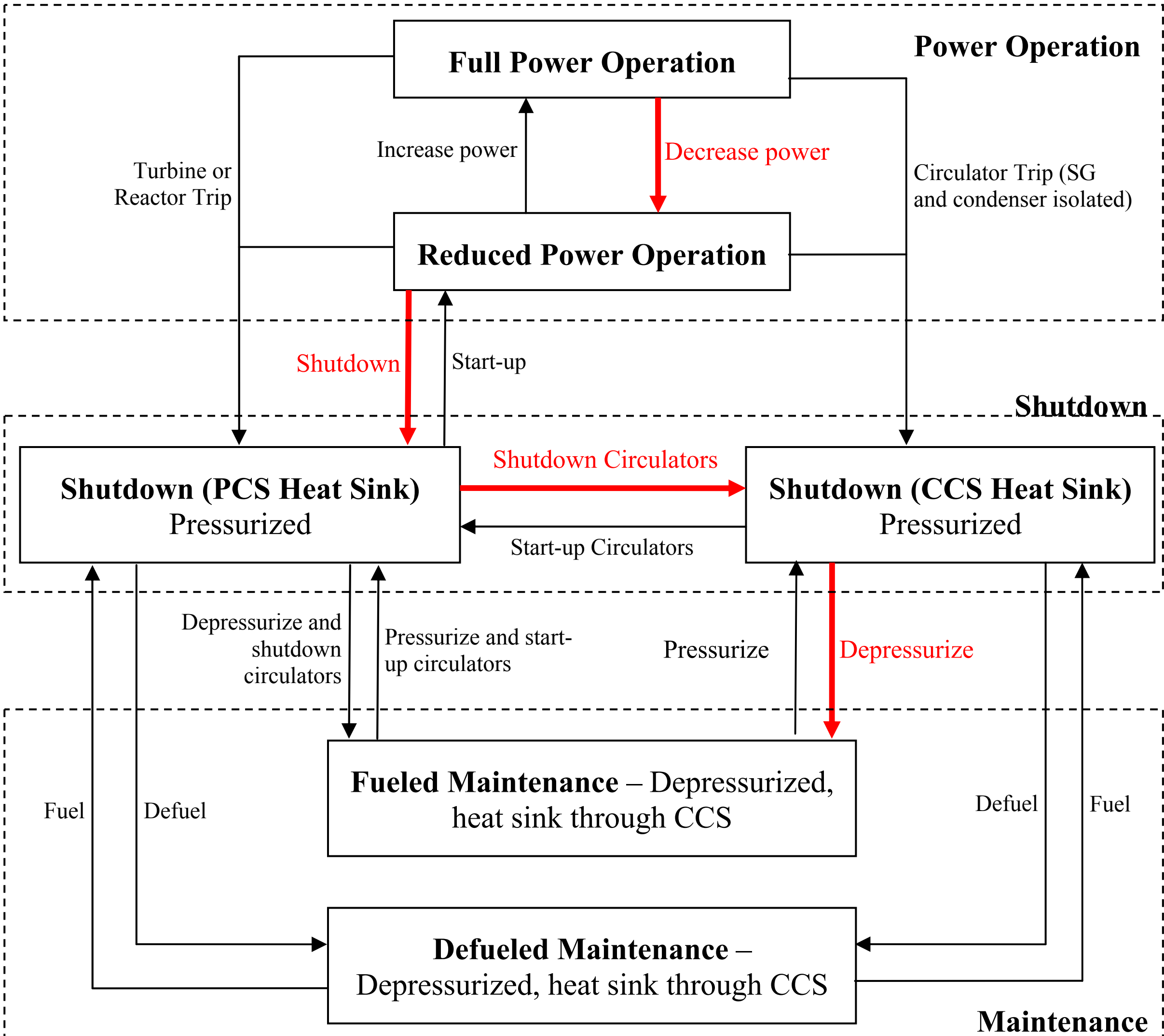

Figure 1-12: Shutdown Path on States Diagram

The different phases that were analyzed for the shutdown are listed below:

- PHASE I (Decrease power)
  - The reactor power is ramped down from 100% to 40% power (by reducing ROT at 100°C/hr).
  - The PHTS and SHTS circulator speeds are used to control the cold temperatures in the two circuits respectively.
  - The feedwater flow rate is used to control steam temperature at 567°C.
  - The feedwater temperature is reduced from 164°C at 100% power to 120°C at 40% power.
  - The CCS circulator is in idle mode (at 10% speed).
- PHASE II (Shutdown)
  - The ROT is further ramped down at 100°C/hr.

  - When the ROT drops below 330°C, the reactor is shut down by inserting control rods at the maximum controlled insertion rate (1cm/s).
- PHASE III (Shutdown circulators)
  - When the ROT drops below 300°C, the PHTS and SHTS circulators are stopped and the circulator outlet check valve closes.
  - The CCS circulator speed is ramped up.
  - The CCS outlet check valve opens with positive differential pressure across the valve.
  - The CCS circulator speed is used to control the ROT ramp-down at 100°C/hr until 200°C is reached.
  - The feedwater flow is stopped.
  - The ROT is stabilised at 200°C for 2 hours (using the CCS circulator speed).
- PHASE IV (Depressurization)
  - The inventory is extracted until 200kPa is reached (helium was extracted at an assumed rate of 0.1kg/s out of the PHTS and 0.15kg/s out of the SHTS).
  - When the reactor mass flow rate dropped below 3kg/s, the CCS blower speed is used to control reactor mass flow rate at 3kg/s.

The results of the shutdown transition are shown on in Figure 1-13 to Figure 1-15. From Figure 1-15 it can be seen that the pressure of the SHTS drops quite suddenly the moment the circulators are stopped. This pressure then remains below the pressure of the PHTS for the remainder of the transient. This is due to the drop in temperature in the SHTS. When the circulators are switched off, the mass flow in the SHTS drops to a very low value, thus the approach temperature of the SG becomes much smaller. This causes the helium at the SG outlet to get a lot closer to the water inlet temperature, which is 35°C at this stage. It must be remembered that for this simulation, the circulator was not stopped totally. The change in temperature therefore might look different if the circulators are totally stopped.

Towards the end of depressurization, the RIT dropped slightly below 50°C (the minimum reached was about 44°C; refer to Figure 1-13). This is mainly due to the expansion of the gas during depressurization. The minimum temperatures reached can be increased by starting depressurization sooner while the temperatures are still higher. The minimum RIT of 44°C reached is not expected to be a problem (radiation embrittlement of the RPV), since the pressures are quite low at this stage (the pressure is about 1 800kPa when the RIT drops below 50°C and it drops to about 200kPa when the RIT reaches its minimum of 44°C).

Similar to the start-up, an extraction rate of 0.1kg/s for the PHTS and 0.15kg/s for the SHTS was assumed (requiring about 11 hours for blowdown). Higher extraction rates will ensure an accelerated shutdown, but it might also influence the minimum temperatures reached due to the quicker expansion of the gas during depressurization.

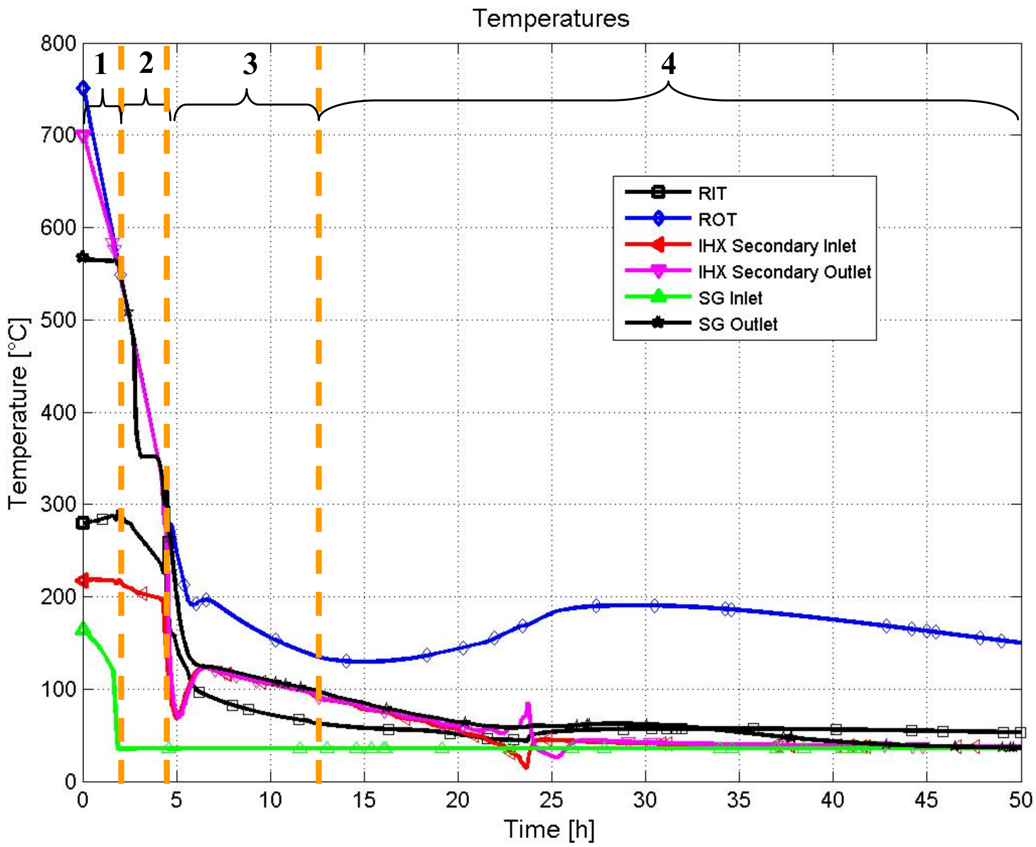

Figure 1-13: Helium and Water Temperatures (Shutdown)

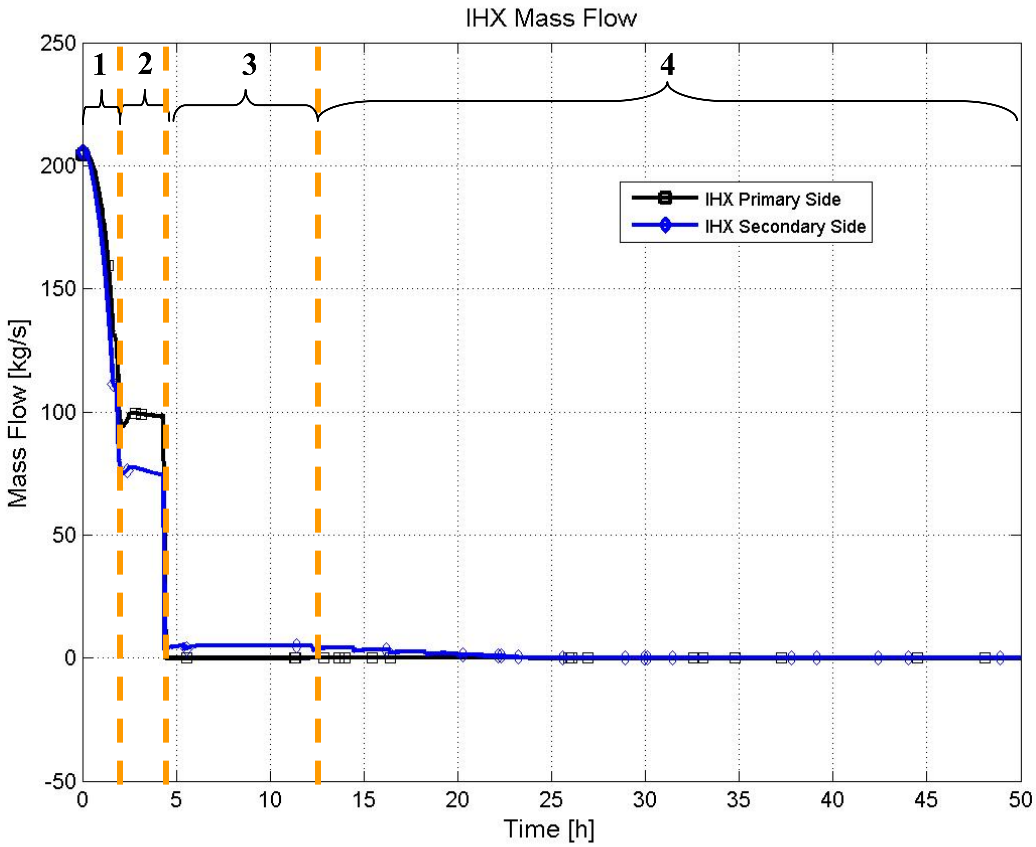

Figure 1-14: IHX Mass Flow (Shutdown)

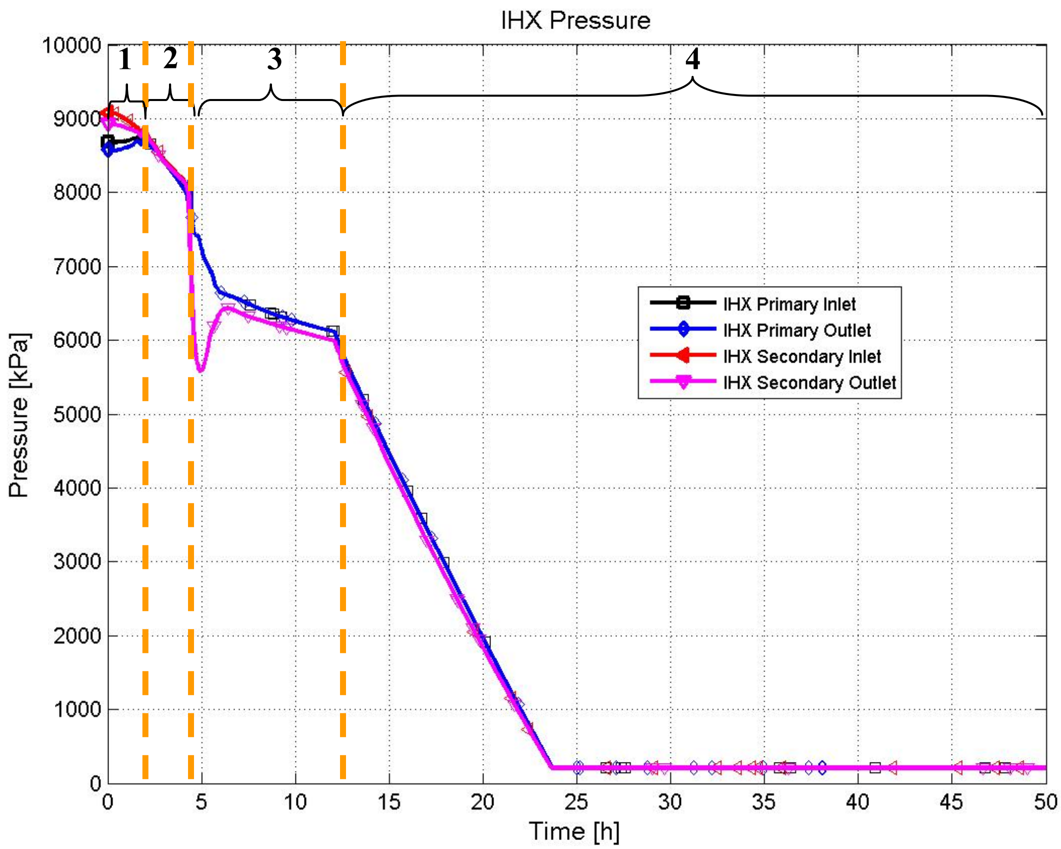

Figure 1-15: IHX Pressure (Shutdown)

1.5 CONCLUSIONS AND RECOMMENDATIONS

In general, the analysis has indicated two important factors that must be considered in the design. Firstly, it indicates that very careful design of the control strategies is necessary to ensure that the pressure of the SHTS remains higher than the pressure of the PHTS and that the pressure difference between the primary and secondary side of the IHX remains within limits. Secondly, the CCS has to be sized carefully to ensure it can supply the flow needed for the depressurized shutdown while not exceeding the maximum flow for the pressurized case.

The conclusions from the steady state results are summarized below.

- Normal operating condition: The desired operating point is achievable with the current plant layout.
- Lower operating condition: In order to prevent the necessity of inventory control, the pressure bias on the IHX can be maintained by lowering the hot gas temperature in the NHSS and maintaining the cold gas temperature. Alternatively, additional preheating of

the feedwater can be applied. The recommended and simpler option is the lowering of the hot gas temperature.
- Shutdown (PCS heat sink): The ROT can be maintained at the required level by adjusting the water flow through the SG. It must be verified that the SG can be operated with this low water flow (about 3% of the flow at full power) under these conditions. The low water flow rate is not expected to be a problem, since no boiling is required at this stage.
- Shutdown (CCS heat sink): To prevent the RIT and ROT from dropping below acceptable limits, either the CCS mass flow can be throttled further by using a fine control valve in parallel with the CMIV, or a bypass for the CCS heat exchanger can be implemented. The fine control is recommended because a CCS cooler bypass valve will receive gas in excess of 700°C and would therefore be classified as a hot valve. The CCS heat exchanger size cannot be reduced as it must be sized for the depressurized condition.
- Depressurized condition: Although the ROT obtained is higher than the original requirement, a bigger problem may be the very small mass flow rate through the reactor. The minimum mass flow rate needed to prevent buoyancy effects in the reactor must be determined and, if required, the CCS circulator size can be increased. It must be kept in mind, however, that the pressurized shutdown condition would also be affected by this.

The conclusions and recommendations for the start-up transition are given below:

- The main concern during the start-up is the sudden change in pressure on the secondary side of the IHX the moment the SG water flow is started (which furthermore causes the pressure in the SHTS to drop below that of the PHTS). This is due to the fact that the preheating of the feedwater has not been activated at this stage (feedwater temperature is still 35°C). The dip can be lessened by starting to heat the feedwater before the water flow is started.
- The pressurization of the start-up takes about 11 hours (almost half of the total start-up time) at the assumed injection rates of 0.1kg/s into the PHTS and 0.15kg/s into the SHTS. The exact injection rates that can be achieved must still be verified, which will impact the start-up time.
- It is recommended that the injection rate ratio of the PHTS and SHTS be chosen such as to ensure that the pressure of the SHTS stays above that of the PHTS during pressurization.
- With the start-up strategy used in this analysis, the PHTS and SHTS circulators are only started once full inventory is reached. The total start-up time can possibly be reduced by starting up the circulators whilst pressurizing, thus starting to heat up the system whilst pressurizing.
- A cold start-up still needs to be performed to determine how long the start-up will take if all components are cold (at ambient conditions) and there is no decay heat present. It is expected that the same start-up strategy can be used; the heat-up phase with the circulators will only take a bit longer.

The conclusions and recommendations for the shutdown transition are given below:

- The SG helium outlet temperature dropped quickly the moment the SHTS circulator was switched off, causing the pressure in the SHTS to also drop sharply to below that of the

PHTS. This drop in temperature and pressure can possibly be reduced by ramping down the SHTS circulator speed at a slower rate.

- The temperature of the RIT did drop slightly below 50°C (minimum reached was about 44°C), but due to the pressure being quite low at this stage, it is not expected to be a problem. Depressurization can however be started sooner (whilst the temperatures are still relatively high) to increase this minimum temperature reached.
- The assumed extraction rates of 0.1kg/s for the PHTS and 0.15kg/s for the SHTS must still be verified and the impact of faster or slower rates on the minimum temperatures reached must be investigated.

2. PLANT LEVEL ANALYSES FOR PHTS HELIUM PRESSURE BOUNDARY LEAKS AND BREAKS

This section evaluates the radionuclide releases from a spectrum of leaks and breaks in the Helium Pressure Boundary (HPB) of the Primary Heat Transport System (PHTS) to determine environmental dose rates and best estimate release fractions for the various RN barriers which will be used in Section 3 to evaluate the RN barrier retention allocations.

Firstly, the NGNP plant design and the characterization of the leaks and breaks analyzed are described. This is followed by a description of the calculation chain employed and the calculation models created for each analysis. Finally the results for the analysis are described and assessed.

2.1 NGNP PLANT DESIGN AND HPB BREAK CHARACTERIZATION

The analysis for the RN releases is based on the PBMR NGNP Steam Cycle with SHTS Helium Loop. The major plant parameters, the break size and location selection as well as the plant system responses assumed are outlined in the next sub-sections.

2.1.1 Summary of Major Plant Parameters

A summary of the major plant parameters that is used in the analysis of HPB breaks is provided in Table 2-1.

Table 2-1 Summary of Major Plant Parameters and Assumed Design Features

Plant Parameter	Value
Plant Design Configuration	PBMR NGNP Steam Cycle with SHTS Helium Loop
Power Level	500MWth
PHTS Helium Pressure	9.0Mpa
RIT	280°C
ROT	750°C
Normal Operation PHTS Mass Flow Rate	204.5kg/s
PHTS Volumes and Sub-Volumes	Based on Flownex NHSS Model
PHTS Helium Inventory	4038kg
Initial Circulating RN Inventories	Calculated
Distribution of Initial RN Inventory (gas-borne, dust, plate-out)	Calculated
Modeled RB design features for pressure relief, RB isolation, and RN filtration	Blow-out panels to relieve pressure between RB compartments and to open Depressurization Vent Shaft (DVS); DVS isolation dampers to re-close the Pressure Relief System (PRS) relief shaft, filtration

Plant Parameter	Value
	capability for releases out the relief shaft, no filtration for other RB release pathways, RB leakage defined
RB and Reactor Building Vent Volume (RBVV) Initial Atmospheric Composition	Ambient air with 50% humidity
Site Boundary Distance	400 meters

The RB and RBVV were defined according to the latest NGNP building design. The schematic layout analyzed is shown in Figure 2-1. Note that the two DVS were combined into one due to an undesirable numerical solution issue, i.e. the formation of an artificial convection loop.

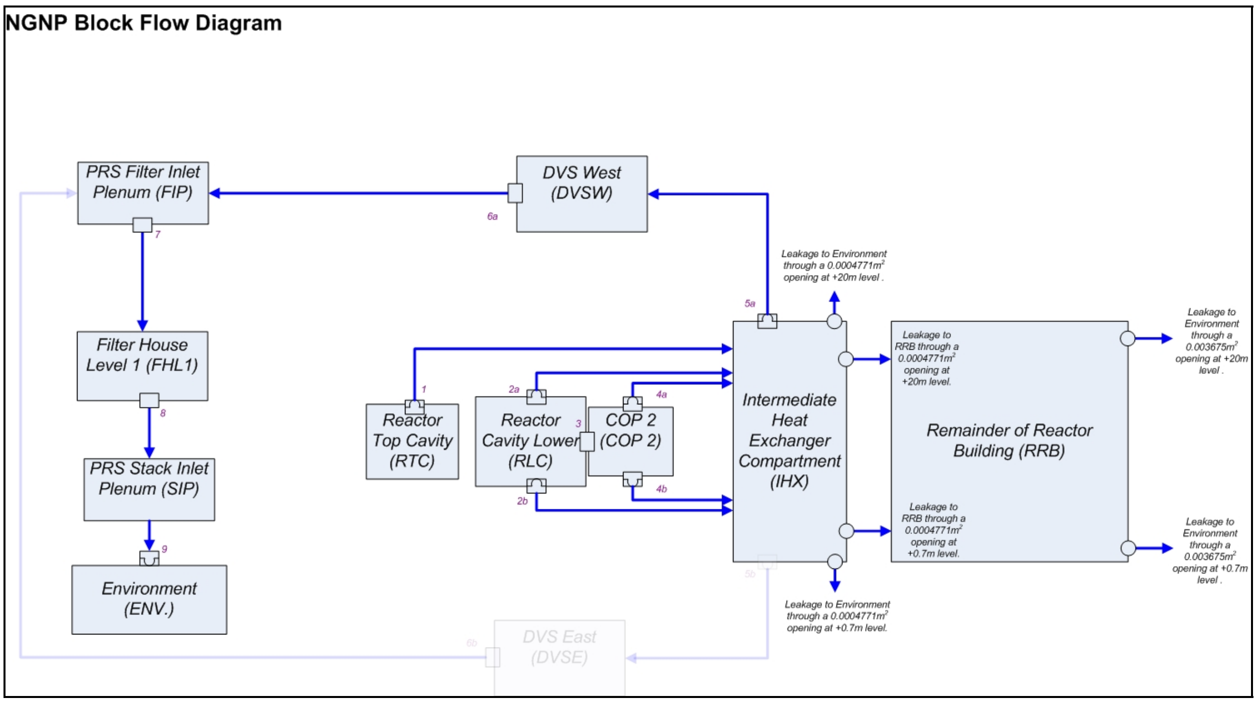

Figure 2-1 Model of Reactor Building Volumes

2.1.2 Break Location

The analyses performed in this study cover a break location in the Core Inlet Pipe (CIP) at the highest elevation above the core and at the top of the pipe located in the Reactor Cavity of the Reactor Building. The location of the break is shown in Figure 2-2.

The choice of break location was based on the following factors

- Consistency with the 2008 study
- The core inlet pipe is the largest pipe with a single wall design
- Isolation is not feasible in this location

- The elevated location was considered the highest potential for RB helium/air ingress to the PHTS after blowdown

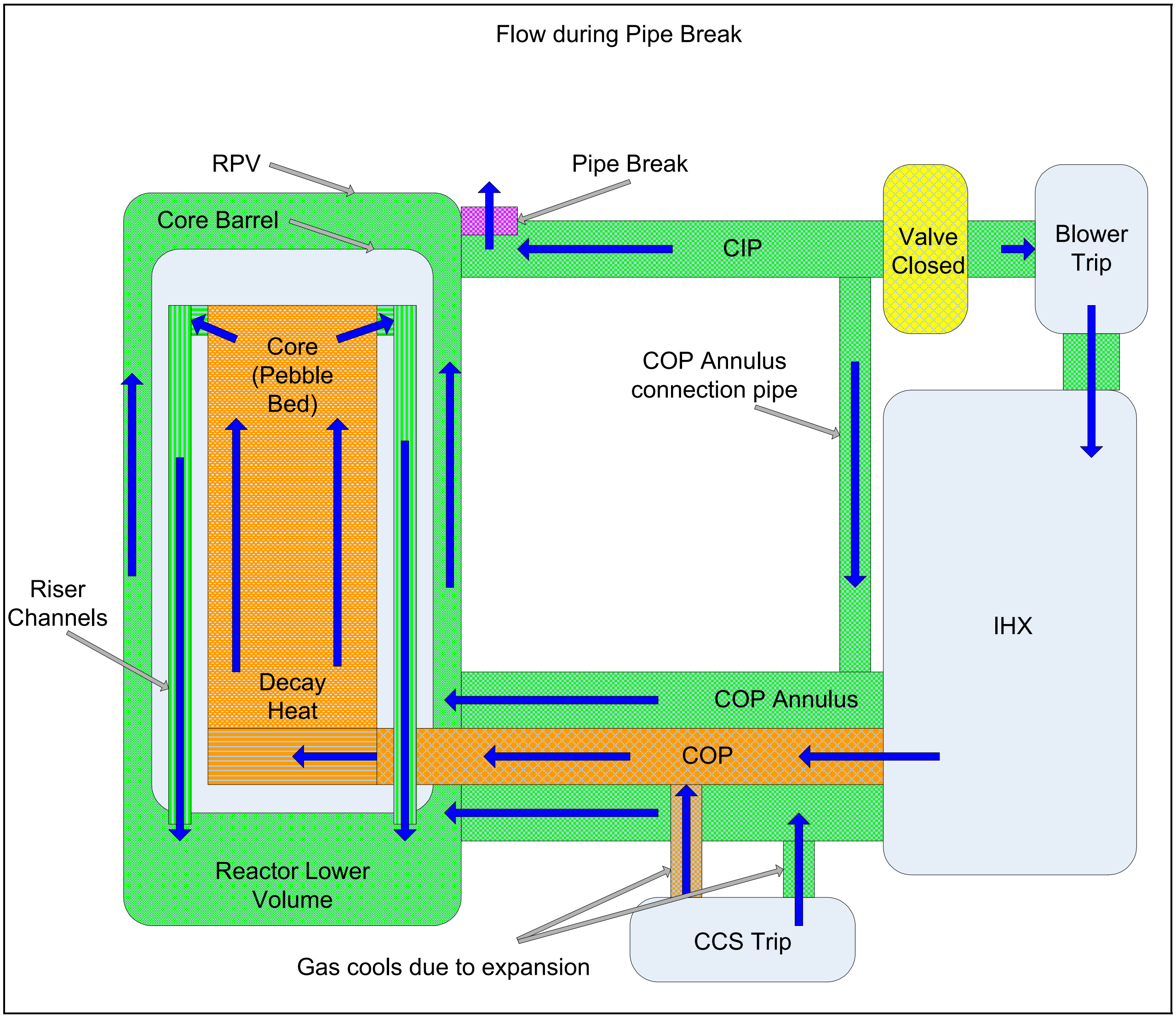

Figure 2-2 Location of the HPB Break in the Core Inlet Pipe showing Break Induced Flows

2.1.3 Selection of Break Sizes

For purposes of evaluating the thermo-fluid behavior of the depressurization of the PHTS a range of HPB break sizes was considered from 2mm Equivalent Break Size (EBS) up to and including a double ended guillotine break (DEGB) of the CIP. This pipe has an inside diameter of 710mm and the EBS is thus 1000mm. For the purpose of evaluating the RN releases to the environment and site boundary radiological doses, two break sizes were considered, one small break of 4mm that was selected to maximize the delayed releases from the fuel into the reactor building, and one medium size break of 100mm EBS which is assumed to be the limiting design basis event break size for event sequences involving Depressurized Loss Of Forced Cooling (DLOFC).

2.1.4 Characterization of Plant System Responses

The following assumptions were made about the response of the plant systems to each modeled HPB break:

- Reactor scram, PHTS and SHTS circulator trip and coast down at the first safety grade scram signal. All control rods insert.
- PHTS and SHTS circulator discharge valves close as designed
- Core Conditioning System (CCS) fails to start
- Helium Purification System HPS isolated from the PHTS HPB at t=0
- Fuel Handling and Storage System (FHSS) remains isolated via the isolation blocks; the He inventory in the non-isolated parts of the FHSS inlet lines. In-core Distribution System (ICDS) line, Small Absorber Sphere (SAS) return lines are assumed to be accounted for in the He inventory data (a very small fraction of the PHTS inventory).
- Reactor Cavity Cooling System (RCCS) in permanent water boil-off mode: Heat-up to 135 ºC, then holds steady (assumes makeup from "firewater truck" after boundary condition temperature is reached).
- RB Heating, Ventilation Air Conditioning (HVAC) system fails to cool or filter RB atmosphere at t=0.
- No process controls except for scram and circulator trips.
- All RB blowout panels (Rupture Panels No. 1, 2a, 2b, 4a, 4b, 5a, 5b and 9) in Figure 2-1 open at 5kPa forward pressure.
- The openings (No. 3, 7 and 8) in Figure 2-1 are normally open and stay open

2.1.5 Characterization of Reactor Building Responses

For each of the break size cases selected for RN analysis (4mm and 100mm EBS) four different responses of the RB design features for isolation and filtration are modeled:

- No filtration, DVS damper fails to open
- No filtration, DVS damper closes at the end of blowdown
- With filtration, DVS damper fails to open
- With filtration, DVS damper closes at the end of blowdown

2.2 RELEASE CALCULATION CHAIN AND CALCULATION MODELS

In order to perform realistic analysis of the PHTS break scenarios, a calculation chain was evaluated. The detail of the flow of calculations, the codes used and the data that is passed between them is provided in Figure 2-3.

The thermal-fluid behavior in the PHTS during the break transient is first evaluated using the Flownex code. For the 100mm break case, the analysis is extended to include the evaluation of PHTS and RB gas exchange behavior after blowdown. Using these results, the transient neutron kinetics code TINTE determines the details of the reactor core behavior. GETTER then uses the fuel temperature behavior and neutronic data to determine delayed releases from the fuel. This information is passed to EXCEL1 which models the RN releases from the PHTS to the RB. EXCEL1 also uses data on the normal operation source term to determine the initial RN releases. This source term is based on results obtained from previous SPECTRA calculations as well as from NOBLEG steady-state fission product release calculations. The ASTEC code then uses the specification of the releases from the PHTS to model the RN distribution in the RB and the releases to the environment, both from the DVS and specified leakage paths. Finally, the RN releases determined are converted into offsite doses using the EXCEL2 model.

The following sections provide further details on each of the codes used and the models that were developed for the analysis.

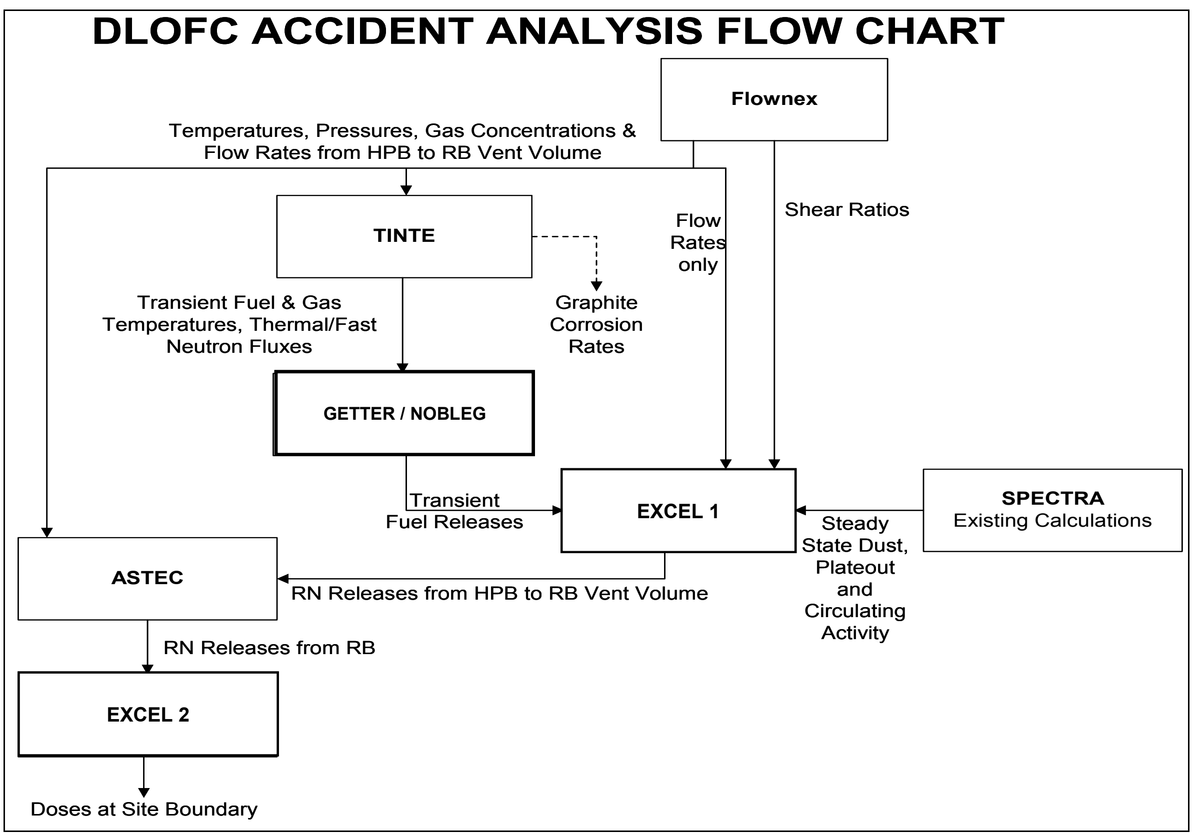

Figure 2-3 Flow Chart for the Radionuclide Release Calculation Chain

2.2.1 Flownex

Flownex models the thermo-fluid behavior in the PHTS and its interaction with the RB. The model provides pressures, gas concentrations and flow rates to TINTE and temperatures, pressures, gas concentrations and flow rates to ASTEC and flow rates and shear force ratios to the Excel1 model of the PHTS.

2.2.1.1 Flownex Model Layout

The NGNP NHSS Flownex Model is shown in Figure 2-4 and is identical to the model used in Section 1 of this study. In order to investigate the thermo-fluid interaction between the PHTS and the RB the NGNP PRS Flownex Model (also referred to as the Reactor Building (RB) Flownex Model) as shown in Figure 2-5 was developed. The PRS model consists of different components:

- Free volume in compartments.
- Ducts or openings connecting compartments to relieve pressure through the Depressurization Vent Shaft (DVS) and Filter House compartments to atmosphere.
- Depressurization (rupture) panels to seal compartments during normal operation.
- Leakage paths from the IHX compartment to the remainder of Reactor Building and further to the environment.
- Heat transfer through walls and roofs/floors between compartments.

The Flownex network layout of the PRS is done according to the different levels (referring to heights) of the RB. The flow path is derived from the NGNP Block Flow Diagram as depicted in Figure 2-1. To simulate a break that occurs in a certain compartment, the two models are coupled via the “pipe break” element available in Flownex, as shown in Figure 2-6.

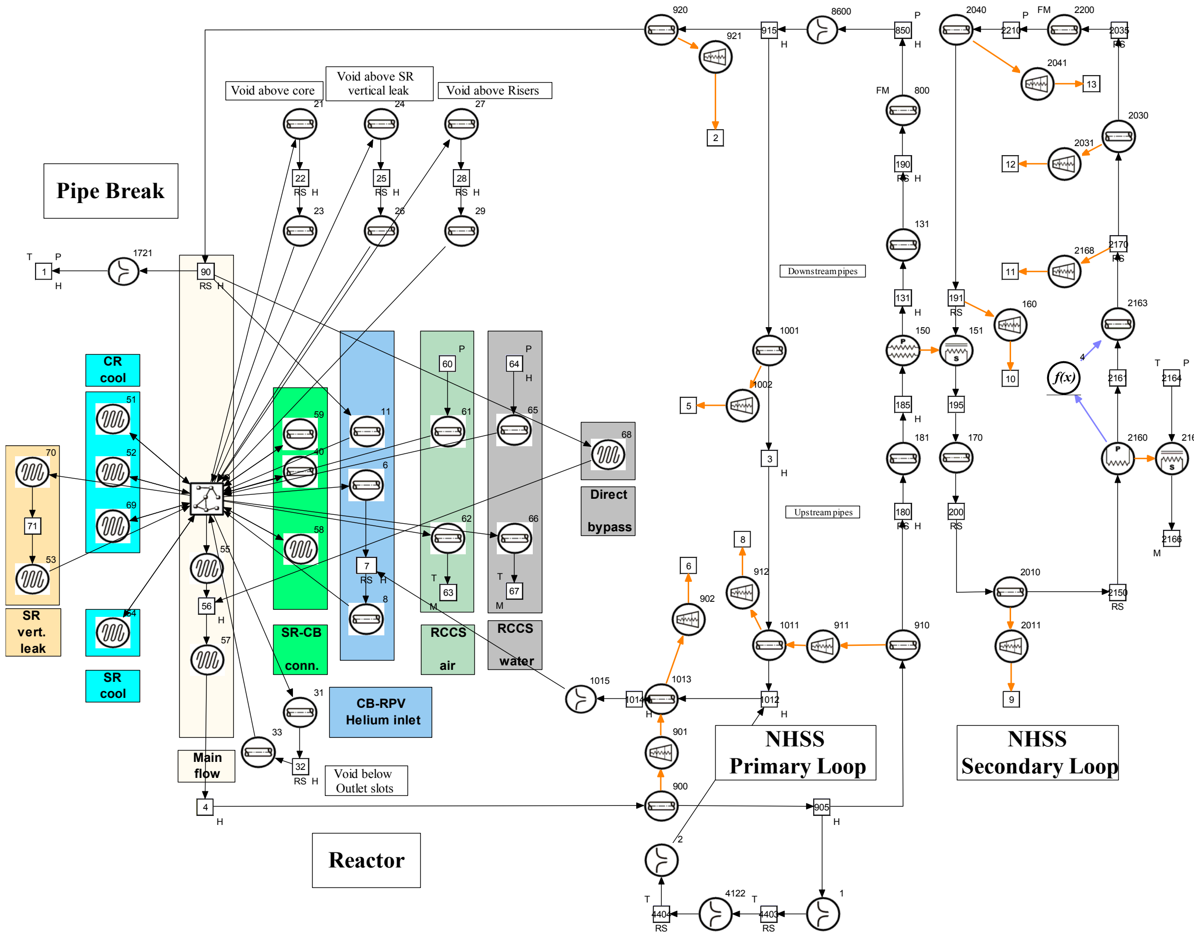

Figure 2-4 Flownex presentation of the NGNP NHSS model

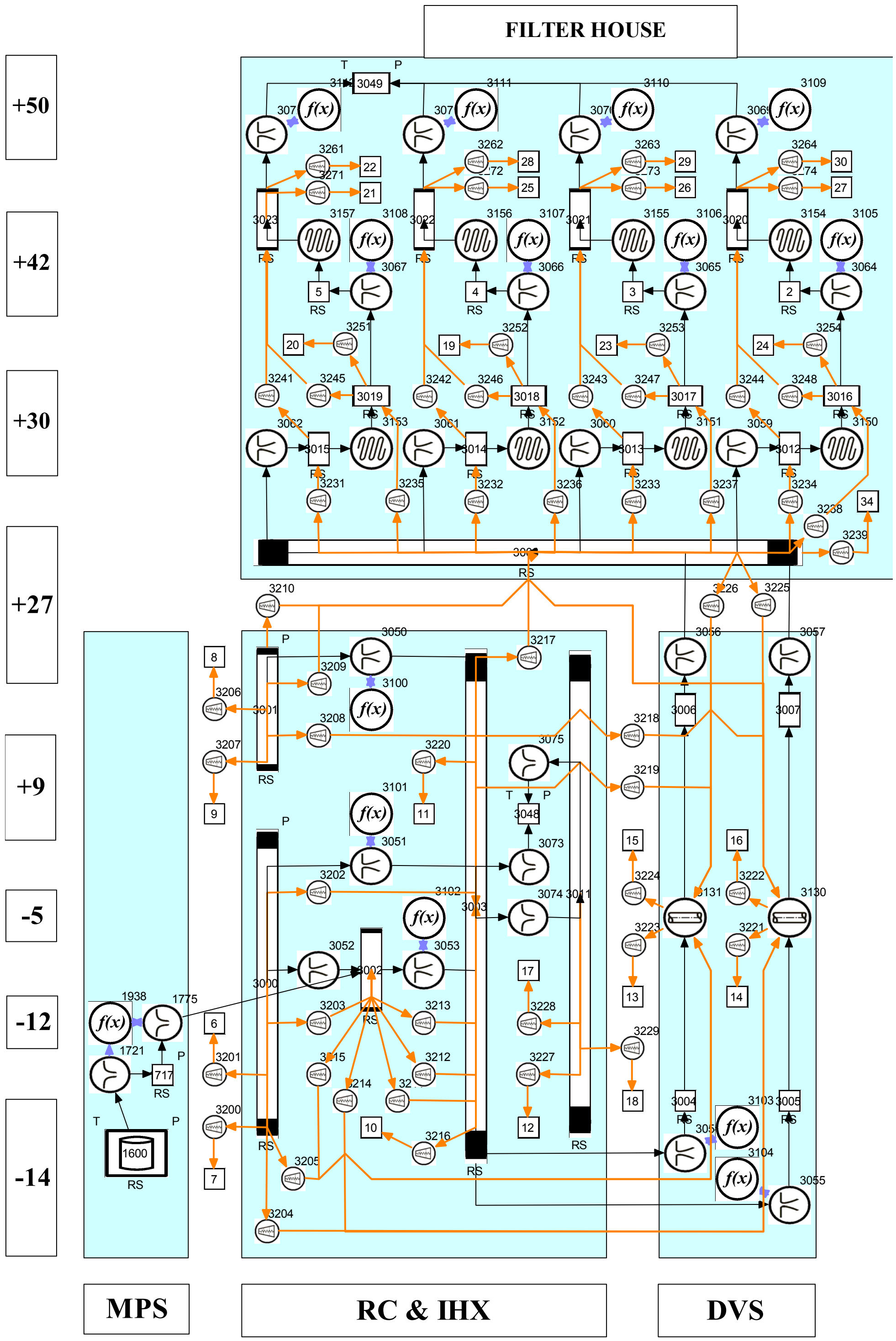

Figure 2-5 Flownex presentation of the NGNP PRS model

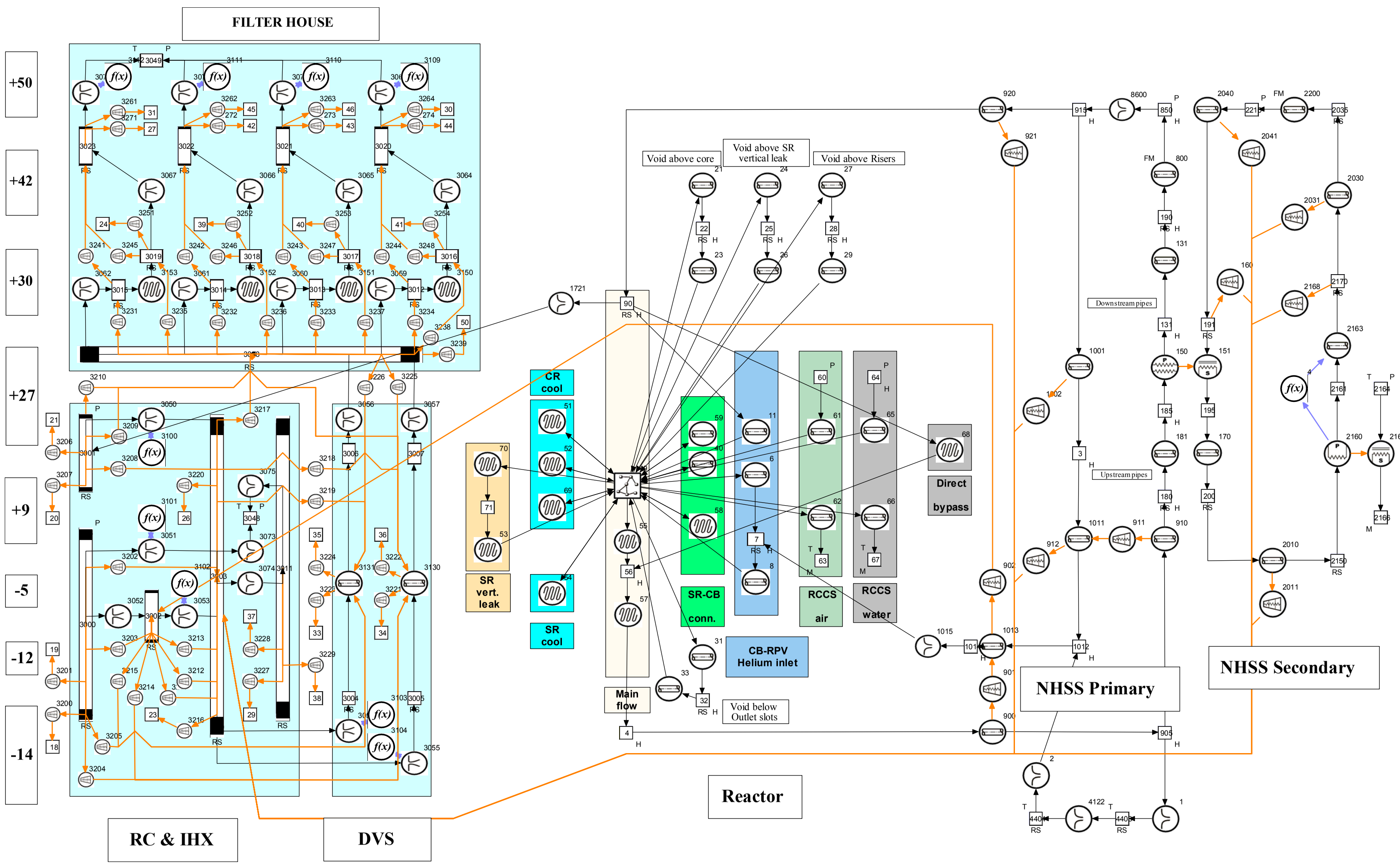

Figure 2-6 Flownex presentation of the coupled NGNP NHSS and NGNP PRS models

2.2.2 TINTE

TINTE determines the time dependent transient behavior of the core during the DLOFC event. Using the pressure and flow rates provided by Flownex, TINTE calculates the core response and provides the fuel temperatures as well as neutron fluxes to GETTER for the RN release calculations.

TINTE has the ability to model corrosion due to air ingress, and this was used to evaluate the possible effects of air ingress in the larger break case. Note that this investigation was performed as a sensitivity study only and was not aimed to be directly included in the calculation chain.

2.2.2.1 TINTE Code

TINTE (Time Dependent Neutronics and Temperatures) is mainly used to model time-dependent transients in HTGRs. These events can be slow (DLOFC over 24 hours, Xenon oscillations over a few days), or fast (Control Rod ejection). The code provides transient temperature data for core component design and design limits (fuel, reflectors, control rods, etc), as well as fission and total power indicators.

TINTE implements the 2-dimensional (r-z cylindrical geometry), time-dependent neutron diffusion equations, with a coarse mesh finite difference solver using 2 neutron energy groups (3.07eV thermal cut-off) and 6 delayed neutron groups. Cross-section data, fuel element burnup history and spatial isotopic distributions are supplied from the neutronics code VSOP99.

The thermal hydraulics solver determines the 2-dimensional heat transport in cylindrical geometry. Gas and solid temperatures are calculated separately from the neutronic power. Fuel element surface temperatures define the effective heat conductivity in the pebble-bed and the convective heat transport.

2.2.2.2 TINTE Model Layout

The general NGNP TINTE model layout is shown in Figure 2-7. The indicated geometry is based on the latest PBMR NGNP design.

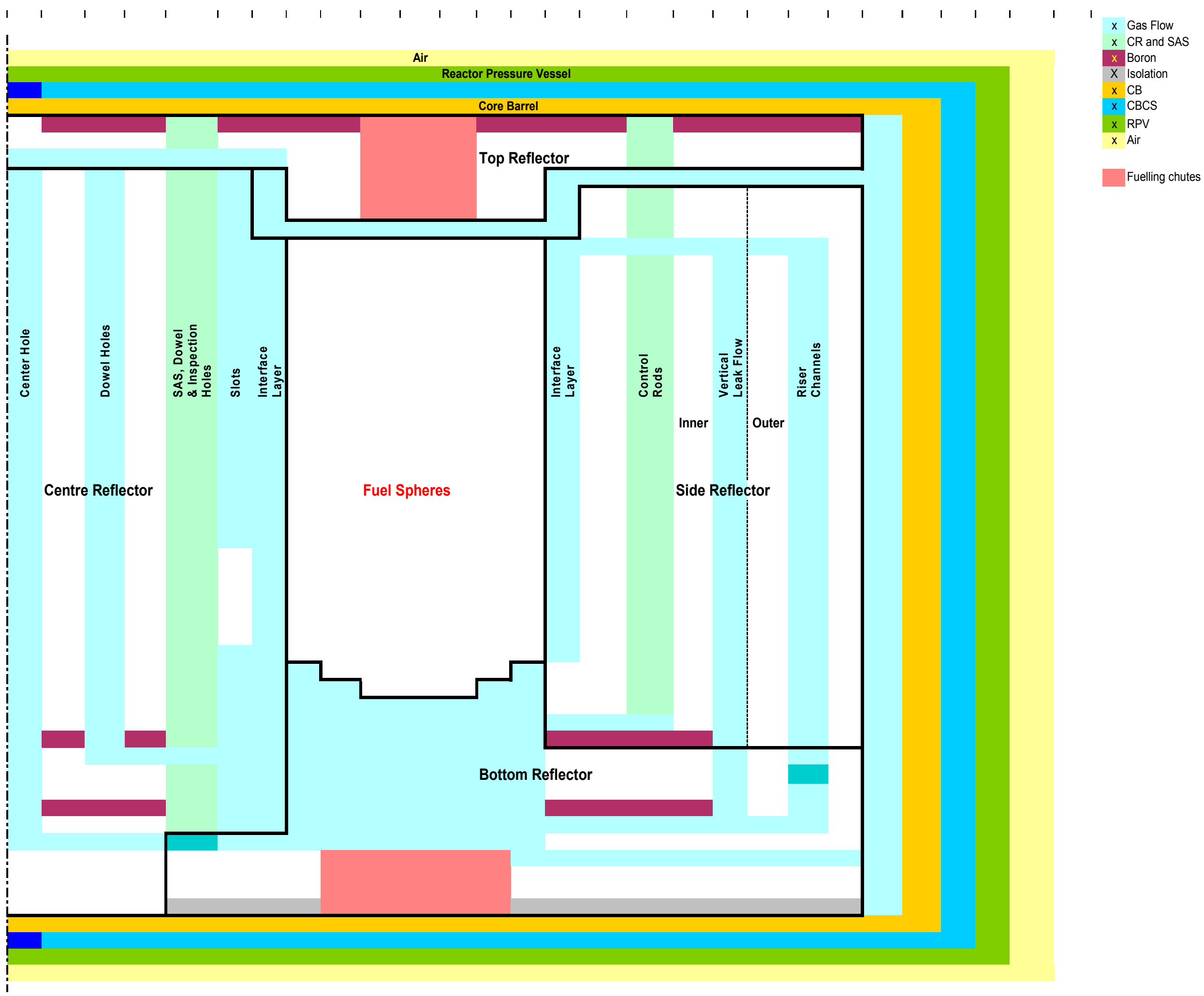

Figure 2-7: General TINTE NGNP Model layout

The main coolant mass flow path enters the model at the upper void between the Core Barrel and the Reactor Pressure Vessel, from where it flows downwards between the radial components of the two SSCs, and then enters the riser channels from the bottom section of the Core Barrel.

In accordance with the PBMR "design-to" philosophy on the treatment of bypass flow modeling, the core bypass and leak flows were simplified to 3 flows, totaling 20% of the total flow:

- Control Rod channel - 5.1 kg/s or 2.5% of the total inlet flow
- Reactivity Control System (RCS) channel - 4.1 kg/s or 2.0% of the inlet total flow
- Direct inlet-outlet bypass flow - 31.7 kg/s or 15.5% of the total inlet flow.

For the model, the fast fluence exposure period on the reflector blocks was defined as 9 Full Power Years (FPY). All other material parameters were used at their best estimate values (e.g. graphite and steel density, specific heat, conductivity and emissivity).

The 2009 500 MW DPP model utilized a Control Rod (CR) bank inserted position of 200 cm below the bottom of the top reflector (i.e. 122 cm into the pebble bed region). This location was based on a critical VSOP99 core configuration, coupled with a load-follow requirement of 100-40-100%. Since the load-follow requirements are assumed to be similar for the NGNP, the rods were kept at this location in the TINTE model.

The VSOP99 code supplied the spatial isotopic distribution (i.e. number densities) and decay heat data that is necessary for the TINTE steady-state calculation. A dedicated VSOP99 NGNP model has been created, and the TINTE tn4 file has been updated with the latest isotopic distribution and decay heat data set
.

The boundary conditions are defined as follows:

- Reactor inlet gas temperature: 280°C.
- Reactor inlet mass flow rate: 204.5 kg/s.
- Reactor outlet pressure: 8.77 MPa.

2.2.2.3 General Model Assumptions

The following general assumptions were made during the development of this model:

- The geometry of the TINTE model corresponds to the cold (room temperature) dimensions of the reactor. The Z-axis expansion of the reactor due to linear thermal expansion is small compared to the dimensions of the reactor along that axis, and it is therefore acceptable to use the cold dimensions.
- The graphite side reflector blocks that have a flat inner and outer face in the radial direction, have been approximated as curved surfaces on radii touching the mid points of the inner and outer faces.
- The domed upper and lower shells of the RPV are being modeled as flat plates due to modeling limitations in TINTE. This approach is made acceptable through the application of the principle of conservation of mass on those RPV sections and also on the void spaces enclosed by them.
- The TINTE model contains no metallic connections between the core barrel and the RPV, i.e. the core barrel support, the control rod drive tubes and the SAS tubes are not explicitly modeled. The only mechanism of heat transfer between the core barrel and the RPV is therefore through radiative heat transfer. This approach will most likely lead to conservative (higher) estimates of temperatures within the core barrel and the fuel spheres.
- The control rod drive equipment, i.e. motors, tubes and chains, is not included in calculating the mass of the upper domed lid of the reactor pressure vessel. The assumption was also made that the top core barrel plate could be modelled as a solid plate, i.e. that all the piping material above the core barrel top plate equates

approximately to the volume of all the many holes in the core barrel top plate. Thirdly, the volume of the SAS basket and container material is lumped to the RPV upper domed section, and the core barrel support structure is lumped to the core barrel support plate.

- The upper and lower fuel core surfaces are approximated with flattened surfaces. The upper flattened surface is located at the volume averaged surface of the fuel sphere peaks and valleys. The fuel cones are also approximated on a volume averaged basis but with flat surfaces stepped in over three axial levels to resemble the flow of pebbles towards the de-fuel chutes.
- A special 10 mm radial contact zone is being used to model the interface of the fuel pebbles with the centre- and side reflector surfaces. This approach is an optional modeling feature available in TINTE for improved modeling of heat transfer in the pebble to reflector contact zones, and has been shown in previous sensitivity studies to be a required feature of any TINTE model.

2.2.3 NOBLEG/GETTER

NOBLEG and GETTER are codes used to analyze fission product transport from the fuel into the coolant gas. NOBLEG determines steady-state fuel releases while GETTER calculates transient behavior.

Fission products formed during the operation of a high temperature gas-cooled reactor that are not completely retained in the uranium oxide kernel, may be released from the fuel elements through failed coated particles and uranium and thorium contamination of the fuel materials. Long-lived fission products may also diffuse through intact TRISO-particle layers (albeit very slowly). Fission products are transported from their origin, the fission sites, through the fuel materials to the surface of the fuel elements, where the fission products are desorbed into the coolant gas.

Fission product transport through the material layers is dependent on two basic theoretical models, first the transport process that describes the movement of fission products, and second, the thermo-fluid model that determines material temperatures that influence the rate of the first process. Both models are incorporated into the fission product release software GETTER. The software product FIPREX acts as a wrapper around GETTER, creating input files, controlling GETTER operation, and performing post-calculation data reduction of the GETTER output.

Two physical models are applied when using the calculation model. Firstly the fuel element model is based on German reference fuel made up of TRISO-particles embedded in A3-3 graphite matrix material. Secondly, the reactor model is based on a spherical fueled HTGR core design with a static central column as modeled by VSOP and TINTE (section 2.1.2.2).

This calculation model is based on German reference fuel and assumes that the fuel utilized will be the same or better quality than German reference fuel. Therefore all transport and fuel parameters as developed and determined by the German fuel program are used. The calculation is performed for the best estimate or expected case using all best estimate input parameters and values. A sensitivity analysis is performed on all uncertain input parameters and values to determine design limits.

There are three distinct sources of fission products in fuel spheres. A fourth source also exists that is important only for activation products, the natural contamination of the activation product precursor in the fuel materials. They are modeled as follows:

Uranium and thorium contamination of the fuel materials

This contamination is primarily in the matrix material of the fuel sphere and release of fission products created by fissions of this contamination only have to diffuse through the matrix material before being released. The contamination is expressed as an effective uranium fraction of the total uranium and thorium content of a fuel element.

Defective and failed coated particles

A particle is considered failed or defective if its coating layers are absent or are damaged sufficiently to allow the release of fission gases. Even under the best manufacturing conditions a small fraction of coated fuel particles will be defective. Furthermore, under abnormally high temperatures and power surges, coated fuel particles may start to fail. Statistical analyses of German production fuel were used to determine PBMR-manufactured fuel failure fractions. Further analyses of German fuel during irradiation and heat-up testing derived fuel failure versus temperature expected curves and their uncertainty ranges. Phenomena that may influence coated particle performance (amoeba effect, Palladium-SiC interactions, etc.) were included in this evaluation.

Intact TRISO coated particles.

Intact coated particles are defined as particles that have all their coating layers intact, are impervious to fission gas release, and release only a very small fraction of their 137Cs inventory. Fission products are modelled to recoil from their fission sites and then to diffuse through the fuel materials to be desorbed in the coolant gas.

2.2.4 EXCEL1

Releases of radionuclides (RNs) from the PHTS circuit out the HPB break and into the reactor building (RB) were calculated using an Excel spreadsheet (EXCEL1 in Figure 2-3) in which information from the Flownex results on the time dependent transport of helium mass into the RB and the RN releases from the fuel into the PHTS developed by NOBLEG/GETTER were used to calculate the time dependent releases of RNs into the RB. Radioactive decay is accounted for in the PHTS.

The radionuclide inventory in the PHTS at the start of the transient was estimated using the normal operation radionuclide release rates from the NOBLEG/GETTER calculations and insights from previous NGNP mechanistic source term calculations. Results from a mechanistic study for the current NGNP design were considered not to be achievable within the time and budget constraints of this project. This approach is reasonable for the current study since only break sizes (≤100 mm) in which the shear ratios around the PHTS circuit are all less than 1.0 resulting in minimal liftoff/re-suspension are being considered. The RNs included in the

EXCEL1 calculation all typically attach to dust or plate out during normal operation, therefore a simplifying assumption was made that the normal operation radionuclide inventory is assumed to all be attached to settled dust in the PHTS at the start of the transient.

The dust mass in the PHTS at the start of the transient is assumed to be the same as in the NGNP Contamination Report [4]. The circulating dust mass at the start of the transient is 0.639 kg and the deposited dust mass at the start of the transient is 1610 kg. The dust that is deposited in the HPS filter is not included.

2.2.4.1 Key Model Assumptions

The following key assumptions were made in the model:

- For the purpose of calculating the dust and radionuclide releases from the PHTS to the RB, the entire PHTS, which includes the reactor vessel, Core Outlet Pipe (COP), CIP, PHTS circulator, IHX and COP annular cooling circuit, and the helium inventory in the Core Conditioning System (CCS) inlet is treated as only one fully mixed volume. The total initial inventories of circulating dust and RNs are assumed to be uniformly distributed in this one PHTS volume.
- Liftoff of initially deposited RNs and dust and RNs released from the fuel during the transient are assumed to instantaneously and uniformly mix in the PHTS volume. Therefore, the transport of the RNs released from the core to the break location is neglected. The dust and RNs are then released in proportion to the helium released from the PHTS to the RB.
- The particle size distribution of the dust to which the RNs that are released from the PHTS are attached is not modeled.
- During each time step, the transient radionuclide fractional release from the PHTS to the RB is assumed to be the same as the transient helium fractional release rate from the PHTS to the RB.
- During each time step, the transient dust fractional release rate from the PHTS to the RB is assumed to be the same as the transient helium fractional release rate from the PHTS to the RB.
- The RNs that are circulating in the PHTS, either attached to dust or as free species that are not attached to dust, remain circulating unless they are released from the PHTS to the RB along with the helium as the PHTS depressurizes or heats following the depressurization. Settling of the RNs in the PHTS after the start of the transient is neglected.
- The RNs released from the fuel to the PHTS during the transient remain circulating and do not become attached to dust and do not plate out throughout the transient.
- The RNs initially circulating in the PHTS that are not attached to dust and RNs that liftoff from the metallic components in the PHTS remain circulating and do not become attached to dust throughout the transient.
- The RNs initially circulating in the PHTS that are attached to dust and the RNs that are circulating due to dust re-suspension remain circulating and attached to dust throughout the transient.

- Simplified models for the desorption of plateout and for dust re-suspension are assumed and used for all RNs.
- The estimate of the normal operation radionuclide inventory in the PHTS at the end of plant life neglects the removal by the Helium Service System during normal operation and the production by means other than the release directly from the fuel pebbles.
- The radionuclide steady state release rate from the fuel to the PHTS is assumed constant for the plant life.

2.2.4.2 Calculation Assumptions

The following calculation assumptions were made:

- For the seven RNs included in the calculation (Ag-110m, Ag-111, Cs-137, I-131, I-133, Sr-90 and Te-132), the normal operation radionuclide inventory is assumed to all be attached to settled dust in the PHTS at the start of the transient. Accordingly, the initial radionuclide circulating and plateout inventories are all assumed to be zero and hence, desorption of plateout is also assumed to be zero.
- The shear ratios during the blowdown for the leak sizes (< 100 mm) in the current study are all less than 1.0. So a minimal dust resuspension is conservatively assumed for all RNs of 0.2%.
- For the 4 mm break, zero release from the PHTS to the RB is assumed post-blowdown, after 91 hrs. He-air ingress into the PHTS from the RB is assumed post-blowdown due to thermal contraction.
- For the 100 mm break, the blowdown is complete in 11 min and release from the PHTS to the RB continues until 50 hrs due to thermal expansion of the helium coolant in the PHTS. From 0-3 hrs, the helium mass in the PHTS is taken directly from the Flownex results. From 3-50 hrs, the helium mass is calculated from fitted Flownex flow rates from the break to smooth out the oscillations in the Flownex results. After 50 hrs, zero release from the PHTS to the RB is assumed as the start of He-air ingress into the PHTS is indicated from the Flownex results.
- Release of helium and RNs from the PHTS to the RB due to buoyancy or convective driven mechanisms after blowdown is assumed to be zero for both break sizes.

2.2.5 ASTEC

2.2.5.1 ASTEC Code Description

The ASTEC software, Version 1.3 Rev 2, CPA module was used. ASTEC (Accident Source Term Evaluation Code) has been developed jointly over a number of years by the French group IRSN (L'Institut de Radioprotection et de Sûreté Nucléaire) and its German counterpart, GRS (Gesellschaft für Anlagen und Reaktorsicherheit mbH). The aim of the code is to simulate an entire LWR severe accident sequence from the initiating event through to the RN release out of the containment.

The CPA module used consists of two main sub-modules, THY and AFP, which simulate the thermal-fluid and aerosol behavior in a containment. In ASTEC, the containment is discretized through a "lumped-parameter" approach (i.e. volumes are represented by nodes connected by junctions). This approach allows the simulation of simple or multi-compartment containments with possible leakages to the environment or to normal buildings.

2.2.5.2 Reactor Building Model

Figure 2-1 shows the block flow diagram of the Reactor Building with the compartments to be modeled indicated. Compartment volumes and areas as well as junction input data are specified in Table 2-2 and Table 2-3. The rupture junctions can be seen, for example between the reactor top cavity (RTC) compartment and the IHX compartment. Other junctions are open, atmospheric junctions.

Table 2-1 also specifies areas for leakage paths from the IHX compartment to the remainder of the reactor building (RRB) compartment and IHX compartment to Environment based on a leakage rate of 50%/day at 0.1 bar-d. The leakage areas from the RRB compartment to the environment are also specified based on leakage rates of 100%/d at 0.1 bar-d. Leakage areas have been sized to give these leak rates by rewriting and solving the incompressible steady-state momentum equation for the leakage area using a user specified flow resistance coefficient value of 1.0.

Each compartment shown in Figure 2-1 was assigned to a single zone in ASTEC. No further nodalization of the compartments was performed. In doing this the model assumes a homogeneous state within one zone. This nodalization is sufficient for the short term behavior where the main processes are driven by pressure differences but may prove to be insufficient in modeling medium and long term behavior where slow convective motions, mainly buoyancy and density driven, are dominant. Further nodalization is also motivated by potential inhomogeneities in compartments such as significant temperature gradients within a compartment caused by strong heat transport and very small flow rates, allowing weak processes to have local effects.

All compartments were implemented using the Non-Equilibrium zone option available in ASTEC. In the Non-Equilibrium zone option, the zone is subdivided into two parts: the atmosphere part similar to the equilibrium zone model and a sump part (if existing) specified by the temperature and water mass. Between both parts heat exchange by convection and condensation (or evaporation) correlations is possible. The choice of zone model is not significant due to the gas injection being helium and due to there being no water present at the start of calculation.

2.2.5.3 Input and Output

The thermal-hydraulic input was provided by the Flownex model whilst the dust and fission product input was provided by Excel1. The dust size distribution was based on the AVR size distribution using 12 size classes.

Zones in ASTEC are defined by their floor area, volume, floor height and zone centre height. The initial conditions of the zone such as the initial pressure, temperature and humidity need to be specified. The initial temperature and humidity in the reactor building was specified as 20 deg C and 1.0% respectively. The value of humidity was chosen so as to ensure that pressures in the reactor building zones could be calculated using the value of the density of air. The initial zone pressures have been set according to the formula $P_{atm} - \rho_{air} \cdot g \cdot h\left(\rho_{air} = 1.2kgm^{-3}\right)$ with and $P_{atm} = 101.325kPa$ at ground level and h the height difference from ground level.

Table 2-2: Initial Conditions and Geometry of Reactor Building Compartments

Compartment *	Initial Pressure (Pa)	Floor Elevation (m) (ASTEC)	Centre Elevation (m) (ASTEC)	Floor Area (m^2)	Total Heat Transfer Surface Area (m^2)	Zone Volume (m^3)
RLC	101355	0.1	11.5	82.0	707	736
RTC	101114	23.0	31.5	82.0	577	1184
COP2	101423	2.5	5.9	81.0	418	477
IHX	101251	0.1	20.1	355.0	3801	11306
DVS WEST	101251	0.1	20.1	70.0	2044	2814
FIP	100985	41.1	42.3	425.0	1082	1085
FHL1	100898	44.5	49.6	451.0	1766	4584
SIP	100775	55.6	59.7	451.0	1600	3702
RRB	101230	0.1	21.9	1600.0	10240	59840
ENVIRON1	100726	0.1	63.8	1.0E4	n/a	1.0E6
ENVIRON2	101085	0.1	34	1.0E4	n/a	1.0E6
ENVIRON3	101317	0.1	14.7	1.0E4	n/a	1.0E6

* Compartment nomenclature as per Figure 2-1

Table 2-3: Junction Data

Junction	From *	To *	Type	Area (m^2)	Length (m)	Elevation (m)
1	RTC	IHX	RUPTURE	12.25	2.0	36.15
2a	RLC	IHX	RUPTURE	1.50	2.0	13.75
2b	RLC	IHX	RUPTURE	1.50	2.0	12.03
3	RLC	COP2	ATMOS_JU	20.8	2.0	5.88
4a	COP2	IHX	RUPTURE	4.00	1.0	5.88
4b	COP2	IHX	RUPTURE	4.00	1.0	5.88

Junction	From *	To *	Type	Area (m^2)	Length (m)	Elevation (m)
5a	IHX	DVSW	RUPTURE	24.50	1.0	5.01
6a	DVSW	FIP	ATMOS_JU	35.28	1.0	41.07
7	FIP	FHL1	ATMOS_JU	12.25	1.0	43.47
8	FHL1	SIP	ATMOS_JU	13.89	1.0	54.63
9	SIP	ENVIRON1	RUPTURE	16.00	1.8	63.84
10a	IHX	ENVIRON2	ATMOS_JU	4.771E-4	1.8	34.00
10b	IHX	ENVIRON3	ATMOS_JU	4.771E-4	1.8	14.70
11a	IHX	RRB	ATMOS_JU	4.771E-4	1.8	34.00
11b	IHX	RRB	ATMOS_JU	4.771E-4	1.8	14.70
12a	RRB	ENVIRON2	ATMOS_JU	3.675E-3	1.8	34.00
12b	RRB	ENVIRON3	ATMOS_JU	3.675E-3	1.8	14.70

* Compartment nomenclature as per Figure 2-1

Leakages to the environment are modeled from the IHX and RRB compartments. Three Environment compartments have been defined to separately account for releases through the stack, releases through leakages in the upper portion of the IHX at 20.0m and releases through leakages in the lower portion of the IHX at 0.7m.

The material properties for concrete walls (heat capacity, heat conductivity, emissivity and density) were specified according to the normal concrete material specification used in the PBMR design.

Fission products were defined as either being attached to dust or not attached to dust, i.e. being transported with the gas. The mass injection rate as a function of time was used for the fission product injection. For the case of modeling fission products as aerosols a new aerosol, with diameter 1E-07 m, was defined and the mass flow rate as a function of time for this aerosol was equal to the sum of the mass flow rates for all the fission products.

2.2.5.4 Assumptions

The flowing assumptions were made in the model

- Junctions 6a and 6b were combined into one junction with the combined cross-section area due to an artificial convection loop appearing.
- Radioactive decay not modeled.
- A friction coefficient of 1.0 is used in the code.
- No fission product chemistry modeled at this stage.
- Assumption of instantaneous mixing in Lumped-Parameter codes and a homogeneous state in a compartment.

2.2.5.5 Limits of Applicability

The model has the following limits of applicability
- The gases in the CPA module are treated as real gases with a set of correlations for their properties valid up to temperatures of 3000°C.
- Codes like ASTEC are based on the lumped parameter modeling concept which may have limitations in representing certain complex spatial interactions.

2.2.6 EXCEL2

The offsite Total Effective Dose Equivalent (TEDE) and thyroid Committed Effective Dose Equivalent (CEDE) to the public at the 400m exclusion area boundary (EAB) are calculated in a Microsoft Excel spreadsheet, referred to as EXCEL2. The TEDE calculation is based on the definition of TEDE in the NRC Regulatory Guide 1.183 (2000). TEDE is defined as the sum of the CEDE from inhalation and the effective dose equivalent (EDE) from external air submersion. The thyroid CEDE is the CEDE to the thyroid organ due to inhalation.

Radionuclide releases from the RB to the environment during the DLOFC transients are input to EXCEL2 and are provided from the ASTEC calculations for seven RNs: Ag-110m, Ag-111, Cs-137, I-131, I-133, Sr-90 and Te-132. These seven RNs are considered the dominant contributors to the offsite TEDE and thyroid CEDE based on insights from previous HTGR studies. EXCEL2 explicitly calculates the doses based on the seven RNs and then estimates the TEDE and thyroid CEDE if all other RNs in addition to the seven were included. Based on the GT MHR Preliminary Safety Assessment Report [5], Table 4.4.3-3, the seven RNs are assumed to account for 80% of the TEDE and 90% of the thyroid CEDE.

The assumptions to calculate the offsite doses are selected to meet the objective of a realistic assessment for a generic site to provide input to the next phase of the NGNP design. This is not to be confused with a conservative evaluation for licensing purposes which can not be supported at this early stage of design. Uncertainties associated with some of these assumptions are assessed in Section 3 as part of the barrier retention allocation study. The EXCEL2 model is based on the following considerations:
- Dose calculation methodology is based on NRC Regulatory Guide 1.183 and methods used in previous HTGR safety evaluations such as those for the MHTGR.
- The cumulative dose is calculated for a 300hr (12.5 days) exposure time for an adult at the offsite boundary, after which relocation is assumed. The breathing rates and weather dispersion factors are constant for this period.
- Dose conversion factors are taken from Federal Guidance Report 13 CD (2002). All of the dose conversion factors are for an adult.
- The daily average breathing rate of 2.32E-4 m^3/s is based on NRC Regulatory Guide 1.4.
- The weather conditions in NRC Regulatory Guide 1.3 for the 1-4 day period are selected as generic weather conditions that yield conservative, 95th percentile weather X/Q values.

  - The generic weather conditions for best estimate calculations are assumed to be such that the best estimate X/Q values are 10% of the conservative values.[1]
  - This approach is consistent with MHTGR PSID [6] and PRA methods and Section 7.1 of NRC Regulatory Guide 4.2.
  - The ground release weather X/Q is 2.60E-5s/ m^3.
  - The stack release weather X/Q is 1.90E-6s/ m^3 for an assumed 50m stack.
- No radioactive decay or deposition of the plume is assumed in transit from the RB to the dose receptor.

Offsite doses for the DLOFC events are compared to the Top Level Regulatory Criteria of the Nuclear Regulatory Commission (NRC) and the Environmental Protection Agency (EPA) for assessing and regulating nuclear power plants in the US. These requirements are shown in Table 2.2 and are the same as used in the 2008 RB Study [1].

Table 2-4 Radiological Dose Limits and Bases

Regulation	Application	Offsite Dose Limits
NRC 10CFR50.34 and NRC 10CFR50.67	Offsite dose limits during design basis events (DBEs)	TEDE < 25rem/event
EPA Manual of Protective Action Guides and Protective Actions for Nuclear Incidents (1992)	Offsite dose limits during DBEs and beyond design basis events (BDBEs) at which sheltering is considered	TEDE < 1rem/event Thyroid CEDE < 5rem/event

2.3 THERMOFLUID BEHAVIOR DURING DEPRESSURIZATION

2.3.1 Impact of Break Size on Depressurization Time

The NGNP NHSS Flownex Model as described in Section 1.1, with a few modifications for the pipe break analyses purpose, was used to obtain the depressurization time and shear force ratio results for the whole range of identified break sizes.

[1] We use the generic site and best estimate for design and will continue to do so throughout the design process, however for licensing when we have a site and the necessary site specific weather data, we will update these generic conditions with site specific weather conditions and the associated or necessary conservatisms.

To determine the depressurization time of the NHSS through the various defined pipe break sizes, the NGNP NHSS Flownex Model was coupled via a pipe break element directly to the environment at normal atmospheric conditions (i.e. assuming a pressure of 100kPa and a temperature of 25°C). The PRS model (Section 2.2.1.1) was excluded for this exercise, because the flow through the "break" is for more than 95% of the time choked (i.e. having a Mach Number of 1) in which case the downstream pressure has virtually no effect on the flow. In the case with the RB model attached, the gas pressure in the break compartment reaches a maximum in the order of 105 to 110kPa early in the transient, versus approximately 9000kPa inside the NHSS HPB. By the time the flow through the break reaches the un-choked condition (which is at a HPB pressure lower than ~300kPa), the gas pressure in the break compartment has equalized to atmospheric pressure. The depressurization time was determined from the break gas pressure data as the first time step data point in the series of decreasing pressure values where the pressure reaches a pressure difference (dP) lower than 0.05kPa. Since atmospheric conditions are defined as 100kPa and 25°C, this relates to the time step when the pressure upstream of the break first reaches 100.05kPa. All Flownex transients for the various break sizes were run for a time duration up to the point where the break pressure is equal to (or just less than) the atmospheric pressure (< 100kPa).

The depressurization (blowdown) time results for the selected pipe break sizes is given in Table 2-5 and can be presented as a quadratic decay curve of blowdown time versus break size (see Figure 2-8 for the break sizes from 3 mm to 30 mm. The larger sizes are not included for visual reasons). The trendline fitted to the data according to $t = m/D^2 + t_0$, where t is the blowdown time (s), D the break diameter (m) (i.e. break size), and m and t_0 are the gradient and intercept of fitted trendline respectively, is $t = 5.12e6/D^2 + 4430$.

Table 2-5 Summary of Depressurisation (Blowdown) Times for the different Break Sizes of the core inlet pipe from the NHSS PHTS

	Break Size (mm)	Max mass flow during break (kg/s)	Blowdown time (s)	Blowdown time (hrs)
Small Breaks	3	0.043	568020	158
	4	0.077	328620	91
	5	0.119	213420	59
	6	0.171	147420	41
	10	0.472	52860	15
	30	4.24	6373	1.8
Large Breaks	100	47.1	674	0.187
	230	247	121	33.6E-3
	1000	4354	12.3	33.3E-4

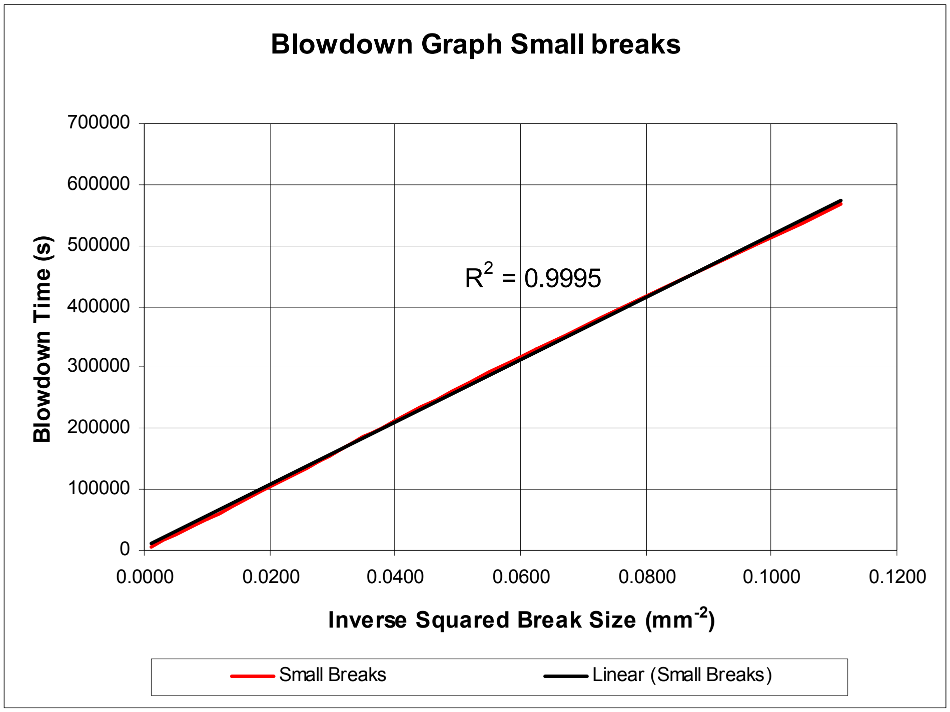

Figure 2-8 Graph of Blowdown Times for small breaks (3 mm to 30 mm EBS)

It was observed that small changes in NHSS He inventory and operation have a large influence on blowdown times. The blow down times indicated may therefore change substantially with changes in the NHSS design. This in turn will lead to changes in the size of the limiting case small break.

2.3.2 Impact of Break Size on Shear Force Ratios

The same transient runs that are used for the determination of blowdown times were also used to extract the required gas pressures, temperatures and velocities from various locations in the NHSS for each break size. The shear force ratio (SFR) is then calculated from

$$SFR = \left(\frac{P_B}{P_N}\right)^{0.75} * \left(\frac{V_B}{V_N}\right)^{1.75} * \left(\frac{T_N}{T_B}\right)^{0.58} \quad (1)$$

where

P is the static pressure	[kPa],
V is the velocity	[m/s],
T is the static temperature	[K].

The subscript “B” signifies blowdown conditions (i.e. after a break occurred) and the subscript “N” signifies normal operation conditions (i.e. during steady state). The break is simulated to occur at time t = 1s, in which case the recorded values for the time between 0s and 1s represents the steady state in the transient results. The shear force ratios are calculated for a few selected locations around the PHTS, namely the Reactor Inlet, Reactor Outlet, Reactor Lower Volume, the CCS Inlet Connection, the IHX Inlet and the Circulator Outlet.

A summary of the shear force ratios for the defined locations is given in Table 2-6. The shear ratios are less than one for all the smaller breaks and close to one for the 100 mm EBS. Only above 100mm EBS are shear force ratios greater than 1 observed. This indicates that liftoff during the two cases analyzed in the calculation chain can be considered minor. Shear forces increase significantly near the break (i.e. at the Reactor Inlet) for the 230 mm and 1000 mm EBS, as expected.

Table 2-6 Summary of Shear Ratios for a core inlet pipe break of various sizes

	Break Size (mm, EBS)								
Location	**3 mm**	**4 mm**	**5 mm**	**6 mm**	**10 mm**	**30 mm**	**100 mm**	**230 mm**	**1000 mm**
Reactor Inlet	0.0306	0.0306	0.0307	0.0308	0.0314	0.0390	0.8269	2.3467	127.45
Reactor Outlet	0.0195	0.0194	0.0195	0.0194	0.0194	0.0188	0.9879	1.0002	1.5147
Reactor Lower Volume	0.0685	0.0685	0.0687	0.0688	0.0695	0.0787	0.9953	2.4003	84.30
CCS Inlet Connection	0.0195	0.0194	0.0195	0.0194	0.0194	0.0188	0.9537	1.0003	1.8534
IHX Inlet	0.0083	0.0083	0.0083	0.0083	0.0083	0.0080	0.2333	0.9999	1.0000
Circulator Outlet	0.0062	0.0062	0.0062	0.0062	0.0062	0.0063	0.0251	1.0000	1.1203

2.3.3 Air Ingress to Reactor Building and PHTS Circuit

To obtain air ingress results for the 100mm EBS HPB break, the NHSS Flownex model was coupled to the NGNP PRS Flownex model. In the calculations the RB remains open to atmosphere all the time. No closing of dampers is modeled. Note that this analysis was not performed for the 4mm break, as the long blowdown timer results in an expected lower air ingress value.

Air ingress into the PHTS of the NHSS following a pipe break is dependant on the amount of air in the break compartment as well as the rate of cooling that occurs from the NHSS pipes. The calculation records the relevant data for a 300 hr period. The pipe break element is coupled to the RB compartment in which the break occurs, while all the heat transfer elements from the pipes around the PHTS and SHTS are connected to the compartments in the RB model in which the NHSS resides.

A 100 mm EBS of the Core Inlet Pipe (CIP) was simulated to occur in the Reactor Top Cavity (RTC) compartment. The helium filled the RTC very quickly, indicated by the helium mass fraction that rose to 1 (see Figure 2-9). The helium fraction started decreasing in the RTC after about 700s, which is the time that blowdown from the break ceased. It decreased to approximately 0.94 after an hour and reached 0.90 at the end of the transient (i.e. after 300 h, not shown on the graph). This implies air content in the break compartment between 6% and 10% during the air ingress period. The helium content in the Filter Inlet Plenum (FIP) increased to 0.44. It follows a similar pattern with a faster decrease down to 0.35 after an hour, as it is situated closer to the RB outlet point.

The results of the air mass fraction response, as recorded at various locations in the reactor and PHTS following a 100mm EBS of the CIP, are shown in Figure 2-10. Apart from small deviations at the reactor outlet and CCS inlet connection points, all the mass fractions inside the reactor (i.e. the reactor inlet, reactor lower volume, void above core and the location below the outlet slots) show a very similar slow increase (graphs on top of each other). An air mass fraction of 0.022 (less than 2.2% air) is reached after 300 hrs, indicating virtually zero air ingress back into the reactor. This result is due to the fact that by the time flow back into the PHTS is established; the RTC compartment contains almost only helium (Figure 2-9). No air is available to be drawn back into the system.

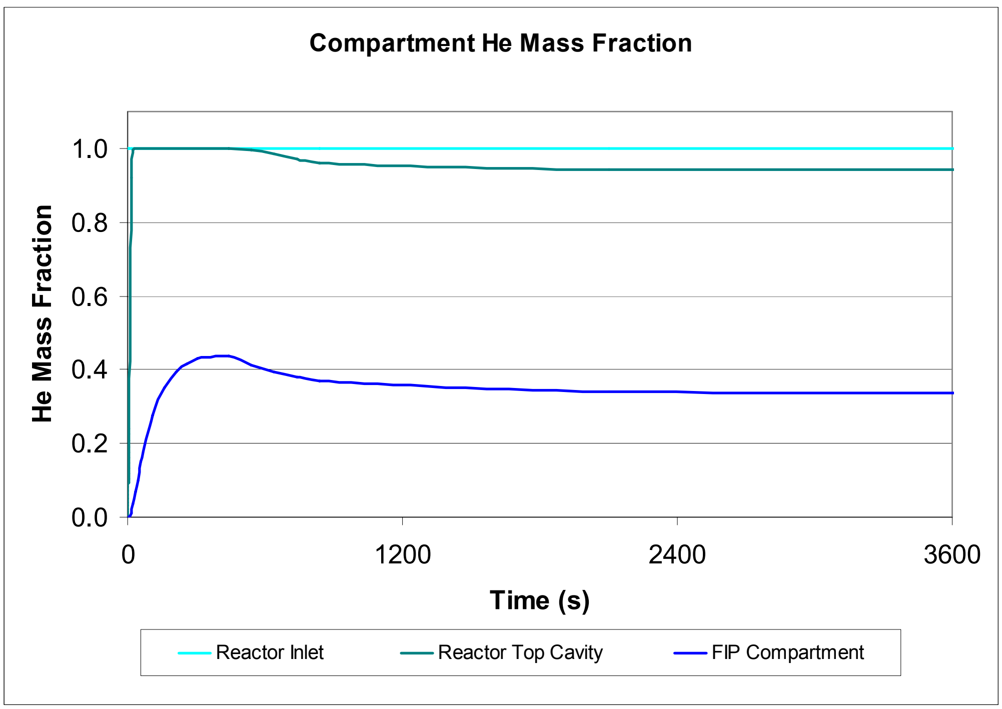

Figure 2-9 Helium mass fraction response in the RTC and FIP compartments of the RB, after a 100 mm EBS of the CIP occurred in the RTC

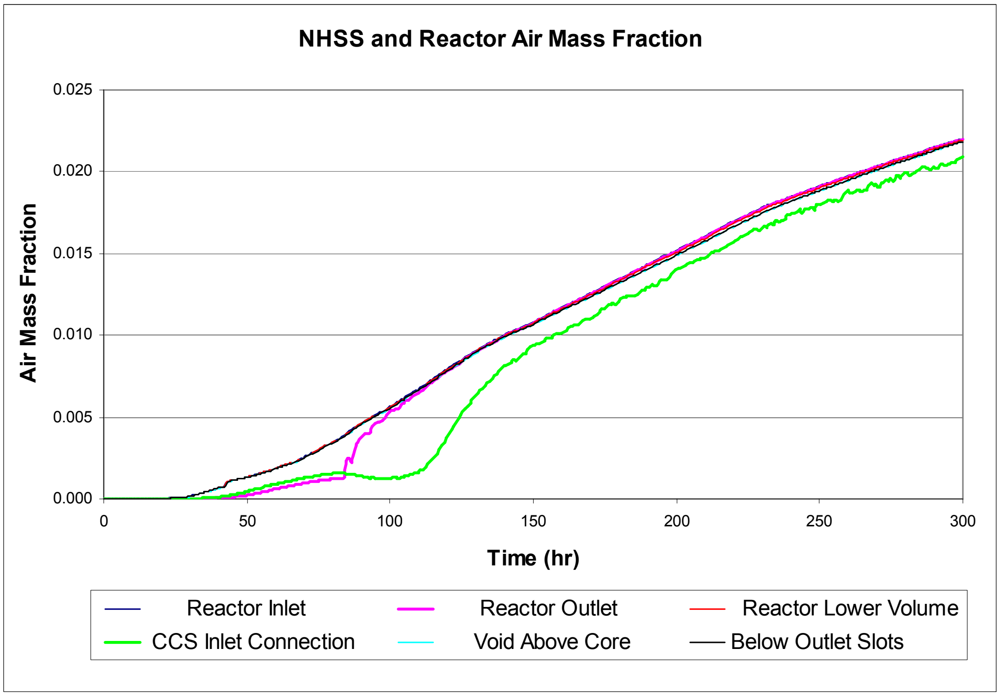

Figure 2-10 Air mass fraction response at various PHTS and reactor locations, after a 100 mm EBS of the CIP occurred in the RTC

The unexpected low air ingress rate observed is mainly due to the small volume of the RTC compartment. The helium released from the PHTS can fill the volume completely. As a sensitivity study a 100 mm EBS of the Core Inlet Pipe (CIP) was also simulated to occur in the Intermediate Heat Exchanger (IHX) compartment. The volume of the IHX cavity is 11306 m^3 as opposed to the volume of the RTC of 1184 m^3, thus one expects a larger fraction of air to be present and available for air ingress after blowdown.

The helium mass fractions in the new break compartment (IHX) and FIP are compared against the original break simulation in the RTC in Figure 2-11. The maximum helium content in the IHX compartment is only 0.61, meaning there is ~39% air available after blowdown to be drawn back into the PHTS. At the end of the transient the helium mass fraction in the IHX compartment decreased to 0.57.

A similar pattern as previously is also observed in the FIP compartment, situated some distance further in the RB. The maximum helium mass fraction of 0.47 is somewhat higher than previously, reaching a value of 0.35 after 300 hrs.

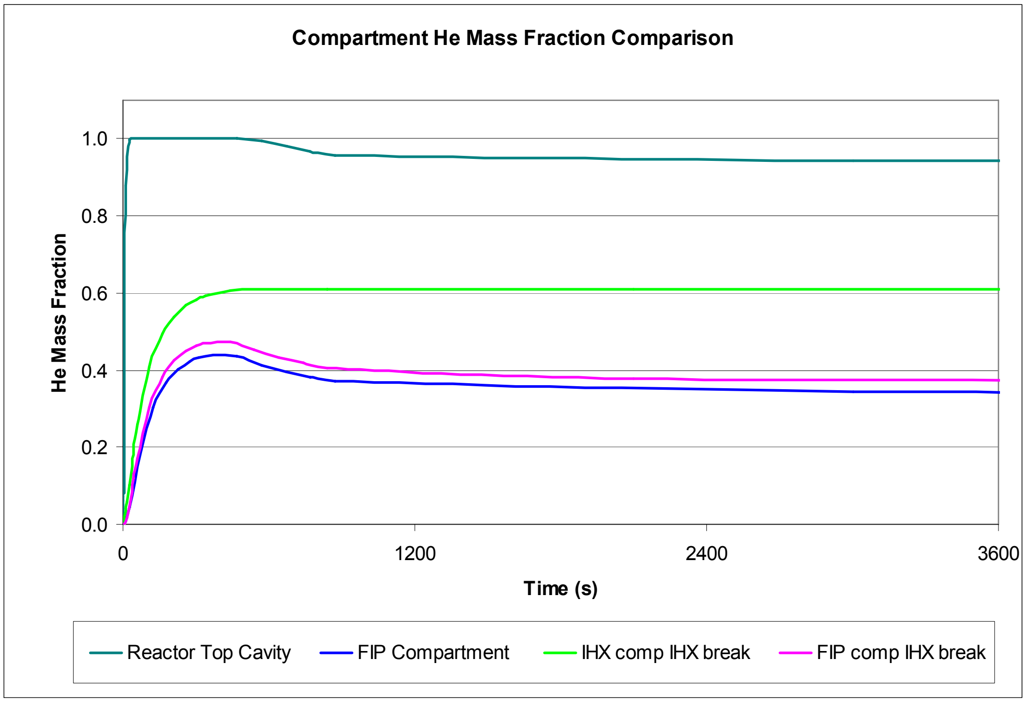

Figure 2-11 Helium mass fraction response in the IHX and FIP compartments of the RB, after a 100 mm EBS of the CIP occurred in the IHX

In Figure 2-12 the air ingress results for the break that occurs in the IHX compartment are compared against the results obtained for the same break that occurred in the RTC compartment of the RB. As expected, a much higher air ingress rate is observed, reaching an air mass fraction of 0.17.

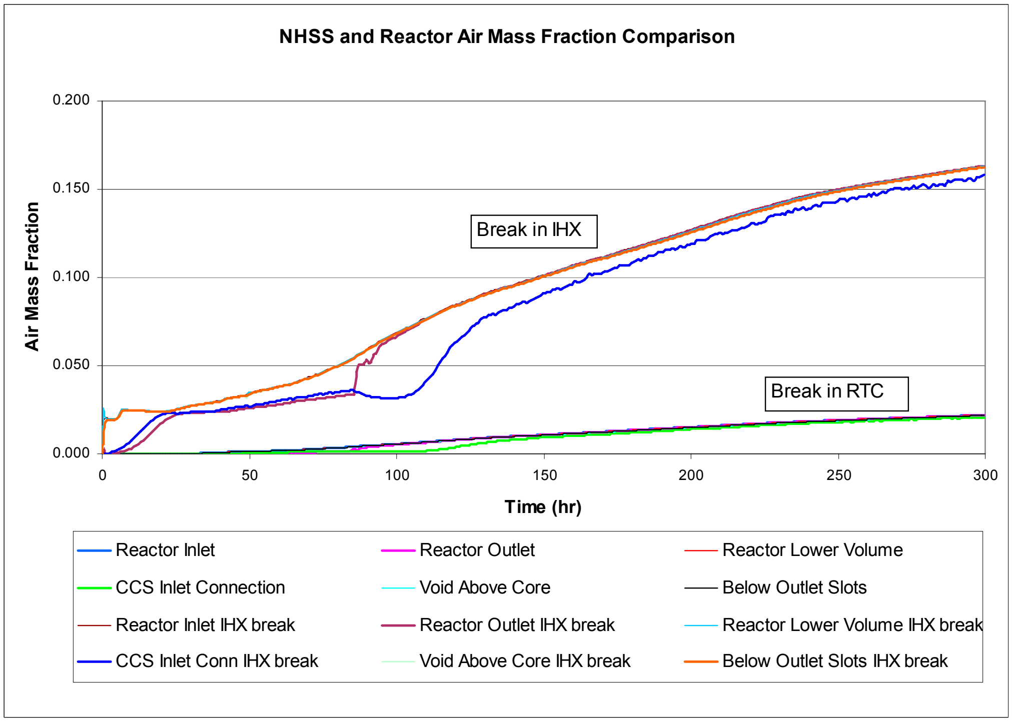

Figure 2-12 Comparison of air mass fraction at various PHTS and reactor locations, after a 100 mm EBS of the CIP occurred in the RTC or in the IHX compartments

For the air ingress calculations, especially after the blow down phase, the mass flows observed were very low. These low mass flows lead to instabilities in the Flownex solution method, especially when lower than the convergence criteria. In order to smooth out the numerical instability observed, a 2nd order polynomial fit was applied to the post-blowdown data and used as input for the Excel1 and TINTE models.

2.3.4 Impact of Break Size on Core Thermal Response

2.3.4.1 DLOFC Transient Assumptions

All the DLOFC transients were started from the same steady state condition, i.e. 500MW power, 280 °C inlet gas temperature, 750 °C outlet gas temperature, inlet pressure 90 bar, and inlet mass flow rate 204.5 kg/s. The following assumptions were made for all cases regarding the transient modeling of Systems, Structures and Components (SSCs):

- A full reactor SCRAM is initiated at t = 300 s, over a period of 16 seconds.
- The RCCS water temperature (which acts as a radial temperature boundary condition in the TINTE model) was ramped from 25 °C to 135 °C at t = 1 s, over a period of 14 hours.

- The inventory pressure blow down period was modeled according to FLOWNEX input data. A typical fit of approximately 15-20 points was used to model the decrease in gas pressure down to 100kPa over the specified durations. The depressurization times are shown in Table 2-7. The differences between the TINTE and FLOWNEX blow down times are small, and on the conservative side for TINTE, since a faster blow down transition would lead to higher fuel temperatures. (If the detailed input data is compared, a second slight mismatch will be found between the FLOWNEX recommended blow down period, and the TINTE implemented periods. This is due to different atmospheric equalization criteria used: FLOWNEX tracked the time when the pressure differential across the break reached 0.05 kPa, while TINTE utilized 1.0045 bar, since its inputs format requires the bar pressure unit and two decimal digits accuracy).
- After the equalization pressure of 100kPa was reached, all gas-related calculations were terminated in TINTE, i.e. the transient then becomes a pure conduction and radiation driven problem.
- The FLOWNEX data exhibited complex positive (incoming) and negative (outgoing) flows at the reactor inlet and break location. Since the magnitude of these flows very quickly becomes very small, it was decided to model the decrease in the TINTE inlet mass flow rate as an exponential drop from 204.5kg/s to 0.0kg/s over the first 60 seconds of each break. The forced mass flow rates then remained at 0.0kg/s for the duration of the pressure drop period. This is a conservative assumption, since this fast decrease in the forced gas flow would lead to higher fuel temperatures (as opposed to modeling the forced flow decrease over 1 hour, for example). Note that TINTE still continues to calculate different rates of natural convection in the core during this period, depending on the gas inventory and the fuel temperatures during the blowdown phase.
- The FLOWNEX variations in the reactor inlet gas temperature were not modeled in TINTE, since the inlet gas mass flow rate falls to 0.0kg/s within the first 60 seconds of each case. This is a conservative assumption, since the fixed inlet gas temperature of 280°C would lead to higher fuel temperatures.

Table 2-7: Event depressurisation times

Break size (mm)	TINTE blow down time (s)	FLOWNEX blow down time (s)
3	561420	568020
4	325920	328620
5	208920	213420
10	51660	52860
100	523	689

2.3.4.2 Fuel Temperature Results: 3 mm - 100 mm Breaks

The maximum and core average fuel temperature behavior of the 4 small breaks (3-10 mm) and the 100 mm medium break are shown in Figure 2-13 and Figure 2-14, respectively. These two parameters are defined as follows:

- **Maximum fuel temperature (MFT)**: The current TINTE model calculates the fuel sphere surface and centre temperatures for 260 spatial positions in the core (10 radial and 26 axial coarse meshes). These two fields are calculated for 6 "types" of fuel (also called "batches"), which consists of the 6 fuel passes through the core. Pass 1 represents the fresh fuel, and pass 6 the most-burnt fuel before final discharge. Of these 6 fuel batches, the fresh fuel usually produces the highest fuel centre temperatures. The "maximum fuel temperature" parameter is then defined as the spatial maximum of the highest fuel centre temperature.

  Note that since the relationship between heat transfer mechanisms in the core (convection, conduction and radiation) varies significantly with time for a typical slow DLOFC event, this spatial maximum temperature changes location in the core. The lines in the plots below therefore do *not* represent the same spatial location in the core over time, nor is it possible to *directly* compare the maximum fuel temperatures (on the plots) between the various cases, since the maxima might not necessary occur at the same location for all cases.

- **Core average fuel temperature**: The volume-weighed average temperature of all the fuel in the core region. Note that his average is calculated over the fuel region in the spheres only (i.e. it is not the total sphere volume average), and it is averaged over all the fuel batch temperatures.

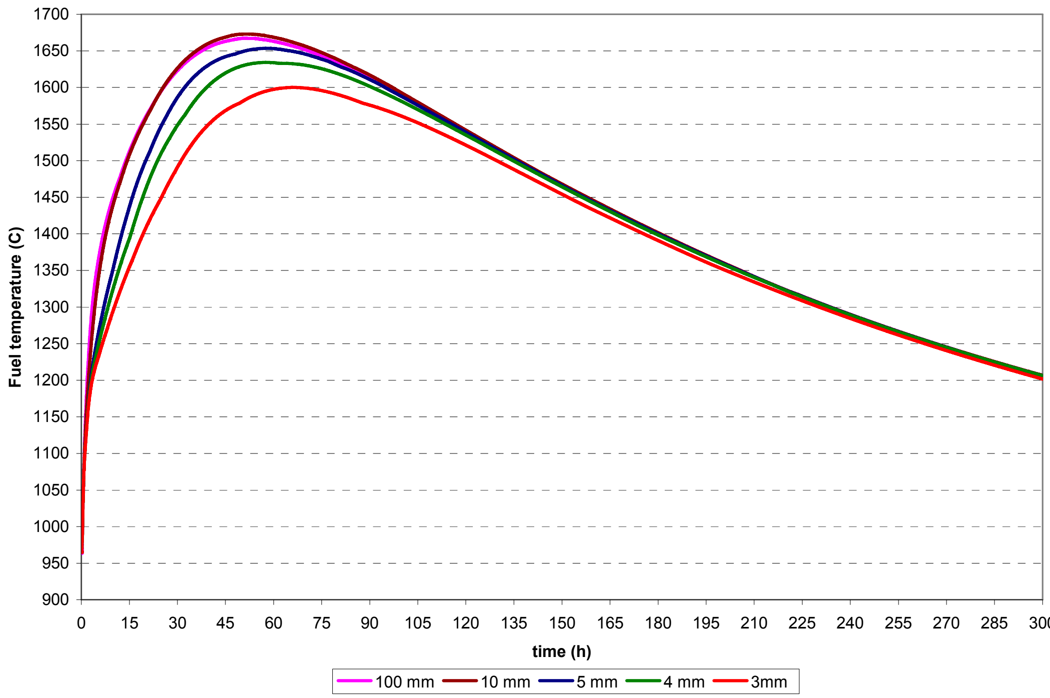

Figure 2-13: Maximum fuel temperatures for 100 mm, 10 mm, 5 mm, 4 mm and 3 mm breaks.

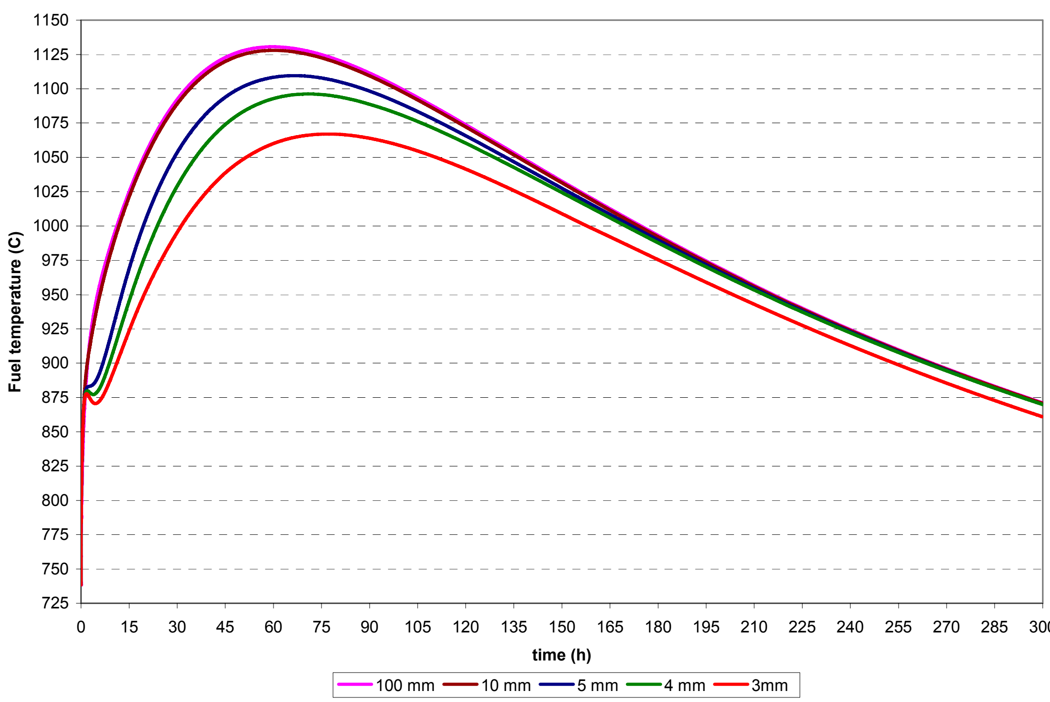

Figure 2-14: Core average fuel temperatures for 100 mm, 10 mm, 5 mm, 4 mm and 3 mm breaks.

The highest/peak values of the data in Figures 1 and 2 are indicated in Table 2-8.

Table 2-8: Peak maximum and core average fuel temperatures (°C) for 3-100 mm breaks

Case	Peak maximum fuel temperature (°C) and time of peak (h)	Peak core average fuel temperature (°C) and time of peak (h)
3 mm break	1600 @ 67 h	1067 @ 78 h
4 mm break	1634 @ 59 h	1096 @ 72 h
5 mm break	1653 @ 59 h	1110 @ 68 h
10 mm break	1673 @ 53 h	1128 @ 61 h
100 mm break	1668 @ 53 h	1131 @ 61 h

The following observations can made from the data presented above:

- The peak values occur sooner for the larger break cases, and appear delayed for the smaller breaks, i.e. the initial gradient of the rise in MFT is steeper for large breaks than smaller breaks. This is due to the increased heat transfer at higher gas inventories to the ex-core structures (mainly to the top and side reflectors).
- The core average fuel temperature peak significantly later than the peak MFT time point, implying that *on average* the core is still getting hotter after the *localized* maxima have been reached. The spatial map in Figure 2-15 show just how small and localized these high temperature volumes are (refer to the small fuel volume in the interval >1600°C, which dominates the fission product release from the fuel).
- The results in Table 2-8 show an unexpected variation in the peak MFT. Generally speaking, higher gas inventories during a slow DLOFC should lead to lower maximum fuel temperatures, since the added convective heat transfer in the core distribute the localized heat more effectively to the cooler areas of the core. This general trend can be seen from the 3, 4 and 5 mm cases, where the 3 mm cases exhibited the lowest peak MFT. However, this is not observed for the 100 mm case, which should have lead to the highest peak MFT. In stead, the 100 mm break case is ~5°C cooler than the 10mm case at their respective peak value time points. Figure 2-16 show however that the 100mm case is hotter than the 10mm case for the first 24 hours. It is also important to note that the core average temperature *does* follow the expected trend, i.e. with the 3mm case being the coldest and the 100mm case the hottest. Also, the 5°C difference between the 10mm and 100mm cases can be seen as insignificant on a base temperature of 1670°C.

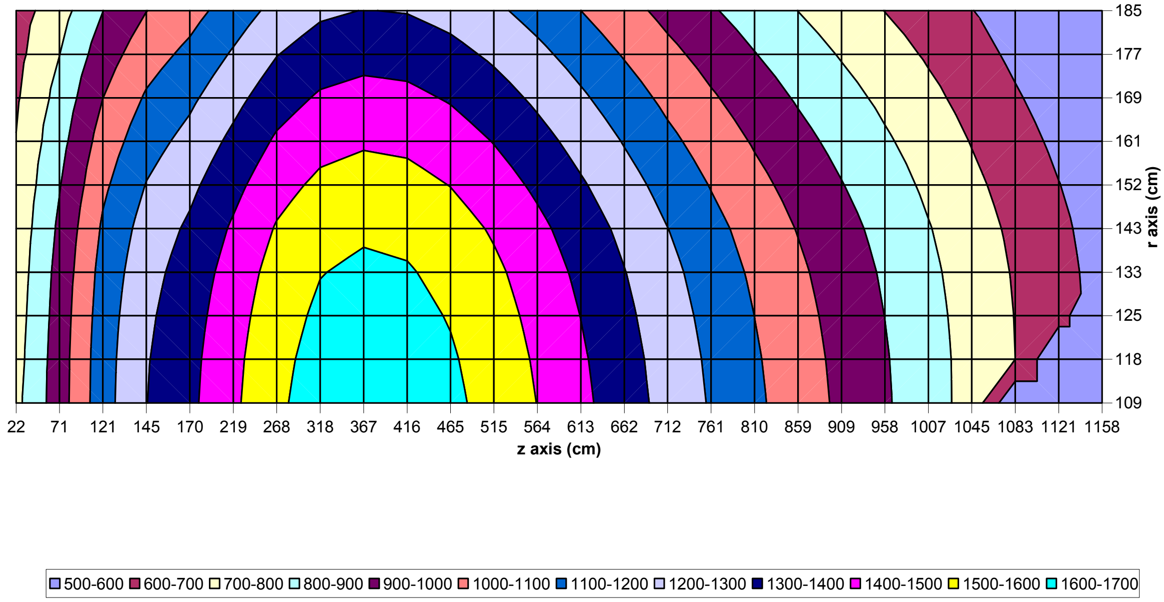

Figure 2-15: Spatial distribution of maximum fuel temperatures for 100 mm break at t = 53 h.

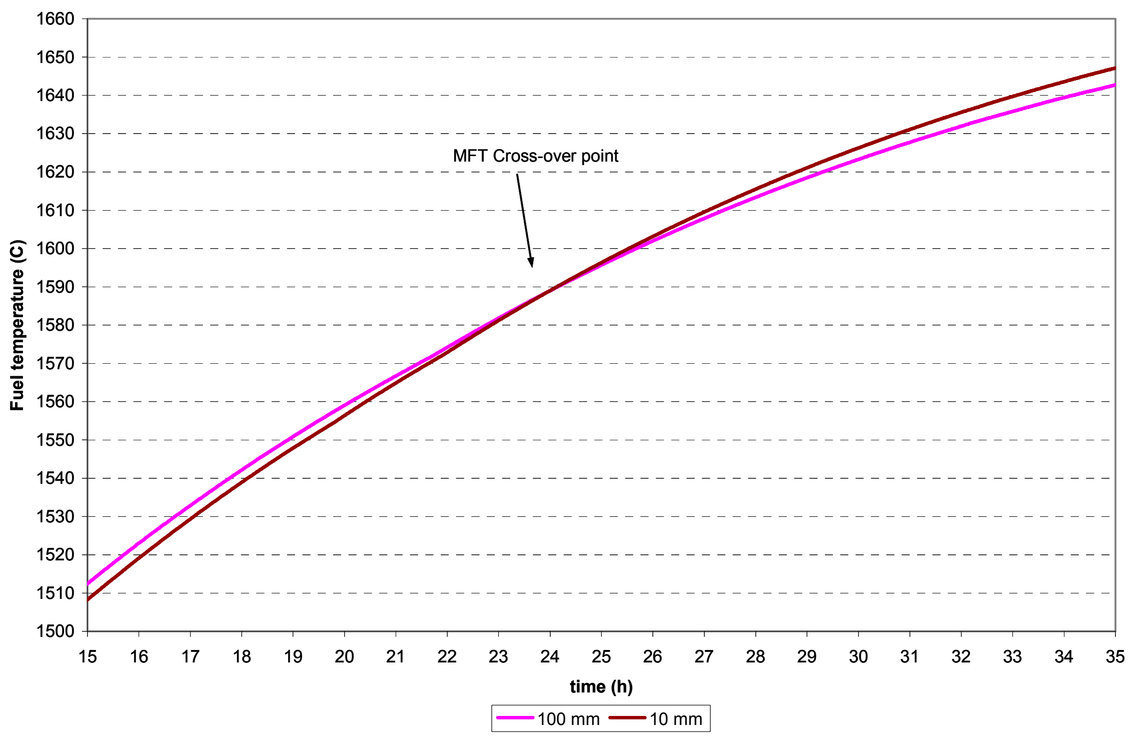

Figure 2-16: Maximum fuel temperatures for 100 mm and 10 mm breaks: 15-35 h.

Figure 2-17 to Figure 2-20 show the behavior of the MFT during 4 different stages of the transients: during the first hour, up to 15 h, between 40-80 h when the peak values are reached, and in the final stage between 280 and 300 h. Figure 2-17 and Figure 2-18 clearly show the cooling effect of the larger gas inventories during the earlier stages of the breaks: at t = 10 h, the MFT varies 154 °C between the 100 mm (1453 °C) and 3 mm (1299 °C) cases. The two larger breaks (10 and 100 mm) also lead to very similar MFT behavior in this period, while the three smaller breaks are more evenly grouped together.

The spread between the 5 cases has decreased to less than 100°C by the time the peak MFT values are reached (Figure 2-19), but at the end of the simulated 300 h period only the 3 mm case is noticeably cooler (~6°C) than the other 4 cases (Figure 2-20). The natural convection-driven differences that exist between these cases are therefore dominant for the first 100-120 hours of the transients – after this period all 5 cases continue as basic decay heat removal events, which are determined by the heat removal capacity of the RCCS system.

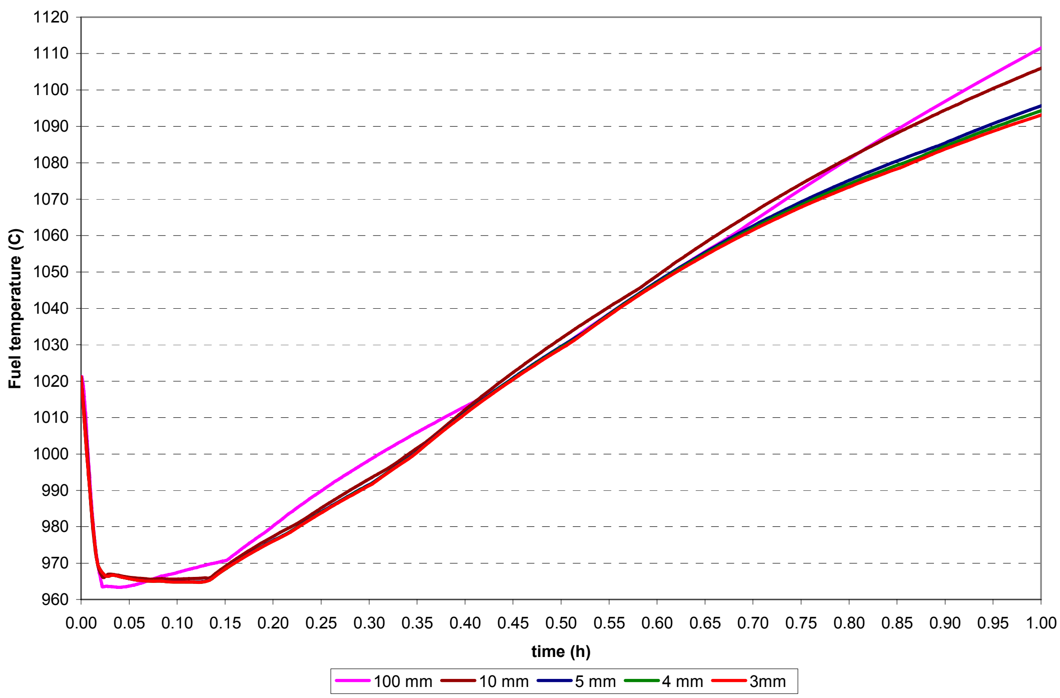

Figure 2-17: Maximum fuel temperatures for 100 mm, 10 mm, 5 mm, 4 mm and 3 mm breaks: 0-3600 s.

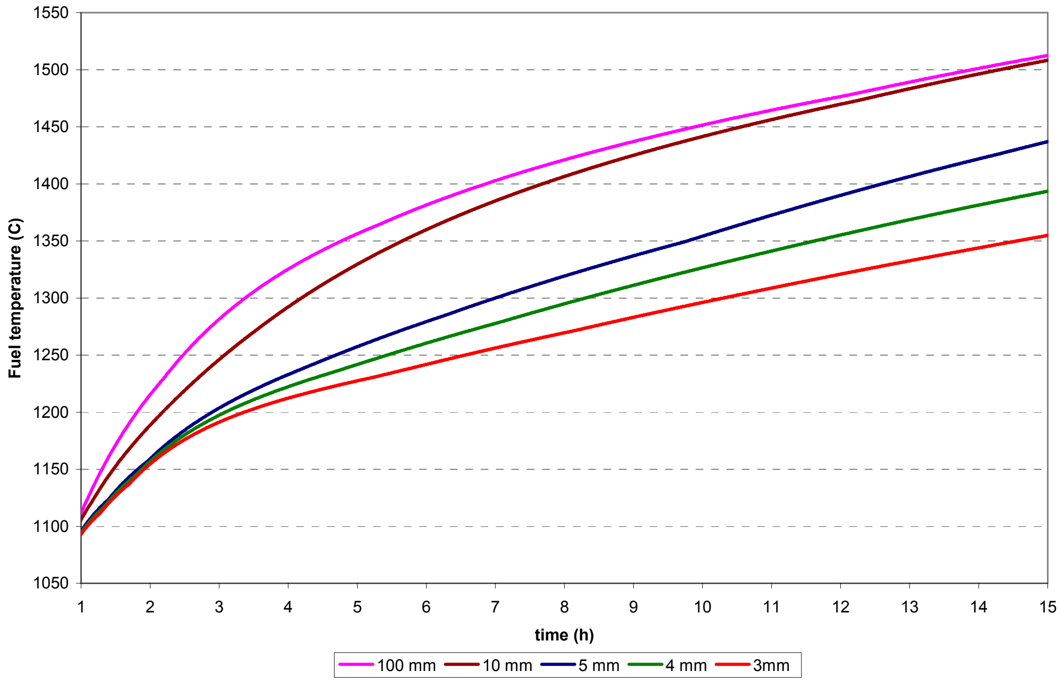

Figure 2-18: Maximum fuel temperatures for 100 mm, 10 mm, 5 mm, 4 mm and 3 mm breaks: 1-15 h.

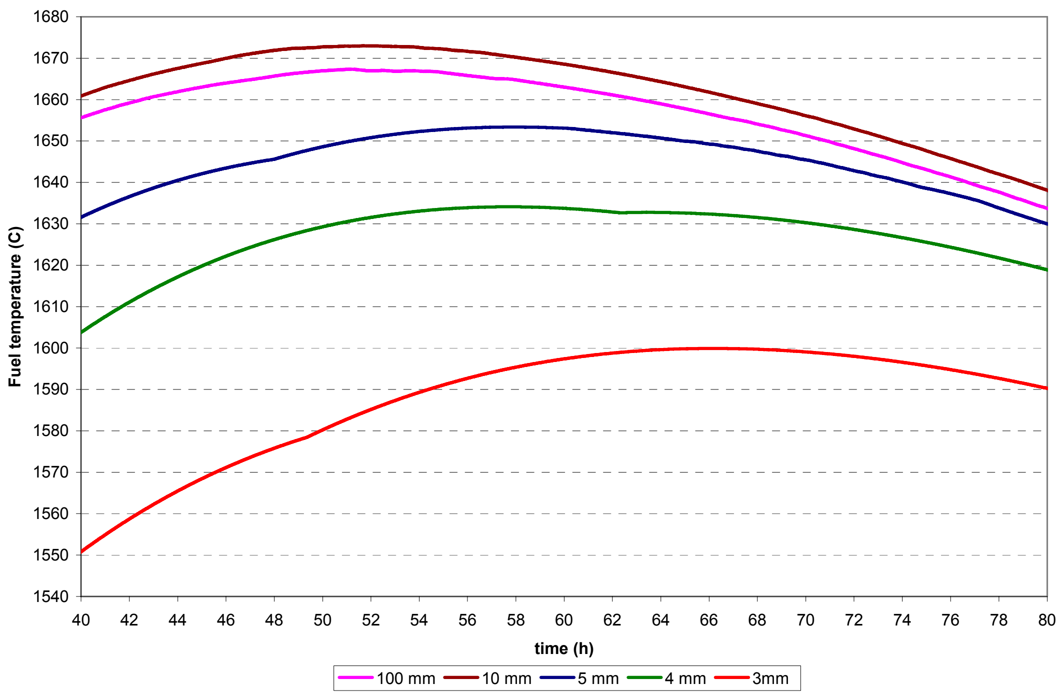

Figure 2-19: Maximum fuel temperatures for 100 mm, 10 mm, 5 mm, 4 mm and 3 mm breaks: 40-80 h.

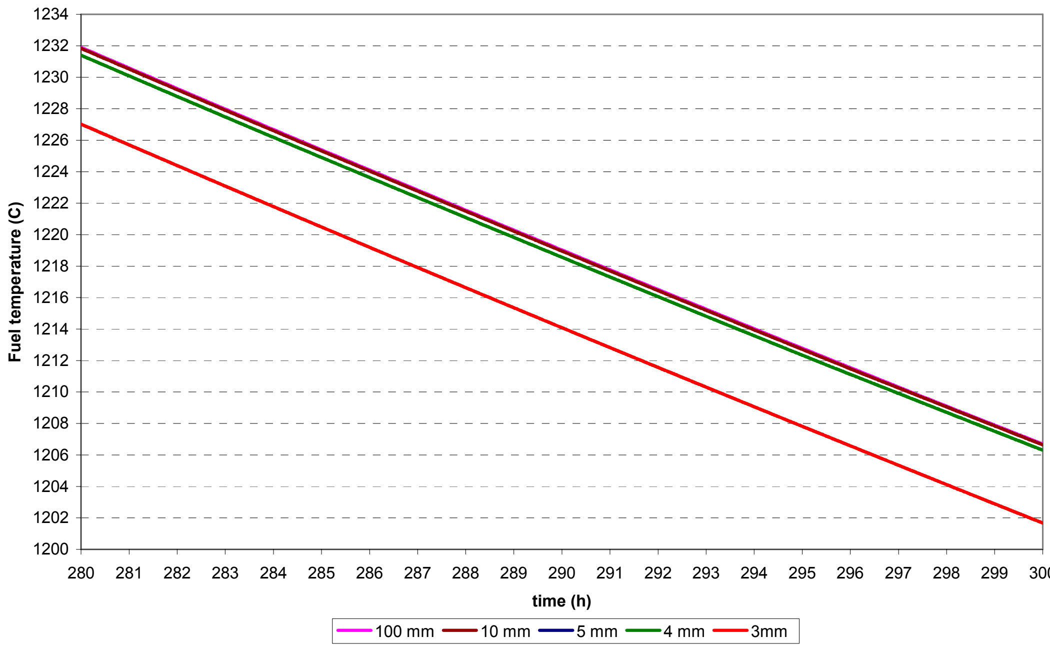

Figure 2-20: Maximum fuel temperatures for 100mm, 10mm, 5mm, 4mm and 3mm breaks: 280h-300h

2.3.4.3 Fuel Temperature Volume Histogram Data

In addition to tracking the behavior of the core maximum and average fuel temperature with time for the 5 small and medium breaks, the maximum fuel temperature volume histogram data can also be analyzed as an additional source of information on spatial heat movement in the core. Figure 2-21 and Figure 2-22 show the % of fuel (as a function of the total core volume) in 100 °C MFT intervals between 1200 °C and 1700 °C, for the first 120 hours of the 100 mm and 3 mm breaks.

Small volumes of fuel (less than 6% of the total core volume) experience MFTs above 1600 °C between 25 h-90 h (Figure 2-21). In contrast to this behavior, the MFT for the 3 mm case never reaches 1600 °C (Figure 2-22), and the exposure period of the fuel between 1500-1600 °C is also less (~90 h) when compared with the 100 mm exposure period for this interval (~ 110 h). Based on this information alone the conclusion can be made that the delayed source term of the 3mm case will be significantly less than the 100 mm case, if the time-at-temperature criterion is used for the migration of FP out of the fuel spheres.

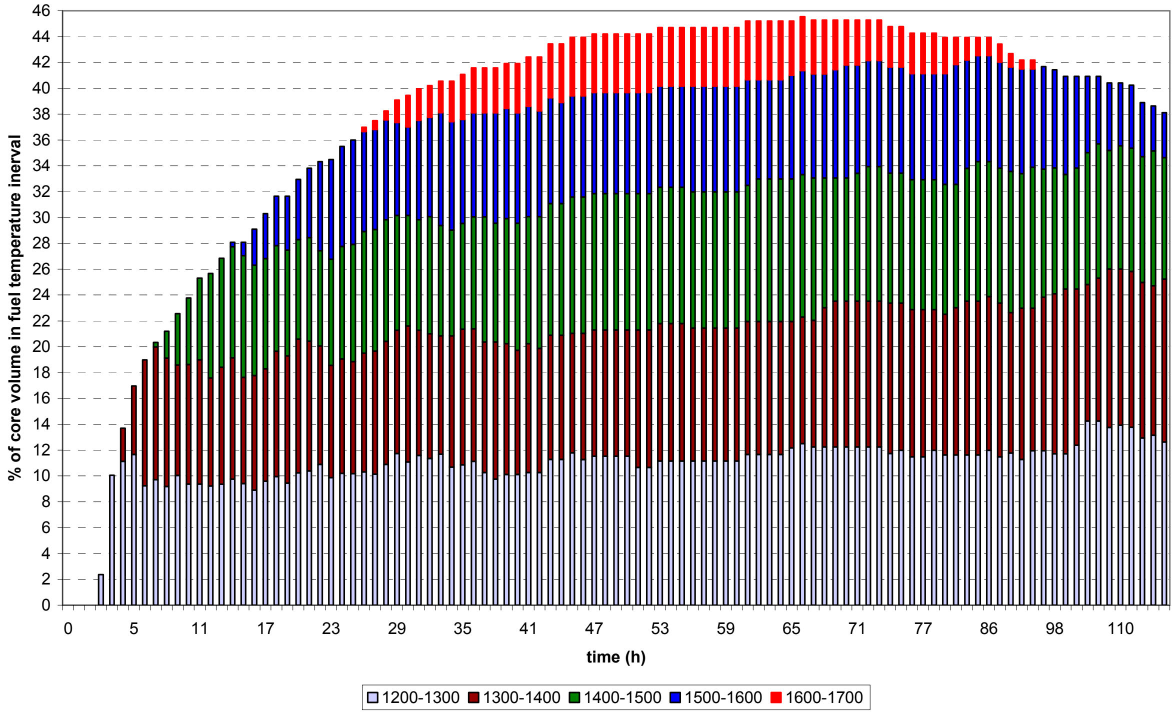

Figure 2-21: Maximum fuel temperatures: % of core fuel volume in 100 °C temperature intervals for the 100 mm break. Transient variation over the first 120 h.

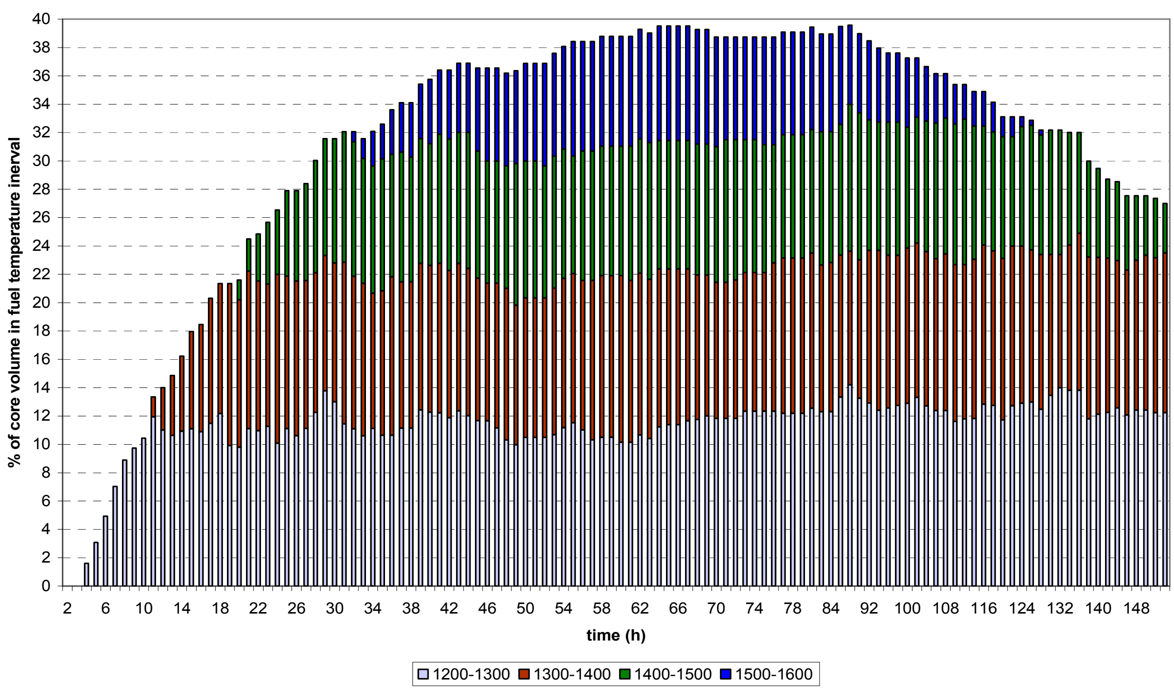

Figure 2-22: Maximum fuel temperatures: % of core fuel volume in 100 °C temperature intervals for the 3 mm break. Transient variation over the first 154 h.

The comparative volumetric MFT behavior at t=5 h and t=50 h for the 3,5,10 and 100 mm cases are shown in Figure 2-23 and Figure 2-24. At t=5 h, the 100 mm case experiences larger fuel volumes in the 1300-1500 °C intervals (total 17%), while the 10 mm case is significantly cooler (total 14%). However, at t=50 h the 10 mm case has 5.1% of the core volume at a MFT > 1600 °C, while the 100 mm case now only has 4.5% in the same interval. A similar trend is shown in Table 2-9, where the 10 mm case has the largest volumes of fuel for longer durations above MFTs of 1600 °C. **On face value of this data, the 10 mm case could therefore lead to the highest delayed FP source term, if fuel temperatures above 1600 °C are the dominant driving mechanism.**

This conclusion cannot however be made from the TINTE data in isolation: for the 100 mm case 18.4% of the core volume has MFTs in the interval 1400-1600 °C, compared to 17.5% of the core volume for the 10 mm case (i.e. the reverse situation to the >1600 °C interval). If it is kept in mind that these are only 2 snapshots out of 300 hour transients, it is clear that only the GETTER data will finally determine which of the 100 mm or 10 mm cases leads to the highest delayed FP source term.

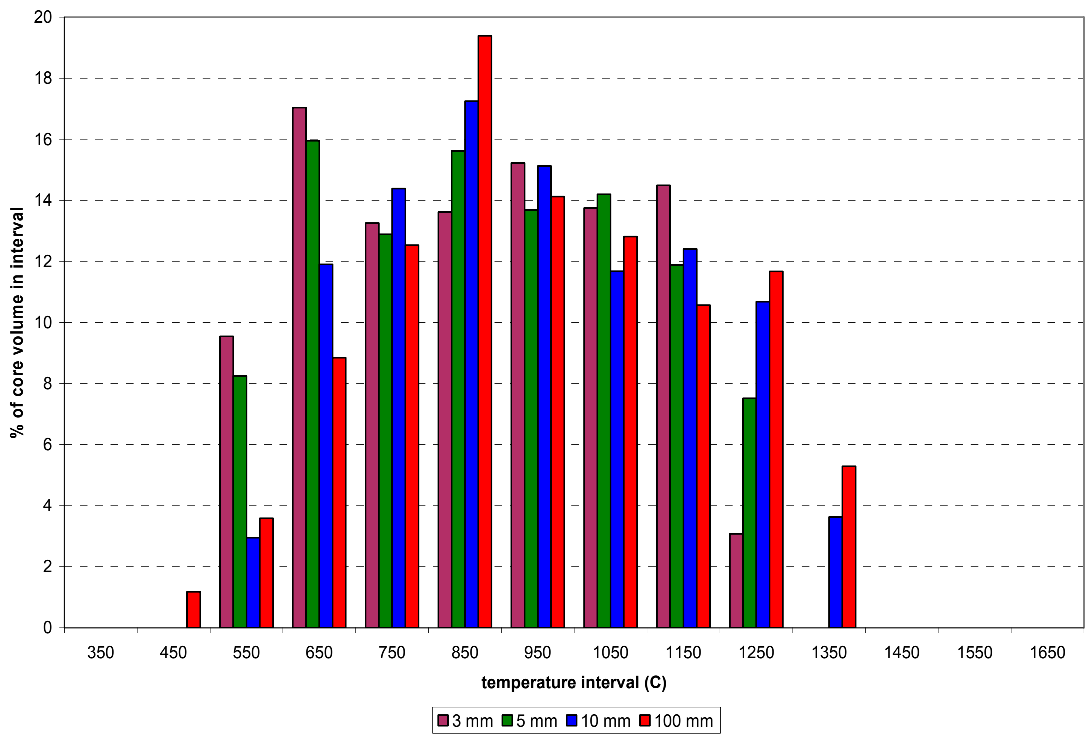

Figure 2-23: Maximum fuel temperatures: % of core fuel volume in 100 °C temperature intervals for the 100 mm, 10 mm, 5 mm, and 3 mm breaks. Snapshot at 5 h.

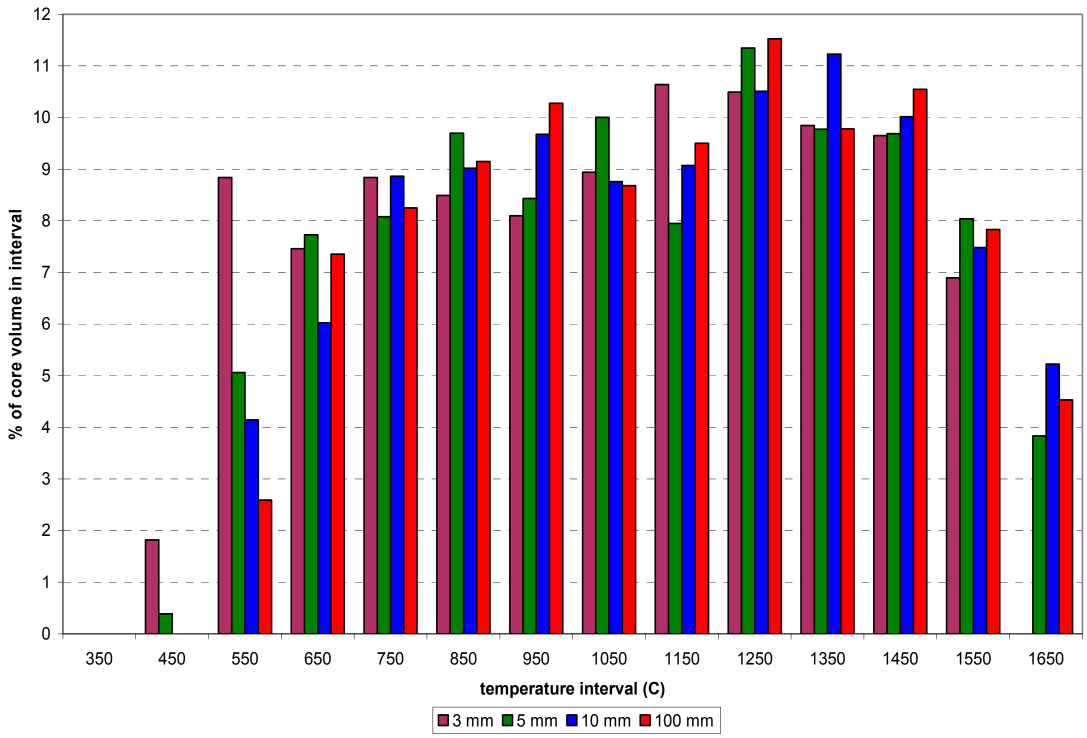

Figure 2-24: Maximum fuel temperatures: % of core fuel volume in 100 °C temperature intervals for the 100 mm, 10 mm, 5 mm, and 3 mm breaks. Snapshot at 50 h.

Table 2-9: 3-100 mm cases: % of Core Volume with MFTs above 1600 °C, and duration exposed to this temperature.

Core volume above 1600C (%)	period above 1600C (h)				
	100 mm	**10 mm**	**5 mm**	**4 mm**	**3 mm**
1%	62	67	57	43	0
3%	45	48	26	0	0
5%	0	6	0	0	0

As indicated earlier, the 10 mm case has the largest volumes of fuel for longer durations above MFTs of 1600°C. The increased convective heat mixing in the core during the 10 mm case distributes the high temperature region over a large core volume than the 100 mm case. The two cases are very close in peak MFT, but the interplay between radiation, conduction and convection seem to combine in the 10 mm case to expose larger fuel volumes for longer to MFTs > 1600°C. This (somewhat surprising) result should be re-assessed with detailed CFD analysis at some point, since TINTE's convective heat flow in a porous medium approach are limited.

2.3.4.4 100mm Break With Air ingress: 1% and 20% Air Molar Fractions

As a sensitivity study, the 100 mm break case was analyzed with air ingress at the break opening. The data for this scenario was also supplied by FLOWNEX, but due to the very low air ingress mass flow rates and oxygen content, a few bounding assumptions were made for the TINTE analysis:

- A mixture of helium and dry air was specified to enter the break location (at the top inlet plenum, close to the RPV). In stead of the varying air *mass* fraction calculated by FLOWNEX (between 0% and 2.2% over 300 hours), a constant *molar* fraction of 1% was assumed to be present over the entire transient. (An example of the conversion of FLOWNEX mass to TINTE molar fractions is shown below in Table 2-10, where it can be seen that the air molar fractions are always less than 1%). At a later stage, a second break location in the IHX volume along the inlet plenum was modelled by FLOWNEX, which resulted in a larger varying air *mass* fraction of up to 17%. For this case, a very conservative constant air *molar* fraction of 20% was assumed to be present.
- The FLOWNEX data also predicted that the ingress of air would only start after ~ 40 hours. This initial helium-only phase was also neglected, and a conservative assumption was used in the TINTE calculation to allow air ingress to start at 60 s.
- The FLOWNEX combined air and helium mass flow ingress rate varied between 0.1 and 4 gram/s (the air component was always lower than 0.02 g/s – see Table 2-10). For the TINTE calculation, a constant mixture flow of 4 g/s was assumed from 60 s onwards. (Note that of the 4 g/s mixture ingress mass flow rate, only 0.02 g/s is air, of which 22% is O_2).
- The air ingress calculation is extremely time consuming (factor 5 slower than real time). This implies a real-time requirement of ~60 days to model a 300 hour air ingress case. Since the air ingress molar fraction, and the air mass flow rate, is very small for these cases, it was therefore decided to only simulate this 100 mm break up to 40 hours for the 1% case, and up to 48 h for the 20% molar fraction case.

Table 2-10: Example of FLOWNEX mass flow rates converted to TINTE molar fraction rates at a few time points

Time (s)	Helium			Dry Air		
	kg/s	mol/s	molar fraction	kg/s	mol/s	molar fraction
59100	-3.44E-03	-8.59E-04	1.0000	-6.47E-09	-1.079E-10	1.26E-07
101100	-3.14E-03	-7.85E-04	1.0000	-3.65E-07	-6.076E-09	7.74E-06
200100	-2.41E-03	-6.01E-04	0.9999	-3.77E-06	-6.286E-08	1.05E-04
302100	-1.80E-03	-4.49E-04	0.9997	-6.81E-06	-1.135E-07	2.53E-04
401100	-1.51E-03	-3.78E-04	0.9995	-1.03E-05	-1.723E-07	4.56E-04
500100	-9.84E-04	-2.46E-04	0.9993	-9.73E-06	-1.622E-07	6.59E-04
602100	-5.97E-04	-1.49E-04	0.9992	-7.32E-06	-1.220E-07	8.16E-04

Due to the very low air ingress rates, and the dominant presence of helium mixing at the break location (as opposed to a pure air ingress scenario), the amount of the corrosion that took place in the core was very low. It is shown in Table 2-11 that for the case where 1% air molar fraction is used, only 0.16 kg of the core fuel graphite was converted to CO and CO_2, while the conservative 20% case resulted in 11 kg core fuel corrosion.

Table 2-11: Total mass of graphite corroded after 40 h of air ingress for two air molar fractions

Air molar fraction	Total mass of graphite corroded (kg)	
	Core graphite	Reflector graphite
1%	0.18 (@ 40 h)	0.25 (@ 40 h)
20%	11.06 (@ 48 h)	1.63 (@ 48 h)

The spatial graphite corrosion concentration (mol/m^3) pattern at t = 40 h for the 1% molar fraction air ingress case is shown in Figure 2-25. The major corrosion activity is concentrated in the bottom parts of the core and the riser channel, and the upper part of the control rod channel. Since gas flow paths are also modeled in the central hole, a small amount of corrosion is also visible in the lower section of the central hole. No corrosion greater than 0.5mol/m^3 has yet occurred at 40 hours in the bottom reflector for this case.

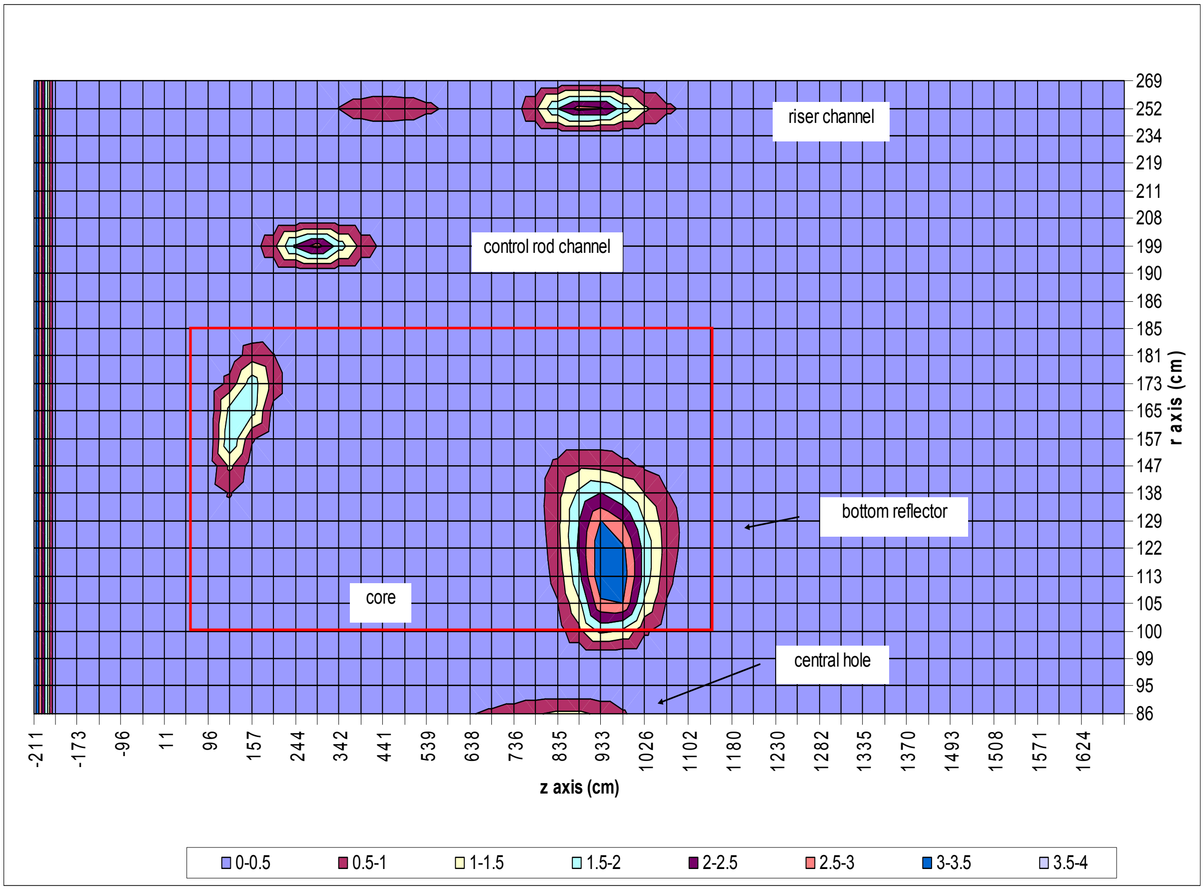

Figure 2-25: 100 mm break with 1% molar fraction air ingress: Graphite corrosion concentration (mol/m^3) distribution at t = 40 h

In contrast to the 1% case, the 20% molar air fraction case distribution (shown in Figure 2-26 to Figure 2-28) indicates that much more corrosion occurs in the core region, and almost none in the bottom reflector structures. Initially, at t = 12 h, corrosion occurs at the bottom and top of the core, mostly driven by the temperature differences and the availability of oxygen. Twelve hours later (Figure 2-27), the corrosion in the bottom of the core dominates, while some central reflector corrosion is also visible in the central hole (air that rises in the cooler side reflector does not yet react, but when it flows downwards in the much hotter central reflector, corrosion occurs). This basic corrosion pattern remains visible at 48 h as well, where no corrosion above 25mol/m^3 has occurred up to 40 hours in the bottom reflector for this case.

It is therefore important to note from these two examples that the degree, as well the spatial location of the observed corrosion, is very sensitive to the amount of air available for chemical reactions.

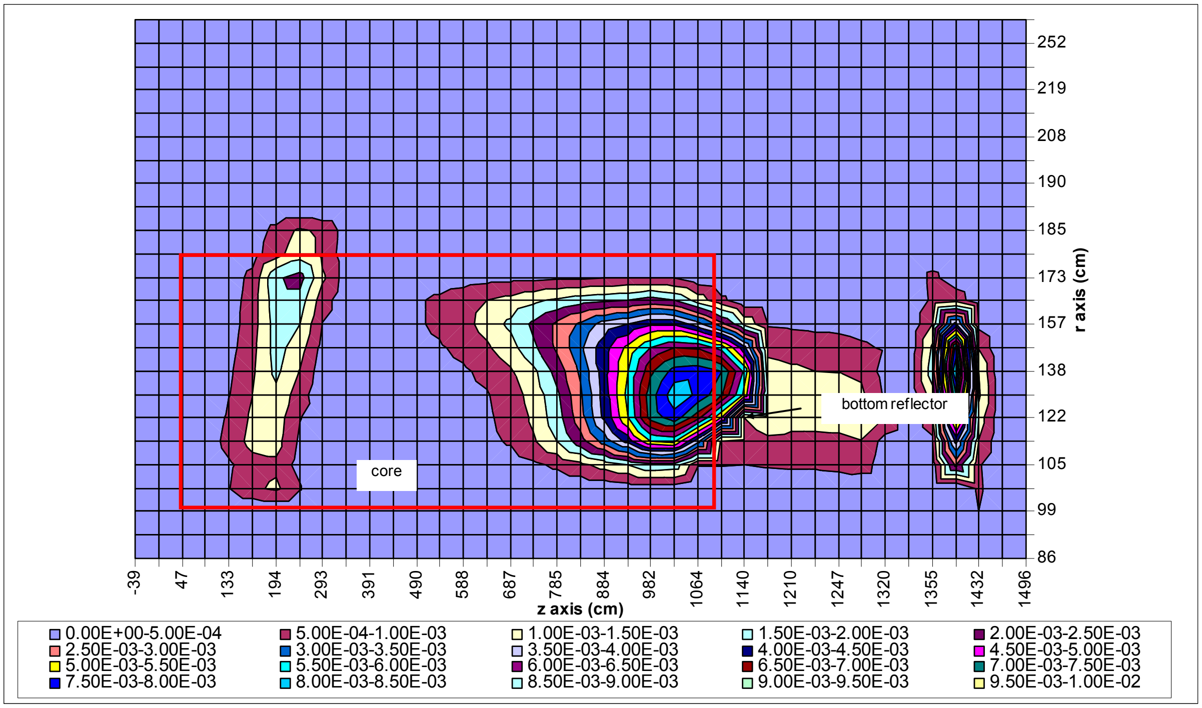

Figure 2-26: 100 mm break with 20% molar fraction air ingress: Graphite corrosion concentration (mol/m^3) distribution at t = 12 h

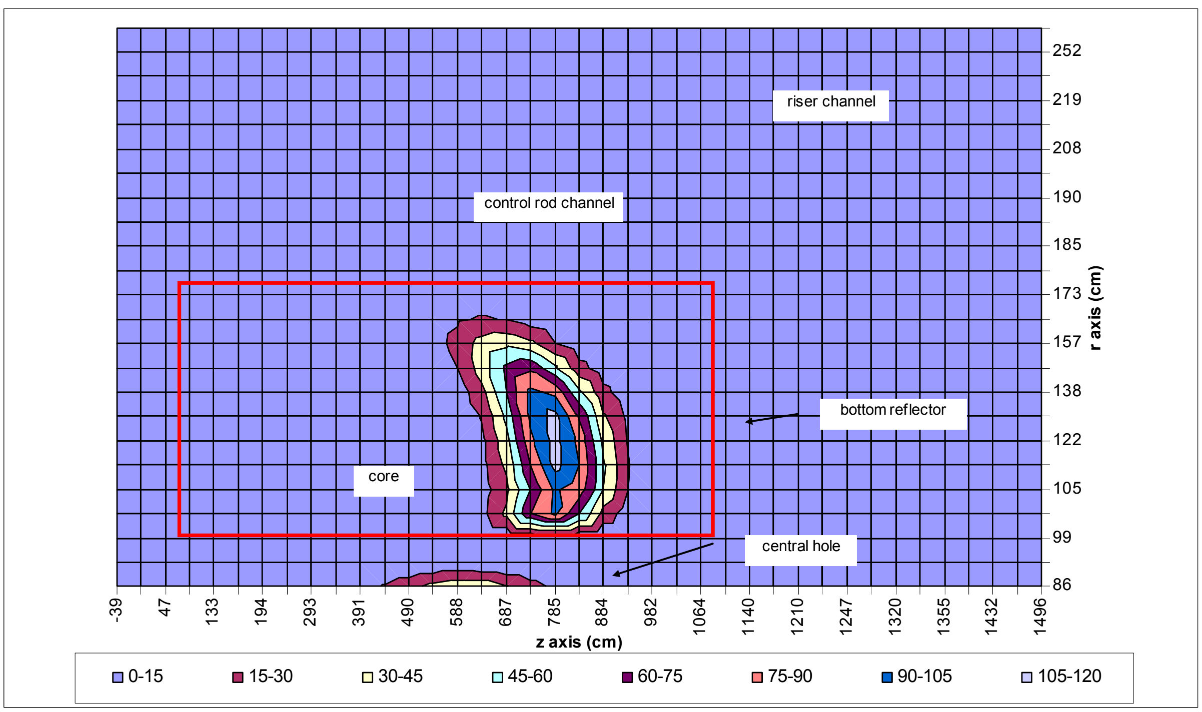

Figure 2-27: 100 mm break with 20% molar fraction air ingress: Graphite corrosion concentration (mol/m^3) distribution at t = 24 h

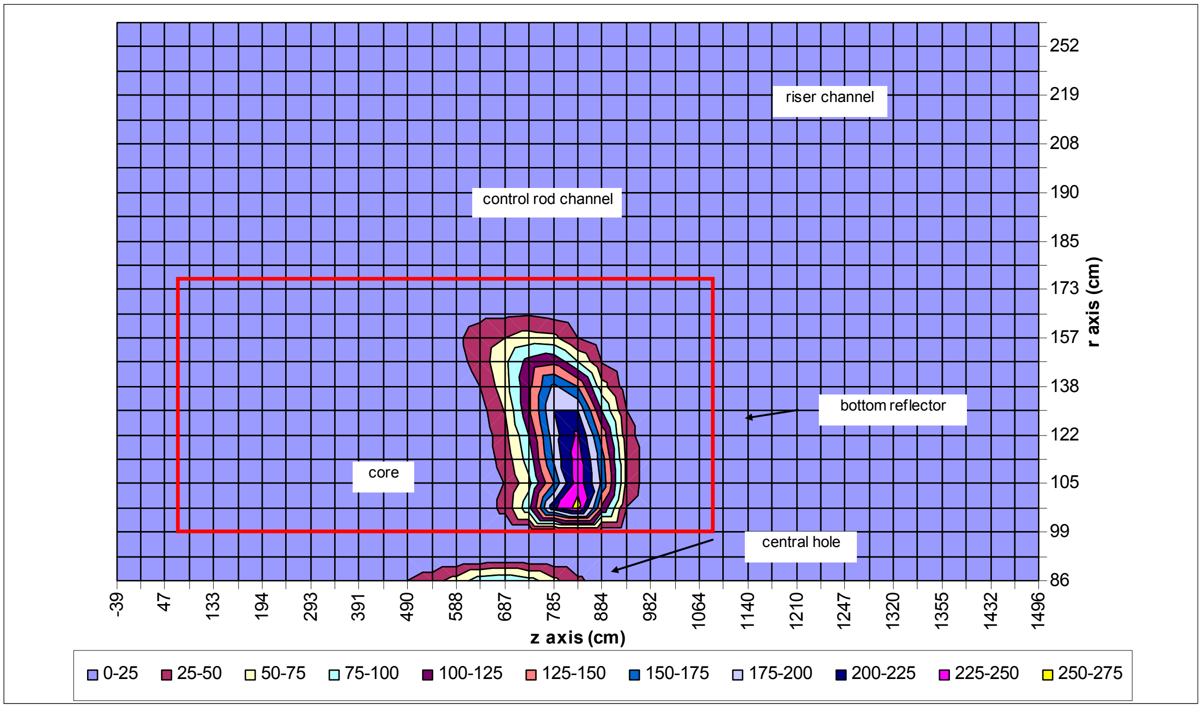

Figure 2-28: 100 mm break with 20% molar fraction air ingress: Graphite corrosion concentration (mol/m^3) distribution at t = 48 h

The non-linear increase in core and reflector corrosion over the first 40 hours of the 100 mm break with 1% air molar fraction can be seen in Figure 2-29. After the discreet changes in gradients around 18 h, the core and reflector corrosion rates continue at a constant gradient up to 40 h. The sharp increase in the reflector mass corroded at t~18 h is mainly caused by the rise in reflector temperatures as the core heat is conducted through the side reflector.
This behavior is *not* observed for the 20% air molar fraction case, which exhibits a much more linear trend in the rate of corrosion. As shown in the spatial distribution above, the core corrosion rate for the 20% case dominates the reflector corrosion rate completely (Figure 2-30), in sharp contrast to the 1% case.

In conclusion; it is difficult to predict the corrosion behavior of the core over the next 260 hours based on data from the first 40-48 hours. However, since the actual mass of core graphite corroded in these 2 cases (<0.3 kg and <11 kg) remains very small compared to the total core graphite mass (~91000 kg), **it can be concluded that no significant additional fission products are released due to corrosion of the fuel elements.**

It is also important to recognize that the analysis is for the 100 mm case where the margin factors to the dose limits are 3 to 4 orders of magnitude larger than for the limiting 4 mm case (details on this are provided in Section 3). Air ingress and oxidation effects for the 4 mm case are not expected to be significant as the essentially zero pressure differential will prevent any air exchange of significance taking place. Therefore for the design basis spectrum of accidents air ingress and oxidation could reduce the margin factors for the larger leaks, but it would not be expected to change the fact that the small leak cases (4 mm) are the limiting cases.

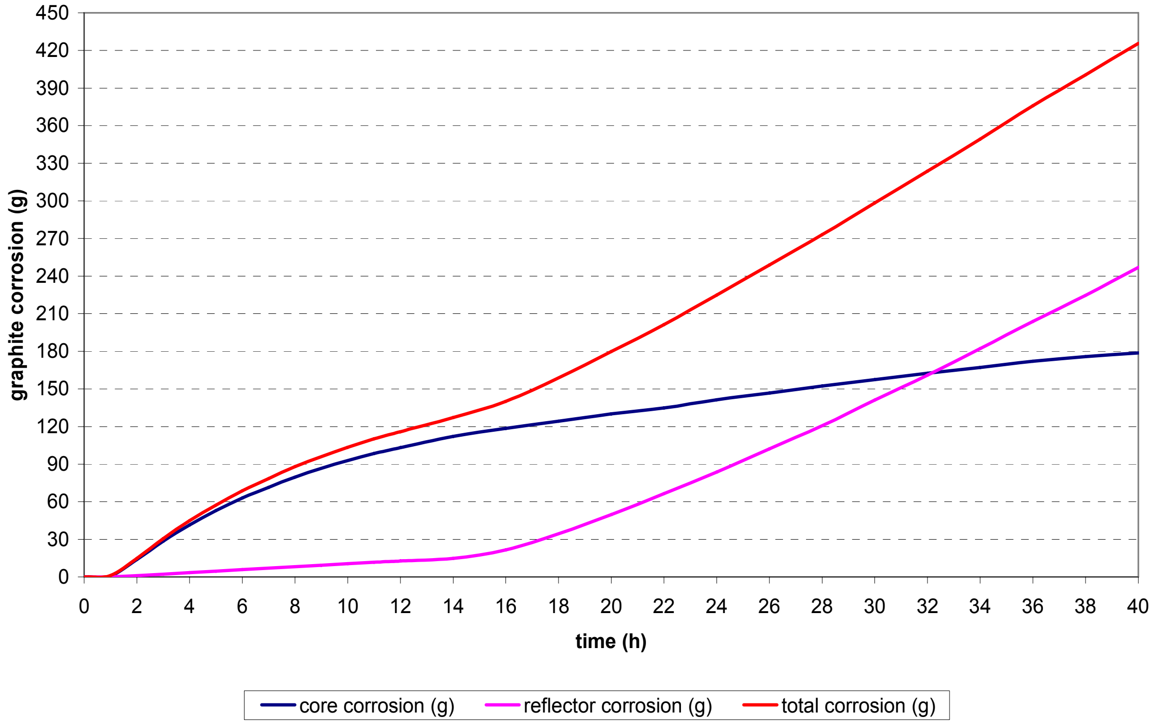

Figure 2-29: 100 mm break with 1% molar fraction air ingress: Graphite corrosion up to 40 h (gram)

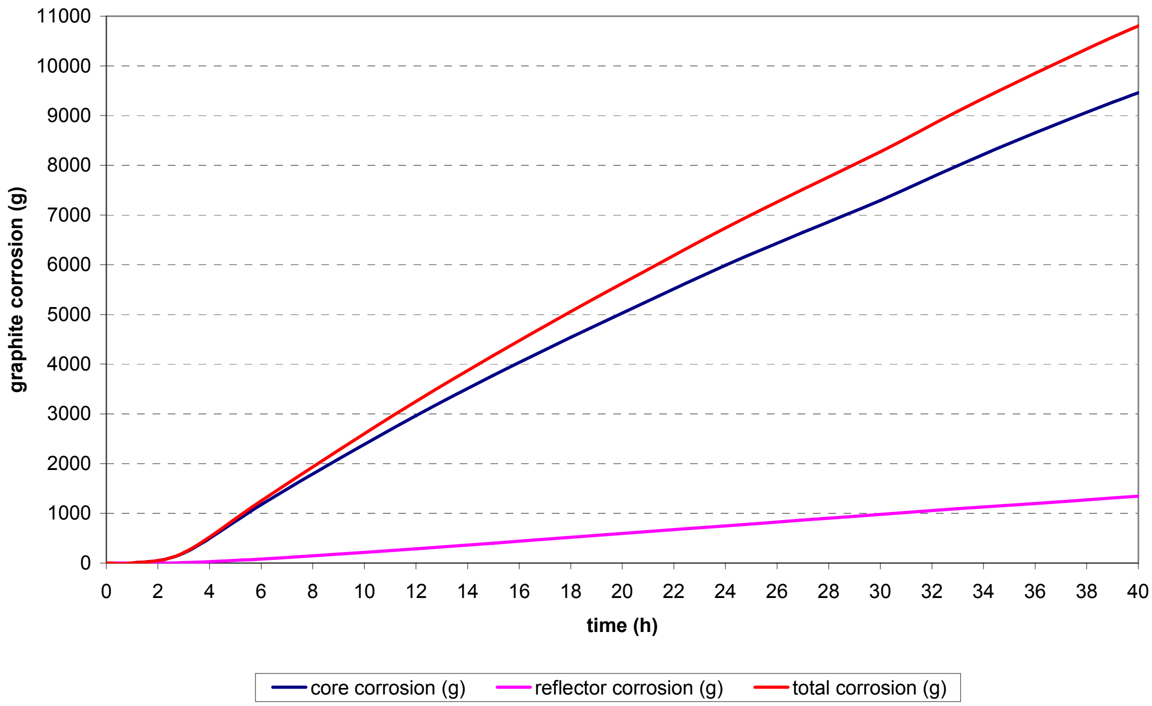

Figure 2-30: 100 mm break with 20% molar fraction air ingress: Graphite corrosion up to 40 h (gram)

2.3.5 Thermofluid Behavior Conclusions and Recommendations

The thermofluid behavior of the PHTS during depressurization is characterized by blowdown times that vary from 158hr to 11min for the range of break sizes (3mm to 100mm break diameter) analyzed. However, small changes in NHSS helium inventory and operation have a large influence on these blowdown times. Changes in the NHSS design are therefore likely to change the blowdown times and as a result the size of the limiting small break.

The results confirm that for DBAs shear force ratios remain below 1 and hence insignificant dust re-suspension and lift-off can be expected.

In terms of the PHTS and RB gas exchange phenomena, the break location as well as the RB compartment layout has a strong effect on the air ingress fractions. Further CFD studies are recommended as well as possible experiments to evaluate PHTS-RB gas exchange phenomena not modeled in Flownex and to evaluate impact of oxidation reactions on flow associated phenomena.

The core thermal response has indicated that the slightly higher 10 mm break MFT results compared with 100mm appear counter intuitive. However, detailed analysis traced the root cause back to increased convective heat mixing in the core during the 10 mm case, which distributes the high temperature region over a larger core volume than the 100 mm case Apart from this insignificant anomaly, the 3 mm to 100 mm cases all confirmed the general trend of cooler fuel temperatures with an increase in gas inventory and blow down time. Since spatial temperature distributions can have an effect on the MFT and can make results appear counter intuitive, it would be useful to extend the analysis chain to a larger set of break sizes.

From the corrosion sensitivity study it was found that over a period of 40-48 hours, the total corrosion in the core ranged from ~1 kg to ~10 kg for 1% to 20% air molar fractions, respectively. This represents an insignificant fraction of the core mass (~90 000 kg). CFD analysis could be used to obtain a clearer understanding of the air ingress and the corrosion associated with such an event, though the indications are that in terms of the dose limits the air ingress will not contribute significantly.

2.4 RADIONUCLIDE RELEASES

2.4.1 Radionuclide Releases from the Fuel to the PHTS

The normal operation (pre-break) total core release rates are listed in Table 2-12~~Table 2-12~~.

Table 2-12: Normal operation core release rates

Nuclide	Release from core (atoms/s)
Ag-110m	5.36E+10
Ag-111	1.48E+09
Cs-134	4.89E+10
Cs-137	6.91E+11
Sr-90	2.17E+06
Kr-88	3.88E+10
Kr-90	5.92E+09
I-131	7.60E+10
I-133	9.44E+10
Te-132	8.62E+10

Release curves for the evaluated breaks and considered radionuclides are presented in Figure 2-31~~Figure 2-31~~ to Figure 2-37~~Figure 2-37~~.

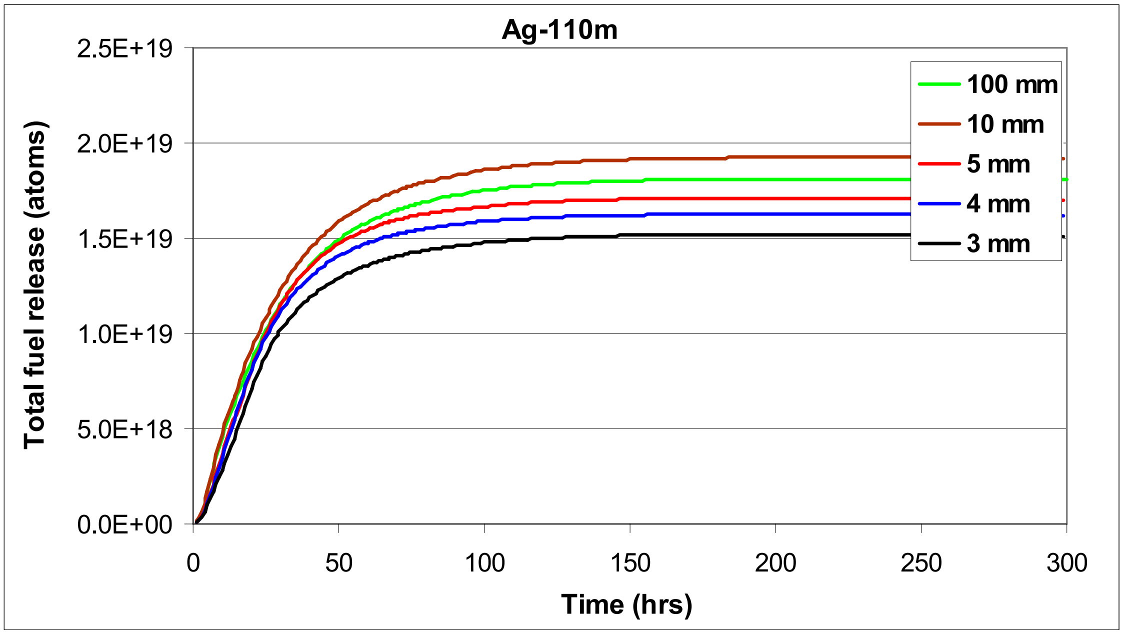

Figure 2-31: Ag-110m releases

In general, releases for the different breaks increases from 3mm, being the lowest releasing, to 4mm, 5mm and 100mm to 10mm which is the highest releasing. This corresponds to the maximum fuel temperatures calculated by TINTE.

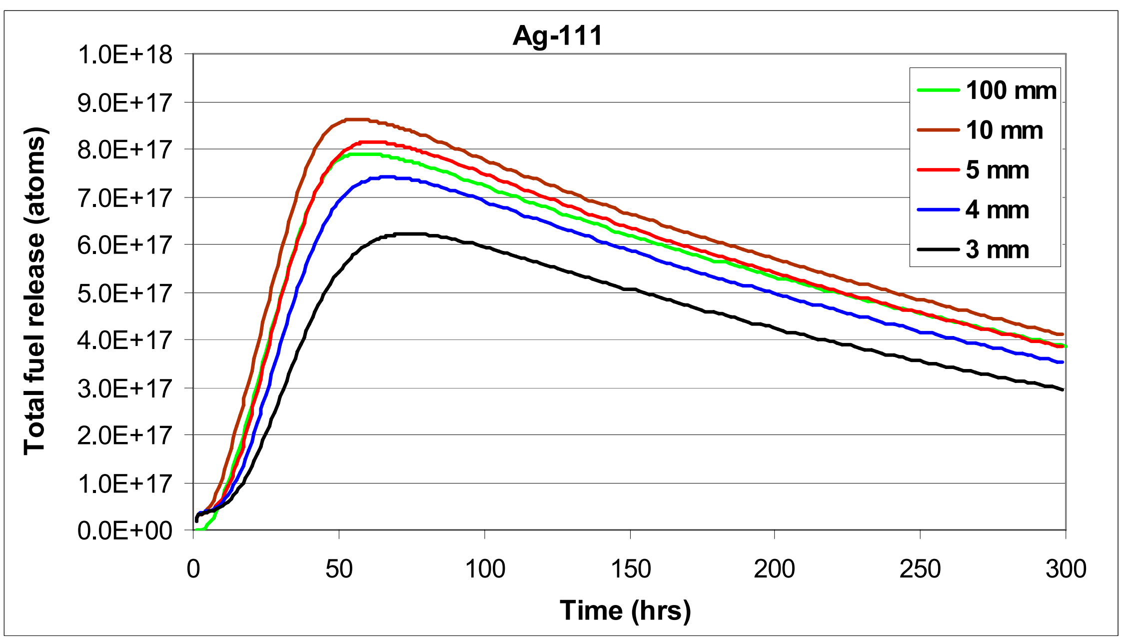

Figure 2-32: Ag-111 releases

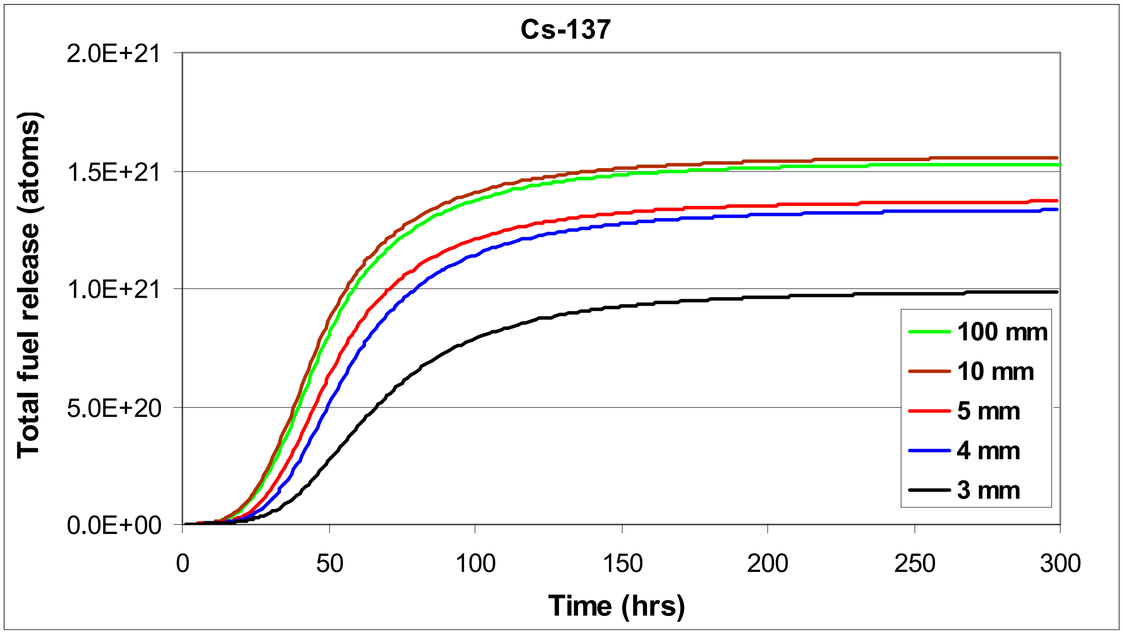

Figure 2-33: Cs-137 releases

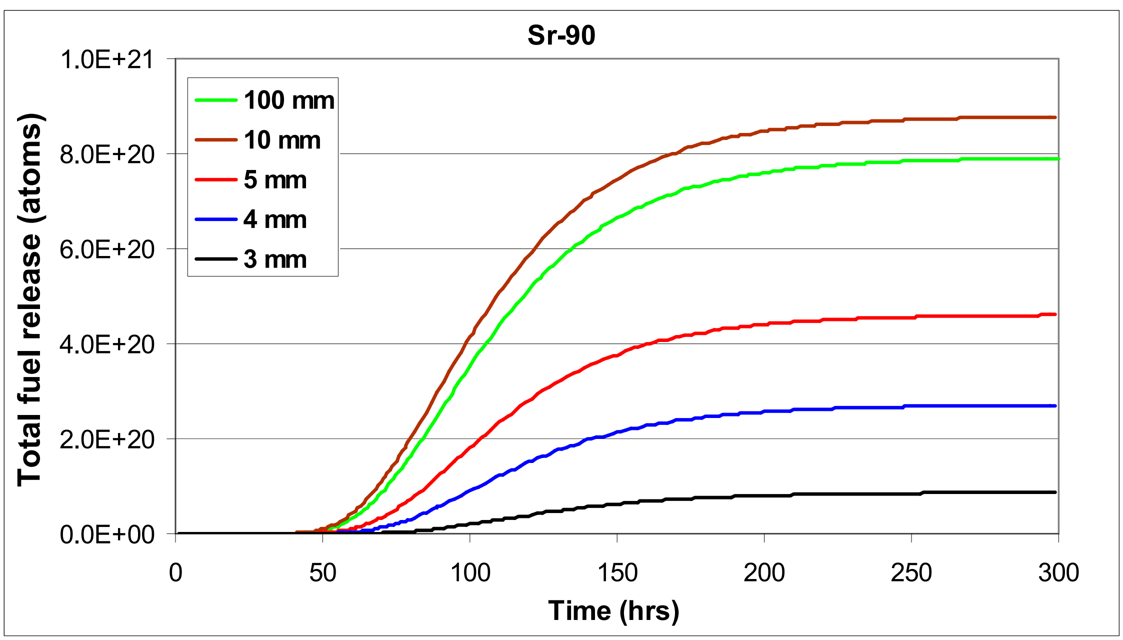

Figure 2-34: Sr-90 releases

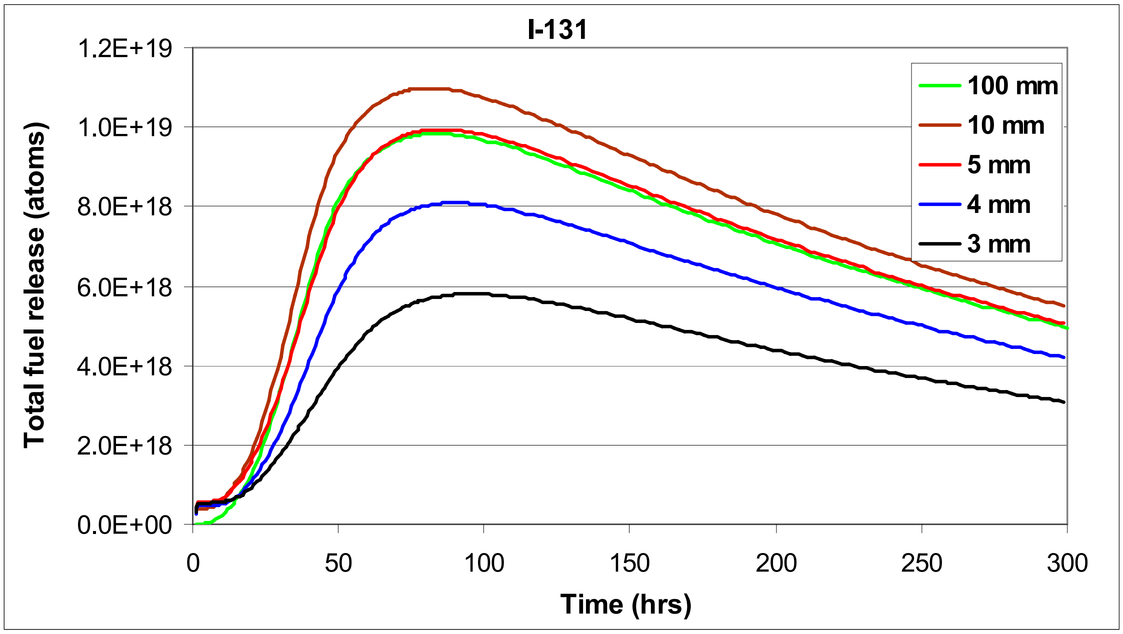

Figure 2-35: I-131 releases

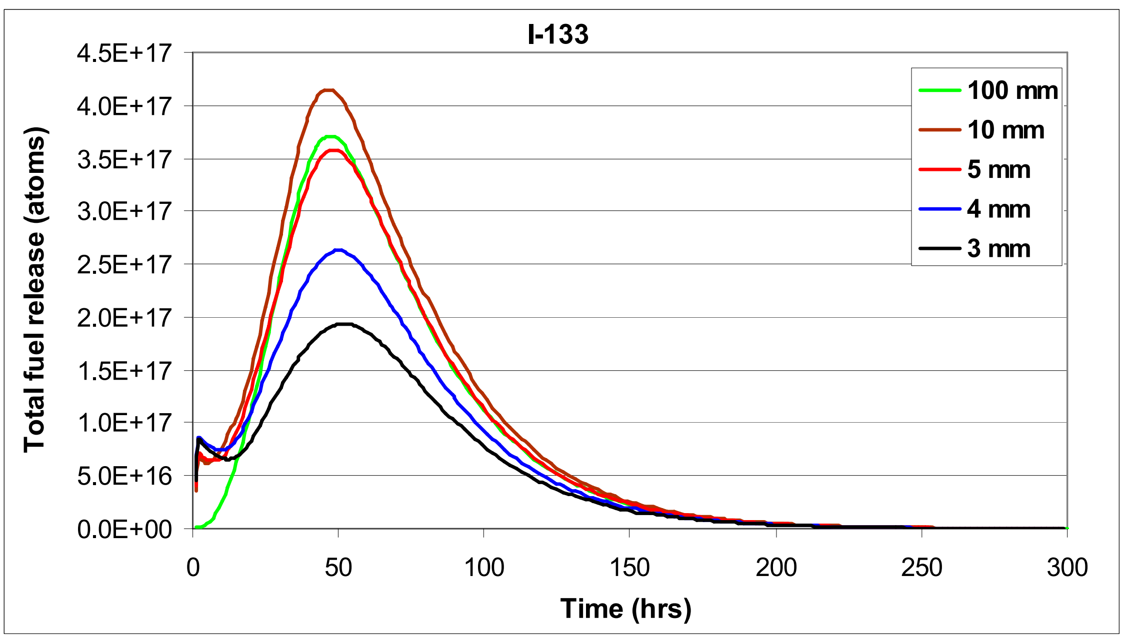

Figure 2-36: I-133 releases

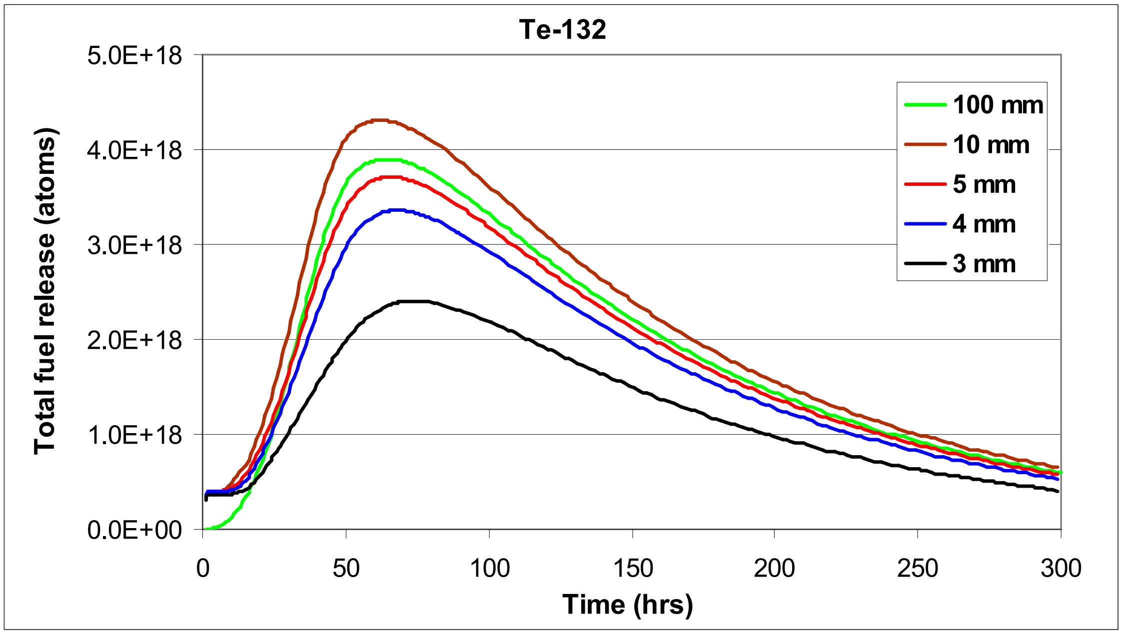

Figure 2-37: Te-132 releases

It is important to remember that all results presented here are based on scaled up calculations and unverified calculation models and should be considered first order scoping calculation results.

2.4.1.1 Break Size Selection

From the results obtained in the thermal-fluid analysis as well as the RN releases from the fuel the decision was taken to use the 4mm case as the small break to analyze in the continuation of the chain. This break size was chosen as it is the largest break for which the blowdown time is long enough (91 hours) to occur after the peak releases of most of the delayed release RNs.

2.4.2 Radionuclide Releases from the PHTS to the Reactor Building

The time dependent I-131 releases from the PHTS to the RB for the 4mm and 100mm CIP HPB break cases are presented in Figure 2-38 and Figure 2-39, respectively. Note that although the releases from the fuel are somewhat higher for the 100mm break, the releases to the RB are more than two orders of magnitude smaller due to the fact that PHTS depressurization occurs prior to the major part of the delayed release from the fuel. Specifically, the 100mm break has 26% more I-131 release from the fuel to the PHTS than the 4mm break due to the higher temperatures during the transient (333Ci versus 265Ci); however because the release from the fuel occurs long after the blowdown is complete much less is released to the RB (0.43Ci versus 155Ci).

For the 4mm break case, it is assumed that no further release of RNs from the PHTS to the RB occurs after the end of blowdown, which has been determined by the Flownex calculations to be about 91 hr. This is because the blowdown extends into the period that the PHTS is no longer thermally expanding (heating) but rather is thermally contracting (cooling) due the core thermal transient during passive core cool-down. For the 100 mm break, the blowdown is complete in 11 minutes, well before the radionuclide releases from the fuel reach their maximum values. After the blowdown, release from the PHTS to the RB continues until 50 hrs due to the thermal expansion of the helium coolant in the PHTS. The blowdown time and the time to the end of thermal expansion for the DLOFC are determined from the Flownex calculations. Continued release from the PHTS to the RB during the PHTS thermal contraction phase is considered in the barrier allocation task as discussed in Section 3.

Releases for all the modeled RNs at 300hr are shown in Figure 2-40 and Figure 2-41 for the 4mm break, and the 100mm break, respectively. For the 4mm break, the contribution from the delayed radionuclide release from the fuel (RNs not attached to dust) represents 99+% of the total release to the RB for all RNs. The release due to the initial dust resuspension is negligible for all the RNs for this small break size. For the 100mm break, the contribution from the delayed radionuclide release from the fuel (RNs not attached to dust) represents 95+% of the total release to the RB for Ag, I and Te isotopes, 46% for Cs-137 and 20% for Sr-90. The release due to the initial resuspension of dust is comparable to the delayed release for Cs-137 and Sr-90 for this larger break size.

The following conclusions are supported by the results for RN releases to the RB for 4mm and 100mm HPB breaks and confirm 2008 study results:

- The larger break sizes have more release from the fuel to the PHTS yet the smaller breaks have more release from the PHTS to the RB. The longer blowdown time for the small break in relation to the time dependent releases from the fuel results in a significantly greater percentage of the delayed RN release from the fuel being transported to the RB
- For breaks up to 100mm EBS the delayed fuel release dominates for I-131

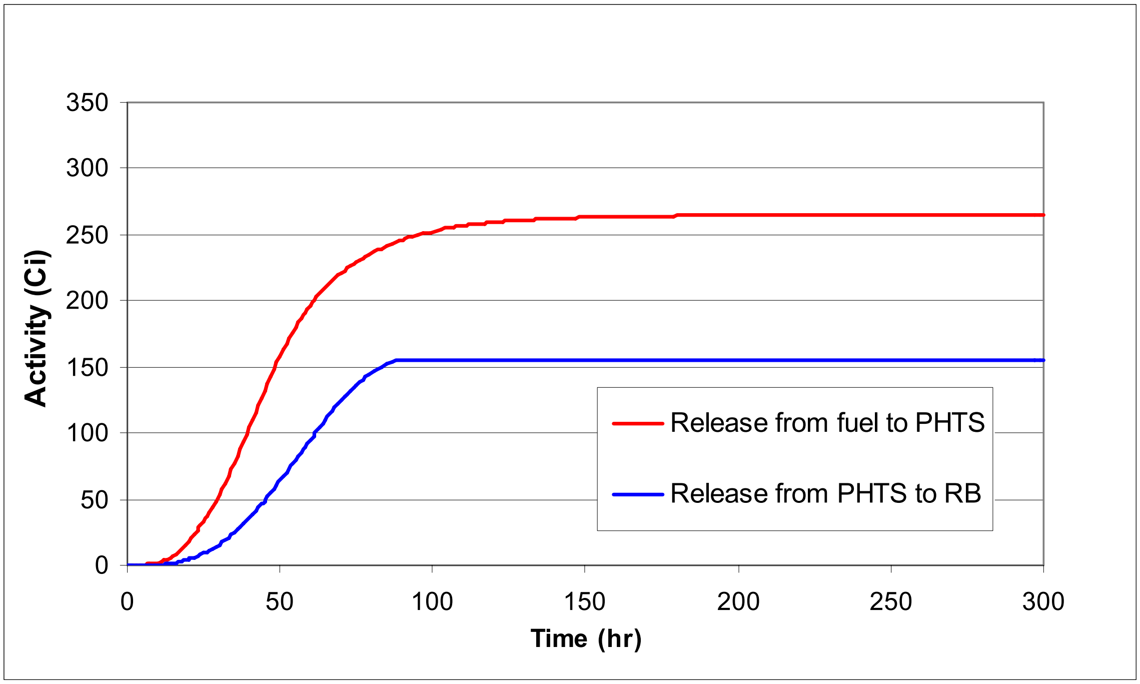

Figure 2-38 Time Dependent Release of I-131 for 4mm Break

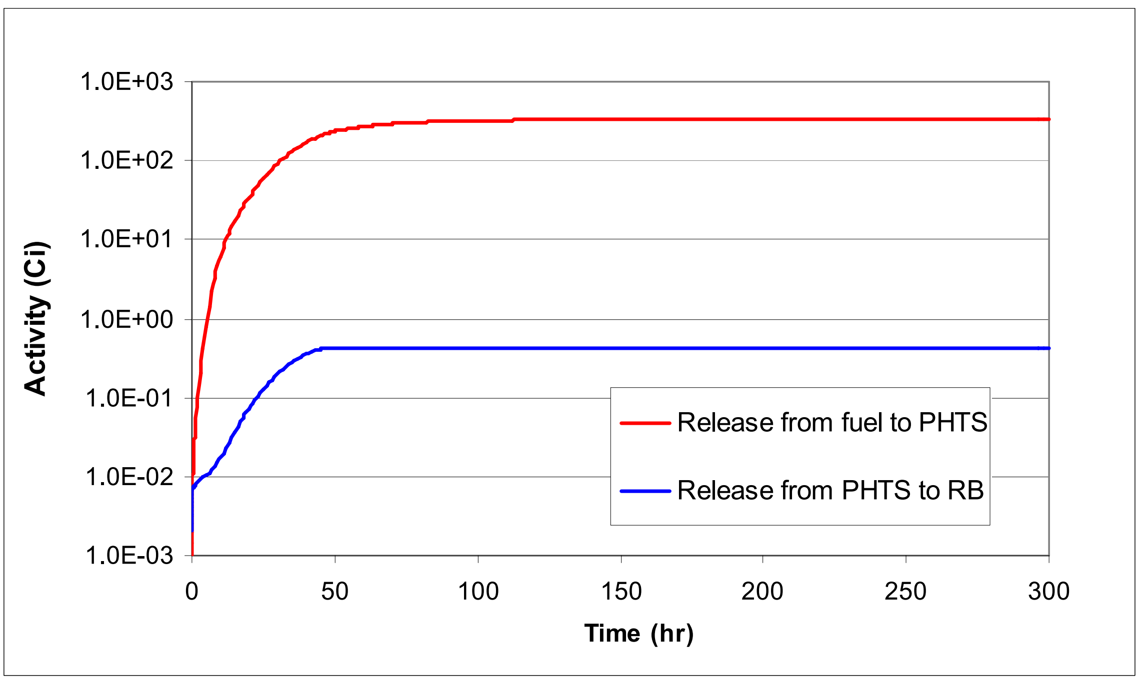

Figure 2-39 Time Dependent Release of I-131 for 100mm break

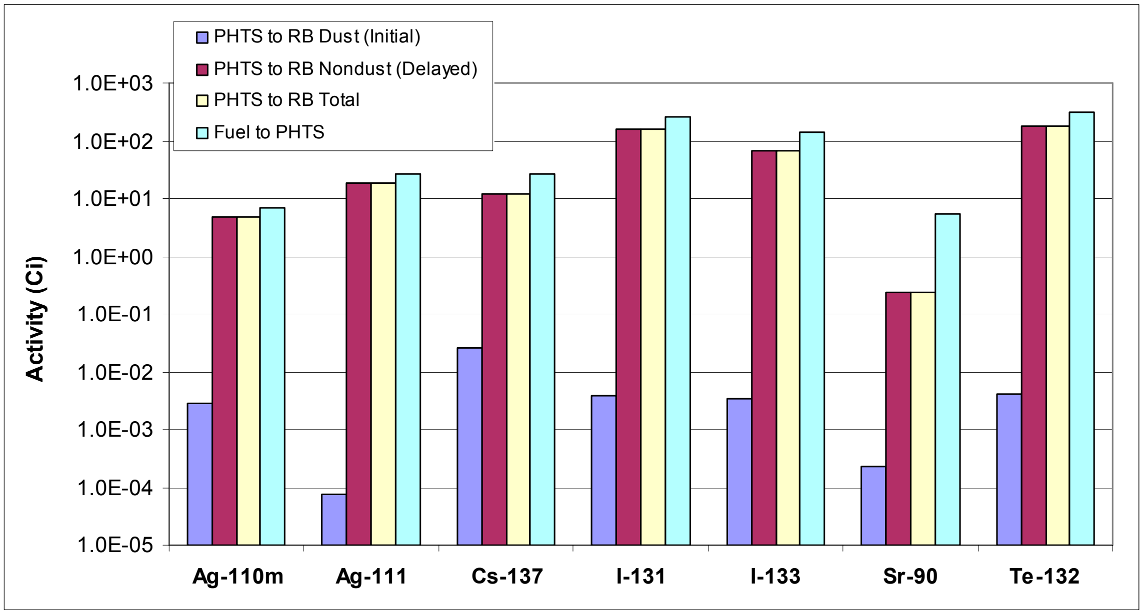

Figure 2-40 Cumulative 300hour releases for 4mm Break

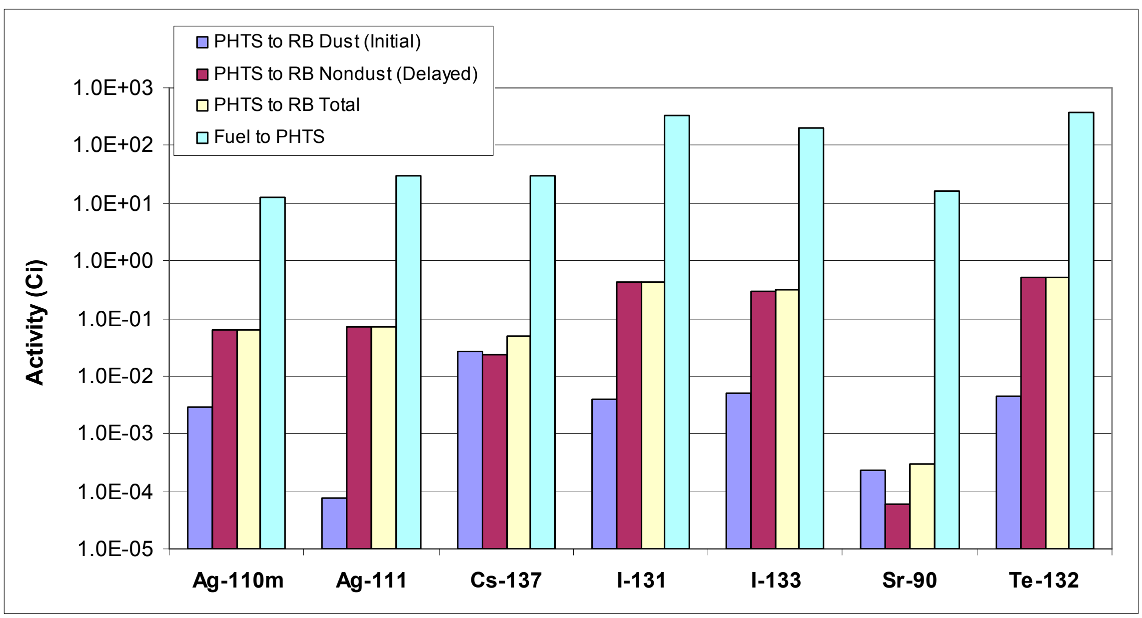

Figure 2-41 Cumulative 300 Hour Releases for 100mm Break

2.4.3 Radionuclide Releases from the Reactor Building to the Environment

2.4.3.1 Reactor Building Analysis Case Descriptions

A 4mm and a 100 mm EBS of the Core Inlet Pipe (CIP) were simulated in the ASTEC RB Model to occur in the Reactor Top Cavity (RTC) compartment. Each of the runs was performed for 300 hours. A case with no leakages was performed as a sensitivity study. Runs were also performed for the option of a damper, on top of the stack, closing at 91 and 50 hours respectively for the 4 mm and 100 mm break which are the times when the delayed release begins). In addition, sensitivity studies were performed modeling the fission products not attached to dust as 1E-7 m diameter aerosols. ASTEC treats the fission products not attached to dust as gases with no deposition taking place. Sensitivity studies, treating the fission products as aerosols, were thus performed to evaluate the effect of fission product deposition on the retention within the reactor building.

The cases run are listed in Table 2-13

Table 2-13: Cases Run during Analysis

	Break Size	Leakage	Damper	Fission Product Form
Case 1	4 mm	No Leakage	No Damper	Gas
Case 2	4 mm	With Leakage	No Damper	Gas
Case 3	4 mm	With Leakage	With Damper	Gas
Case 4	4 mm	With Leakage	No Damper	Aerosol
Case 5	4 mm	With Leakage	With Damper	Aerosol
Case 6	100 mm	No Leakage	No Damper	Gas
Case 7	100 mm	With Leakage	No Damper	Gas
Case 8	100 mm	With Leakage	With Damper	Gas
Case 9	100 mm	With Leakage	No Damper	Aerosol

2.4.3.2 4 mm Break Study

2.4.3.2.1 No Damper Case

Phase 1 (t < 35 minutes) – Rupture Panels Break

At the time of the break the helium, dust and fission product injection from the Helium Pressure Boundary (HPB) to the Reactor Top Cavity (RTC) compartment begins. The RTC compartment begins to pressurize and the temperature and helium mass fraction in the RTC compartment increases as seen in Figure 2-42~~Figure 2-42~~, and Figure 2-43. The temperature increase is relatively sharp in the RTC compartment compared to the remainder of the compartments (Figure 2-42~~Figure 2-42~~).

The rupture panel between the Reactor Top Cavity (RTC) compartment and IHX compartment breaks at approximately 1 minute (Figure 2-42~~Figure 2-42~~). Helium, dust and fission product flow from the RTC compartment to the IHX compartment takes place. The IHX compartment (and also RTC compartment) begins to pressurize. The helium mass fraction in the RTC compartment continues to increase (Figure 2-43). The mean mass density in the RTC compartment decreases due to the gas composition changing from air to a mixture of air and helium, see Figure 2-43.

At approximate 14 minutes the rupture panels between the IHX and DVSW compartments burst. The pressure and temperature in the RTC compartment drops to approximately 103.75 kPa, as seen in Figure 2-42~~Figure 2-42~~, before increasing again. The pressure in the DVSW, FIP, FHL1 and SIP compartments reach this pressure almost instantaneously due to pressure equalization of the gas which was in the IHX and RTC compartments. A temperature drop of approximately 2°C is observed in the RTC and IHX compartments.

Helium, dust and fission product flow from the IHX to the DVSW compartments (and subsequently to the FIP, FHL1 and SIP compartments) takes place. All compartments within the reactor building begin to pressurize. The helium mass fraction in the RTC compartment continues increasing significantly (Figure 2-43), resulting in the density of the gas mixture within the RTC compartment decreasing further. The density in the IHX compartment increases slightly due to the flow of gas from the RTC to the IHX, see Figure 2-43.

The rupture panels between the SIP compartment and the environment burst at approximately 35 minutes which results in helium, fission products and dust being transported to the environment. The reactor building pressures all drop to values close to atmospheric pressure. Reactor Building pressures show differences with the atmospheric pressure of the environment due to the contribution of the hydrostatic head term; $\rho_{zone} \cdot g \cdot h$. A temperature drop is observed in all compartments due to the relief of the gas mixture to atmosphere, the mixture of the helium with the air in the Reactor Building and the heat dissipation of the gas to the concrete structure.

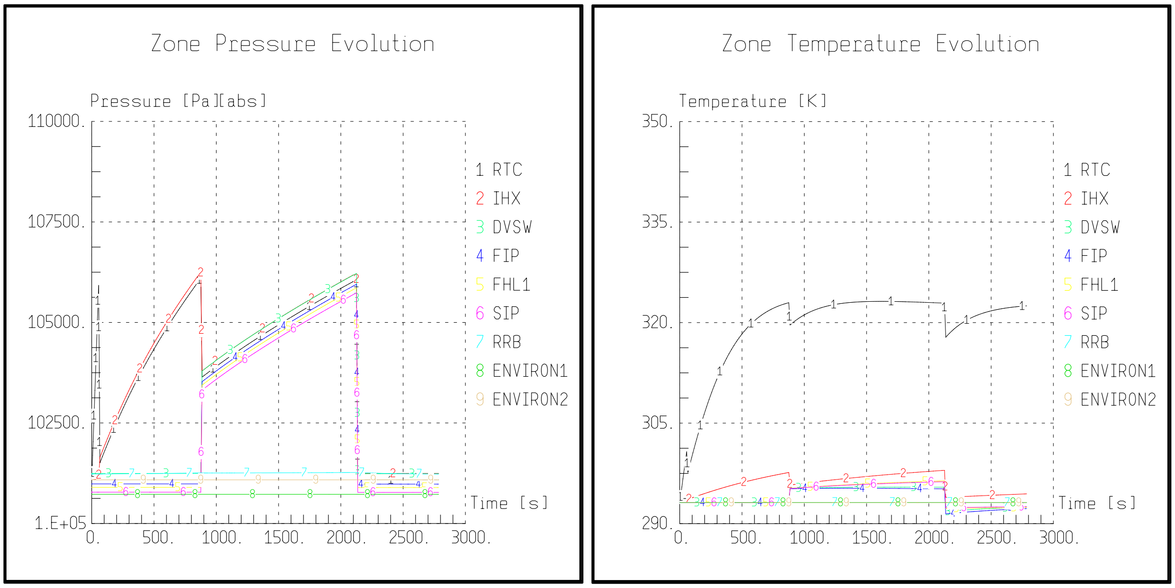

Figure 2-42: Zone Pressure and Temperature Evolution at t = 46.4 minutes

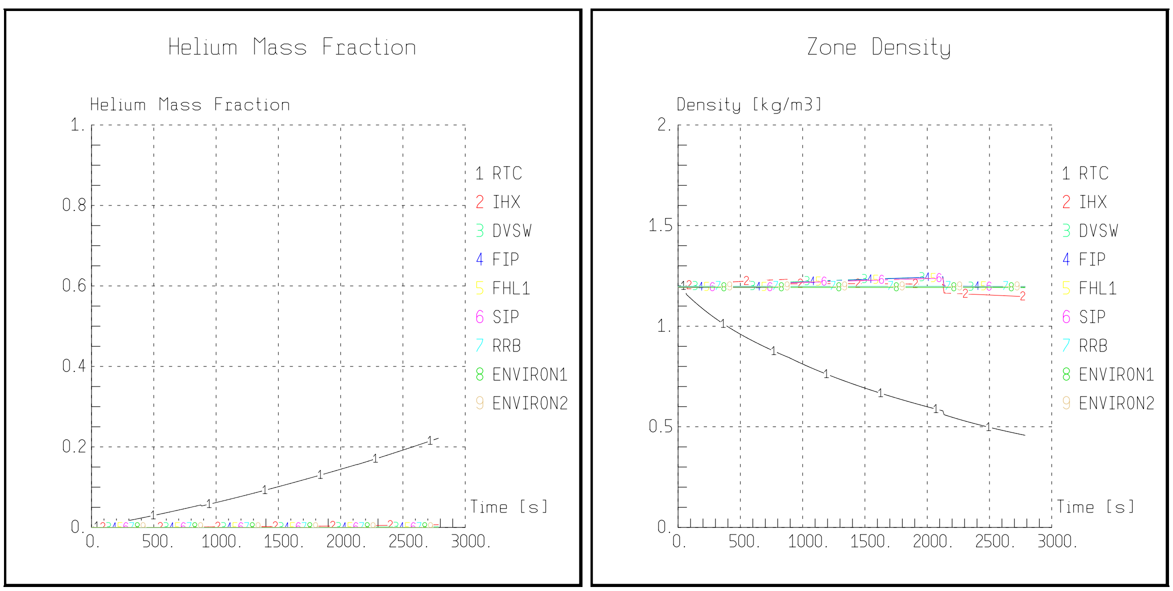

Figure 2-43: Helium Mass Fraction and Zone Mass Density at t = 46 minutes

<u>Phase 2 (t < 91 hours) – Completion of Blowdown</u>

Once the final rupture panel to atmosphere has opened the temperature in the RTC compartment begins to decrease due to heat transfer from the gas to the walls. The temperature in the IHX compartment peaks at 2.8 hours, at which point it begins to decrease. The difference in the temperature evolution in the RTC and IHX compartments, Figure 2-44, is due to the relatively higher gas temperature and larger surface to volume ratio in the RTC compartment as compared to the IHX compartment which results in the temperature in the RTC compartment decreasing at a relatively faster rate than the IHX compartment temperature.

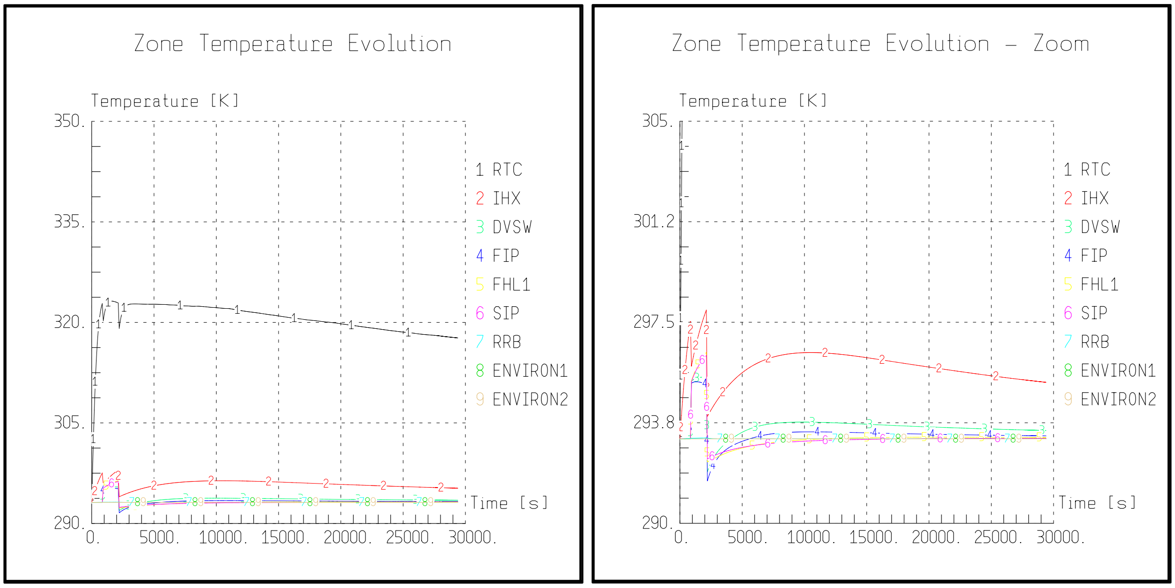

Figure 2-44: Zone Temperature Evolution at 8.2 hours

The pressure at the centre of the IHX compartment, Figure 2-45, decreases due to the cooling of the gas mixture in the IHX compartment. The change in the pressure, using the differential form of the ideal gas law, can be written as

(0.1) $$\frac{\Delta P}{P} = \frac{\Delta n}{n} + \frac{\Delta T}{T}$$

Field Cod

where the molar density in the IHX can be seen in Figure 2-46.

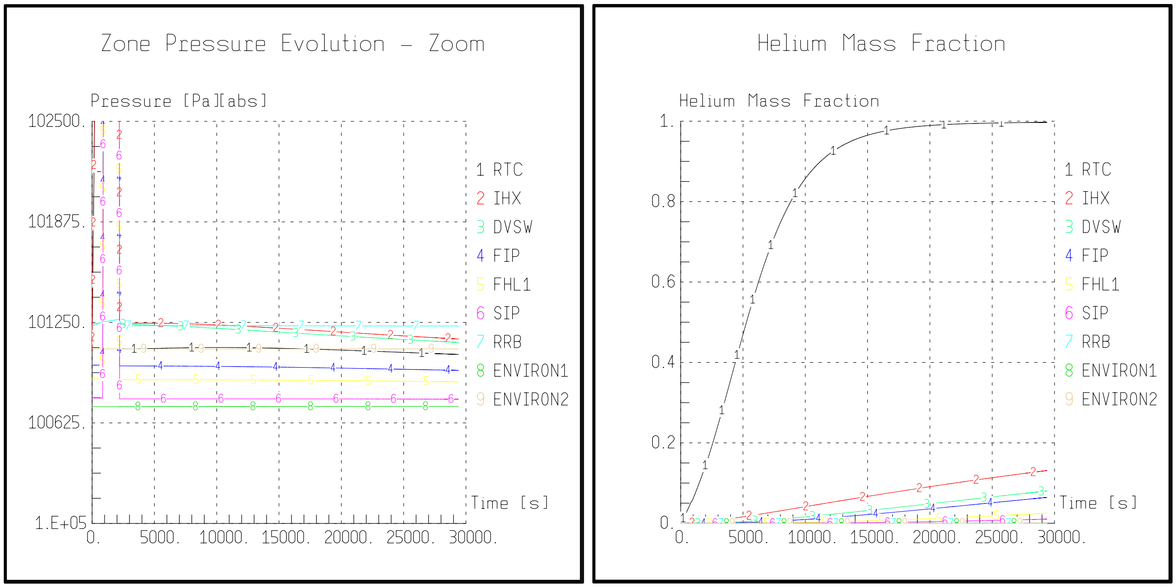

Figure 2-45: Zone Pressure Evolution and Helium Mass Fraction at 8.2 hours

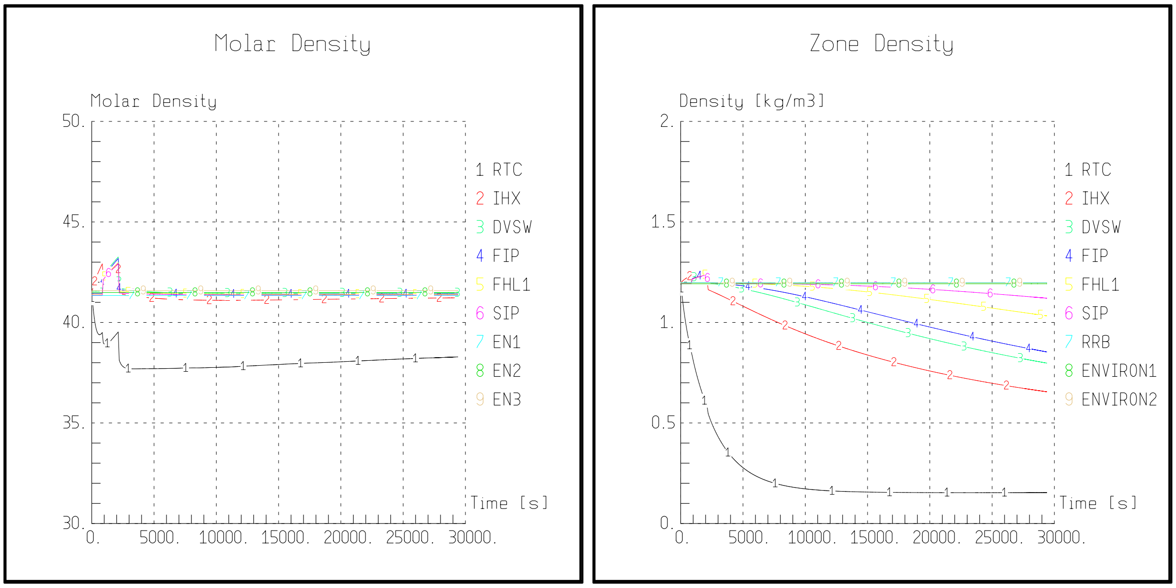

Figure 2-46: Zone Molar and Mass Density at 8.2 hours

At the junctions in the IHX compartment there is also a change in the pressure difference due to the hydrostatic head term: $\rho_{IHX} \cdot g \cdot h$. The mass density in the IHX compartment decreases, see Figure 2-46, which is as a result of the change in the air/helium fraction in the IHX compartment, (Figure 2-45). The helium mass fraction in the RTC compartment and other compartments increases with the RTC compartment approaching 100% He after approximately 7 hours.

The pressure on either side of a junction is given by $P_{zone\_centre} \pm \rho_{zone} \cdot g \cdot h$. Once the pressure difference across a junction becomes negative there is inflow through that leakage junction into the reactor building at which point fission product release through the leakages ends. This occurs at 35 minutes and 5.5 hours for the lower and upper leakage junctions from the IHX to the environment respectively as seen in Figure 2-47. Inflow of air through leakages results in a further driving force for flow through the stack, Figure 2-48.

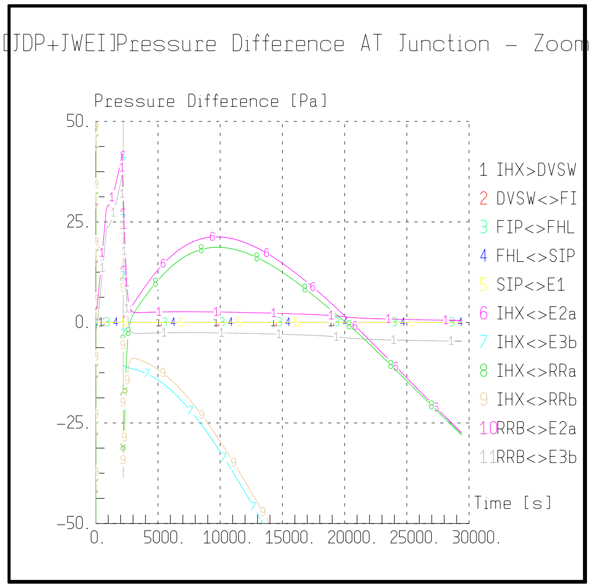

Figure 2-47: Pressure Difference at Junction at 8.2 hours

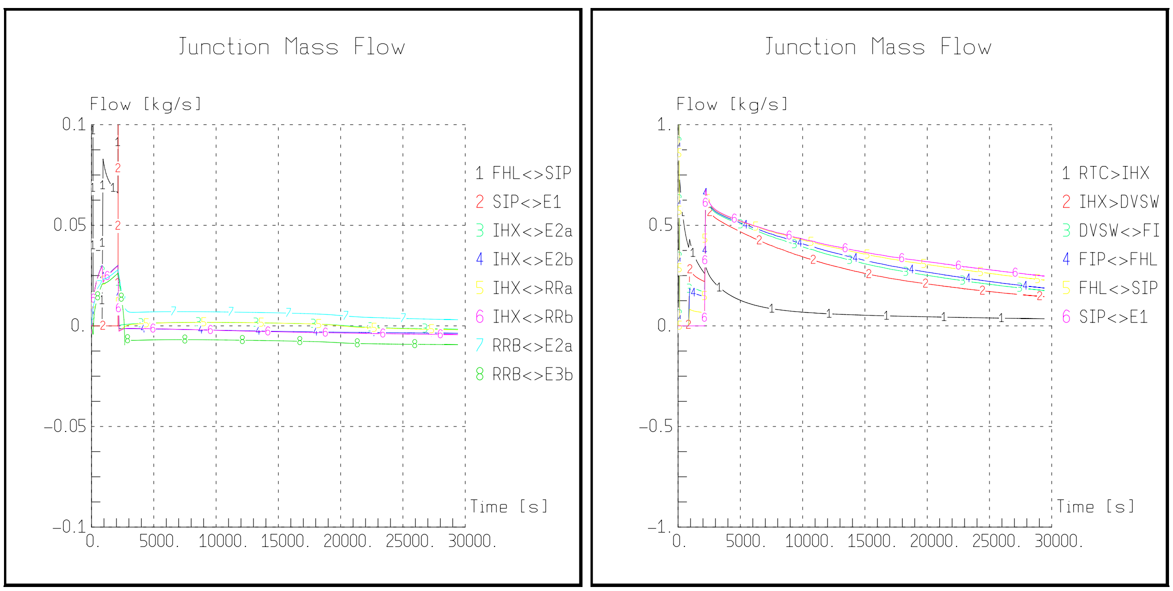

Figure 2-48: Junction Mass Flow at 8.2 Hours

<u>Phase 3 (t > 91 hours) – Post-Blowdown</u>

Flow from the RTC to the IHX compartment reverses after blowdown is completed at 91 hours, see Figure 2-49. This is due to the pressure in the RTC compartment now being lower than in the IHX compartment. The temperature in the RTC compartment decreases faster as it is cooling at a more rapid rate than in the IHX compartment and with the end of blowdown the pressure in the RTC compartment falls below that of the IHX compartment. Due to the reverse of flow between the IHX and the RTC, the Helium mass fraction of the gas mixture within the RTC starts to decrease as a result of air from the IHX flowing back into the RTC.

It should be noted that very small flows are observed post-blowdown, necessitating that the error bounds across junctions are kept very small in order for the code to obtain convergence.

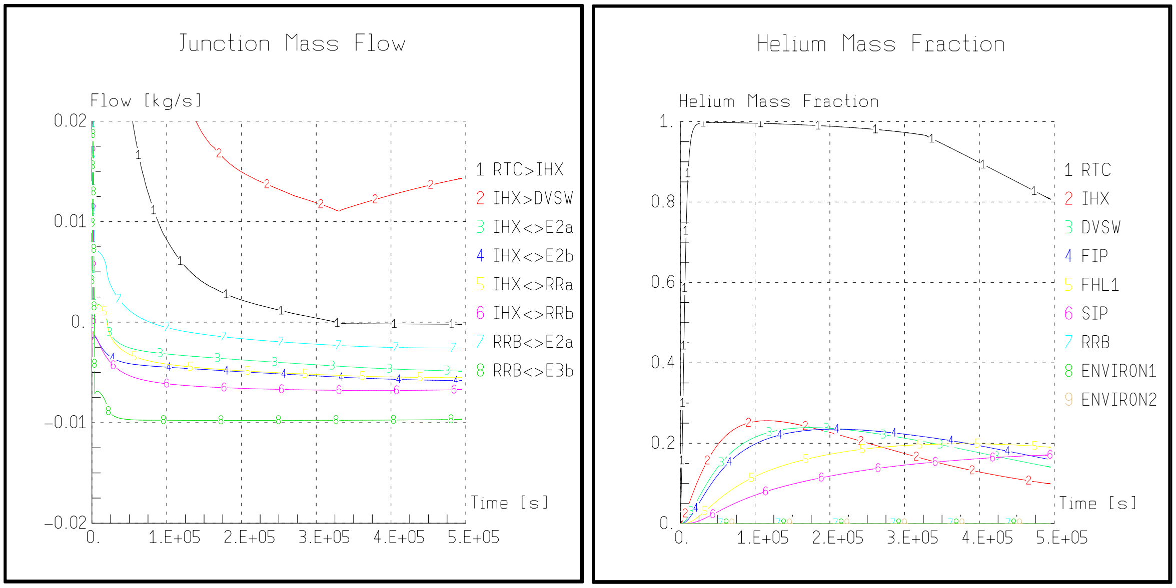

Figure 2-49: Junction Mass Flow and Helium Mass Fraction at 138 hours

2.4.3.2.2 Damper Closure Case

For the case with damper closure at 91 hours the evolution of the break, up until 91 hours, is the same as for the case with no damper closure.

The option of damper closure at the stack at 91 hours results in a rapid pressure buildup in the IHX compartment leading to the pressure difference across the upper leakage junctions changing from negative to positive, as seen in Figure 2-50. Flow reverses for the upper IHX leakage path so that flow is now to the environment again whilst the lower IHX leakage path continues to intake air into the Reactor Building as seen in Figure 2-50. The difference in pressure behavior at the junctions is due to the hydrostatic head term, where the pressures at the lower junction is given by $P_{zone\_centre} + \rho_{zone} \cdot g \cdot h$ and that at the upper junction is given by . $P_{zone\_centre} - \rho_{zone} \cdot g \cdot h$ The result is that a natural convection loop in the IHX renews release to the environment through the upper IHX leakage path, as seen in Figure 2-51.

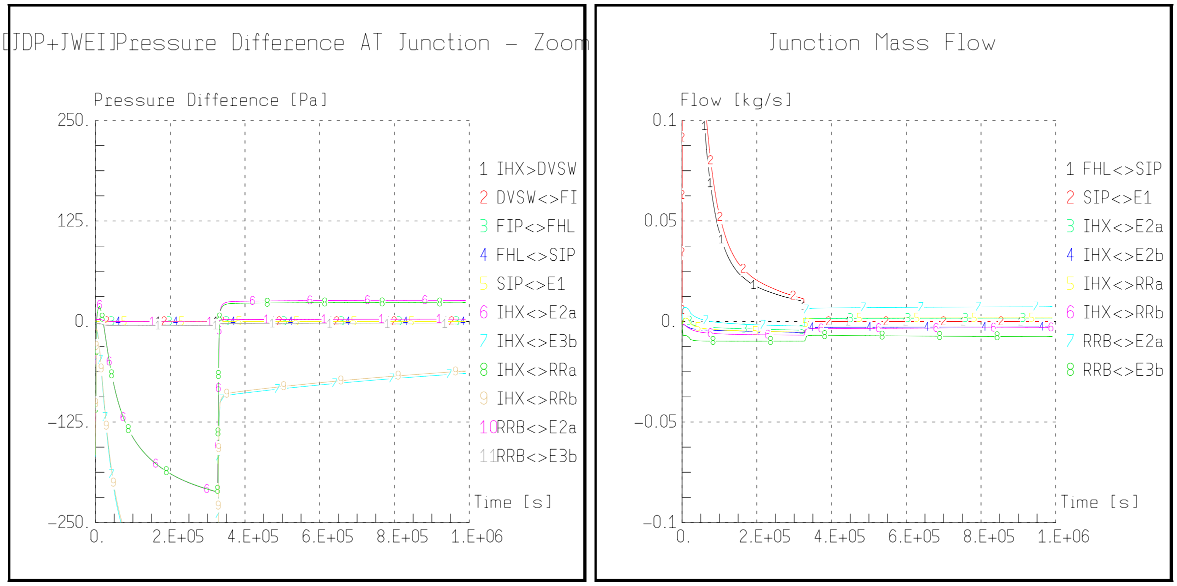

Figure 2-50: Pressure Difference at the Junction and Junction Mass Flow at 277 hours

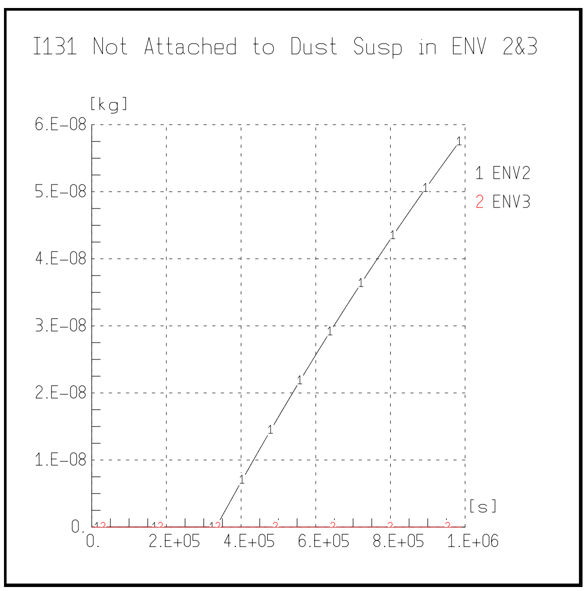

Figure 2-51: FP's not Attached to Dust Released through Leakages at 277 hours

2.4.3.2.3 Dust Distribution and Radionuclide Retention

Results are presented below for the distribution of the dust in the reactor building for the case with no damper and for the I-131 not attached to dust for the case with and without a damper. Note that the dust results for the case of damper closing has not been listed due to damper closing having an insignificant effect on the distribution of the dust due to most dust depositing before damper closing takes place. Therefore, the results in Table 2-14 can be considered correct for both the cases with and without the damper

Table 2-14: Distribution of Dust (% of Total Dust Mass Injected) at 300 Hours for a 4 mm Break with Leakage and with No Damper Closing

	Dust Deposited on Walls	Dust Deposited on Ceiling	Dust Deposited on Floor	Total Dust Deposited in Zone	Dust Suspended in Zone
RTC Compartment	26.11	0.97	< 0.01	27.08	0.31
IHX Compartment	0.05	< 0.01	67.64	67.69	0.00
DVS Compartment	< 0.01	< 0.01	3.47	3.47	< 0.01
FIP Compartment	< 0.01	< 0.01	0.60	0.60	< 0.01
FHL1 Compartment	< 0.01	< 0.01	0.46	0.46	< 0.01
SIP Compartment	< 0.01	< 0.01	0.19	0.19	< 0.01
RRB Compartment	< 0.01	< 0.01	0.01	0.01	< 0.01
ENVIRON1 (Stack Release)	< 0.01	< 0.01	< 0.01	< 0.01	0.20
ENVIRON2 (Leakages at 20.0 m)	< 0.01	< 0.01	< 0.01	< 0.01	0.01
ENVIRON3 (Leakages at 0.7 m)	< 0.01	< 0.01	< 0.01	< 0.01	< 0.01

NOTE: No Filtration is modeled in the ASTEC model

In Table 2-15 details of the percentage of RNs retained in the building are provided for various cases analyzed including the sensitivity cases in which the RNs are modeled as vapors. It can be seen that the retention for the aerosol case much larger than for the equivalent vapor case. The reason for this is that there is minimal retention of vapor in the RB as it does not interact with the surfaces, however the aerosol particles are modeled to interact and adhere to surfaces and hence have a greater retention factor.

Table 2-15: Radionuclide Retention (% Retained) in Reactor Building at 300 Hours for a 4 mm Break

	No Leakage, No Damper, Radionuclides Modeled as Vapor	With Leakage, No Damper, Radionuclides Modeled as Vapor	With Leakage, With Damper, Radionuclides Modeled as Vapor	With Leakage, No Damper, Aerosol Sensitivity Case	With Leakage, With Damper, Aerosol Sensitivity Case
Ag-110m	99.52	72.61	92.01	99.65	99.67
Ag-111	99.75	74.67	92.67	99.76	99.78
C-s137	99.97	85.87	95.33	99.93	99.92
I-131	99.91	80.98	94.17	99.87	99.87
I-133	99.76	74.13	92.53	99.77	99.78
Sr-90	99.99	96.01	98.34	99.98	99.96
Te-132	99.88	78.74	93.66	99.85	99.85

NOTE: No Filtration is modeled in the ASTEC model

The effect of the damper closing on the releases via the leak paths can be seen in Table 2-16 for the I-131 case. The highest leakage to the environment is observed for the damper closing case, with the stack releases being minimal. This has a large effect on the dose rates, with ground releases providing larger doses than stack releases. This is further discussed in Section 2.4.4.

Table 2-16: I-131 Distribution (% of Total I-131 Mass Injected) at 300 Hours for 4 mm Break

Compartment *	No Leakage, No Damper	With Leakage, No Damper	With Leakage, With Damper	With Leakage, No Damper, Aerosol Sensitivity Case	With Leakage, With Damper, Aerosol Sensitivity Case
RTC	48.92	49.39	49.47	88.24	86.73
IHX	45.72	10.86	25.94	9.34	10.76
DVSW	3.55	3.59	7.00	1.45	1.48
FIP	0.73	1.52	2.15	0.38	0.37
FHL1	0.80	8.38	3.42	0.35	0.35
SIP	0.19	7.27	1.11	0.15	0.12
RRB	< 0.01	< 0.01	5.12	< 0.01	0.05
ENVIRON1 (Stack Release)	0.09	19.03	0.69	0.13	0.08
ENVIRON2 (Leakage)	0.00	< 0.01	5.14	< 0.01	0.05
ENVIRON3 (Leakage)	0.00	< 0.01	< 0.01	< 0.01	< 0.01

* Compartment nomenclature as per Figure 2-1
NOTE: No Filtration is modeled in the ASTEC model

2.4.3.3 100 mm Break Study

2.4.3.3.1 No Damper Case

Phase 1 (t < 4 s) – Rupture Panels Break

High helium mass flow rates into the RTC compartment occur at the beginning of the break which results in the rupture panels all opening within the first 4 s as seen in Figure 2-52. Due to the high temperature of the incoming gas the temperature in the RTC compartment increases rapidly in the first few seconds peaking at a value just over 500 K (227°C) after 11 s.

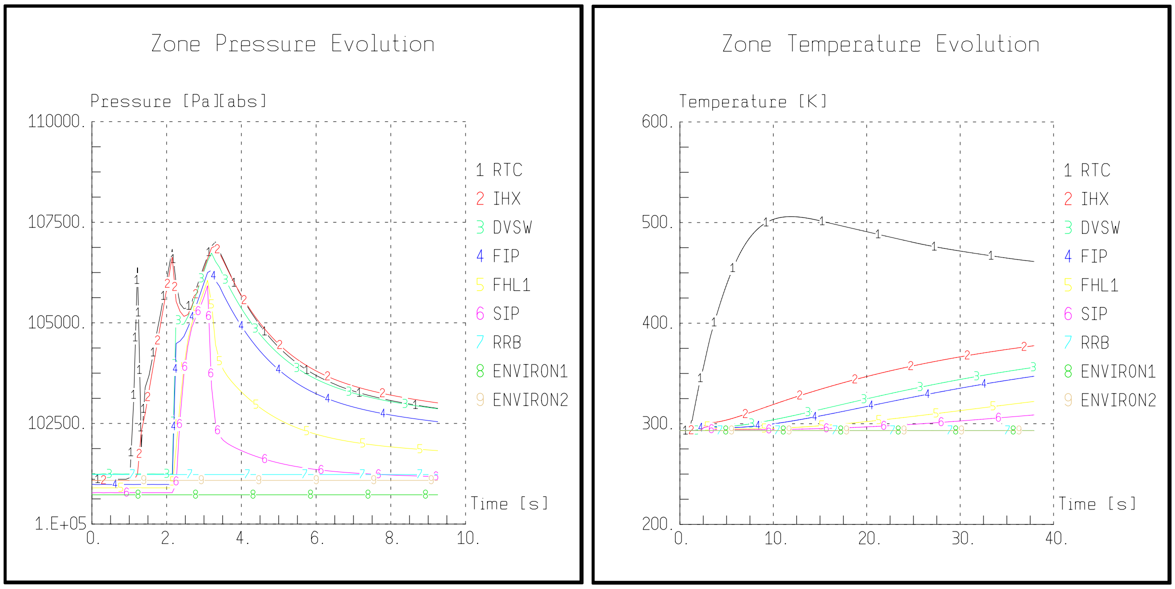

Figure 2-52: Zone Pressure and Temperature Evolution at 9 and 37 seconds

Phase 2 (t < 18 Hours) – Completion of Blowdown

The pressure at the centre of the IHX and connecting compartments, Figure 2-53, decreases rapidly due to the venting to atmosphere. The molar density in the IHX compartment can be seen in Figure 2-54.

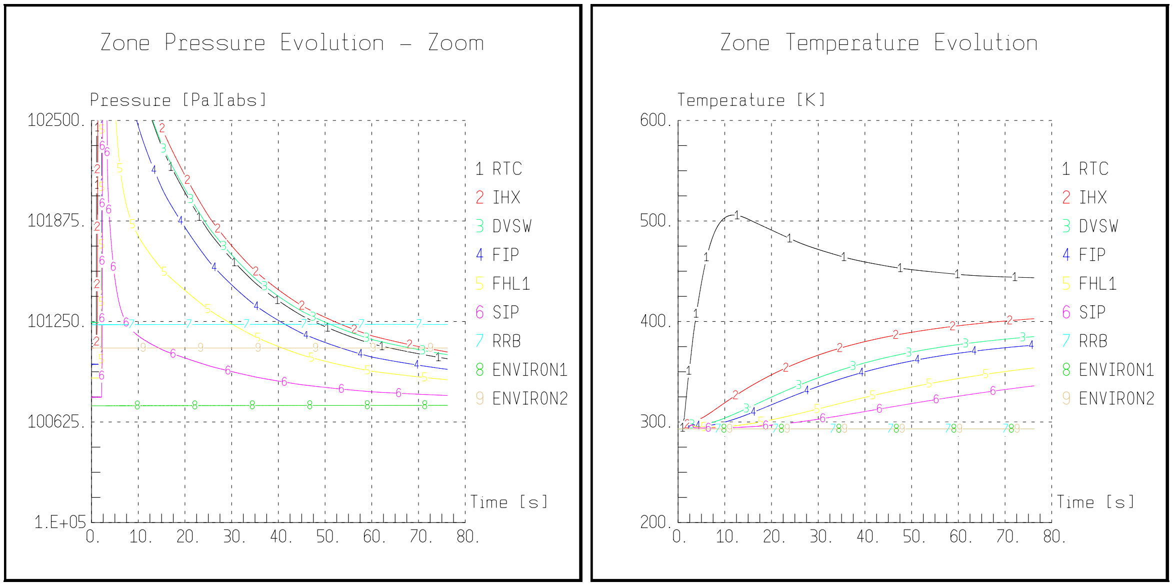

Figure 2-53: Zone Pressure and Temperature Evolution at 76 seconds

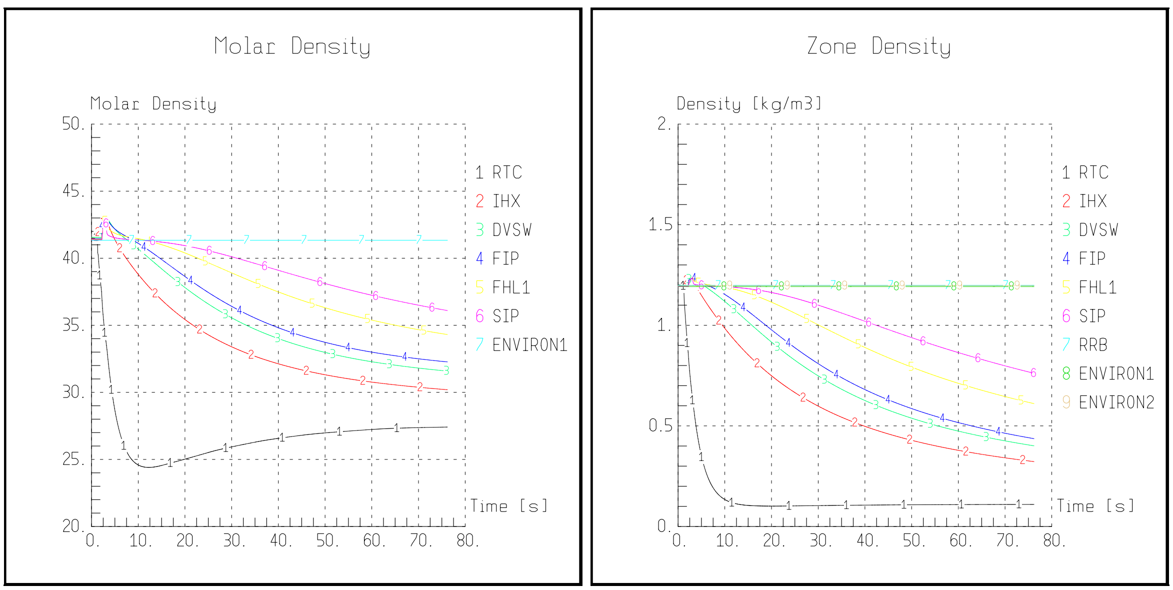

Figure 2-54: Zone Molar and Mass Density at 76 seconds

At the junctions in the IHX compartment there is also a change in the pressure difference due to the hydrostatic head term in the IHX compartment. The mass density in the IHX decreases, see Figure 2-54, which is as a result of the change in the air/helium fraction in the IHX compartment, see Figure 2-55. The helium mass fraction in the RTC compartment and other compartments increases with the RTC compartment helium fraction approaching 100% He after approximately 25 seconds, Figure 2-55.

The pressure on either side of a junction is given by $P_{zone\_centre} \pm \rho_{zone} \cdot g \cdot h$. Once the pressure difference across a junction becomes negative there is inflow through that leakage junction into the reactor building at which point fission product release through the leakages ends. This occurs at 50 – 70 s for the lower and upper leakage junctions to the environment from the IHX respectively as seen in Figure 2-55. Inflow of air through leakages results in a further driving force for flow through the stack, Figure 2-56.

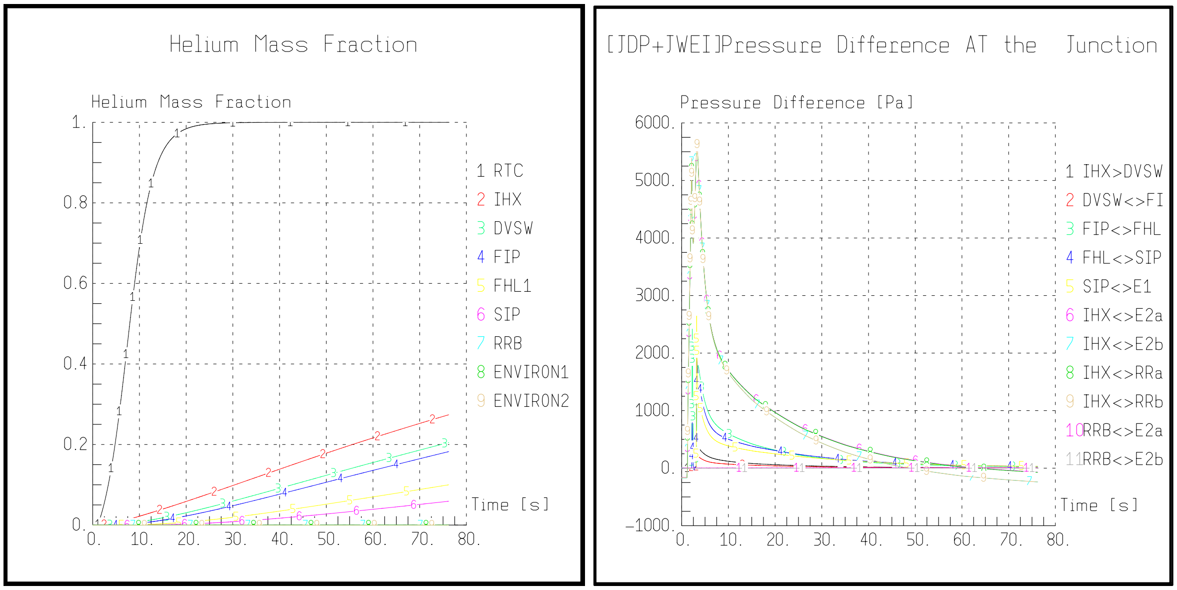

Figure 2-55: Helium Mass Fraction and Junction Pressure Difference at 76 seconds

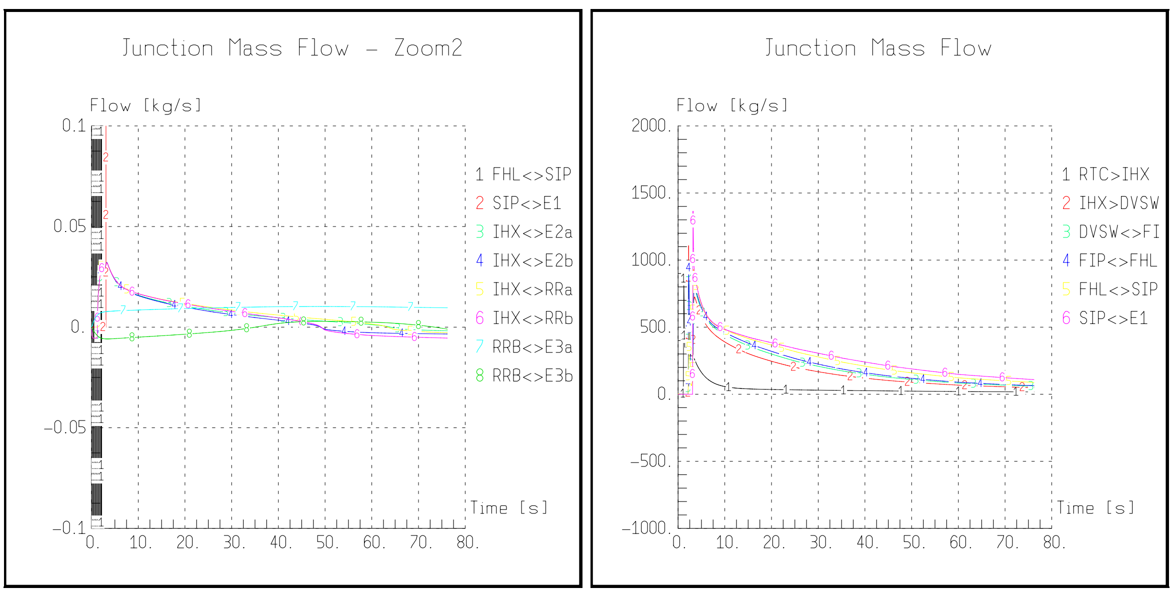

Figure 2-56: Junction Mass Flow at 76 seconds

The temperatures in the compartments drop at different rates, see Figure 2-57, depending on the temperatures and the surface area to volume ratio of the compartment.

The cooling of vent shaft compartments causes the flow from the vent shaft to the environment to reverse at around 7 minutes, see Figure 2-58, and release of fission products and dust out of the reactor building to environment ceases at this point. The building pressure begins to increase slightly due to inflow of air through stack and leakages, see Figure 2-57.

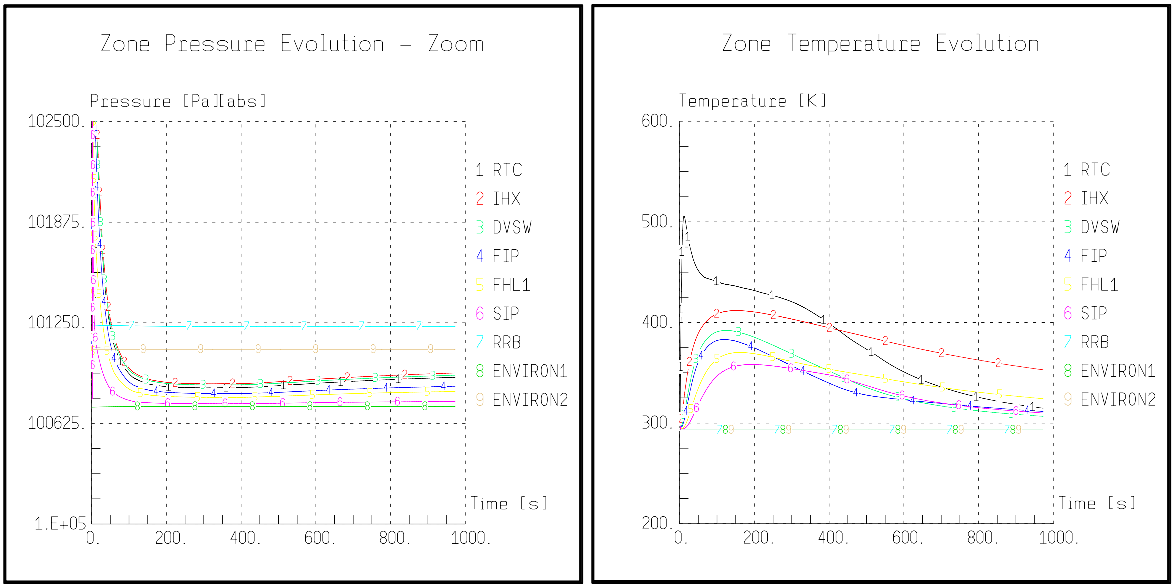

Figure 2-57: Zone Pressure and Temperature Evolution at 16 minutes

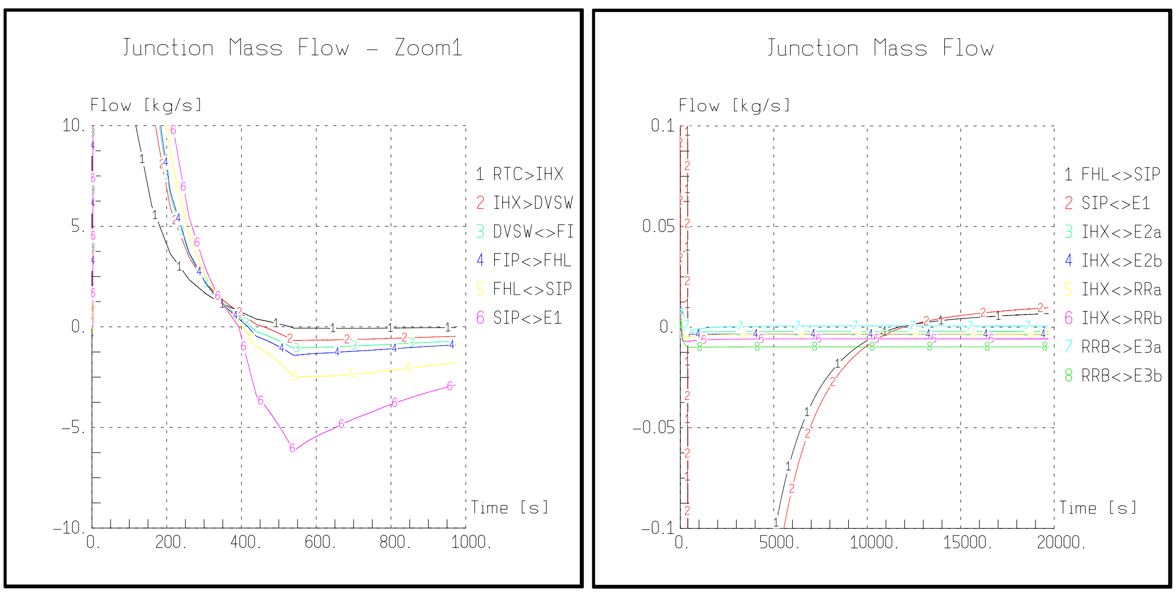

Figure 2-58: Junction Mass Flow at 16 minutes

At approximately 3.5 hours the flow through the vent shaft reverses again and release through the stack resumes, see Figure 2-58.

Phase 3 (t > 18 Hours)

At approximately 18 hours, after blowdown is complete, the flow from the RTC compartment to IHX reverses. This has important implications for the release to environment of fission products released from the core during core heat-up as these are released after the mass flow between the RTC and IHX compartment reverses, see Figure 2-59 and Figure 2-60. Thus, fission products released into the RTC compartment after the flow reverses are retained in the RTC compartment.

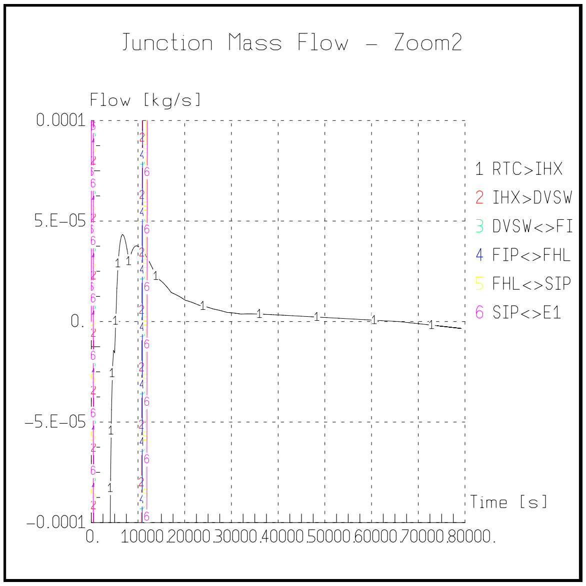

Figure 2-59: Junction Mass Flow at 22 hours

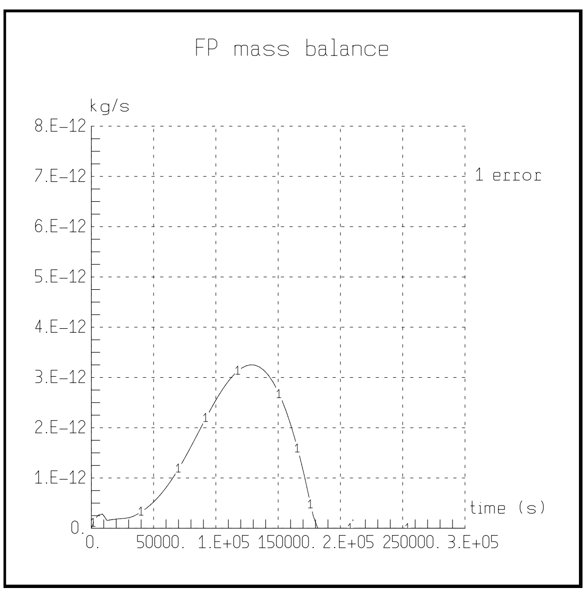

Figure 2-60: Mass Release Rates of Fission Products into RTC Compartment as a Function of Time

2.4.3.3.2 Damper Closure Case

The option of damper closure at the stack at 50 hours results in a rapid pressure build-up in the IHX compartment leading to the pressure difference across the upper leakage junctions becoming positive from having been negative prior to damper closure, see Figure 2-61. Flow reverses for the upper IHX leakage path so that flow is now to the environment again whilst the lower IHX leakage path continues to intake air into the RB as seen in Figure 2-61. The difference in pressure behavior at the junctions is due to the hydrostatic head term where the pressures at the lower junction is given by $P_{zone\_centre} + \rho_{zone} \cdot g \cdot h$ and that at the upper junction is given by $P_{zone\_centre} - \rho_{zone} \cdot g \cdot h$. The result is that a natural convection loop in the IHX renews release to the environment through the upper IHX leakage path, see Figure 2-62.

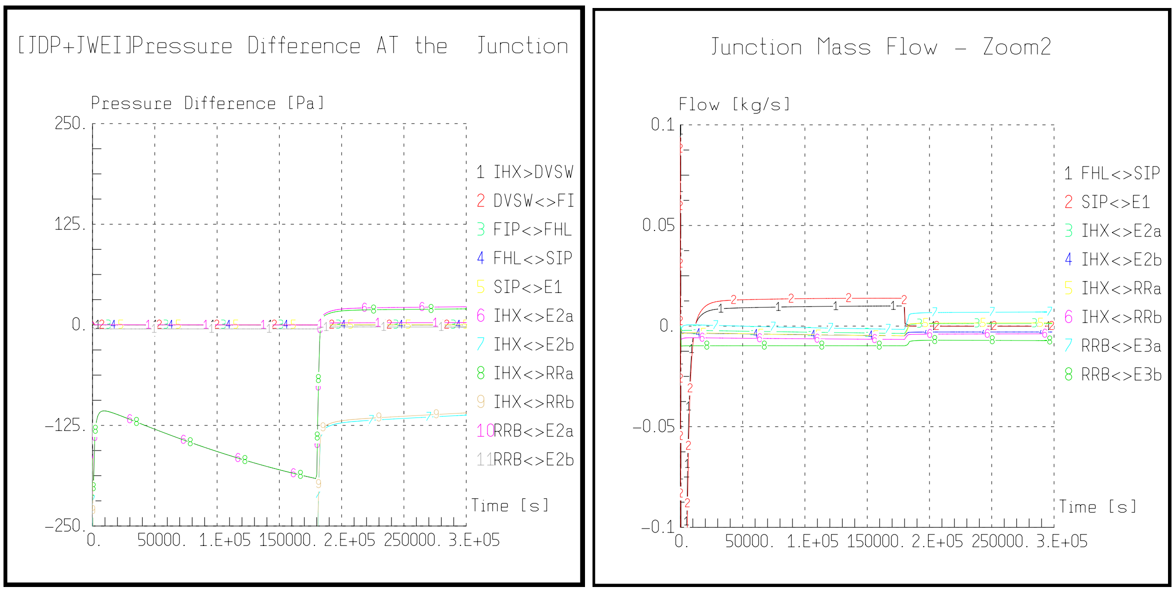

Figure 2-61: Pressure Difference at the Junction at 83 hours

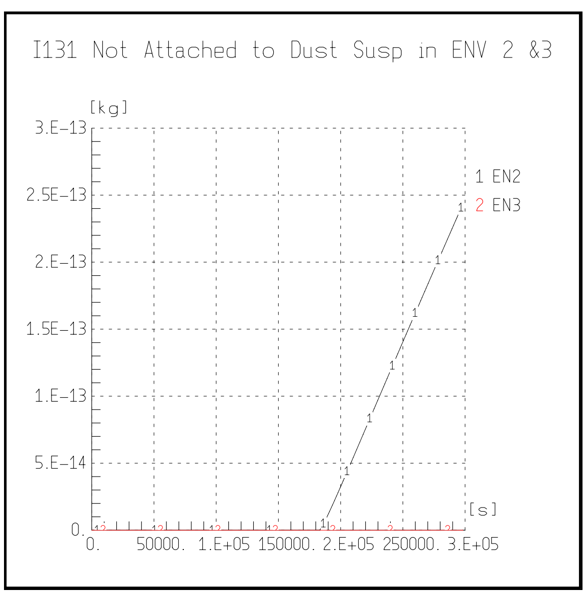

Figure 2-62: I-131 Not Attached to Dust Released Through Leakages at 83 hours

2.4.3.3.3 Dust Distribution and Radionuclide Retention

Similar observations to those made for the 4mm break case in terms of the effect of aerosols and damper closing can be drawn from the results of the 100mm break case as shown in paragraph 2.4.3.3.1 and 2.4.3.3.2 above.

Table 2-17: Distribution of Dust (% of Total Dust Mass Injected) at 300 Hours for a 100 mm Break with No Damper Closing

	Dust Deposited on Walls	Dust Deposited on Ceiling	Dust Deposited on Floor	Total Dust Deposited in Zone	Dust Suspended in Zone
RTC Compartment	0.87	1.80	0.00	2.67	0.49
IHX Compartment	0.13	0.03	41.75	41.91	<0.01
DVS Compartment	0.02	0.12	10.54	10.68	<0.01
FIP Compartment	<0.01	0.01	4.22	4.23	<0.01
FHL1 Compartment	<0.01	<0.01	10.65	10.66	<0.01
SIP Compartment	<0.01	<0.01	4.66	4.66	<0.01
RRB Compartment	<0.01	<0.01	<0.01	<0.01	<0.01
ENVIRON1 (Stack Release)	<0.01	<0.01	<0.01	<0.01	22.09
ENVIRON2 (Leakages at 20.0 m)	<0.01	<0.01	<0.01	<0.01	<0.01
ENVIRON3 (Leakages at 0.7 m)	<0.01	<0.01	<0.01	<0.01	<0.01

* Compartment nomenclature as per Figure 2-1
NOTE: No Filtration is modeled in the ASTEC model

Table 2-18: Fission Product Retention (% Retained) in Reactor Building at 300 Hours for a 100 mm Break

	No Leakage, No Damper	With Leakage, No Damper	With Leakage, With Damper	With Leakage, No Damper, Aerosol Sensitivity Case
Ag-110m	99.33	98.51	99.11	99.33
Ag-111	99.97	99.79	99.92	99.98
C-s137	91.84	91.78	91.87	91.90
I-131	99.86	99.67	99.81	99.86
I-133	99.70	98.76	99.45	99.70
Sr-90	87.44	87.52	87.54	87.53
Te-132	99.86	99.68	99.81	99.86

NOTE: No Filtration is modeled in the ASTEC model

Table 2-19: I-131 Distribution (% of Total I-131 Mass Injected) at 300 Hours for 100 mm Break

Compartment *	No Leakage, No Damper	With Leakage, No Damper	With Leakage, With Damper	With Leakage, No Damper, Aerosol Sensitivity Case
RTC	98.83	98.71	98.71	98.72
IHX	0.73	0.44	0.56	0.70
DVSW	0.12	0.11	0.15	0.13
FIP	0.04	0.04	0.05	0.04
FHL1	0.10	0.14	0.11	0.10
SIP	0.04	0.09	0.04	0.04
RRB	0.00	0.00	0.05	< 0.01
ENVIRON1 (Stack Release)	0.14	0.33	0.15	0.14
ENVIRON2 (Leakage)	0.00	< 0.01	0.05	< 0.01
ENVIRON3 (Leakage)	0.00	< 0.01	< 0.01	< 0.01

* Compartment nomenclature as per Figure 2-1
NOTE: No Filtration is modeled in the ASTEC model

2.4.4 Radiological Consequences at Site Boundary

2.4.4.1 Description of Dose Cases

For each break size, a number of offsite dose cases are analyzed to evaluate various RB options, responses and assumptions regarding the characteristics of the source term. A description of the cases follows:

Case 1: No RB retention cases
Case 2: RB retention with successful opening and failure to reclose the Depressurization Vent Shaft (DVS)
Case 3: RB retention with successful opening and closing of the DVS
Case 4: RB retention with successful opening and failure to reclose the DVS (Case 2) with no RB leakage pathways

The no RB retention cases assume that the release from the PHTS is directly to the environment at ground level with no RB retention. These cases are selected to create a baseline to understand the importance of different RB retention characteristics defined in other cases.

For the RB retention cases, a RB is included containing a DVS that opens at set pressure to the environment at an elevation of 50 m above ground level. Releases from the DVS are referred to as stack releases. In cases 2 and 3, there are also pathways to the environment at ground level to simulate RB leakage pathways. Case 4 is a sensitivity case in which the RB leakage pathways are not included. This case is included to help understand the effect of the natural circulation that develops when the leakage pathways are included.

For the cases in which the reclosing of the DVS is successful, the DVS damper closes at a given time preventing any further release from the RB through the DVS pathway. For the 4 mm break, the damper closes at the end of blowdown, 91 hrs. For the 100 mm break, the damper closes at 50 hr when the release to the RB from the PHTS ends due to the end of PHTS thermal expansion and the onset of PHTS thermal contraction.

For each case, various options regarding DVS filtration and the characteristics of the source term are evaluated. These options for each case are described below:

Option a: No DVS filtration, non-dust RNs are vapor
Option b: DVS filtration, non-dust RNs are vapor
Option c: No DVS filtration, non-dust RNs are 10-7m aerosols
Option d: DVS filtration, non-dust RNs are 10-7m aerosols

Note that all of the initial circulating activity in the PHTS due to resuspension is assumed to be on dust particles. All of the delayed releases are assumed to not attach to dust and be of one form only. Hence, depending on the above option, all of the delayed fuel releases were assumed to be either 100% vapor or 100% aerosol. Mixtures of dust, aerosol, and vapor are considered in the barrier allocation task as discussed in Section 3.

For the filtration cases, 99% filtration is assumed for all DVS dust and aerosol releases and 0% filtration is assumed for all DVS vapor releases. No filtration is assumed for ground level dust, aerosol and vapor releases in all cases.

For the vapor cases, the delayed release from the fuel enters the RB as vapor. There is no deposition in the RB assumed for the vapor RNs. The only RB retention for the vapor RNs is the result of the holdup in the RB due to the transport from one RB volume to the next. Vapor dose conversion factors (DCFs) are used for I and Te isotopes. Vapor DCFs are not currently available for the metallic RNs so the default solubility/particulate class DCFs are used for the metal RNs. The default classes have the greatest DCFs values and result in the largest doses. I and Te vapor DCFs are approximately a factor of 3 greater than the default particulate DCFs. For the aerosol cases, the delayed release from the fuel enters the RB as aerosols. Deposition and settling occur in all compartments for the aerosols. Default particulate DCFs are used for the aerosols.

The complete set of offsite dose cases with various combinations of break size, RB response, filtration, and RN form are listed in Table 2-20.

Table 2-20 Radiological Dose Cases Analyzed

Case No.	PHTS HPB Break Size	RB Retention Modeled	RB Leakage Modeled	DVS Damper Reclosure	Form of Non-Dust RNs	DVS Filtration
1a(4)	**4mm**	**No**	**n/a**	**n/a**	**Vapor**	**n/a**
1c(4)	4mm	No	n/a	n/a	Aerosol	n/a
2a(4)	**4mm**	**Yes**	**Yes**	**No**	**Vapor**	**No**
2b(4)	4mm	Yes	Yes	No	Vapor	Yes
2c(4)	4mm	Yes	Yes	No	Aerosol	No
2d(4)	4mm	Yes	Yes	No	Aerosol	Yes
3a(4)	**4mm**	**Yes**	**Yes**	**Yes**	**Vapor**	**No**
3b(4)	4mm	Yes	Yes	Yes	Vapor	Yes
3c(4)	4mm	Yes	Yes	Yes	Aerosol	No
3d(4)	4mm	Yes	Yes	Yes	Aerosol	Yes
4a(4)	4mm	Yes	No	No	Vapor	No
1a(100)	100mm	No	n/a	n/a	Vapor	n/a
1c(100)	100mm	No	n/a	n/a	Aerosol	n/a
2a(100)	100mm	Yes	Yes	No	Vapor	No
2b(100)	100mm	Yes	Yes	No	Vapor	Yes
2c(100)	100mm	Yes	Yes	No	Aerosol	No
2d(100)	**100mm**	**Yes**	**Yes**	**No**	**Aerosol**	**Yes**
3a(100)	100mm	Yes	Yes	Yes	Vapor	No
3b(100)	100mm	Yes	Yes	Yes	Vapor	Yes

2.4.4.2 Effective Dose Conversion Factors

For the RB retention cases, four contributions to the dose are considered for each RN, the dose resulting from ground level aerosol release, the ground level vapor release, the stack level aerosol release and the stack level vapor release. The differences in the effective dose conversion factor (eDCF) for each of the four release modes are important in the understanding of the differences in the doses in the various RB retention cases. For each release mode, the thyroid CEDE eDCF is the product of the breathing rate, X/Q weather dispersion factor and the DCF. A comparison of the thyroid CEDE eDCFs for I-131 is shown in Table 2-19. Differences in the eDCFs are the result of differences in the X/Q and DCFs. The stack X/Q is an order of magnitude less than the ground level X/Q and the I-131 vapor DCF is a factor of 3 greater than the aerosol DCF. The net result is that the greatest eDCF is for the ground level vapor release and the smallest eDCF is for the stack level aerosol release. These values differ by a factor of approximately 40.

Table 2-21 Evaluation and Comparison of Effective Dose Conversion Factors (eDCF)

	X/Q (s/m³)	DCF (Sv/Bq)	eDCF (Sv/Bq)
Ground level vapor	2.6E-05	3.93E-07	2.4E-15
Ground level particulate/aerosol	2.6E-05	1.47E-07	8.9E-16
Stack level vapor	1.9E-06	3.93E-07	1.7E-16
Stack level particulate/aerosol	1.9E-06	1.47E-07	6.5E-17

2.4.4.3 No Reactor Building Retention Cases

The no RB retention cases evaluate the doses due to releases from the PHTS directly to the environment at ground level with not RB retention. These cases are evaluated to create a baseline to understand the importance of different RB retention characteristics defined in the other cases, but also to compare to results obtained from the 2008 study. The results for the no RB retention cases are listed in Table 2-22

Table 2-22 Radiological Doses for No RB Retention Cases

Case No.	Break Size (mm)	Form of Non-Dust RNs	Total I-131 Release (Ci)	Thyroid CEDE (mrem)	Ratio of Thyroid PAG Limit to Thyroid CEDE	TEDE (mrem)	Ratio of NRC TEDE Limit to TEDE
1a(4)	4	Vapor	1.6E+02	2.0E+03	2.5E+00	1.4E+02	1.8E+02
1c(4)	4	Aerosol	1.6E+02	7.3E+02	6.9E+00	6.3E+01	4.0E+02
1a(100)	100	Vapor	4.3E-01	5.7E+00	8.7E+02	4.3E-01	5.8E+04
1c(100)	100	Aerosol	4.3E-01	2.1E+00	2.4E+03	2.2E-01	1.2E+05

The results indicate that no RB retention is needed in order to meet the offsite dose limits based on the realistic assumptions used in this study. The dose from the most limiting case, 1a(4) is a factor of 2.5 less than the thyroid PAG limit. This conclusion differs from the 2008 NGNP RB Report [1] conclusion for the no RB retention case, in which the thyroid dose limits were exceeded by a factor of 2. An evaluation of the impact of uncertainties in the mechanistic source term and dose calculation on the capability to meet the dose limits is assessed in Section 3 in the course of determining barrier retention allocations.

The smaller, 4mm break size is the more limiting dose case due to the larger releases from the PHTS. The 4mm release from the PHTS is 160Ci vs 0.43Ci for the 100mm break. The larger releases in the smaller break are due to the delayed fuel release occurring concurrent with the blowdown resulting in a larger transport mechanism from the PHTS as opposed to the majority of the delayed fuel release occurring post-blowdown in the 100mm break. The 100mm breaks are not large enough to generate shear force ratios high enough to develop large contributions from lift-off and resuspension of initially deposited RNs.

As expected, if the RNs that are not attached to dust are assumed to be in the vapor form, the doses are higher by a factor of 2-3 compared to the aerosol case, consistent with the difference in the DCFs. The contributions to the total dose for each RN are given in Table 2-21 for the highest dose case, Case 1a(4). I-131 and Te-132 are the key contributors to both the thyroid CEDE and the TEDE. For the thyroid CEDE, I-131 and Te-132 contribute 69% and 16% and for the TEDE, I-131 and Te-132 contribute 50% and 15%, respectively.

Table 2-23 Radionuclide Contributions to Case 1a(4) Dose

Radionuclide	Thyroid CEDE (mrem)	TEDE (mrem)	Contribution to Total Thyroid CEDE (%)	Contribution to Total TEDE (%)
Ag-110m	4.0E-01	1.4E+00	<.1	1.0
Ag-111	3.5E-02	7.0E-01	<.1	0.5
Cs-37	1.0E+00	1.1E+01	<.1	7.9
I-131	**1.4E+03**	**6.9E+01**	**68.7**	**50.3**
I-133	1.1E+02	6.1E+00	5.7	4.4
Sr-90	3.1E-03	8.2E-01	<.1	.6
Te-132	**3.1E+02**	**2.1E+01**	**15.5**	**15.3**
Subtotal	**1.8E+03**	**1.1E+02**	**90**	**80**
Other RNs Estimate	**2.0E+02**	**2.7E+01**	**10**	**20**
Total Estimate	**2.0E+03**	**1.4E+02**	**100**	**100**

The Case 1a(4) TEDE is a factor of 3 less and the thyroid CEDE is a factor of 5 less than the similar 2008 no RB retention case doses for a 3mm break. The differences in the doses are due to many contributing factors which are summarized in Table 2-22. A major contributor to the reduced dose is the reduction in the RN releases from the fuel by a factor of 4 (265 Ci vs 1040 Ci). This can be directly attributed to the lower observed fuel temperatures which in turn are directly related to the lower operating temperatures. Also, a smaller percentage of the RN release from the fuel is released from the PHTS (58% vs 82%) in the current results. This difference is due primarily to differences in the Flownex calculation of the blowdown temperatures throughout the PHTS compared with simple assumptions made for the PHTS average temperatures in the 2008 simplified two volume PHTS model. In addition, the scaling factors are different because the 2008 model only explicitly tracked 2 RNs, Cs-137 and I-131 compared with the 7 RNs in the current model.

Table 2-24 Comparison of Current and 2008 Study for No RB Retention Case

	3mm 2008 RB Report No RB Retention	4mm Current Case 1a(4)
Core inlet/outlet temperatures, °C	350 °C/950 °C	280 °C/750 °C
SS helium mass in PHTS, kg	3272	3920
Helium mass in PHTS at end of blowdown, kg	25	94
Blowdown time, hr	102	91
Maximum fuel temperature for fuel release calculations, °C	1741	1634
Cumulative I-131 release from fuel to PHTS at 300hr, Ci	1040	265
Cumulative I-131 release from PHTS to RB at 300hr, Ci	850 (82% of fuel release)	155 (58% of fuel release)
Weather X/Q, s/m^3	2.3E-5 (425 m EAB)	2.6E-5 (400 m EAB)
I-131 thyroid CEDE DCF for delayed releases, Sv/Bq	2.92E-7 (FGR11 particulate)	3.93E-7 (FGR13 vapor)
TEDE scaling factor	1/0.4 =2.5	1/0.8=1.25
Thyroid CEDE scaling factor	1/0.5=2.0	1/0.9=1.11

2.4.4.4 Reactor Building Retention Cases

For the RB retention cases, the RN releases from the ASTEC RB model are used to determine the offsite doses. Since ASTEC provides details on stack releases as well as ground level leakage releases, the stack and ground level contributions to the doses can be evaluated and then summed to determine the total doses.

The radiological doses for all the RB retention cases are listed in Table 2-25. In Table 2-26 some of the key results from both the no RB retention and the RB retention cases are succinctly summarized. The key cases are:

- Case 1a(4) No RB retention case with the highest dose of all cases
- Case 2a(4) RB retention case with the maximum release
- Case 3a(4) RB retention case with the maximum dose
- Case 2d(100) RB retention case with the minimum dose

Table 2-25 Radiological Doses for RB Retention Cases

Case No.	Break Size (mm)	RB Leakage	DVS Damper Reclosure	Form of Non-Dust RNs	DVS Filtration	Total I-131 Release (Ci)	Thyroid CEDE (mrem)	Ratio of Thyroid PAG Limit to Thyroid CEDE	TEDE (mrem)	Ratio of NRC TEDE Limit to TEDE
2a(4)	4	Yes	No	Vapor	No	**3.0E+01**	2.9E+01	1.7E+02	1.9E+00	1.3E+04
2b(4)	4	Yes	No	Vapor	Yes	3.0E+01	2.9E+01	1.7E+02	1.9E+00	1.3E+04
2c(4)	4	Yes	No	Aerosol	No	1.9E-01	7.2E-02	6.9E+04	6.0E-03	4.2E+06
2d(4)	4	Yes	No	Aerosol	Yes	2.0E-03	8.5E-04	5.9E+06	7.7E-05	3.2E+08
3a(4)	4	Yes	Yes	Vapor	No	9.1E+00	**1.1E+02**	4.7E+01	**7.2E+00**	3.5E+03
3b(4)	4	Yes	Yes	Vapor	Yes	9.1E+00	1.1E+02	4.7E+01	7.2E+00	3.5E+03
3c(4)	4	Yes	Yes	Aerosol	No	2.0E-01	3.9E-01	1.3E+04	3.4E-02	7.4E+05
3d(4)	4	Yes	Yes	Aerosol	Yes	7.6E-02	3.5E-01	1.4E+04	3.0E-02	8.3E+05
4a(4)	4	No	No	Vapor	No	1.4E-01	1.5E-01	3.3E+04	1.0E-02	2.4E+06
2a(100)	100	Yes	No	Vapor	No	1.4E-03	1.4E-03	3.5E+06	4.3E-04	5.9E+07
2b(100)	100	Yes	No	Vapor	Yes	8.5E-04	1.2E-03	4.3E+06	9.4E-05	2.7E+08
2c(100)	100	Yes	No	Aerosol	No	5.7E-04	2.5E-04	2.0E+07	3.4E-04	7.4E+07
2d(100)	100	Yes	No	Aerosol	Yes	5.8E-06	**2.6E-06**	1.9E+09	**3.6E-06**	7.0E+09
3a(100)	100	Yes	Yes	Vapor	No	8.3E-04	4.1E-03	1.2E+06	6.4E-04	3.9E+07
3b(100)	100	Yes	Yes	Vapor	Yes	2.7E-04	3.9E-03	1.3E+06	3.0E-04	8.2E+07

Table 2-26 Dose Results for Key RB Retention Cases

Dose Analysis Case	I-131 Ground Release (Ci)	I-131 Stack Release (Ci)	I-131 Total Release (Ci)	Thyroid CEDE (mrem)	TEDE (mrem)
Case 1a(4) **No RB Retention Max Dose Case** **4 mm break, non-dust RNs are vapor**	**155**	**n/a**	**155**	**2000**	**140**
Case 2a(4) **RB Retention Max Release Case** **4 mm break, DVS damper fails to reclose, no filtration, non-dust RNs are vapor**	**2.8E-5**	**30**	**30**	**29**	**1.9**
Case 3a(4) **RB Retention Max Dose Case** **4 mm break, DVS damper recloses, no filtration, non-dust RNs are vapor**	**8.0**	**1.1**	**9.1**	**110**	**7.2**
Case 2d(100) **RB Retention Min Dose Case** **100 mm break, DVS damper fails to reclose, 99% filtration of stack particulates/aerosols, non-dust RNs are aerosol**	**2.2E-8**	**5.7E-6**	**5.8E-6**	**2.6E-06**	**3.6E-06**

The RB retention case that results in the maximum I-131 total release is case 2a(4), a 4mm break with unsuccessful reclosing of the DVS damper, without filtration and the non-dust RNs are assumed to be in vapor form. The I-131 release for this case is 30Ci compared to 155Ci for a similar no RB retention case, a reduction of a factor of 5. For the same two cases, the doses are reduced by a much larger factor, a factor of about 70 because the release is mainly via the stack which has a X/Q that is an order of magnitude less than the X/Q for the ground level release in the no RB retention case. In this case, in which the DVS damper remains open, release through the stack dominates and ground level release is negligible in comparison. A RB natural circulation pattern develops that continues release through the stack post-blowdown.

Interestingly, the RB retention case with the maximum I-131 release is not also the case that results in the maximum offsite doses. The case that results in the maximum offsite doses is case 3a(4), a 4mm break, with successful reclosing of the DVS damper, without filtration and the non-dust RNs are assumed to be in vapor form. For this case, the total I-131 release is 9Ci but of these, 8Ci are ground level release. When the damper closes, there is no further release from the stack but as pressure builds slightly in the RB more release exits through the ground level RB leakage paths relative to the open damper case. Since, the ground level X/Q is an order of magnitude greater than the stack X/Q, this case has higher doses than the open damper maximum release case which had a greater total release of 30Ci. For cases with RB retention, the maximum offsite thyroid CEDE is 110mrem and the maximum TEDE is 7.2mrem, both well within dose limits and a factor of approximately 20 less than the no RB retention case.

The RB retention case with the minimum doses is case 2d(100), a 100mm break with unsuccessful reclosing of the DVS damper, with filtration and the non-dust RNs are assumed to be in aerosol form. The minimum offsite thyroid CEDE is 2.6E-06mrem and the TEDE is 3.5E-06mrem for this case. The thyroid CEDE is 6 orders of magnitude less than the comparable no RB retention case, case 1c(100). This large difference is the net result of including a multivolume RB DVS, RB settling and deposition for the aerosols and DVS filtration of the aerosols.

2.4.4.5 Interpretation of Radiological Dose Results

2.4.4.5.1 Effect of Break Size on RB Retention Cases

Comparisons of the 4mm Case 2a(4) and 100mm Case 2a(100) dose results for the cases in which the DVS damper fails to reclose, with no DVS filtration and the non-dust aerosols are assumed to be vapors are given in Figures 2-63 and 2-64. In the 100mm cases, the contribution of the initial release that is attached to dust to the total dose is greater than in the 4mm cases because the blowdown ends before the time of any significant delayed release from the fuel. Early in the transient, the cumulative dose is greater for the 100mm cases. The dose due to the prompt release of the RNs attached to dust is greater in the larger break due to the shorter blowdown and increased rate of transport to the RB during the blowdown. Conversely, the dose due to the delayed release is much less in the 100 mm break as the blowdown is complete before any significant delayed release from the fuel occurs. This is consistent with 2008 RB study results.

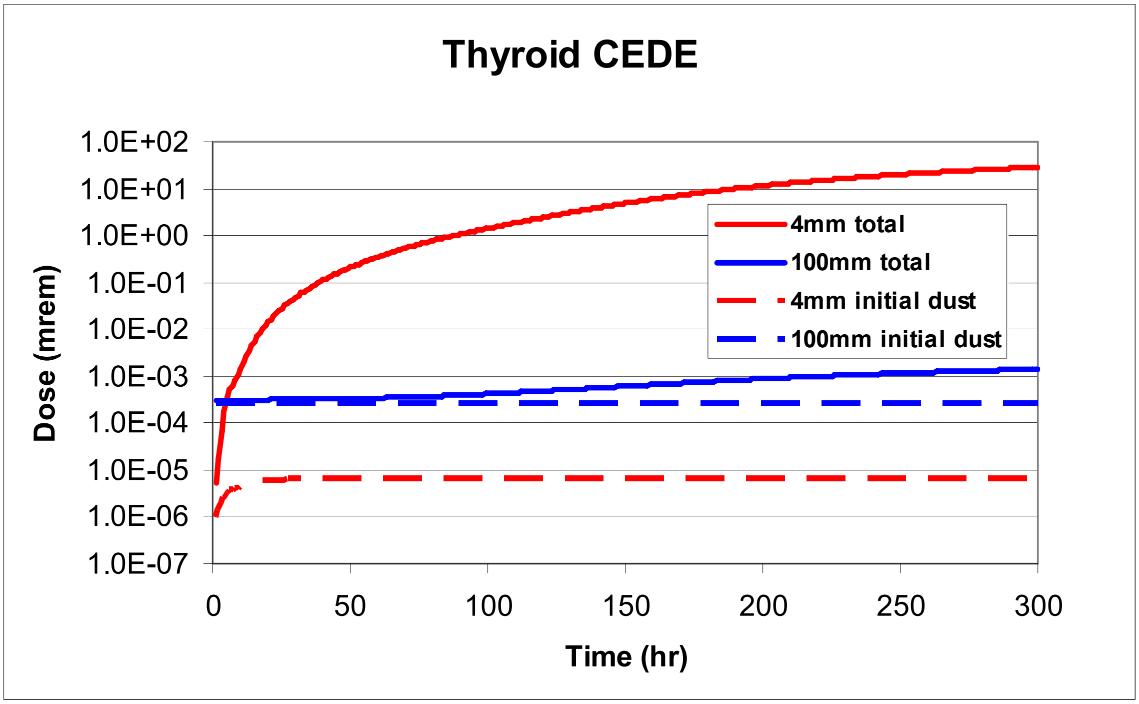

Figure 2-63 Comparison of Time Dependent Thyroid CEDE for 4mm [2a(4)] and 100mm [2a(100)] Breaks

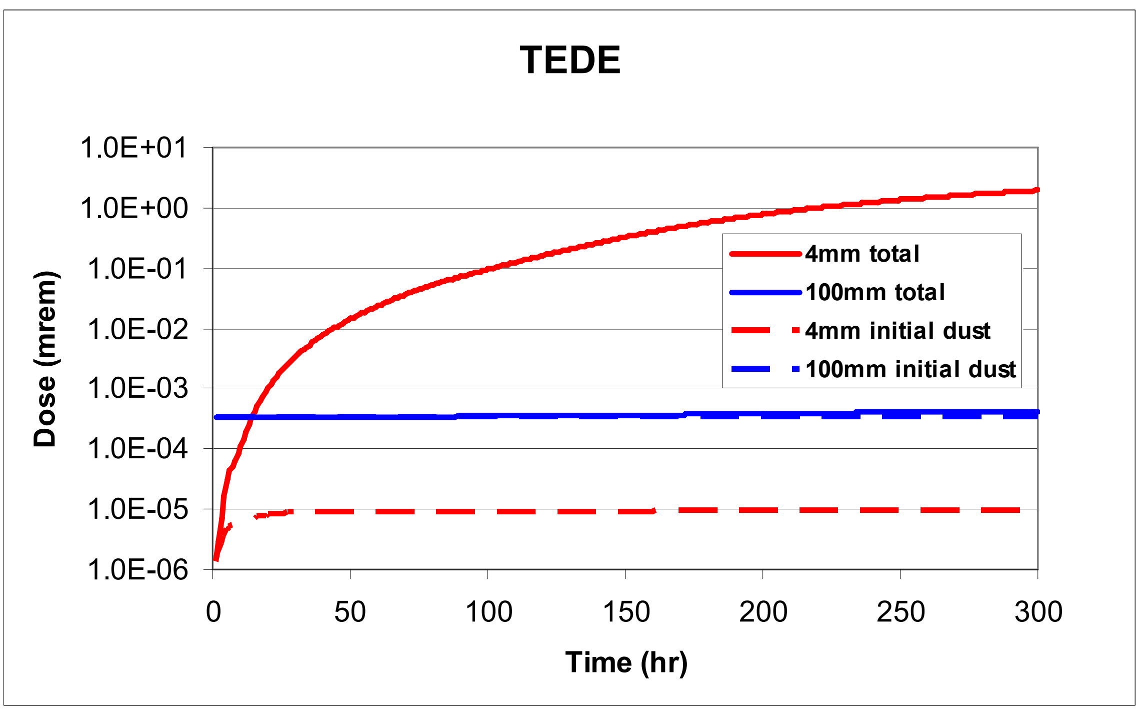

Figure 2-64 Comparison of Time Dependent TEDE for 4mm [2a(4)] and 100mm [2a(100)] Breaks

2.4.4.5.2 Effect of Filtration

The effect of adding DVS filtration is different for the 4mm vs. 100mm cases and the vapor vs. aerosol cases. For the 4mm cases, the total release is dominated by the contribution from the delayed non-dust RN release from the fuel. Therefore, for the 4mm cases in which the delayed non-dust release is assumed to be in vapor form, filtration has no effect on the 300hr cumulative doses. For the 4mm aerosol cases when the DVS damper remains open, the effect of the filtration is to reduce the doses by 2 orders of magnitude consistent with the assumed DVS filtration efficiency. For the 4mm aerosol cases when the DVS damper recloses, the effect of the filtration is small since the majority of the release is ground level as discussed above and not filtered. For the 100mm vapor cases, a small reduction in doses from DVS filtration is evident since in the 100mm cases a larger percentage of the total release is from the initial release of the RNs that are attached to dust and are filtered. Similar to the 4mm case, the 100mm aerosol cases with filtration also have doses that are 2 orders of magnitude less.

2.4.4.5.3 Effect of RN Form (Aerosol vs. Vapor)

A comparison of the cumulative releases across the fuel, PHTS and RB barriers is made in Figure 2-65 for the 4mm cases in which the DVS damper fails to reclose, without filtration and for the aerosol and vapor options for the non-dust RNs. The 1-131 release from the fuel is 265Ci, from the PHTS is 155Ci and from the RB is 30Ci for the vapor delayed release RN case and 0.19Ci for the aerosol delayed release case. Deposition and settling of the aerosols in the RB reduces the releases by about 2 orders of magnitude. Doses for these two cases differ more than the release difference because the aerosol DCFs are less than the vapor DCFs by a factor of about 3 for I and Te.

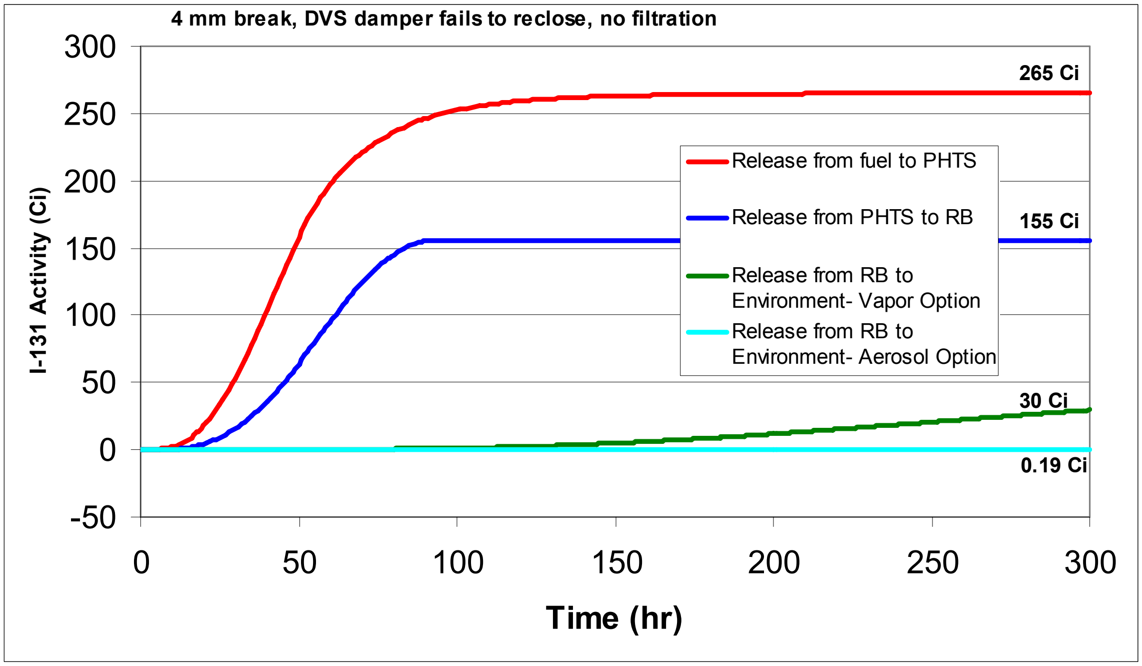

Figure 2-65 Comparison of Time Dependent Releases across Barriers

2.4.4.5.4 Effect of RB Leakage Pathways

Case 4a(4) is a sensitivity case in which the RB leakage pathways are not included. This case is included to help understand the effect of the natural circulation that develops when the leakage pathways are included. Case 4a(4) is similar to Case 2a(4), a 4mm break with unsuccessful reclosure of the DVS damper without filtration vapor case, except that in Case4a(4) there are no RB leakage paths modeled.

A comparison of the thyroid CEDE for these two cases shows that the dose is higher in the case with leakage paths by a factor of nearly 200. This increase in dose is primarily due to air intake to the RB through the leakage paths which provides an additional driving force for release through the stack. The release from the leakage paths is negligible compared to the stack release as shown previously in Table 2-24. The sensitivity of the doses to the modeling of the release paths in the RB ASTEC model requires additional investigation. More study is also needed to understand buoyancy driven helium-air exchange phenomena.

2.4.4.6 Comparison of RB Retention Cases to the 2008 Study

A comparison of the RB retention case 2c(4), 4mm break, DVS opens and never recloses, no filtration, RNs not attached to dust are aerosols is made with a similar 3mm break case from the 2008 RB Study [1] in Table 2-25. The 2008 RB study [1] case is for a 3mm break, RB damper opens and never recloses, no filtration, RNs not attached to dust are aerosols with a 20% RB vent volume. The break size modeled in the 2008 RB study [1] was 3mm, however, the analysis showed a similar blowdown time for this case as was obtained in the 4mm case in the current study. It is therefore viable to compare equivalent cases.

Table 2-27 Comparison of Doses for the 2008 RB Study and the Current Study

Dose	3mm 2008 RB Report RB Retention	4mm Current Case 2c(4)
TEDE, mrem	8.5	.006
Thyroid CEDE, mrem	210	.073

The Case 2c(4) TEDE is a factor of 1400 less and the thyroid CEDE is a factor of 2800 less than the similar 2008 RB study [1] retention case dose. The differences in the doses are due to many contributing factors which are summarized in Table 2-26.

The more significant differences are the reduced source term to the RB that was discussed previously in the no RB retention section and the additional retention of the RB as modeled in ASTEC compared to the simple RB model used in the 2008 RB study [1]. Another major contributor to the dose difference is the use of a 50m stack X/Q for the DVS releases in the current study. The stack X/Q is an order of magnitude less than the ground level X/Q.

Table 2-28 Comparison of Dose Evaluation of 3mm 2008 and 4mm 2009 Cases

	3mm 2008 RB Report RB Retention	4mm Current Case 2c(4)
Cumulative I-131 release from PHTS to RB at 300hr, Ci	850	155 (reduced fuel temperatures)
Cumulative I-131 release from from RB at 300hr, Ci	18 (2% of release to RB)	0.19 (0.1% of release to RB)
Ground level weather X/Q, s/m^3	2.3E-5 (425m EAB)	2.6E-5 (400m EAB)
Stack level weather X/Q, s/m^3	n/a (all ground level releases)	1.9E-6 (400m EAB)
I-131 thyroid CEDE DCF for aerosols, Sv/Bq	2.92E-7	1.47E-7
TEDE scaling factor	1/0.4 =2.5	1/0.8=1.25
Thyroid CEDE scaling factor	1/0.5=2.0	1/0.9=1.11
RB DVS compartments (More retention due to transport and larger size in multi volume model.)	single (20,000m^3)	multi (23,491m^3)
I-131 RB deposition/settling rate (1/hr)	0. 3	0.4-0.01
RB cooling, density and elevation differences effect on flow in and from RB considered.	no	yes (RB in flow from leakage paths increases stack releases)
Stack filtration for I-131 aerosols	95%	99%
RB radioactive decay of RNs	yes	no

This comparison supports the following conclusions and insights:

- Lower initial core temperatures evaluated in the current study result in lower initial RN inventories and lower delayed fuel releases into PHTS for all break sizes in the current study. This can be directly attributed to the reduction in the ROT.
- Convection cooling for slow depressurization reduces delayed fuel releases into PHTS in the 2009 results for break sizes less than 10mm due to lower time at temperature
- Cumulative release of I-131 to RB at 300hr for 4mm breaks are factor of 5 less due to the combined effects of reduced initial temperatures, convection cooling during blowdown, and model refinements
- Temperature and density effects are important in the evolution of the flows in the RB
- Multi-compartment ASTEC RB model indicates higher RB retention than single compartment 2008 model
- Modeling of multiple leakage paths from the RB to the environment allows for natural circulation of air into and helium air mixture out of the RB
- Assumptions made about the RB operation, RB features and characteristics of the source term greatly influence the offsite doses

Differences in results from the 2008 RB study [1] are all understood and are attributed to differences in the design, models, codes and assumptions.

2.4.5 Radionuclide Release Conclusions and Recommendations

From the PHTS and RB analysis it was shown that

- The longer blowdown time for the small break results in a significantly greater percentage of the delayed RN release from the fuel being transported to the RB.
- Significant retention of dust and fission products occurs in the RB especially in the RTC and IHX compartments.
- Air intake to the RB through the leakage paths provides an additional driving force for release through the stack.
- Closure of the stack damper significantly reduces the stack release and increases the leakage release for the 4mm break. The reduction in stack release is less for the 100mm break because the contribution of the initial release that is attached to dust is more significant and unaffected by the damper closing.
- Releases from the RB are very sensitive to assumptions made regarding the form of the RNs entering the RB (aerosol or gas).
- The helium fraction in the RTC and IHX compartments increases to dominant levels reducing the density and thereby affecting the pressure difference between compartments.
- The surface areas of the compartments within the RB play a significant role in the cooling of the gas which also influences the pressure in the compartments.

It was observed that temperature and density effects are important in the evolution of the flows in the reactor building. Counter intuitive behavior can occur due to the pressure and density effects induced by the lower density helium gas.

Note should also be taken in the design that a multi compartment RBVV will retain more RNs than a single compartment RBVV.

Further nodalization of the IHX and RRB compartments would be useful to investigate buoyancy effects that were not included in this study but may contribute to the RN releases.

The key conclusions of the dose evaluation include the following:

- Minimum ratios of the PAG thyroid CEDE limit to calculated dose:
    - 2.5 for the 4mm no RB retention cases, Case 1a(4)
    - 47 for the 4mm RB retention cases, Case 3a(4)
- Minimum ratios of the NRC TEDE limit to dose:
    - 180 for the 4mm no RB retention cases, Case 1a(4)
    - 3500 for the 4mm RB retention cases, Case 3a(4)
- No RB retention is required to meet dose limits based on realistic assumptions used in this study.
- The RB retention cases included in this study reduce the offsite doses by 1 – 6 orders of magnitude relative to the no RB case providing additional margin to limits
- Assumptions made about the RB response and characteristics of the source term greatly influence the offsite doses.
    - Cases in which the DVS damper recloses have higher doses than when it remains open due to the increase in ground level releases for these cases.
    - Cases with DVS filtration result in the same (for the 4mm vapor cases) or lower doses (for all other cases) especially for cases in which the non-dust RNs are assumed to be in aerosol form.
    - Cases in which the non-dust RNs are assumed to be in vapor form as opposed to aerosol form have higher doses. Significant RB deposition occurs for RNs assumed to be in aerosol form.
- Dose is more sensitive to ground level releases than DVS stack releases due to the 50m stack influence on X/Q.
- For each comparable case, the 100mm break dose is one to four orders of magnitude less than the 4mm break dose. Results confirm 2008 RB study results that longer blowdown time for the small break results in a significantly greater percentage of the delayed RN release from the fuel being transported to the RB and accordingly greater doses.
- Differences in trends for the 4mm and 100mm cases are a result of the larger contribution of the initial release that is attached to dust to the total dose in the 100mm cases. The RNs that are attached to dust do deposit in the RB and are filterable when released through the vent shaft
    - For the 100mm vapor case when the damper remains open, filtration reduces the doses, 20% for the thyroid CEDE and by a factor of 5 for the TEDE. For the 4mm vapor cases, filtration has no effect on the overall doses.

- The reduction in doses is significantly larger between the RB vapor case with open damper and the no RB retention case for the 100mm case than for the 4 mm case.
- The opposite is true for the reduction in doses for the RB aerosol case with open damper. The 4mm shows a greater reduction in doses relative to the no RB retention case.

It is obvious from the results that the forms of the RNs in the RB play an important part in the retention and filtration. Experimental investigation into the form of the RNs (vapor / aerosol) as well as the adsorption to dust is therefore important.

2.5 EVALUATION OF UNCERTAINTIES AND SENSITIVITIES

The results presented in this section are all based on point estimates of parameters that are either best estimate when a basis can be established to support it, or conservative in selected areas where a best estimate is not currently available. An evaluation of the uncertainties in these parameters was performed as part of the barrier retention allocations as discussed in the following section.

3. RADIONUCLIDE BARRIER RETENTION ALLOCATIONS

3.1 OVERVIEW

The purpose of this section is to document the results of the radionuclide barrier retention allocations which have been developed for use in the conceptual design of the NGNP as well as in subsequent design and plant life cycle stages. The RN barriers considered are:

- Fuel barrier
- PHTS Helium Pressure Boundary barrier
- Reactor building barrier

For each of these barriers retention allocations were established for the next phase of design. The scope of the barrier allocation task includes the following:

- Review current and 2008 RB study [1] results relative to radionuclide (RN) barrier retention capability
- Evaluate and analyze uncertainties significant for barrier retention allocations
- Define an appropriate set of parameters that define the barrier retention capability
- Establish the barrier allocations for the next phase of design
- Document the assumptions and boundary conditions for the allocations
- Propose a process for using and updating the barrier allocations in the future
- Define design data needs (DDNs) to aid in the next phases of design

3.2 TECHNICAL APPROACH TO BARRIER ALLOCATIONS

The technical approach to barrier allocations was comprised of the following steps.

Step 1 Review current best estimate dose calculations to define barrier retention capability
Step 2 Perform uncertainty analysis on the doses from a selected limiting HPB break scenario
Step 3 Define the parameters that describe the barrier retention capability
Step 4 Assess the uncertainties in the barrier performance parameters
Step 5 Assign barrier allocation targets and a method for using them in design
Step 6 Define DDNs identified in the uncertainty analysis

The first step was to review retention allocations supported by the results of the radiological dose evaluations presented in Section 2 as well as the results of the dose evaluations that were developed in the 2008 RB study [1]. As discussed in Section 2, the limiting design basis events for the NGNP are expected to involve DLOFC scenarios initiated by HPB breaks in the range of 3mm to 100mm equivalent break size. As shown in both of these studies, among these breaks, the radiological doses from breaks on the smaller end of this range are limiting because of the interaction of the very slow delayed fuel release with the slow rate of depressurization. Breaks on the larger end of this range are expected to release much less RNs into the reactor building due to a lack of pressure driving force during the delayed fuel release. Breaks larger than 100mm are expected to be so unlikely that such breaks would fall into the beyond design basis event (BDBE) range.

The next step was to perform an uncertainty analysis for scenarios resulting from the 4mm break in the CIP at the top of the RPV in the RTC which was analyzed on a best estimate basis in Section 2. Of the various 4mm break cases that were analyzed, the following scenario is selected to perform the uncertainty analysis:

- Blow-out panels open and vent gases out the Depressurization Vent Shaft (DVS) through the 50m stack on the top of the RB assuming no engineered filter in the shaft
- The DVS damper is closed at the end of blowdown, i.e. when the PHTS reaches pressure equilibrium with the RB atmosphere
- The plant design and boundary conditions used in the Section 2 evaluations are valid

Based on its dominance in the evaluation of the thyroid PAG dose which has been established as the limiting dose metric based on the results of Section 2.4, the focus of the uncertainty analysis was on I-131

In Steps 3 and 4 the barrier allocation parameters were defined and evaluated with respect to radiological dose uncertainties. In Step 5 the barrier allocation targets for the next phase of the design were established as well as a process for using and updating these allocations in the future. These allocations consider whether barrier allocations based on the evaluation of 4mm CIP breaks are adequate to account for a more complete set of scenarios and plant conditions that will be evaluated in future safety analyses as the design matures. Boundary conditions necessary to maintain the validity of the barrier allocations are also documented as part of this step. In Step 6, DDNs were identified to reduce the major drivers of uncertainty in the ability to meet the allocation targets.

The results of each step of the barrier allocation process are discussed in the following sections.

3.3 REVIEW BARRIER RETENTION CAPABILITY SUPPORTED BY EXISTING STUDIES

The barrier retention capabilities supported by the current radiological dose assessments are summarized in Table 3-1. The following parameters are used to define the barrier retention capability:

Fuel Barrier — Fraction of fuel inventory released into PHTS circuit during normal operation and during the DLOFC transient (the fuel RN releases during normal operation produce a normal circulating activity in the PHTS in the form of dust and plateout that is attached to HPB surfaces at the time of the break. During a DLOFC there is an additional delayed fuel release that occurs over the course of several days after the initiating event)

PHTS HPB Barrier — Fraction of RNs existing at the time of the break and released into the PHTS by the fuel during the DLOFC transient that is released into the reactor building

RB Barrier — Fraction of RNs released into the RB that are released to the environment

Table 3-1 Barrier Retention Factors from Current Best Estimate Results

I-131 Form	Analysis Case (Break Size mm)	Initial I-131 Inventory (Ci)		Fraction Released From Fuel	Fraction Released From PHTS	Fraction Released from RB ground level	Fraction Released from RB elevated	Thyroid CEDE (mrem)	Margin Factor to Thyroid CEDE Limit
Vapor	3a(4)	Fuel	1.29E+07	2.05E-05	5.85E-01	5.14E-02	6.83E-03	1.1E+02	4.5E+01
		Circ.	0	1					
		Non-circ.	2.05E+00	2.00E-03					
Aerosol	3c(4)	Fuel	1.29E+07	2.05E-05	5.85E-01	4.81E-04	7.79E-04	3.9E-01	1.3E+04
		Circ.	0	1					
		Non-circ.	2.05E+00	2.00E-03					
Vapor	3a(100)	Fuel	1.29E+07	2.57E-05	1.29E-03	4.74E-04	1.46E-03	4.1E-03	1.2E+06
		Circ.	0	1					
		Non-circ.	2.05E+00	2.00E-03					
Aerosol	2008(3)	Fuel	1.29E+07	8.03E-05	8.17E-01	2.12E-02	n/a	2.1E+02	2.4E+01
		Circ.	0	1					
		Non-circ.	3.61E+00	2.00E-03					
Aerosol	2008 (1000)	Fuel	1.29E+07	8.03E-05	8.33E-04	6.57E-01	n/a	6.5E+00	7.7E+02
		Circ.	0	1					
		Non-circ.	3.61E+00	2.50E-01					

As seen in this table the fuel barrier has the greatest RN retention capability relative to the other barriers. The HPB barrier is much more effective for larger break sizes than is the case for breaks in the 3mm to 4mm range. The reactor building appears to have a significant retention capability; however there is an order of magnitude change between the vapor case and the aerosol case in the current best estimate analysis. It is already apparent in the current results that the physical and chemical form of the RNs is a significant source of uncertainty. These and other sources of uncertainty are explored further in the sections below.

3.4 RADIOLOGICAL DOSE UNCERTAINTY MODEL

3.4.1 Overview of Model and Workshop

The approach chosen for the uncertainty analysis is to develop a simple model of the progression of the RN transport during an accident from the fuel kernels to the environment and to identify the major uncertainties in each step of the progression. The interrelationship between the individual steps of the model is shown in the flowchart of Figure 3-1.

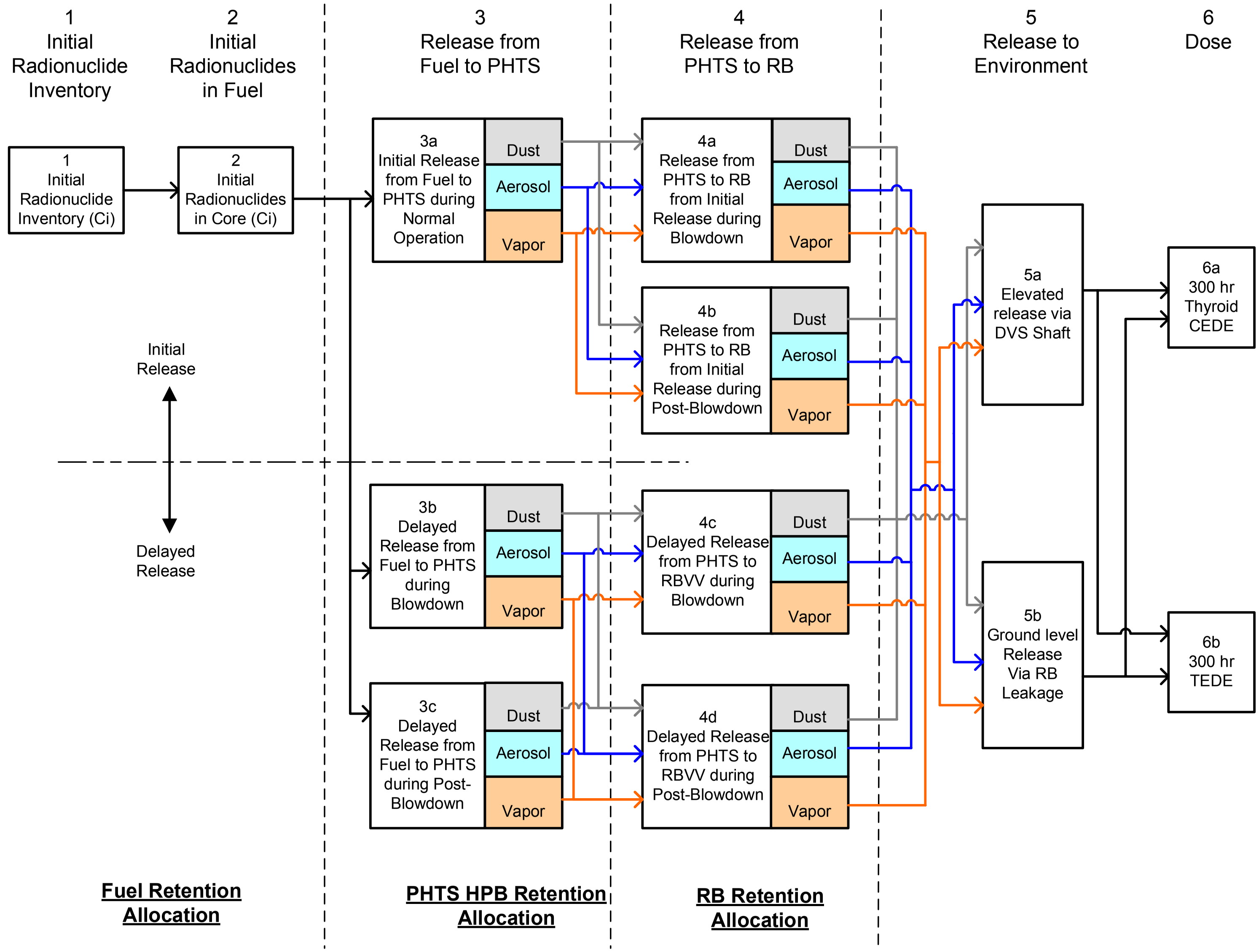

Figure 3-1 Radionuclide Transport Flow Chart for Uncertainty Analysis Model Development

The parameters of this model were quantified in an expert elicitation workshop held at PBMR from August 24 to 28. Some of the steps (boxes) in the flow chart are dependent on the fission product (radionuclide) group and accident case. The quantification of the parameters involves the following steps:

Determine for each parameter, radionuclide group and accident case that:

(a) The uncertainties involved are small and the value determined or used in the accident analysis are best estimate values. In this case the parameter is quantified with the best estimate value from the accident analysis without an explicit quantification of uncertainties.

(b) The uncertainties are large or the value determined or used in the accident analysis are not best estimate values. In this case the parameter is quantified with an uncertainty distribution.

The model and flowchart was converted into an Excel spreadsheet under the Crystal Ball software. The Crystal Ball software allows each input parameter in Excel to be represented by an uncertainty distribution and Crystal Ball then quantifies the uncertainty distribution of the output parameters by Monte Carlo propagation of the input uncertainties. The barrier allocations are developed from the Crystal Ball quantification as degree of confidence levels for meeting the barrier requirements. The top part of the Excel spreadsheet is shown in Figure 3-2.

The quantification of a parameter as an uncertainty distribution involves the following steps:

1. Determine the as calculated value for the parameters for the all vapor case. As calculated values for the all aerosol cases are also useful to help define the distributions for the aerosol and vapor release parameters.
2. Assign percentiles to the as calculated values.
3. Estimate the lower bound percentile (1 %tile or 5 %tile) and the upper bound percentile (99 %tile or 95 %tile)
4. Estimate the 50 %tile value
5. Characterize the shape of the uncertainty distribution and the distribution parameters (usually 2) that define it.
6. Determine any correlations between the uncertainties of this parameter to other parameters in the model (fully correlated, partly correlated, not correlated).
7. The uncertainty assessments will be used to guide the definition of DNNs

The objective of the FP Allocations Workshop was to determine the uncertainty distributions and fixed values for all the input parameters of the model. The workshop team was comprised of all the experts responsible for the best estimate analysis of Section 2. The workshop participants reviewed the uncertainty analysis model presented here, identified key sources of uncertainty for each parameter in the model, and captured the current best state of knowledge about the uncertainty in each parameter. A consensus was reached on the uncertainty distribution for each parameter in the model which is discussed in the next section.

2009 RN Retention Allocation
Case: 4mm Damper Reclose End of Blowdown, No DVS Filtration
RN Group: I-131
Net Retention at 300 h:

Barrier	Source in Bq	Retained in Barrier BQ	% Retai'd in Barrier Source in	Fraction Not Retained		
					Release to Env. (Bq)	1.72E+10
Fuel	4.79E+17	4.79E+17	100.00%	2.07E-05	Total Thyroid CEDE (Sv)	5.39E-05
PHTS	9.91E+12	9.24E+12	93.25%	6.75E-02	Total TEDE (Sv)	3.63E-06
RB	6.69E+11	6.52E+11	97.43%	2.57E-02		
					Fraction of Initial Inv Released to Env	3.59E-08

Net Retention at 300 h:

Barrier	Source in (Ci)	Retained Net (Ci)	% Retai'd of Source in		
				Release to Env. (Ci)	4.64E-01
Fuel	1.29E+07	1.29E+07	100.00%	Total Thyroid CEDE (mrem)	5.39E+00
PHTS	2.68E+02	2.50E+02	93.25%	Total TEDE (mrem)	3.63E-01
RB	1.81E+01	1.76E+01	97.43%		

1 Total Initial Invent'ry (Bq)	2 Initially in Fuel (Bq)	3 Release to PHTS (Bq)	4 Release to RB (Bq)	5 Release to Environm't (Bq)	6 Release to Environm't (Bq)	7 I-131 300 h Dose (Sv)	8 Total 300 h Dose (Sv)
4.79E+17	4.79E+17	7.62E+10	3.68E+07	2.26E+05	2.21E+05	1.43E-11	2.15E-11
		In. Rel. BD	In. Rel. BD	Att. To Dust	Elev-Filt	Thy CEDE	Thy CEDE
			Dust			7.27E-13	1.45E-12
						TEDE	TEDE
					5.49E+03	4.87E-12	7.30E-12
					Gd-Unfilt	Thy CEDE	Thy CEDE
						2.47E-13	4.94E-13
						TEDE	TEDE
			1.84E+07	1.13E+05	1.10E+05	7.16E-12	1.07E-11
			In. Rel. BD	Aerosol	Elev-Filt	Thy CEDE	Thy CEDE
			Aerosol			3.63E-13	7.27E-13
						TEDE	TEDE
					2.74E+03	2.43E-12	3.65E-12
					Gd-Unfilt	Thy CEDE	Thy CEDE
						1.24E-13	2.47E-13
						TEDE	TEDE
			1.84E+07	1.13E+06	1.10E+06	1.91E-10	2.87E-10
			In. Rel BD.	Vapor	Elev-Filt	Thy CEDE	Thy CEDE
			Vapor			9.68E-12	1.94E-11
						TEDE	TEDE
					2.60E+04	6.15E-11	9.23E-11
					Gd-Unfilt	Thy CEDE	Thy CEDE
						3.11E-12	6.22E-12
						TEDE	TEDE

Only part of tree shown - remaining part covers Initial fuel releases during post blow-down and delayed fuel releases during blow-down and post blow-down phases

Figure 3-2 Top Part of Excel Calculation Model for Uncertainty Analysis

The workshop took several person weeks to prepare, involved about a dozen different experts, and lasted for a full five day period. The workshop group agreed on the approach to using the results of the uncertainty analysis to establish the RN retention allocations and was responsible for completing the entire task on RN barrier allocations. It was agreed at the workshop to focus on the RN transport of I-131 and to also evaluate the uncertainties associated with the remaining RNs. The total doses are then estimated using scaling factors to account for the other RNs.

3.4.2 RN Barrier Allocation Model

The model is defined by the flowchart in Figure 3-1. The model distinguishes between the initial release comprised of the normal circulating activity and RNs deposited on internal PHTS surfaces at the time of the initiating event, and the delayed release from the fuel during the DLOFC transient. For each of these two release types a distinction is made between the blowdown phase of the release and the post-blowdown phase of the release, yielding four combinations:

Initial release during blowdown
Delayed release during blowdown
Initial release during post-blowdown
Delayed release during post-blowdown

The 4mm case has the following event timing:

Time of peak fuel temperatures	~60 hours
End of blowdown	91 hours
Time of maximum I-131delayed release	~90 hours
End of post-blowdown phase	300 hours

Since the blowdown extends past the end of PHTS thermal expansion and into the period of PHTS thermal contraction, only two divisions, the blowdown and post-blowdown phases are necessary to characterize the transient.

Larger breaks, such as the 100 mm break, exhibit three distinct release phases, namely the blowdown phase, followed by the PHTS thermal expansion phase which starts after the blowdown is complete, and followed by the PHTS thermal contraction phase of the release. Therefore, the model may have to be modified when applied to larger breaks.

The flowchart is converted to the RN Allocation Quantification Tree which is developed in a Microsoft Excel™ spreadsheet. Each node or box in the flowchart is numbered. Each column in the flowchart corresponds to a column in the quantification tree. In the following each flowchart node is defined.

Box 1: Total Initial Inventory of Fission Products and Contamination Products (TII)

Fission Product Groups: Thirteen fission product groups collect fission product elements that behave chemically similar. They are:

- Noble Gases (Xe) — Not modeled, does not contribute to dose
- Alkali Metals (Cs) — Only Cs-137 modeled
- Alkaline Earths (Ba) — Only Sr-90 modeled
- Halogens (I) — Only I-131 and I-133 modeled
- Chalcogens (Te) — Only Te-132 modeled
- Platinoids (Ru) — Not modeled, included in remainder fraction
- Early Transition Elements (Mo) — Not modeled, included in remainder fraction
- Tetravalents (Ce) — Not modeled, included in remainder fraction
- Trivalents (La) — Not modeled, included in remainder fraction
- Uranium (U) — Not modeled, included in remainder fraction
- More volatile Main Group (Cd) — Not modeled, included in remainder fraction
- Less volatile Main Group (Sn) — Not modeled, included in remainder fraction
- Cesium-Iodide Cs-I — Important in LWRs due to steam environment.

Cs-I may be significant in NGNP designs involving steam generators in the PHTS in which case water and steam ingress scenarios will need to be considered.

Contamination:

• Silver (Ag)	Only Ag-110m and Ag-111 modeled
• Uranium (U)	Not modeled
• Other (Oth)	Not modeled

For the dose calculation the radioactive isotopes of the individual elements or groups are of importance. However for the physical processes that determine the release characteristics, such as aerosol formation and settling, it is the total mass inventory of each group, including stable isotopes that determines the behavior. This must be kept in mind when defining the uncertainty distributions for the release parameters.

Box 2: Initial Radionuclides in Fuel

Fuel here is defined as the fuel pebbles, including the outer graphite layer. The initial quantity of radionuclides in the fuel is the amount retained in the fuel at the core equilibrium condition, which is also the initial condition for the transient. The difference between Box 1 and Box 2 is what is released to the PHTS during normal operation which is addressed in Box 3a .

Box 3a: Initial Release from Fuel to PHTS during Normal Operation

The initial release from the fuel to the PHTS during normal operation involves the following processes for which uncertainties need to be assessed. The sources of uncertainties for each bullet are evaluated in the following sections:

- Release from exposed Kernels (SiC and PyC coatings failed) normal operation
- Release from defective coated particles (SiC coating failed) during normal operation
- Release from intact kernels during normal operation
- Diffusion of Ag and other contamination during normal operation
- Fission of U contamination outside coated particles during normal operation
- Activation of other contamination outside coated particles during normal operation
- Release from graphite to PHTS during normal operation

Box 3b: Delayed Release from Fuel to PHTS during Blowdown

The processes for which uncertainties need to be assessed are:

- Delayed release from exposed kernels during blowdown
- Delayed release from fission of U-contamination outside particles

- Delayed release from defective particles during blowdown
- Diffusion of Ag and other contamination during blowdown
- Delayed release from intact kernels during blowdown
- Delayed release from graphite to PHTS during blowdown

Box 3c: Delayed Release from Fuel to PHTS during Post-Blowdown

The processes for which uncertainties need to be assessed are:

- Same Items as 3b plus:
    - Release due to effects of oxidation in graphite or coatings

Box 4a: Release from PHTS to RB from Initial Release during Blowdown

The processes for which uncertainties need to be assessed are:

- Initial aerosol, vapor and dust circulating activity in PHTS
- Initial non-dust circulating activity
    - Initial non-dust circulating activity as aerosols
    - Initial non-dust circulating activity as vapor
    - Resuspension of deposited dust during blowdown
- Plateout Activity
    - Initial plateout activity in PHTS
    - Lift-off/revolatilization of plateout activity forming aerosols during blowdown
    - Lift-off/revolatilization of plateout activity forming vapors during blowdown
- Transport of RNs to the RB during blowdown

Box 4b: Release from PHTS to RB from Initial Release during Post-Blowdown

The processes for which uncertainties need to be assessed are:

- Same Items as 4a plus:
    - Transport of RNs from the core to the RB during post-blowdown

Box 4c: Delayed Release from PHTS to RB during Blowdown

The processes for which uncertainties need to be assessed are:

- Delayed RN release to PHTS attaching to dust
- Delayed RN release to PHTS forming aerosols
- Delayed RN release to PHTS remaining as vapors
- Transport of RNs from the core to the RB during blowdown

Box 4d: Delayed Release from PHTS to RB during Post-Blowdown

The processes for which uncertainties need to be assessed are:

- Same Items as 4c plus:
    - Transport of RNs from the core to the RB during post-blowdown

Box 5a: Elevated Release RBVV via DVS Shaft to Environment

The processes for which uncertainties need to be assessed are:

- Distribution of RNs into dust, aerosol, and vapor
- Particle size distribution of dust and aerosol
- Radioactive decay, deposition, and plateout out the release path

Box 5b: Ground Level Release via RB leakage to Environment

The processes for which uncertainties need to be assessed are:

- Distribution of RNs into dust, aerosol, and vapor
- Particle size distribution of dust and aerosol
- Radioactive decay, deposition, and plateout out the release path

Box 6a: 300 hr Thyroid CEDE

The processes for which uncertainties need to be assessed are:

- Radioactive decay
- Daughter buildup
- X/Q for elevated release
- X/Q for ground release
- Building wake factor
- Building wake factor for elevated release
- Building wake factor for ground release
- Breathing rate
- Dose conversion factor for dust
- Dose conversion factor for aerosols
- Dose conversion factor for vapors
- Scaling factor for total dose from I-131 dose

Box 6b: 300 hr TEDE

The processes for which uncertainties need to be assessed are:

- Same as Box 6a

3.5 BOUNDARY CONDITIONS

Boundary conditions define a minimum set of plant capabilities that are necessary to make the barrier allocations valid. It was decided at the workshop that the barrier allocations shall be consistent with PBMR safety design philosophy and the 2008 RB study [1]. Some of the most important requirements for barrier allocation considerations include the following:

- Need to have a building and means of controlling releases during normal operation; this will likely lead to an HVAC with controlled pressure zones which may or may not have an accident mitigation role
- Need to provide a pressure relief capability and structural features to protect RB and all the safety related SSCs for design and beyond design basis events
- Will need to control leakage post blowdown to limit air ingress to building and post blowdown releases
- Need for filtration should not be driven by the allocations and will be resolved in later stages of design
- All retention allocations are based on the current NGNP 500MW 750°C ROT design, including the PHTS and RB layouts. Changes in these factors will lead to changes in the retention allocations
- It is assumed that a DLOFC from a 4mm break in CIP near RPV in reactor cavity of RB will represent a bounding design basis event for the NGNP design
- Plant response same as in current RN dose evaluation
- Blowout panels open to relieve RB pressure and exhaust release out the depressurization vent shaft (DVS)
- DVS damper is closed at end of PHTS blowdown for the damper closed cases and is left open for the damper fails open cases
- No filtration and no filtration flow resistance is assumed for the DVS release
- RB HVAC is assumed to be switched off at time of break so that RB retention is only influenced by passive NGNP characteristics

3.6 EVALUATION OF UNCERTAINTIES

During the workshop, the uncertainties associated with radionuclide transport were assessed across each barrier. This included an identification of the sources of uncertainty including parameters in the current calculations, factors not considered in the current calculations, limitations imposed by boundary conditions of the analysis, and the uncertainties associated with the early state of design of the NGNP. A discussion of the results of this evaluation is provided for each barrier in the sections below.

3.6.1 Uncertainties in Releases from Fuel Barrier

When considering the RN releases from the fuel, both the uncertainties in the fuel temperature analysis during the transient as well as the uncertainties associated with the RN releases under those temperatures have to be considered. The major parameters of the fuel release calculation that are important to consider in the evaluation of fuel release uncertainties include:

- Major factors leading to fuel temperature uncertainties
  - Core bypass and leak flows
  - Added pressure drops in by-pass channels
  - Core thermal dispersion
  - Pebble bed heat transfer coefficients
  - Reflector and core graphite conductivity
- Major factors leading to RN release uncertainties
  - Transport parameters (diffusion coefficients and sorption isotherms)
  - Heavy metal contamination
  - Fuel failure fractions as a function of time at temperature, burn-up, etc.

The uncertainties assigned to the release of I-131 during the transient are based on previous parametric Monte Carlo analysis performed on the VSOP-TINTE-GETTER chain. The distributions for delayed fuel release fractions for delayed fuel release during blowdown and post-blowdown phases in Figure 3-3 and Figure 3-4, respectively. They are characterized as log-normal distributions with mean values linked to the best estimate values calculated in Section 2, having values of 1.9E-5 and 1.4E-6 for the blowdown phase, and post-blowdown phase respectively. The post-blowdown values are much smaller because the core temperatures have significantly decreased below the peak by the time of the end of blowdown. The lognormal range factors (ratio of the 95%ile to 50%tile) for each distribution is 20.

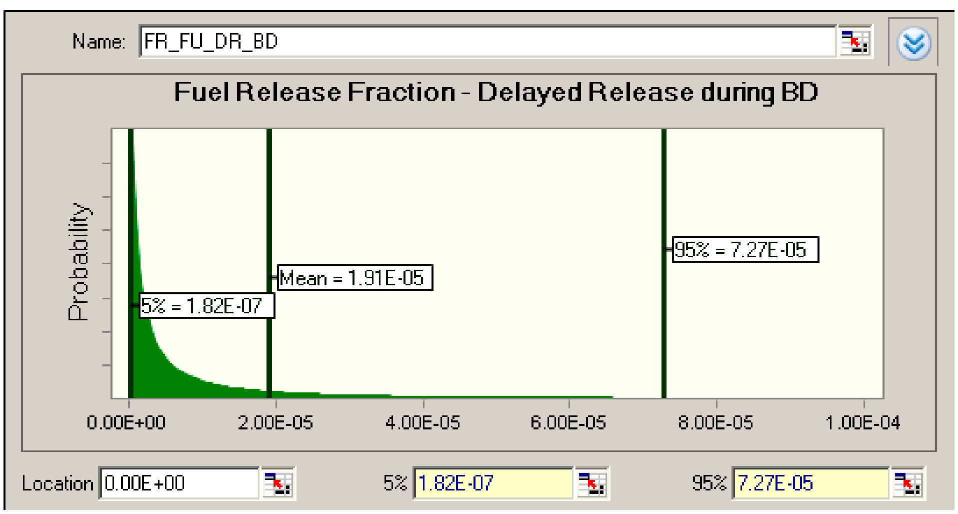

Figure 3-3 Uncertainty Distribution for Fraction of I-131 Released from Fuel During Blowdown

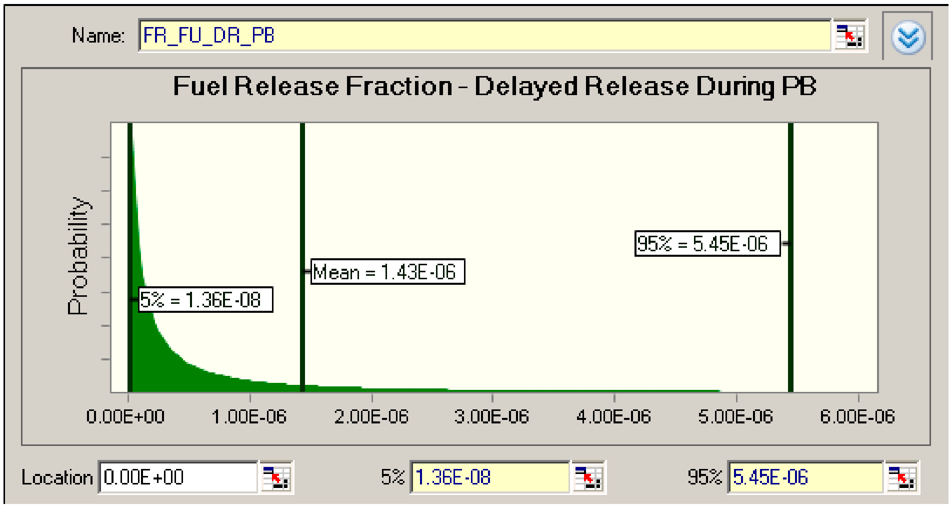

Figure 3-4 Uncertainty Distribution for Fraction of I-131 Released From Fuel During Post-Blowdown

The uncertainty distributions assigned to the fuel release fractions are based on the following additional boundary conditions:

- Fuel quality must be equal or better than the current German qualified fuel
- Fuel temperatures during the transient do not exceed 1700 °C
- Burnup measurement and on-line refueling is sufficiently accurate that the limiting fuel burnup is not exceeded
- There is no water ingress during the event
- In the 4mm break analysis the maximum temperature of the fuel does not exceed the temperature at which Sr90 release becomes dominant. This uncertainty is added as an uncertainty in the scaling of the 7 isotopes to the overall TEDE

As a result of analyzing the uncertainties associated with the fuel barrier performance, the following items were identified as possible candidates for future DDNs:

- Fuel qualification
- Core by-pass and leak flow analysis and measurements during hot conditions
- RN release from fuel physical phenomena investigation
- Graphite (including fuel sphere graphite) thermal conductivities under irradiation
- Fuel graphite impurities

3.6.2 Uncertainties in Releases from PHTS HPB Barrier

The evaluation of uncertainties associated with the release of RNs inside the PHTS circuit into the RB is dependent on the phase of the event i.e. blowdown or post-blowdown. The uncertainty associated with the initial inventory at the time of the break must also be considered.

Areas of uncertainty that are considered:

- Initial inventory at time of break
    - Circulating and non-circulating activity
    - Form of the circulating I-131 (dust / vapor / aerosol)
- Blowdown Phase
    - Re-suspension of normal operation plated-out or deposited I-131
    - Thermo-fluid behavior (blowdown and thermal expansion)
    - Retention of delayed release I-131 in the PHTS
    - Form of delayed release I-131 (dust / vapor / aerosol)
- Post-blowdown Phase
    - Thermo-fluid behavior (thermal contraction, diffusion, natural circulation)

Note that the thermo-fluid behavior during the post-blowdown phase is not currently modeled in the models. This effect is however considered in the uncertainty analysis.

For evaluating the RN initial inventory during the time of the break the following sources of uncertainty were identified:

- Circulating vs. non-circulating activity
    - Analyses of AVR data and experiments have indicated that most activity is either plated-out or deposited. Circulating activity within the PHTS during normal operation was found to be of the order of 1%
- Dust vs. non-dust
    - Significant uncertainties in sorption interaction between RNs and graphite
    - Previous experience (e.g. AVR data) has not been sufficiently analyzed to determine I-131 dust ratios
    - Assumption is that there is no knowledge on the dust vs. non-dust distribution of I-131 during normal operation (flat distribution)
- Vapor vs. aerosol
    - Lack of knowledge of I-131 chemistry in a dry helium/air environment
    - Section 2 analysis only considers vapor form
    - Flat distribution between 0 and 1 represents state of knowledge about fraction of initial and delayed releases of I-131 as vapor vs. aerosol

For evaluating the releases from the PHTS during the blowdown phase, the following sources of uncertainty were identified:

- Re-suspension of plated-out and deposited I-131
    - Flownex calculations indicate shear force ratios < 1 and hence insignificant liftoff/resuspension. There is some uncertainty involved in this analysis, but it is seen as relatively small
- Thermal-fluid behavior
    - Low coolant flow rates close to the limit of the calculational model
    - Flow path reversal and directional changes

  - Buoyancy not modeled
  - Time of completion of blowdown
  - Transport of I-131 from the core to the break location
- Retention of delayed release I-131 in the PHTS
  - Low surface temperatures and its effect on the plate-out rate
  - Low flow velocities effect on both plate-out and deposition rates
  - Form of the I-131 effect on the plate-out and deposition
  - Reduction in effective surface area available as flow paths bypass certain components (e.g. IHX)
- Form of delayed release I-131
  - Less time available for I-131 sorption to the dust than in normal operation
  - Sorption is more likely on deposited dust than circulating dust
  - Most delayed release of I-131 is expected to reach the RB in non-dust form

For evaluating the releases from the PHTS during the post-blowdown phase, the following sources of uncertainty were identified:

- Thermal-fluid behavior
  - Time of blowdown exceeds the time of peak core temperatures; PHTS is in state of thermal contraction at end of blowdown
  - Low coolant flow rates close to the limit of the calculation model and hence estimates of the time to complete blowdown are uncertain
  - Buoyancy effects and diffusion not yet included in computer models but considered in this uncertainty analysis
  - Transport path of I-131 from the core to the break location and extent of mixing in PHTS circuit is uncertain
  - Uncertainty distribution applied based on engineering judgment to bound the flow rates for gas-exchange
  - Plate-out and settling along release path if gas-exchange occurs is not modeled in computer models but is expected; magnitude of these phenomena is uncertain

As a result of these sources of uncertainties, uncertainties in the fractional releases from the PHTS were evaluated. Some of the key uncertainty distributions are provided in the following Figures.

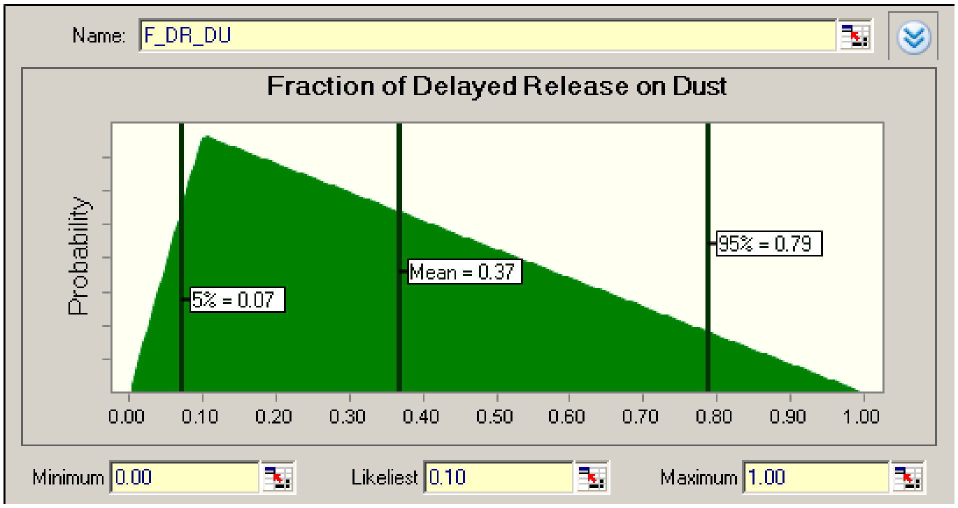

Figure 3-5 Uncertainty distribution on the Fraction of the Delayed Fuel Release Attached to Dust in the PHTS Prior to Release

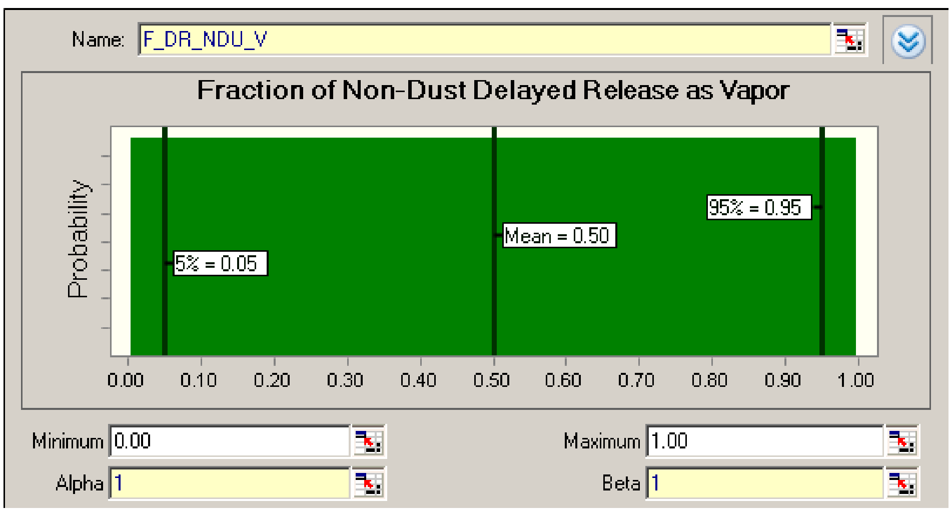

Figure 3-6 Uncertainty Distribution on the Fraction of Non-Dust Delayed Fuel Release That is Vapor

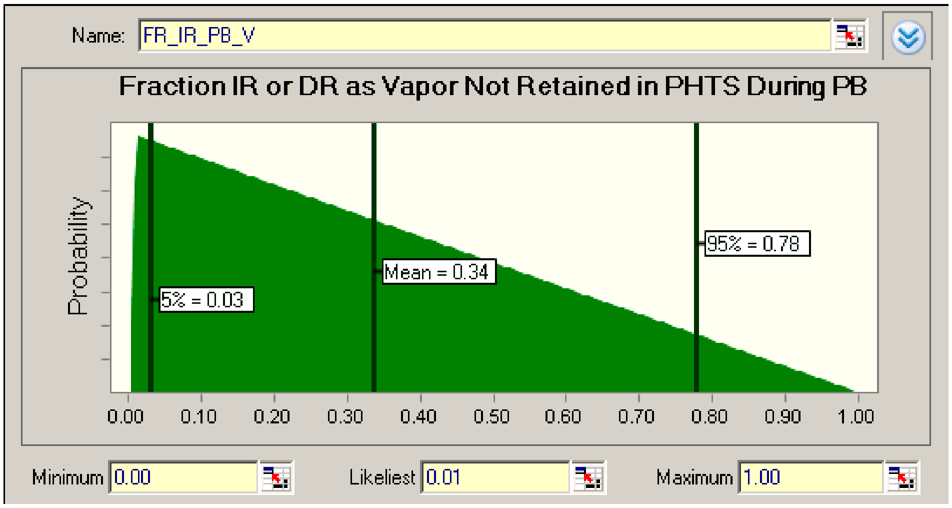

Figure 3-7 Fraction of RNs as Vapor Released to the RB During Post-Blowdown

Items for further study and consideration of future DDNs for the PHTS HPB barrier include:

- Computer Code validation
- Reduce uncertainty on distribution of I-131 and other radiologically significant RNs on dust, aerosol, and vapor as well as dust and aerosol size distributions
- Reduce uncertainty on plate-out, settling, and other PHTS retention phenomena
- Reduce uncertainty on PHTS-RB gas exchange phenomena
- Reduce uncertainty on the formation, size and chemical interaction of metallic dust
- Reduce uncertainty in heat transport coefficients of the pebble bed and other thermal-fluid factors, such as component flow restrictions

3.6.3 Uncertainties in Releases from Reactor Building

The major sources of uncertainty identified in the workshop for the RB barrier included the following items:

- Same uncertainties about distribution of RNs on dust, vapor, and aerosol as in PHTS as well as how these distributions change after release into the RB
- Uncertainty in dust size distribution input leading to uncertainty in dust deposition rates
- Location and size of reactor building bypass leakage
    - Leaks from RBVV direct to environment
    - Leaks from RBVV into other RB compartments
    - Ingress of air into building and impact on gas mixtures
- Timing of DVS damper closure

- Uncertainties in RN retention phenomena for each form of RN (dust, vapor, aerosol)
- Model Uncertainties
- Limited validation of ASTEC for HTGR conditions

As a result of these sources of uncertainty, the uncertainty distributions developed for key aspects of the release calculation are shown in the following figures.

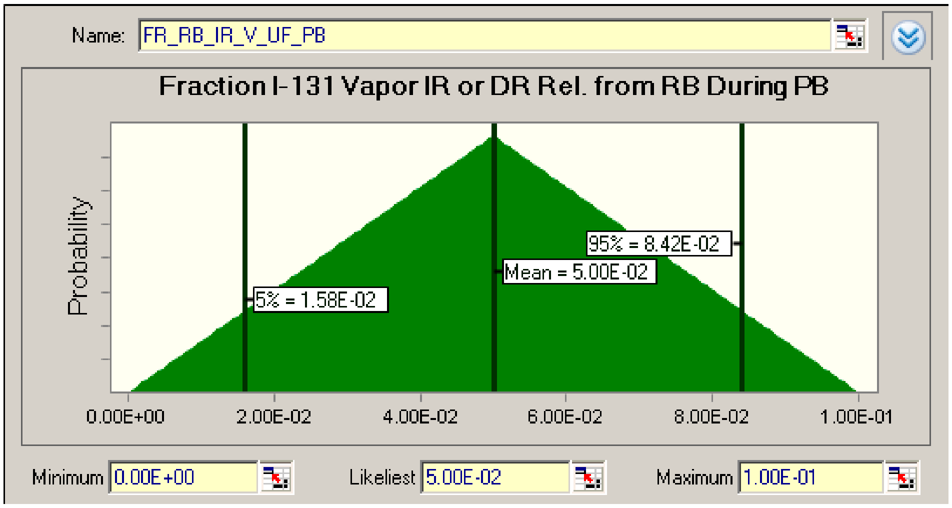

Figure 3-8 Uncertainty Distribution for Fraction of I-131 as Vapor Released from RB at Ground Level Post-blowdown

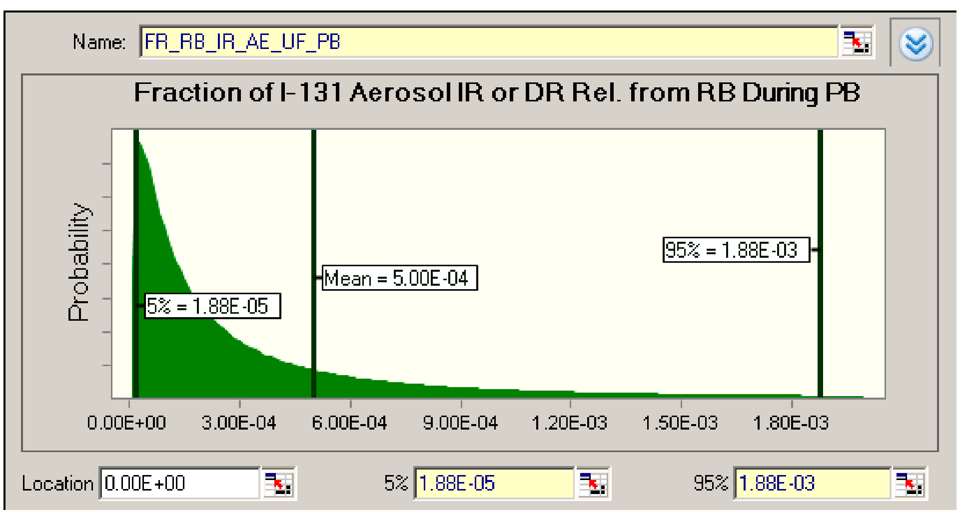

Figure 3-9 Uncertainty Distribution for Fraction of I-131 as Aerosol Released from RB at Ground Level Post-blowdown

These distributions are based on the following additional boundary conditions that were identified during the RB barrier session of the workshop.

- A multi-compartment building with blow-out panels must exist
- DVS has a tall (> 50m) stack and an effective closure mechanism with minimal leakage compared to the normal RB leak rates
- The building leak rate is close to the assumed commercial grade leak rate
- The surface area to volume ratios of the building are comparable to what was modeled
- The HVAC system and systems injecting Helium into the PHTS shut down at the time of the break, i.e. these system does not negatively influence the releases
- The PHTS break does not adversely impact the RB an safety classified SSCs – e.g., no consequential second break scenario exists

For future consideration the candidates for future DDNs include the following for the RB barrier:

- Computer code validation
- Reduce uncertainty on outside air-RB-PHTS gas exchange phenomena
- Reduce uncertainty on changes in the distribution of I-131 and other radiologically significant RNs on dust, aerosol, and vapor as well as dust and aerosol size distributions in the RB
- Reduce uncertainty on plate-out, settling, and other retention phenomena along the two major release paths: DVS with damper open and RB leakage with DVS closed.

3.6.4 Uncertainties in Radiological Dose Calculation

Dose calculation performed in this study are based on Regulatory Guide rules and definitions of the NRC TEDE and the PAG CEDE in a manner consistent with realistic assumptions and a generic site. While there are considerable uncertainties in the dose calculation due to lack of defined site, weather variability, etc. these uncertainties can only be quantified for specific sites. The decision was made at the workshop to treat dose parameters as fixed values. The most significant uncertainty that can be influenced by the design is the extent to which I-131 is indicative of the total dose. So the only uncertainty distributions assigned for this part of the release and dose calculation is those in the scaling factor used to predict total dose from I-131 dose. One such uncertainty factor was needed for each the thyroid CEDE and the TEDE. These distributions are shown in the following figures.

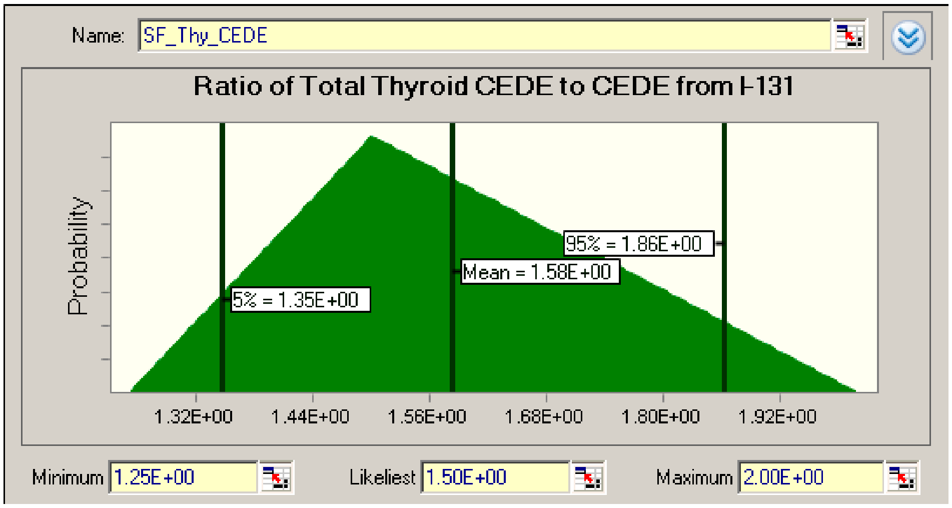

Figure 3-10 Uncertainty in the Scaling Factor to Calculate Total Thyroid CEDE from I-131 Thyroid CEDE

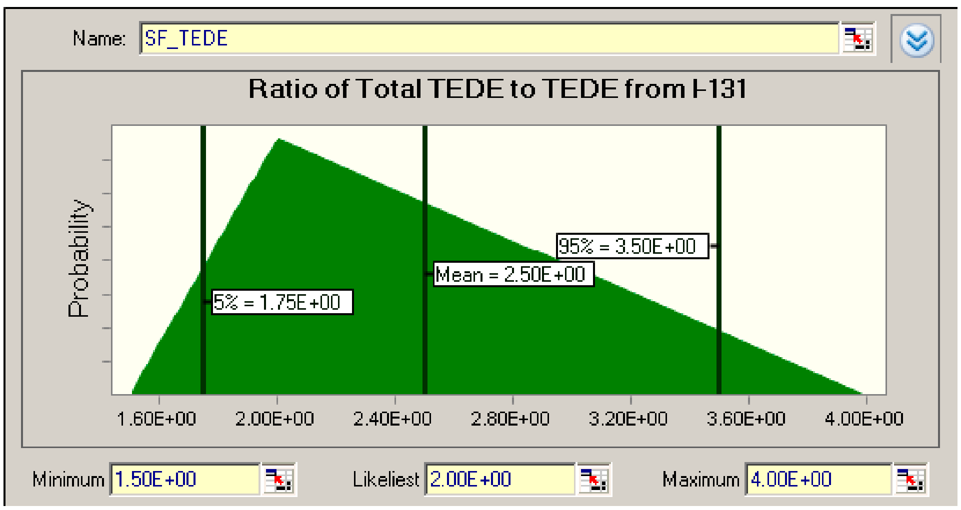

Figure 3-11 Uncertainty in the Scaling Factor to Calculate Total TEDE from I-131 TEDE

The following items were identified for future consideration as DDNs for the radiological dose part of the model.

- Need to confirm applicability of existing Dose Conversion Factors (DCFs) for HTGR source terms including impact of:
    - Distribution of RNs as dust, aerosol, and vapor
    - Particle size distributions for dust and aerosol
    - Possible chemical reactions during transit to dose receptor

3.6.5 Uncertainty Distributions Assigned to Crystal Ball Input Variables

A summary of the input distributions for all the independent variables that were developed for the Crystal Ball model is provided in Table 3-2.

Table 3-2 Uncertainty Distributions for Independent Variables in Crystal Ball Model

Parameter	Point Estimate [Note 2]	Flow-chart Box	Input Distributions						
			LB	BE	UB	Distribution Parameters [Note 1]			
			5%tile	50%tile	95%tile	Type	Para. 1	Para. 2	Comment
Fraction of TII released from Fuel to PHTS during normal operation (IR)	1.59E-07	2, 3a	1.89E-09	3.40E-08	6.11E-07	Log-normal	1.59E-07	18.0	1=mean; 2=RF
Fraction of initial release from fuel (IR) in PHTS that is circulating	1.00E-02	4a, 4c	1.00E-03	1.00E-02	1.00E-01	Log-normal	2.7E-02	10	
Fraction of IR Circulating in PHTS that is dust	0.5	4a, 4c	0.05	0.5	0.95	Beta	1	1	1=Alpha; 2=Beta
Fraction of IR non-dust circulating in PHTS that is vapor	0.5	4a, 4c	0.05	0.5	0.95	Beta	1	1	1=Alpha; 2=Beta
Fraction of IR Non-Circulating that is dust	0.5	4a, 4c	0.05	0.5	0.95	Beta	1	1	1=Alpha; 2=Beta
Fraction of IR non-circulating dust that is re-suspended during blowdown	4.00E-04	4a	4.00E-05	4.00E-04	4.00E-03	Log-normal	1.1E-03	10	1=mean; 2=RF
Fraction of IR non-circulating non dust that is lifted off during blowdown	4.00E-04	4a	4.00E-05	4.00E-04	4.00E-03	Log-normal	1.1E-03	10	1=mean; 2=RF
Fraction of IR non-circulating lifted off non-dust that is vapor	0.5	4a	0.05	0.5	0.95	Beta	1	1	1=Alpha; 2=Beta
Fraction of IR in PHTS Released RB due to pressure equib.	0.93	4a	0.5	0.93	0.95	Triangle			[Note 3]
Complement of the PHTS Settling fraction for dust during blowdown	0.1	4a, 4c	0	0.1	1	Triangle			[Note 3]
Complement of the PHTS Settling fraction for aerosol during blowdown	0.1	4a, 4c	0	0.1	1	Triangle			[Note 3]
Complement of the PHTS plateout fraction for vapor during blowdown	0.1	4a, 4c	0	0.1	1	Triangle			[Note 3]
Fraction of DR that is dust	0.1	4b, 4d	0	0.1	1	Triangle			[Note 3]
Fraction of non-dust DR that is vapor	0.5	4b, 4d	.05	.50	.95	Beta	1	1	1=Alpha; 2=Beta
Fraction released from PHTS during blow down phase due to thermo-fluid behavior	0.63	4a, 4c	0.315	0.63	0.8	Triangle			[Note 3]
Complement of the PHTS Settling fraction for dust during post blowdown	0.01	4b, 4d	0	0.01	1	Triangle			[Note 3]

Parameter	Point Estimate [Note 2]	Flow-chart Box	Input Distributions						
			LB	BE	UB	Distribution Parameters [Note 1]			
			5%tile	50%tile	95%tile	Type	Para. 1	Para. 2	Comment
Complement of the PHTS Settling fraction for aerosol during post blowdown	0.01	4b, 4d	0	0.01	1	Triangle			[Note 3]
Complement of the PHTS plateout fraction for vapor during blowdown	0.01	4b, 4d	0	0.01	1	Triangle			[Note 3]
Fraction of RB dust released via DVS during blowdown given non-dust is vapor	2.00E-03	6a	1.90E-05	3.81E-04	7.62E-03	Log-normal	2.00E-03	20.0	1=mean; 2=RF
Fraction of RB dust released via DVS during blowdown given Non-dust is aerosol	1.00E-02	6a	9.52E-05	1.90E-03	3.81E-02	Log-normal	1.00E-02	20.0	1=mean; 2=RF
Fraction of RB dust released via RB Leakage during blowdown given vapor	1.00E-04	6b	9.52E-07	1.90E-05	3.81E-04	Log-normal	1.00E-04	20.0	1=mean; 2=RF
Fraction of RB dust released via RB Leakage during blowdown given aerosol	2.00E-04	6b	1.90E-06	3.81E-05	7.62E-04	Log-normal	2.00E-04	20.0	1=mean; 2=RF
Fraction of RB aerosols released via DVS during blowdown	8.00E-04	6a	7.62E-06	1.52E-04	3.05E-03	Log-normal	8.00E-04	20.00	1=mean; 2=RF
Fraction of RB IR aerosols released via RB Leakage during blowdown	1.00E-07	6b	3.93E-10	1.18E-08	3.54E-07	Log-normal	1.00E-07	30.00	1=mean; 2=RF
Fraction of RB IR vapor released via DVS during blowdown	7.00E-03	6a	7.00E-04	7.00E-03	1.00E-01	Triangle			[Note 3]
Fraction of RB IR vapor released via RB Leakage during blowdown	2.00E-07	6b	7.86E-10	2.36E-08	7.07E-07	Log-normal	2.00E-07	30.00	1=mean; 2=RF
Total Initial Inventory (TII) of I131 (Bq)/1e16	4.79E+01	1	4.00E+01	4.79E+01	5.58E+01	Normal	4.79E+01	4.79	1=mean; 2=SD
Fraction of IFI released from Fuel to PHTS as Delayed Release (DR) during blowdown	1.91E-05	3b	1.82E-07	3.64E-06	7.27E-05	Log-normal	1.91E-05	20.00	1=mean; 2=RF
Fraction of RB dust released via DVS during post-blowdown (PB)	0.00	6a	Fixed value to force assumption that damper closed after blowdown						
Fraction of RB IR aerosols released via DVS during PB	0.00E+00	6a	Fixed value to force assumption that damper closed after blowdown						
Fraction of RB aerosols released via RB Leakage during PB	5.00E-04	6b	1.88E-05	1.88E-04	1.88E-03	Log-normal	5.00E-04	10.00	1=mean; 2=RF
Fraction of RB IR vapor released via DVS during PB	0.00E+00	6a	Fixed value to force assumption that damper closed after blowdown						

Parameter	Point Estimate [Note 2]	Flow-chart Box	Input Distributions						
			LB	BE	UB	Distribution Parameters [Note 1]			
			5%tile	50%tile	95%tile	Type	Para. 1	Para. 2	Comment
Fraction of RB IR vapor released via RB Leakage during PB	5.00E-02	6b	0.00E+00	5.00E-02	1.00E-01	Triangle			[Note 3]
Fraction of IFI released from Fuel to PHTS as delayed release (DR) during PB	1.43E-06	3c	1.36E-08	2.72E-07	5.45E-06	Log-normal	1.43E-06	20.00	1=mean; 2=RF
X/Q for elevated release (s/m^3)	1.90E-06	7a, 7b	Uncertainty in Dose Parameters Not Addressed						
X/Q for ground release (s/m^3)	2.60E-05	7a, 7b	Uncertainty in Dose Parameters Not Addressed						
Building wake factor for elevated release (-)	1.00E+00	7a, 7b	Uncertainty in Dose Parameters Not Addressed						
Building wake factor for ground release (-)	1.00E+00	7a, 7b	Uncertainty in Dose Parameters Not Addressed						
Breathing Rate (m^3/s)	2.32E-04	7a, 7b	Uncertainty in Dose Parameters Not Addressed						
Thyroid CEDE dose conversion factor for particulates (Sv/Bq)	1.47E-07	7a	Uncertainty in Dose Parameters Not Addressed						
TEDE CEDE dose conversion factor for particulates (Sv/Bq)	7.39E-09	7b	Uncertainty in Dose Parameters Not Addressed						
TEDE EDE dose conversion factor for particulates (Sv/Bq)	1.69E-14	7b	Uncertainty in Dose Parameters Not Addressed						
Thyroid CEDE dose conversion factor for vapor (Sv/Bq)	3.93E-07	7a	Uncertainty in Dose Parameters Not Addressed						
TEDE CEDE dose conversion factor for vapor (Sv/Bq)	1.98E-08	7b	Uncertainty in Dose Parameters Not Addressed						
TEDE EDE dose conversion factor for vapor (Sv/Bq)	1.69E-14	7b	Uncertainty in Dose Parameters Not Addressed						
Radionuclide decay factor for dust release	1.00E+00	7a, 7b	Uncertainty in Dose Parameters Not Addressed						
Radionuclide decay factor for aerosol release	9.00E-01	7a, 7b	Uncertainty in Dose Parameters Not Addressed						
Radionuclide decay factor for vapor release	5.00E-01	7a, 7b	Uncertainty in Dose Parameters Not Addressed						

Parameter	Point Estimate [Note 2]	Flow-chart Box	Input Distributions						
			LB	BE	UB	Distribution Parameters [Note 1]			
			5%tile	50%tile	95%tile	Type	Para. 1	Para. 2	Comment
Radionuclide daughter buildup factor	1.00E+00	7a, 7b	Uncertainty in Dose Parameters Not Addressed						
Scaling Factor I-131 Dose to Total Dose for Thyroid CEDE	1.50E+00	7a	1.25E+00	1.50E+00	2.00E+00	Triangle			[Note 3]
Scaling Factor I-131 Dose to Total Dose for TEDE	2.00E+00	7b	1.50E+00	2.00E+00	4.00E+00	Triangle			[Note 3]

Notes:
1. Comment column defines the definition of Parameter 1 and Parameter 2
2. Only the independent input parameters are given; other model parameters are calculated from these; certain values are treated as constants as explained in the table entries
3. For the Triangle distribution the LB = lower bound is the 0%tile, BE = Most likely is the peak value of the triangle; UB = upper bound is the 100%tile

3.7 BARRIER ALLOCATION RESULTS

3.7.1 Summary of Barrier Allocations

Barrier retention allocations were assigned in terms of following parameters:

- Limits on fuel release fractions during normal operation and transient
- Limits on PHTS HPB release fraction
- Limits on RB release fraction
- Limits on composite 3-barrier release fraction across 3 barriers
- Factor Margins to PAG and 10CFR50.34 dose limits

Design target values for each parameter are given in terms of:

- Best estimate based on mean and 50%tile values
- Upper bounds based on 95%tile
- Lower bounds based on 5%tile

Each barrier expected to meet or exceed targets in next phase of design. The limits on the composite 3-barrier release fractions are used to assess integrated performance of all three barriers and to facilitate barrier performance trade-offs in future design stages. This parameter is given a higher priority than the individual barrier allocations as this parameter controls the margins to the dose limits. The margins to dose limits are used to provide allowance for risks due to:

- Evolution of design
- Improvements and changes to analysis models and data
- Licensing acceptance

A summary of the barrier allocations for the above listed parameters is provided in Table 3-3 and Figure 3-12. Table 3-3 includes the mean values of the uncertainty distributions that were developed as well as selected percentiles. It can be seen that the fuel, as a barrier, provides the most important contribution to retention. For the fuel release parameter, there is more than a factor of 300 spread between the 5%tile and 95%tile values. This uncertainty is driven by the input uncertainty on the delayed fuel releases during blow down and post-blowdown phases of depressurization from DLOFC resulting from a 4mm break. The HPB barrier is seen to provide somewhat more than a factor of 2 reduction in the release for these same 4mm breaks with more than a factor of 4 spread between the 5%tile and 95%tile values. The RB barrier provides more than a factor of 50 reduction in the release with a factor of 30 spread between the lower and upper percentiles. As seen in Figure 3-12, the composite retention capability of all three barriers is nearly 7 orders of magnitude reduction in the release against the baseline of the RN inventory and it is clear that, while the fuel retention is most important component, all three barriers contribute to this result.

Table 3-3 RN Retention Barrier Design Target Allocations for NGNP Conceptual Design

Parameter	Mean	5%tile	50%tile	95%tile
Fuel Release Fraction	2.05E-05	2.68E-07	4.10E-06	7.87E-05
PHTS HPB Release Fraction	4.40E-01	1.47E-01	4.19E-01	8.00E-01
Reactor Building Release Fraction	1.73E-02	1.34E-03	1.31E-02	4.68E-02
Composite Three Barrier Release Fraction	1.64E-07	4.73E-10	1.86E-08	6.00E-07
I-131 Release to Environment - Curies	2.12E+00	6.05E-03	2.39E-01	7.81E+00
Margin Factor to 5rem Thyroid CEDE PAG Limit [Note 1]	1.85E+02	7.77E+04	1.67E+03	4.99E+01
Margin Factor to 25rem TEDE DBA Dose Limit [Note 1]	1.16E+04	4.99E+06	1.06E+05	3.14E+03
Note 1: These values are obtained by dividing the dose limit by the corresponding percentile of the dose uncertainty distribution; hence the higher doses have lower margins to the limit				

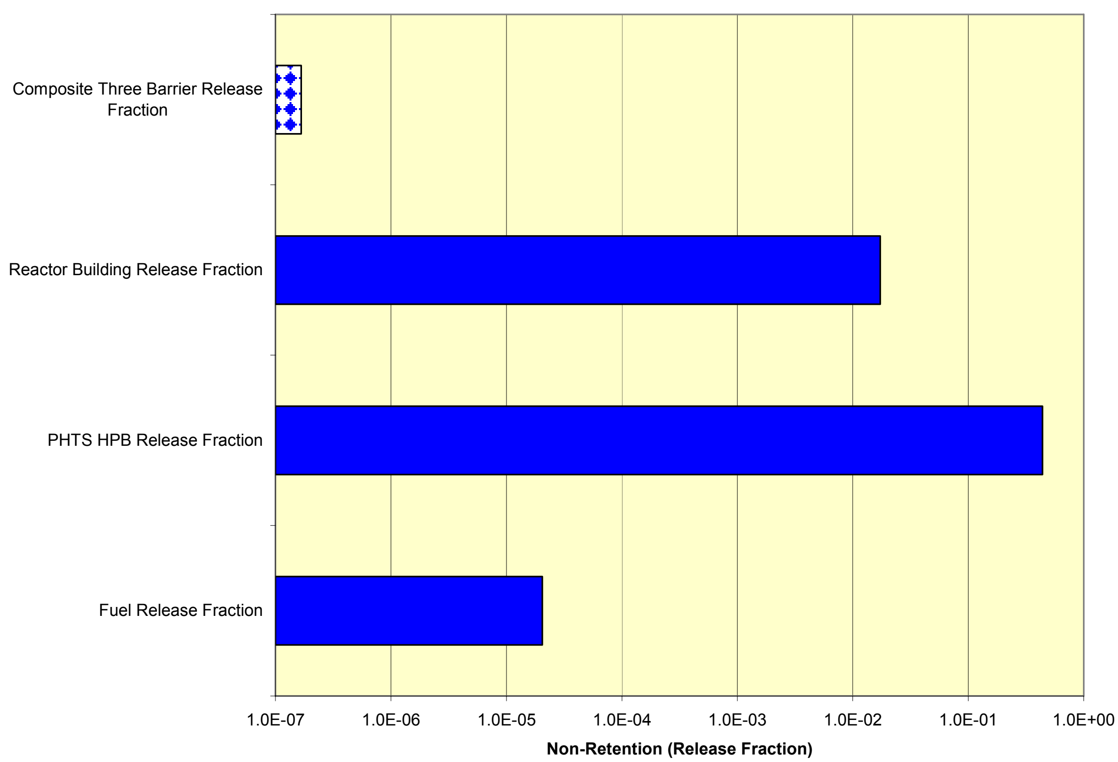

Figure 3-12 Mean Values of Barrier Release Fractions

3.7.2 Uncertainties in Barrier Performance

Uncertainties in the barrier allocation parameters are given in Table 3-3 in terms of mean values and selected percentiles of the uncertainty distributions obtained using Crystal Ball using straight Monte Carlo sampling and 100,000 trials. Further information on uncertainties is provided in the following figures for each parameter.

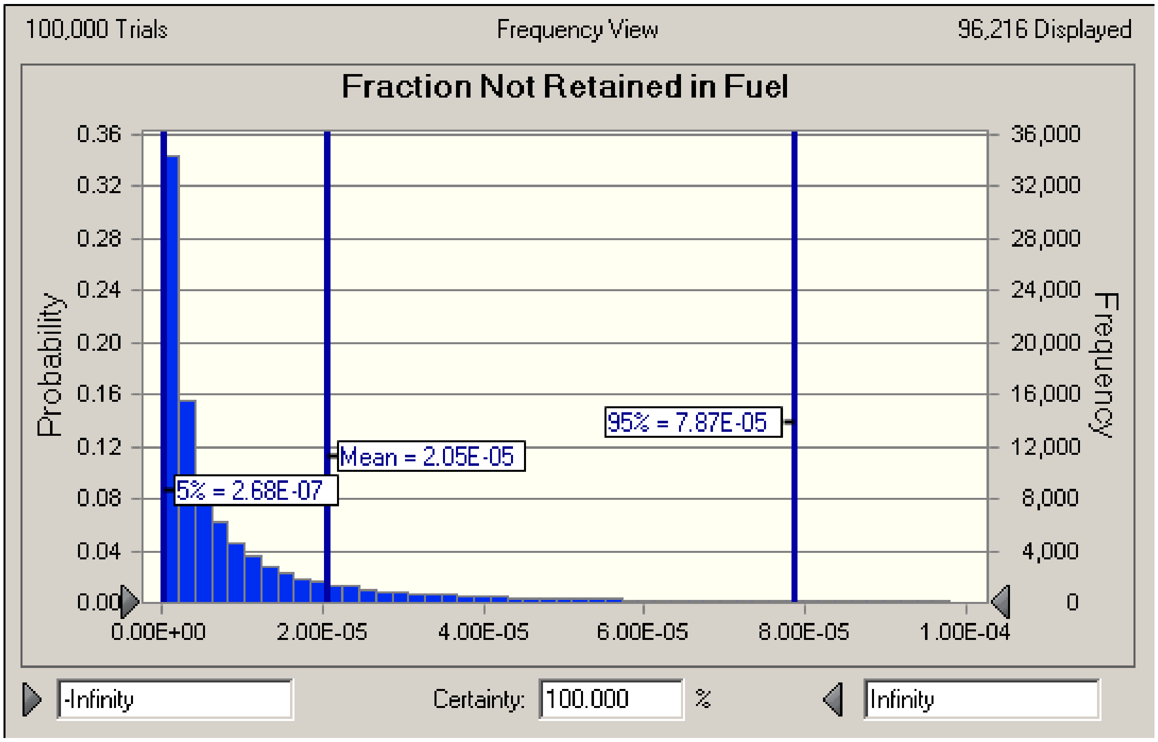

Figure 3-13 Fuel Barrier Release Fraction Uncertainty Distribution

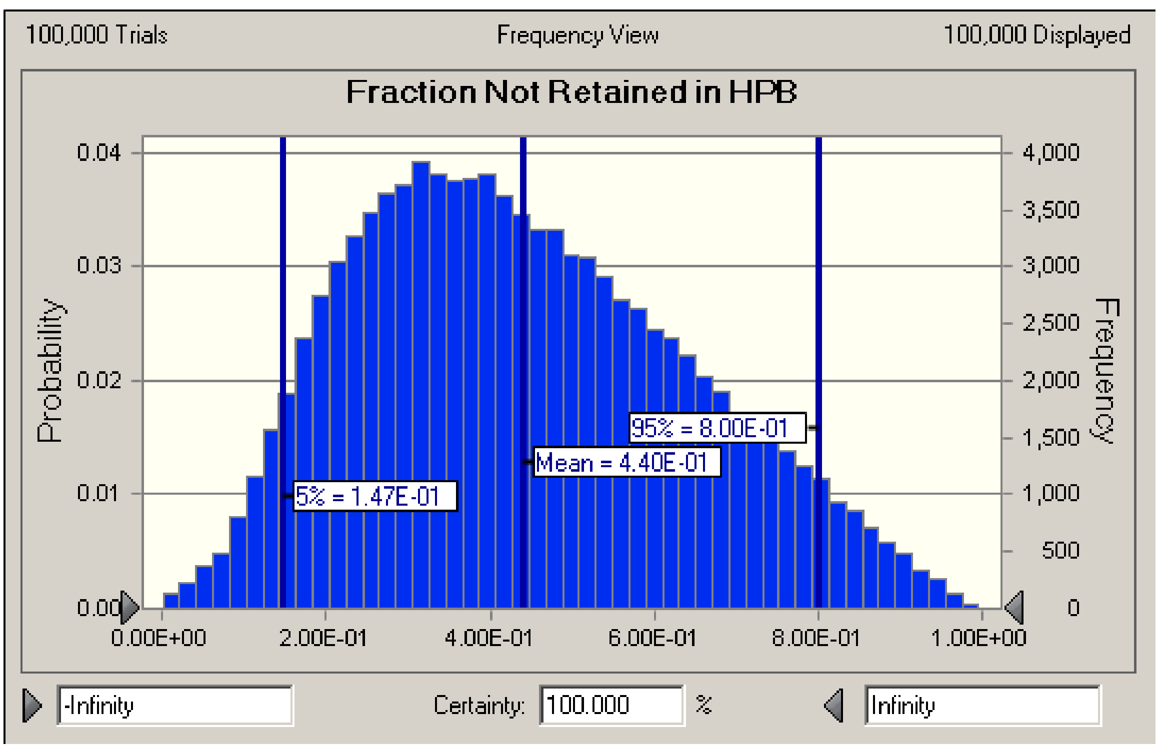

Figure 3-14 PHTS HPB Barrier Release Fraction Uncertainty Distribution

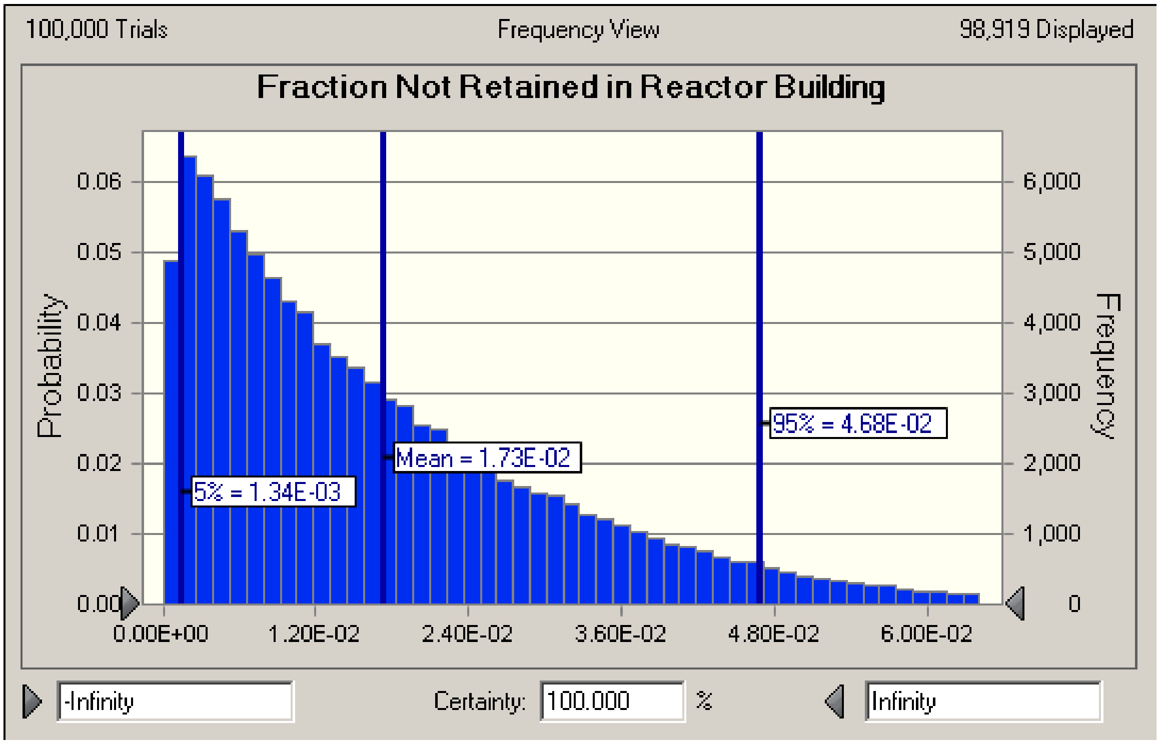

Figure 3-15 Reactor Building Barrier Release Fraction Uncertainty Distribution

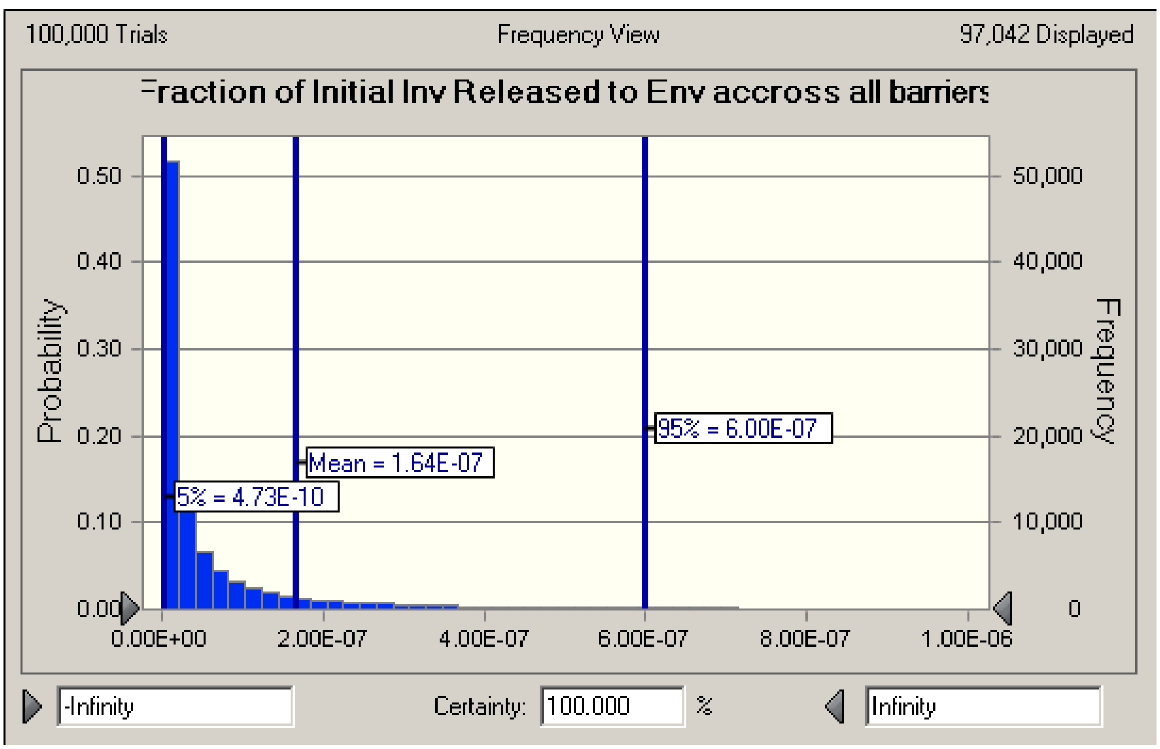

Figure 3-16 Composite Three- Barrier Release Fraction Uncertainty Distribution

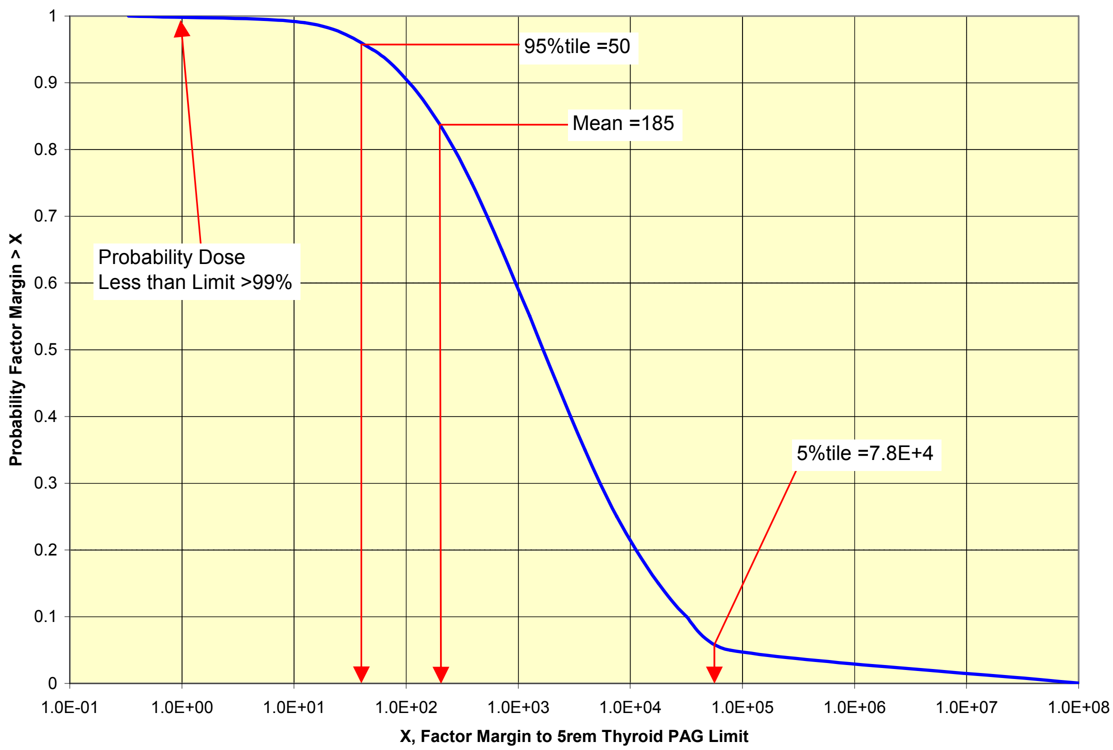

Figure 3-17 Uncertainty Distribution on the Factor Margin to the Thyroid PAG Dose Limit

3.7.3 Use of Barrier Allocations in Future Design Phases

The following conclusions and insights from the Barrier Allocation task will shape future design phases of the NGNP:

- Barrier retention factors are design targets to guide next phase of NGNP design; not to be confused with regulatory requirements.
- There is an expectation that barrier retention capabilities will be evaluated in the next design phase and changes are expected due to:
    - Design changes and greater level of detail in design
    - Improvements in state of knowledge due to improved and more detailed models and data
    - More complete evaluation of HPB break sizes, locations, and plant response scenarios; treatment of more radio-nuclides; limiting scenarios to set allocations likely to change
- Barrier retention allocations may change as design is optimized to maintain margins against limits
- Margins to limits may be reduced if warranted by reduced uncertainties in performance

- Barrier allocations completed are based on HPB break size and location expected to be limiting for design basis events for an assumed set of boundary conditions defined in this section
- RN retention allocation for reactor building, a factor of 10 reduction in source terms for I-131 and Cs-137, have been enhanced in this study by factor of more than 5 relative to that specified in the 2008 RB study [1]
- RN retention allocation for the HPB is rather limited for small breaks but it is important to include to demonstrate barrier defense-in-depth capability; HPB barrier retention is more significant for larger breaks due to lack of pressure driving force during delayed fuel release based on the 2008 and 2009 study results
- RN retention allocation targets for the fuel augments the fuel performance specification
- Thyroid PAG dose dominated by delayed fuel releases at ground level from RB that occur post-blowdown after DVS damper is closed
- Methodology for evaluating barrier performance and barrier allocations should be updated for each future design stage to maintain adequate margins against dose limits

It is rather noteworthy that the potential releases during the post-blowdown phase of the 4-mm DLOFC were found to dominate the results and provide the limiting conditions for determining the barrier allocations. This is noteworthy because in the point estimate evaluations provided with the computer models in Section 2, there is no release predicted from the HPB into the RB following blowdown for the 4mm break because the core temperatures are decreasing and the PHTS helium is contracting during this period. It is noted however that in the point estimate analysis, RN transport from the RB to the environment continues post-blowdown and makes a significant contribution to the dose. In the uncertainty analysis, based on engineering judgment, some RN transport into the RB was postulated due to phenomena such as diffusion and natural convection that were not modeled in the computer programs. These RNs had been release from the fuel in the computer simulations but were retained in the PHTS due to lack of a modeled transport mechanism. This insight points to the importance of future work to resolve the uncertainties associated with gas-exchange phenomena.

3.7.4 Topics for Further Study

Topics for Further Study include the following:

- Improved mechanistic analysis of buoyancy and natural circulation phenomena on gas exchange among the barriers and resulting impacts on core oxidation and RN releases from HPB and RB
- Improved understanding of the distribution of RNs between dust, vapor, and aerosol forms in the PHTS and in the RB
- Improved understanding of RN transport phenomena for dust, vapor, and aerosol in the PHTS and RB including those associated with settling, plateout, and radioactive decay
- Expansion of the range of leak and break locations and variations on plant response for a full spectrum of LBEs

- More realistic treatment of lift off and dust resuspension for beyond design basis larger HPB breaks (>100mm)
- Inclusion of filter resistance and aerosol formation in RB model
- Improved Coupling of Core, PHTS, and RB models
- Better characterization of Dose Conversion Factors for HTGR source terms
- Improved understanding of the contribution of nuclides other than those modeled in this study.

A summary of the most important candidates for future consideration as DDNS is provided as follows:

- Fuel Barrier
    - Current fuel performance demonstration
      (currently covered by DDN NHSS-01-01, DDN NHSS-01-02)
- HPB Barrier
    - Computer code validation
    - Reduce uncertainty on distribution of I-131 and other radiologically significant RNs on dust, aerosol, and vapor as well as dust and aerosol size distributions
    - Reduce uncertainty on PHTS-RB gas exchange phenomena
    - Reduce uncertainty on plate-out, settling, and other retention phenomena
- RB Barrier
    - Computer code validation
    - Reduce uncertainty on outside air-RB-PHTS gas exchange phenomena
    - Reduce uncertainty on changes in I-131 distribution in RB
    - Reduce uncertainty on plate-out, settling and other retention phenomena
- Radiological Dose
    - Confirm applicability of DCFs for HTGR releases for dust, aerosol, and vapor

Final determination and definition of necessary DDNs will be undertaken as part of forthcoming conceptual design studies.

REFERENCES

[1] NGNP-NHS 100 RB-RXBLD, Revision 0, *NGNP and Hydrogen Production Conceptual Design Study - Reactor Building Functional and Technical Requirements and Evaluation of Reactor Embedment*, Westinghouse Electric Company, 16 September 2008

[2] NGNP-NHS-HTS-RPT-M-0004, Revision 0, *NGNP: Intermediate Heat Exchanger Development and Trade Studies*, Westinghouse Electric Company, 18 September 2009

[3] Flownex Version 7.018 *Nuclear Transient Premium*, Flownex International

[4] NGNP-NHS 50-CC, Revision 0, *NGNP and Hydrogen Production Preconceptual Design Study: Contamination Control*, Westinghouse Electric Company, May 2008

[5] DOE-GT-MHR-100230, Revision 0, *GT MHR Preliminary Safety Assessment Report,* General Atomics, September 1994

[6] DOE-HTGR-86-024,Ammendment 8, *Preliminary Safety Information Document for the Standard MHTGR*, US Department of Energy

DEFINITIONS

None

ASSUMPTIONS

All assumptions are stated in the report where they are used.

APPENDICES

APPENDIX A: FINAL DESIGN REVIEW PRESENTATION TO BEA

Plant Level Assessments Leading to Fission Product Retention Allocations

90% Design Review

10 September 2009

PBMR TEAM

P B M R

Shaw®

Discussion Topics

- Objectives and Scope
- *Plant Level Analyses I:* Normal Operation and Anticipated Transients
  - Requirements and Functional Analyses (Bullet 1 In SOW 6793)
  - Operating Range and Initial Transitions Analyses (Bullet 2)
- *Plant Level Analyses II:* DLOFC for a Range of Primary HPB Leaks and Breaks
  - Depressurization for Range of Leaks and Breaks (Bullet 3)
  - Coupled Thermo-fluid Analysis of PHTS and Reactor Building Response (Bullet 4)
  - Radioactive Material Release Source Terms and Site Boundary Doses (Bullet 5)
  - Retention Allocations and RN Retention DDNs (Bullet 5)
- Path Forward

Objectives and Scope

- Develop requirements and functional analyses in support of critical SSC development
- Perform operating range (upper and lower limits) and initial transition analysis providing the basis for the normal operation radionuclide source term within the fuel and Helium Pressure Boundary (HPB)
- Perform HPB depressurization analyses for a spectrum of leaks and breaks (ranging from 3mm to guillotine break of the largest pipe)
- Perform coupled thermo-fluid analyses for the heatup and cooldown of the fuel, the gas in the HPB and the gas in the Reactor Building (RB) in order to determine the extent and timing of the transport of the radionuclides released from the fuel and the extent and timing of the ingress of the gas mixture from the RB into the HPB
- Based on the above, perform plant level assessments to assess the source terms relative to the offsite requirements.
- Allocate RN retention requirements for the Fuel, HPB and RB
- Define RN retention Design Data Needs (DDNs)

Key Contributors

- PBMR
  - Roger Young, Diana Naidoo, Wilma van Eck, Desna Pretorius, Joachim van der Merwe, Bernard Muller, Gerhard Strydom, Johan Strauss, Hanno van der Merwe, Alastair Ramlakan, Nilen Naidu, Pieter Swanepoel
- Technology Insights
  - Karl Fleming, Fred Silady, Lori Mascaro, Fred Torri, Scott Penfield, Dan Allen

Frequently Used Acronyms

- CCS Core Conditioning System
- CIP/COP Core Inlet/Outlet Pipe
- DLOFC Depressurized Loss of Forced Cooling
- EBS Equivalent Break Size
- PHTS Primary Heat Transport System
- SHTS Secondary Heat Transport System
- HPB Helium Pressure Boundary
- RB Reactor Building
- RBVV Reactor Building Vent Volume
- PRS Pressure Relief System (for the RB)
- SG Steam Generator
- IHX Intermediate Heat Exchanger
- RCCS Reactor Cavity Cooling System
- PCS Power Conversion System
- RIT/ROT Reactor Inlet/Outlet Temperature
- RN Radionuclide
- DDN Design Data Need

Plant Level Analyses I

Normal Operation and Anticipated Transients

PBMR TEAM

Current Topic

- Objectives and Scope
- ***Plant Level Analyses I:*** **Normal Operation and Anticipated Transients**
  - **Requirements and Functional Analyses (Bullet 1 In SOW 6793)**
  - **Operating Range and Initial Transitions Analyses (Bullet 2)**
- *Plant Level Analyses II:* DLOFC for a Range of Primary HPB Leaks and Breaks
  - Depressurization for Range of Leaks and Breaks (Bullet 3)
  - Coupled Thermo-fluid Analysis of PHTS and Reactor Building Response (Bullet 4)
  - Radioactive Material Release Source Terms and Site Boundary Doses (Bullet 5)
  - Retention Allocations and RN Retention DDNs (Bullet 5)
- Path Forward

Requirements and Functional Analysis

- Requirements and functional analysis in support of critical SSC development
  - SRM input support captured in CORE™ database.
  - Functional analysis performed as an ongoing interactive task with analysis personnel in support of performance modelling
  - Modes and states
  - SE support of steady-state, transition & accident analysis
  - Consolidation of ’08 RB functions and technical requirements

Discontinued on April 17, 2009

Current Topic

- Objectives and Scope
- ***Plant Level Analyses I:* Normal Operation and Anticipated Transients**
  - **Requirements and Functional Analyses (Bullet 1 In SOW 6793)**
  - **Operating Range and Initial Transitions Analyses (Bullet 2)**
- *Plant Level Analyses II:* DLOFC for a Range of Primary HPB Leaks and Breaks
  - Depressurization for Range of Leaks and Breaks (Bullet 3)
  - Coupled Thermo-fluid Analysis of PHTS and Reactor Building Response (Bullet 4)
  - Radioactive Material Release Source Terms and Site Boundary Doses (Bullet 5)
  - Retention Allocations and RN Retention DDNs (Bullet 5)
- Path Forward

Operating Range and Initial Transitions Analyses

by

Wilma van Eck

Bernard Muller

NHSS Thermal Hydraulic Model

- NHSS model contains
  - Reactor
    - Detailed model developed for DPP400 (power level adjusted)
  - IHX
    - Based on compact layout designed in accompanying IHX & HTS priority task
  - SG
    - Preliminary sized based on MHTGR layout
  - PHTS and SHTS Circulators
    - Preliminary sized as no design data available
  - PHTS circulator outlet valve (non-return valve)
  - 2 x 100% CCS
    - Preliminary sized to keep Reactor Outlet Temperature < 300°C at atmospheric decay heat removal conditions
  - Piping and insulation
  - Control system
    - Control strategy proposed for purpose of this task

Flownex Model

- The Flownex model includes
  - Volume / inventory
  - Metal mass for thermal capacitance in transients
  - Area available for heat transfer
  - Turbo machines and heat exchanger
    - Modelled using empirical performance maps (user input)
  - Reactor
    - Modelled using point kinetics
  - Pressure drop
    - Calculated based on user input loss factors or friction factor correlations
  - Heat transfer
    - Calculated based on user input Nusselt number correlations

Steady State Definitions

- Power operation:
  - Nominal operating point (Reactor at 100% power, full inventory)
  - Upper operating point (Currently defined the same as nominal)
  - Lower operating point (Reactor at 40% power, full inventory)
- Shutdown state:
  - Pressurized maintenance (heat sink through Power Conversion System)
  - Pressurized maintenance (heat sink through Core Conditioning System)
- Maintenance:
  - Depressurized maintenance (atmospheric pressure, heat sink through Core Conditioning System)

Proposed Plant Modes and States Diagram

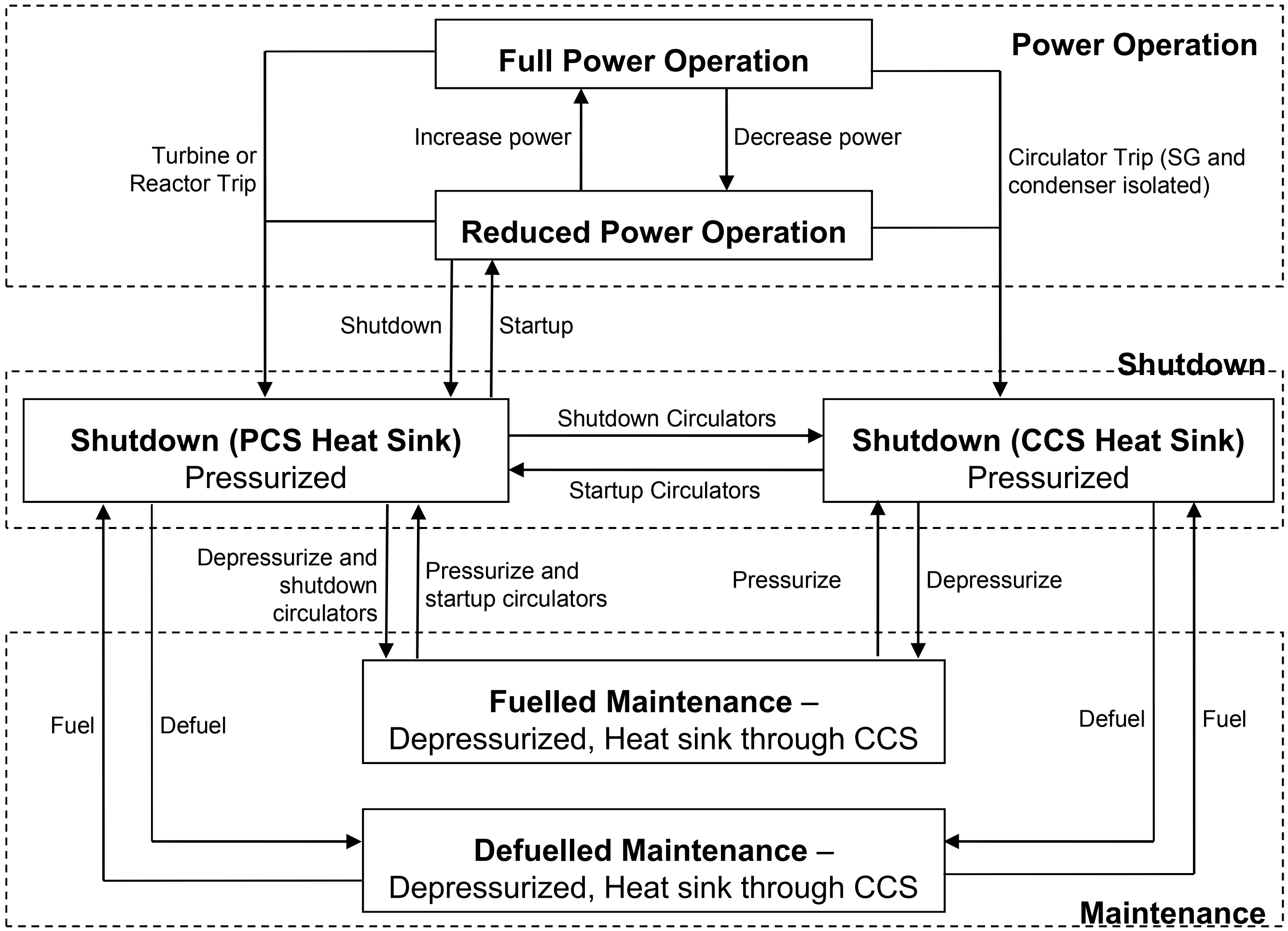

Nominal Operating Point (100% Power)

- Nominal operating point parameters
  - 500MWt reactor power (100%)
  - Reactor outlet temperature 750°C
  - Reactor inlet temperature 280°C
  - Steam conditions: 567°C at 16.9MPa
  - Feedwater conditions: 164°C
  - Mass flow rate PHTS/SHTS ~ 205kg/s
  - 9.0MPa in PHTS
  - 9.1MPa in SHTS
  - PHTS full inventory ~4 ton
  - SHTS full inventory ~6.3 ton

Nominal Operating Point (100% Power)

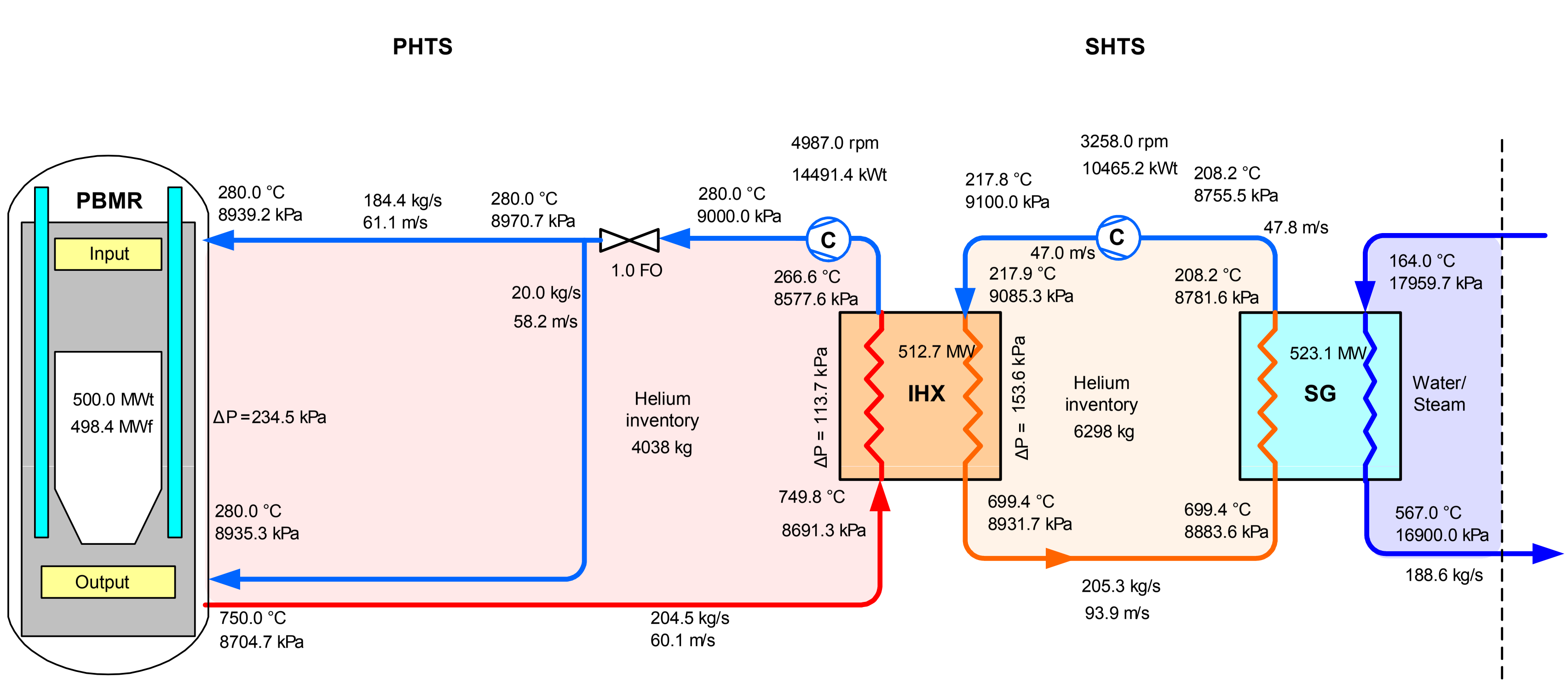

SG - Steam Generator
IHX - Intermediate Heat Exchanger
C - Circulator

Lower Operating Point (40% Power)

- Options to prevent pressure bias reversal between PHTS and SHTS
  - Lower ROT (preferred)
  - Increase feedwater temperature
  - Active He inventory control

- Lower operating condition therefore defined as
  - 200MWt reactor power (40%)
  - Reactor outlet temperature ~600°C
  - Reactor inlet temperature 280°C
  - Steam conditions: 567°C at 16.9MPa
  - Feedwater conditions: 120°C
  - 8.74MPa in PHTS
  - 8.76MPa in SHTS
    - Only marginally higher than PHTS
    - Recommendation: SHTS pressure can be increased by increasing cold gas temperature in SHTS slightly
  - PHTS full inventory ~4 ton
  - SHTS full inventory ~6.3 ton

Lower Operating Point (40% Power)

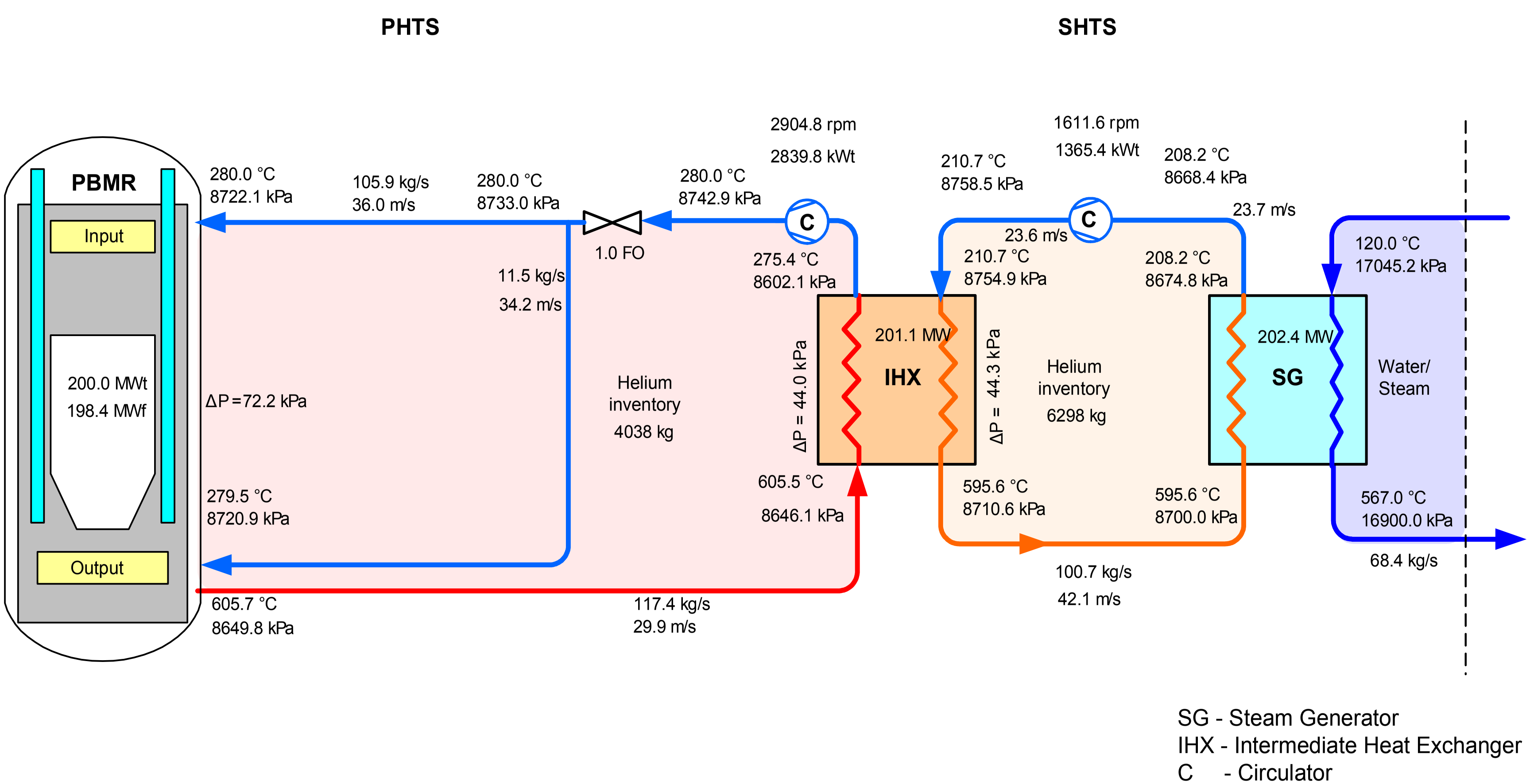

Pressurized Maintenance

Decay heat removal via Power Conversion System

- Pressurized maintenance via PCS
  - Decay heat at 12 hours after shutdown
  - Reactor outlet temperature 150°C
  - Reactor inlet temperature 130°C
  - Circulators at 10% speed
  - Feedwater temperature 35°C
  - Feedwater flow rate reduced to remove heat required
  - Pressure in PHTS 6.3MPa
  - Pressure in SHTS 6.6MPa
  - Full inventory

Pressurized Maintenance
Decay heat removal via Power Conversion System

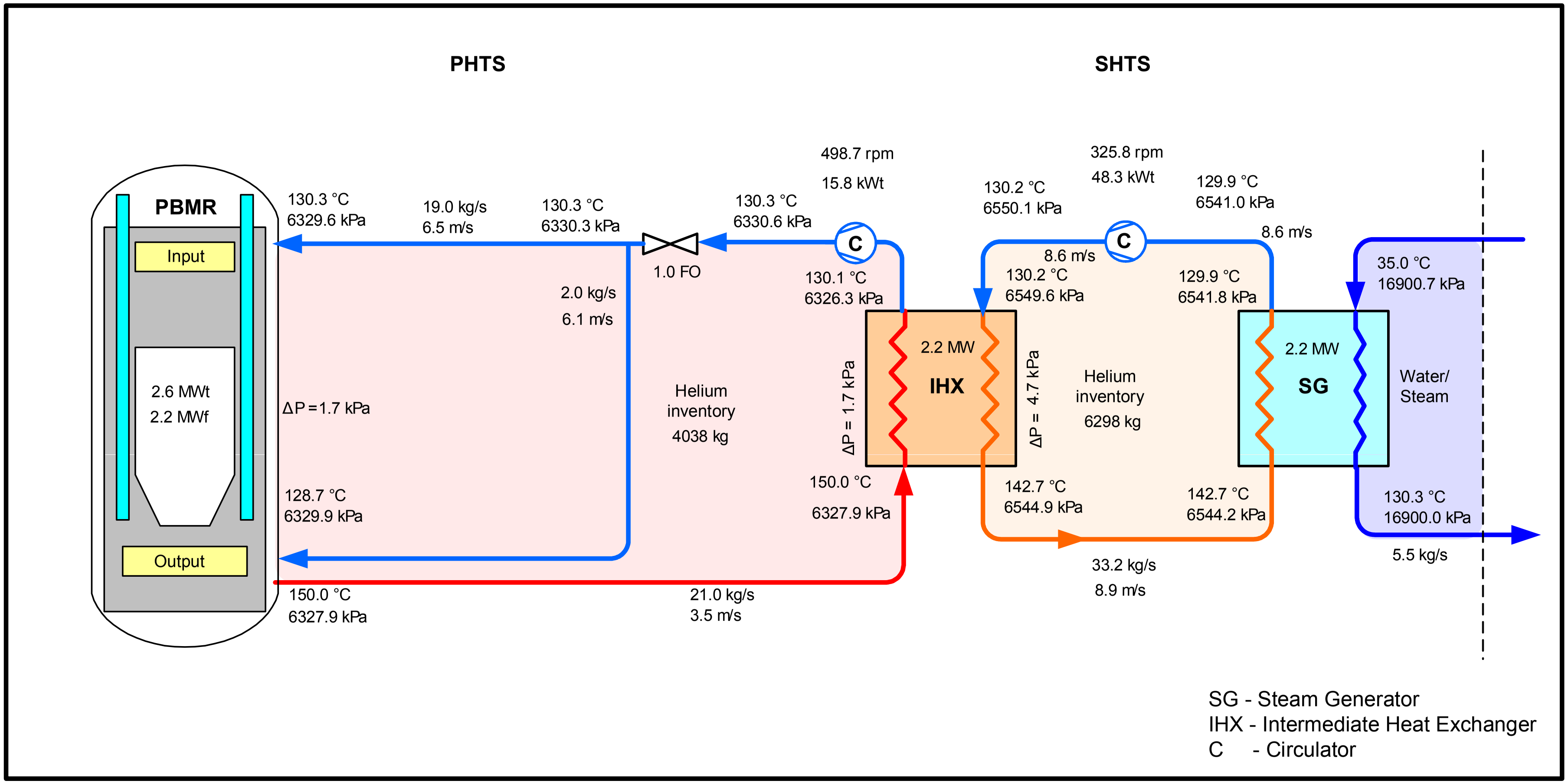

P B M R

Pressurized Maintenance

Decay heat removal via Core Conditioning System

- Pressurized maintenance via CCS
  - Decay heat at 12 hours after shutdown
  - Reactor outlet temperature ~ 120°C
  - Reactor inlet temperature ~ 50°C
  - PHTS and SHTS circulators stopped
  - CCS circulator at 10% speed
  - Pressure in PHTS 5.5MPa
  - Full inventory

Pressurized Maintenance

Decay heat removal via Core Conditioning System

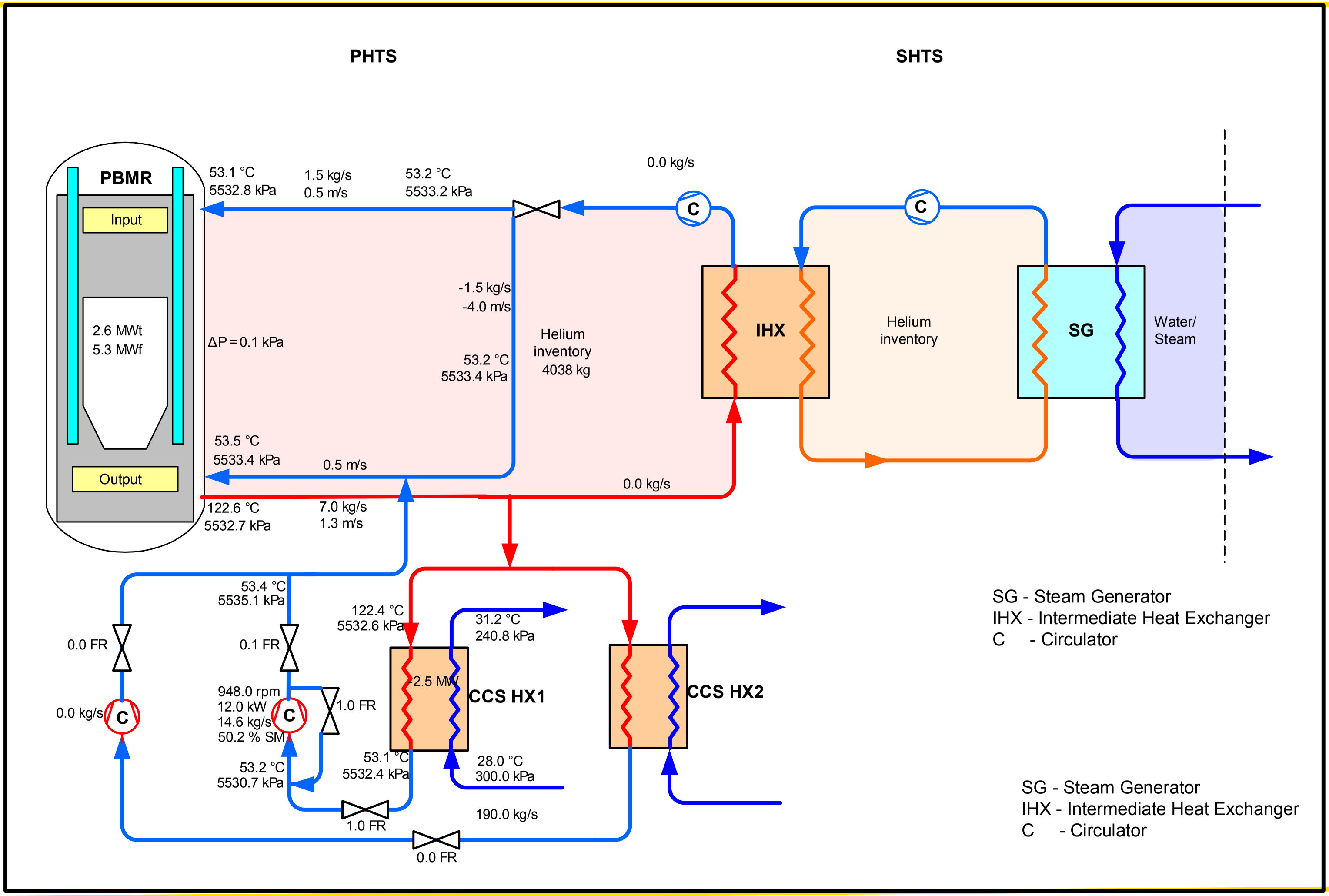

Depressurized Maintenance
Decay heat removal via Core Conditioning System

- Depressurized maintenance via CCS
  - Decay heat at 24 hours after shutdown
  - Reactor outlet temperature ~250°C
  - Reactor inlet temperature ~60°C
  - PHTS and SHTS circulators stopped
  - CCS circulator at 100% speed
  - Atmospheric pressure
  - Minimum inventory

Depressurized Maintenance
Decay heat removal via Core Conditioning System

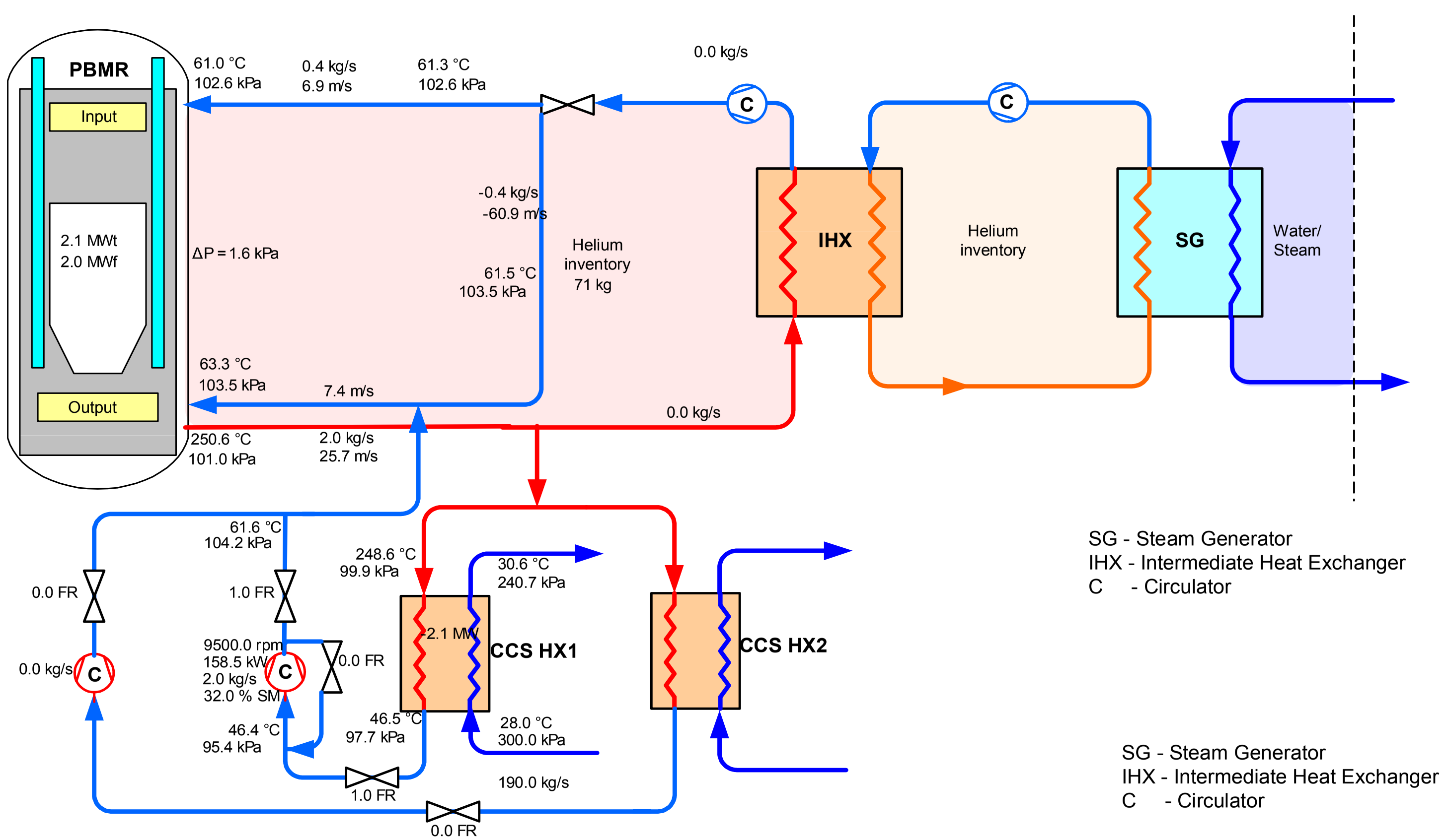

SG - Steam Generator
IHX - Intermediate Heat Exchanger
C - Circulator

Steady State Heat Balance Observations

- Nominal operating point
  - Flownex steady state heat balances are different from original reference flow sheet due to better estimates for pressure drop and component performance.
- Lower operating point
  - When decreasing power, the NHSS is operating at part load and therefore component efficiencies change. This results in temperature changes in the network.
  - To maintain primary/secondary pressure bias, the SHTS cold temperature must be controlled and ROT allowed to decrease.
  - *Recommendation*: Cold gas temperature in SHTS should be increased slightly to maintain pressure bias of 100kPa
- Pressurized maintenance/shutdown condition
  - CCS at minimum throughput (as currently sized) keeps reactor outlet temperature at ~100°C.
- Depressurized maintenance condition
  - CCS at maximum throughput (as currently sized) keeps reactor outlet temperature at ~250°C.

Start-up Strategy

- PHASE I (Pressurize)
  - Pressurize PHTS and SHTS to full inventory
  - CCS removes decay heat
- PHASE II (Startup Circulators):
  - Main circulators ramped up to full speed to heat up reactor, CCS reverts to idling
  - SG closed off (no water flow), thus water pressure builds up to 16.9MPa
- PHASE III (Startup: 0 to 40% power):
  - SG helium outlet temperature >208°C (normal operating point):
    - SG water flow started and used to control SG helium outlet temperature at 208°C
  - Reactor made critical and reactor power is ramped up to 40% power (100°C/hr)
  - Primary circulator speed set at 40%
  - RIT controlled at 280°C with secondary circulator speed
- PHASE IV (Increase Power):
  - Reactor power ramped up from 40% to 100% power (100°C/hr):
  - SG feedwater temperature increased from 125°C at 40% power to 164°C at 100% power
  - RIT controlled to 280°C with primary circulator speed
  - SG helium outlet controlled to 208°C with secondary circulator speed
  - Steam temperature controlled at 567°C using water mass flow, steam pressure maintained at 16.9MPa
  - Inventory topped up to full pressure (Prim = 9MPa, Sec = 9.1MPa)

Start-up Results

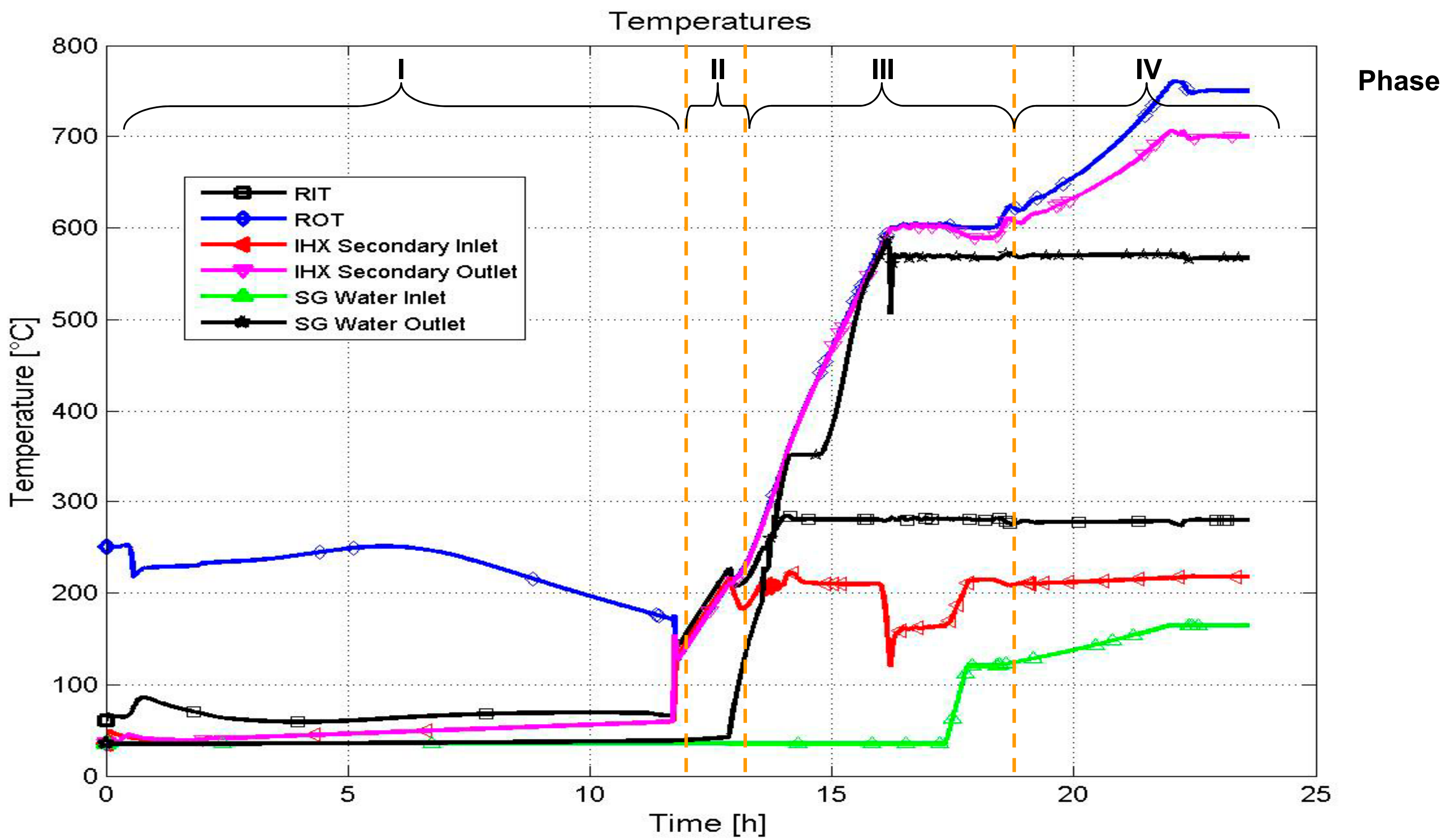

Start-up Results

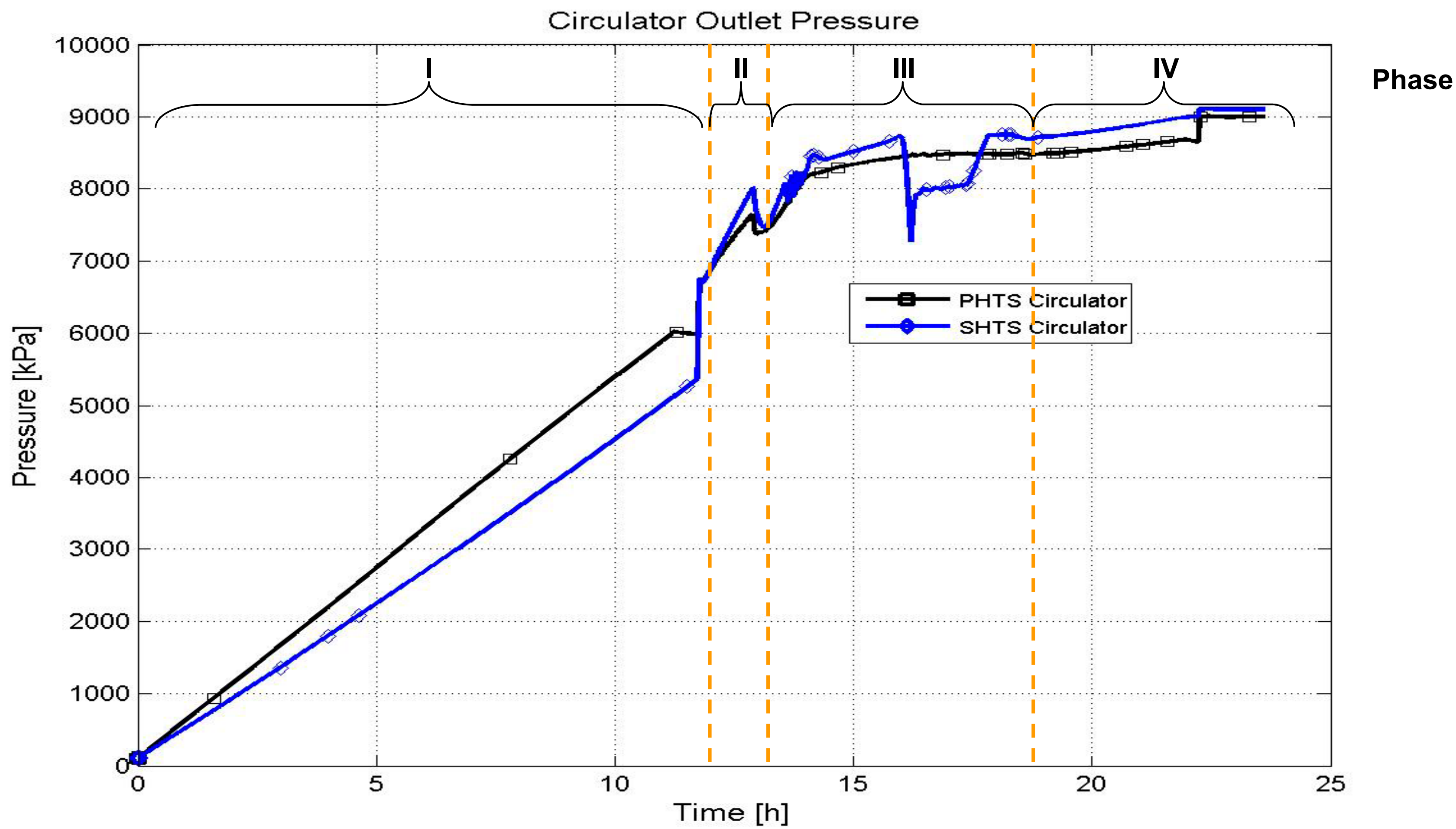

P B M R

Start-up Observations

- ROT and RIT can be controlled satisfactorily using circulators
- SHTS pressure lower than PHTS during Phase I (pressurize)
  - Can easily be rectified by pressurizing SHTS at slightly faster rate
- Cold side temperature of SHTS dips suddenly during Phase III (Startup)
  - Due to the water flow through SG being started while feedwater temperature is not preheated (still 35°C)
  - Causes SHTS pressure to drop below the PHTS pressure
    - May be desirable to detect small leaks from PHTS
    - May be undesirable due to induced stresses in SG, then auxiliary preheating of feedwater will be required
- During Phase IV (40% to 100% power transition), feedwater is preheated
  - SHTS cold side temperature can be controlled using secondary blower
  - SHTS pressure remains above PHTS pressure

Shutdown Strategy

- PHASE I (Decrease Power)
  - Reactor Power ramped down from 100% to 40% power (by reducing ROT at 100°C/h)
  - Circulator speed controlled to maintain cold temperatures in PHTS and SHTS
  - Feedwater flow rate used to control steam temperature at 567°C
  - Feedwater temperature reduced from 164°C at 100% power to 120°C at 40% power
  - CCS circulator in idle mode (10% speed)
- PHASE II (Shutdown)
  - ROT further ramped down at 100°C/h
  - ROT < 330°C: Reactor shut down by inserting control rods at maximum rate (1cm/s)
- PHASE III (Shutdown Circulators)
  - ROT < 300°C: PHTS and SHTS circulator stops and circulator outlet check valve closes
  - CCS circulator started
  - CCS outlet check valve opens with positive differential pressure across valve
  - CCS circulator speed used to control ROT rampdown at 100°C/h until 200°C is reached
  - Feedwater flow stopped
  - ROT is stabilised at 200°C for 2 hours (using CCS circulator speed)
- PHASE IV (Depressurization)
  - Inventory extracted until 200kPa is reached
  - Reactor mass flow rate < 3kg/s:
    - CCS blower speed used to control reactor mass flow rate at 3kg/s

Shutdown Results

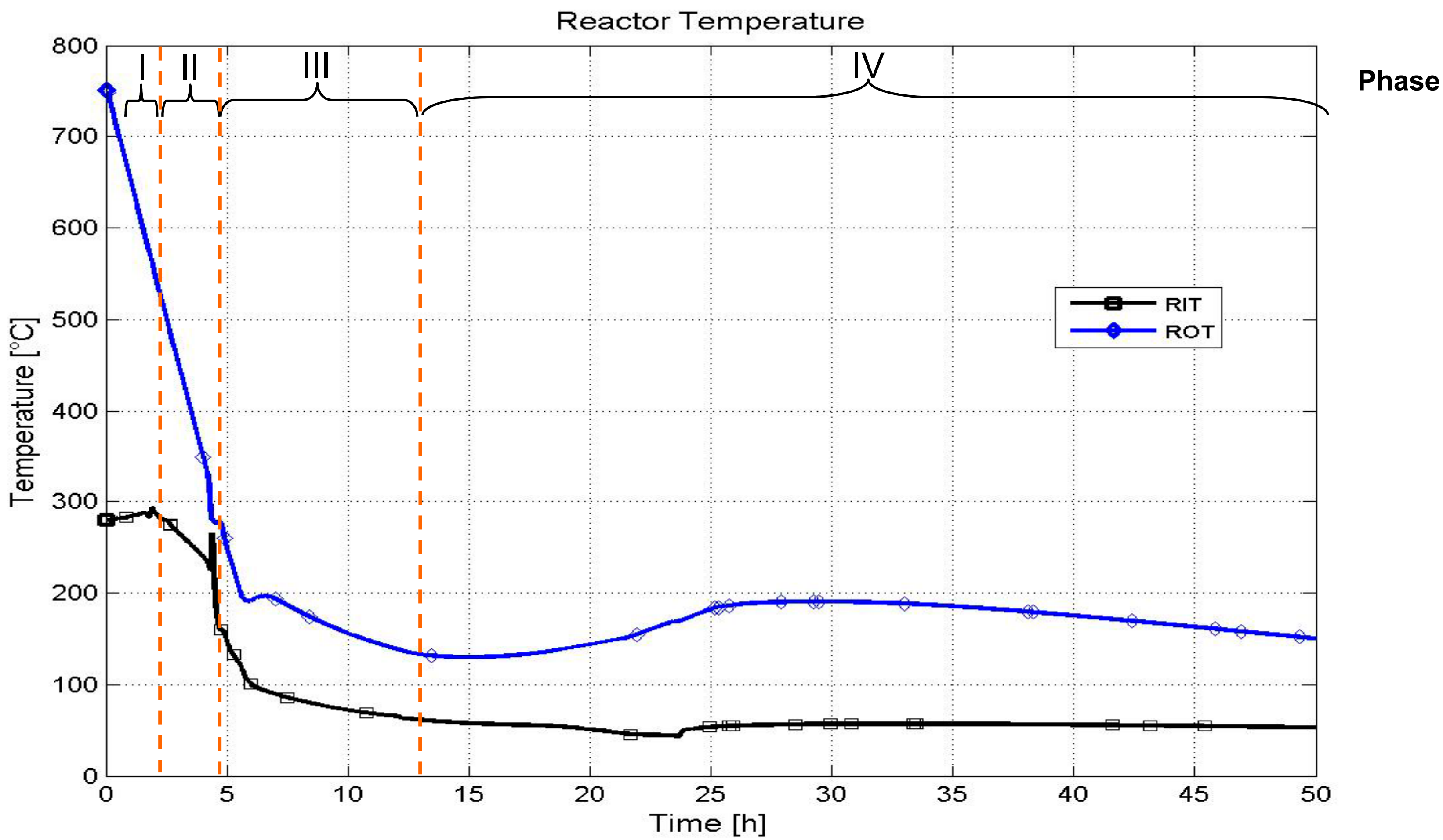

Shutdown Results

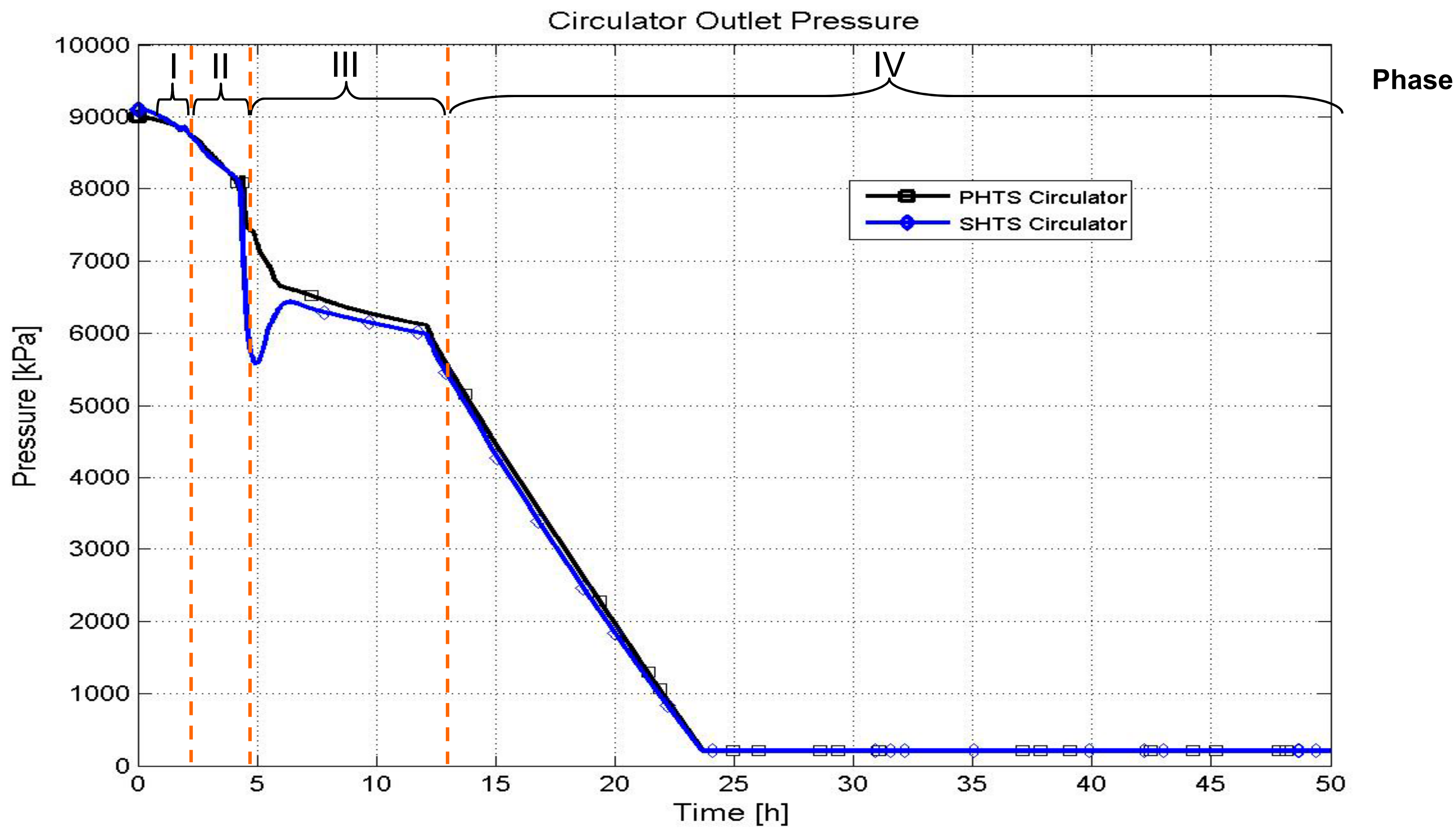

Shutdown Observations

- To keep pressure bias during Phase I, the circulators must be used to control cold gas temperature
- SHTS pressure dropped below PHTS pressure during Phase III (when circulators were switched off)
  - Due to drop in temperature of SHTS
  - SHTS circulator not stopped totally – low mass flow in SHTS causes SHTS temperature to approach feedwater temperature (35°C at this stage)
- CCS still to be optimally sized
  - Sufficient flow (in the order of 10 kg/s) through reactor is required to overcome buoyancy effects and to ensure good heat transfer and core cooling
  - Current CCS can only maintain about 3 kg/s during depressurization
- To prevent reductions in temperatures as a result of depressurization
  - As soon as all steam has condensed, stop feed water flow
  - Use circulators to add heat to the system

Lessons Learned and Future Work

- Lessons Learned
  - Careful design of the control strategies will be required to ensure the following during all transitions:
    - That the pressure of the SHTS remains higher than that of the PHTS
    - That the pressure difference between the primary and secondary side of the IHX remains within it limits
  - The CCS has to be sized carefully to ensure it can supply the required minimum and maximum flows for the pressurized and depressurized conditions respectively
- Future work
  - Optimize controllers
  - Refine control strategy
  - Determine exact behavior of SG feedwater temperature during transitions

Plant Level Analyses II

DLOFC for a Range of Primary HPB Leaks and Breaks

PBMR TEAM

Objectives

- Build on knowledge gained in 2008 Study on HPB break source term phenomena
- Improve understanding of key RN transport mechanisms for DLOFC events via best currently available models
  - HPB blowdown, effects on core temperatures and releases from HPB
  - Thermal expansion and contraction of PHTS gas
  - Gas exchange between PHTS and RB and between RB and environment
- Apply more detailed multi-compartment RB model and associated RN transport mechanisms
- Provide enhanced RN retention allocations to fuel, HPB, and RB
- Provide RN retention DDNs

Dose Behavior vs. Break Size for Unfiltered Vented RB from 2008 Study

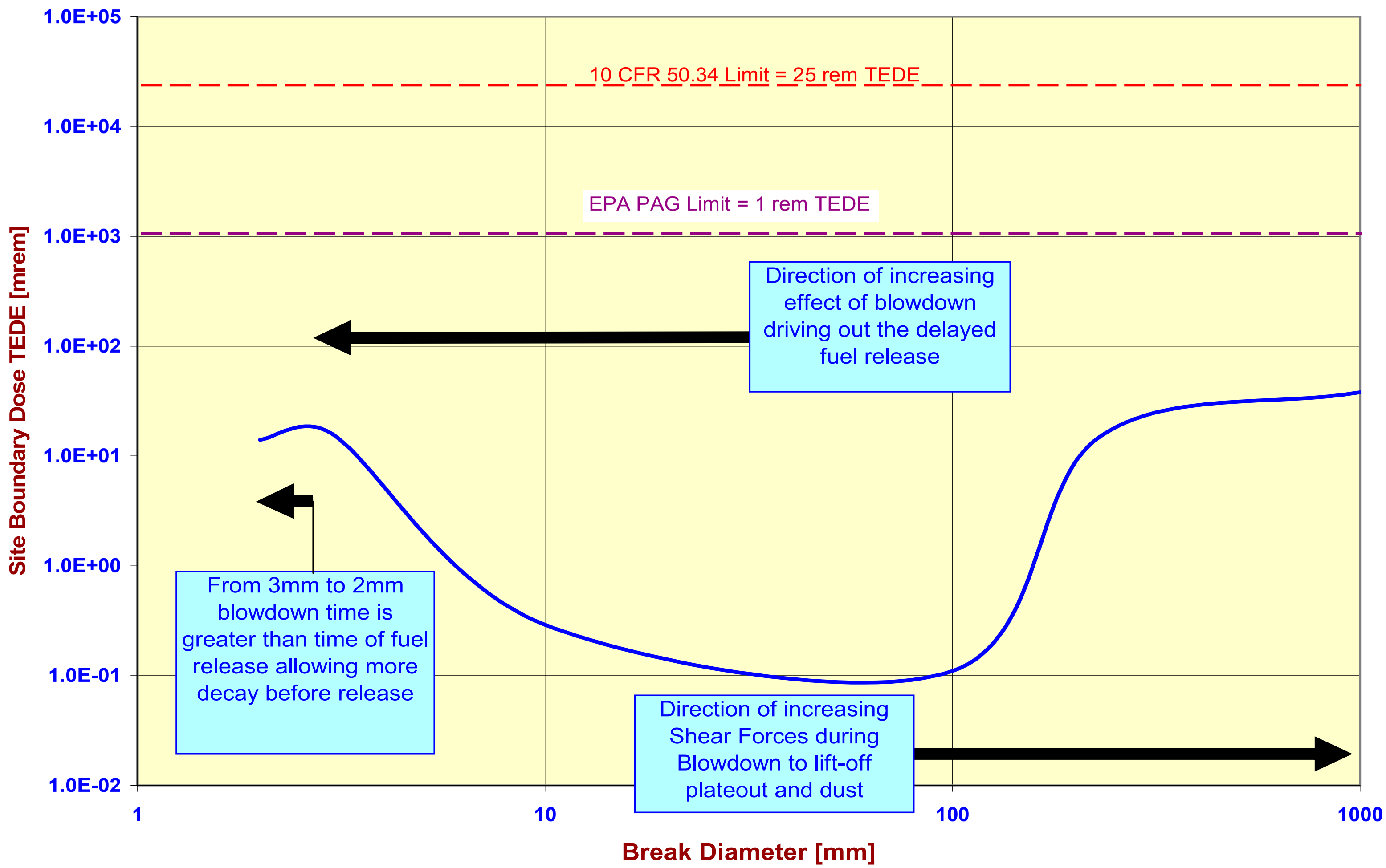

Comparison of Current and 2008 Studies

Parameter	2008 Study	Current Study
Convection cooling of core during blow-down	Neglected	Modeled
Thermo-fluid model of PHTS	Two volume mass balance with isentropic break flow and ideal gas law coupled to RB model	Flownex model of PHTS, SHTS, PCS coupled to Flownex RB model for 100mm breaks
RN release from PHTS model	Transport within PHTS calculated as part of the two volume thermo-fluid model	Simplified model using Flownex calculated gas flows neglecting transport within PHTS
Thermo-fluid model of RB	Single volume RB model with PRS single relief shaft dampers and filters with direct release and leakage to environment	Astec multi-compartment model with blow-out panels, DVS, damper and multiple leak paths. He-air mixtures in RB and PHTS calculated. PHTS calculated.
RN retention and releases from RB	Simple retention constant based on 2 RNs	Mechanistic retention based on 7 RNs

Characterization of Leak and Break Scenarios

- All breaks assumed to occur at top of CIP inside Rx cavity
  - Consistent with 2008 study
  - Largest pipe with single wall design
  - Isolation is not feasible in this location
- Parametric study of break sizes from 2mm to 1m Equivalent Break Size (EBS) corresponding to double ended break of 700mm CIP
  - Evaluation of time to depressurize
  - Calculation of shear force ratios
- Selection of cases for RN transport
  - 4mm selected to maximize delayed fuel release from PHTS HPB
    - For smaller break sizes pressure driven blowdown continues into the heatup phase, increasing releases from HPB
    - Smaller break sizes increase core heat removal lowering temperatures and releases from fuel
    - Smaller break sizes increase pressure driving force increasing releases from HPB
    - Smaller break sizes allow more time for radioactive decay of I-131 and other short lived radionuclides
  - 100mm selected as limiting break size for design basis accident selection

Assumed Response of Key Systems to HPB Breaks

- Control rods insert normally
- PHTS and SHTS circulators stop and non-return valves close; no decay heat removal via PCS
- No isolation of break and no He extraction from PHTS via HSS
- Core Conditioning System remains off in standby configuration (DLOFC transient); no water cooling of CCS HX
- Helium Services System (HSS) and Fuel Handling and Storage System (FHSS) isolated and do not add He mass to blowdown
- Reactor Cavity Cooling System modeled to simulate water boil-off mode of operation
- No RB HVAC circulation or filtration

Assumed Response of Reactor Building

- Multi-compartment model with engineered pressure relief shaft and multiple bypass leak paths
- Design Features
  - Blow-out panels to protect structures from blowdown loads and control release pathways
    - Reactor cavity to IHX cavity
    - IHX cavity to Pressure Relief System (PRS)
  - Isolation damper to reclose Depressurization Vent Shaft (DVS)
- Alternative RB responses considered
  - With and without PRS re-closure following blowdown
  - With and without assumed PRS filtration

Computer Codes and Models for HPB Break Evaluations

DLOFC ACCIDENT ANALYSIS FLOW CHART

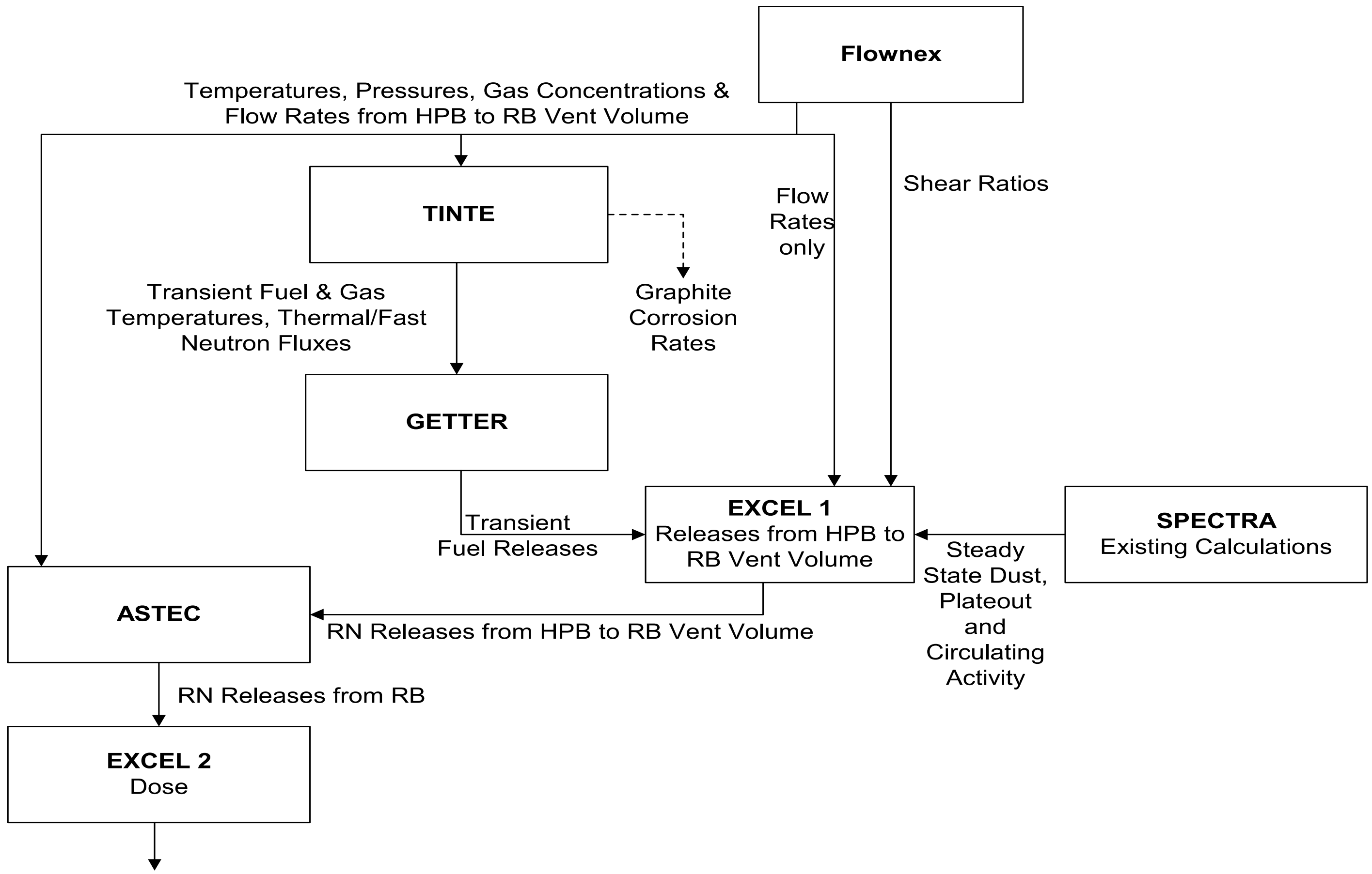

Current Topic

- Objectives and Scope
- *Plant Level Analyses I:* Normal Operation and Anticipated Transients
  - Requirements and Functional Analyses (Bullet 1 In SOW 6793)
  - Operating Range and Initial Transitions Analyses (Bullet 2)
- ***Plant Level Analyses II:* DLOFC for a Range of Primary HPB Leaks and Breaks**
  - **Depressurization for Range of Leaks and Breaks (Bullet 3)**
  - **Coupled Thermo-fluid Analysis of PHTS and Reactor Building Response (Bullet 4)**
  - Radioactive Material Release Source Terms and Site Boundary Doses (Bullet 5)
  - Retention Allocation and RN Retention DDNs (Bullet 5)
- Path Forward

Depressurization for Range of Leaks and Breaks and Coupled Thermo-fluid Analysis of PHTS and Reactor Building Response

by

Johan Strauss

Flownex DLOFC Models

- NHSS model is the same as used in the operating range and initial transitions analyses

- Determination of blowdown time:
  - Model is coupled via a pipe break element directly to the environment at atmospheric pressure @ 25°C because flow through the HPB break is choked for more than 95% of the time
  - Blowdown time is defined as time from break until pressure upstream of the break is 0.05kPa above atmospheric
- Determination of Shear Force Ratios (SFR):
  - Same model as above used to extract gas pressures (P), temperature (T) and velocities (V) from various locations in the PHTS:

$$SFR = \left(\frac{P_B}{P_N}\right)^{0.75} * \left(\frac{V_B}{V_N}\right)^{1.75} * \left(\frac{T_N}{T_B}\right)^{0.58}$$

  with N = steady state, B = max during break
- Determination of PHTS-RB gas exchange
  - Model coupled via a pipe break element to RB vent volume model and data recorded for 300 hour period
  - Flownex models gas exchanges due to thermal expansion and contraction. Buoyancy driven natural convection gas exchanges are not modeled.

Blowdown Time Results

Blowdown time results for a range of Equivalent Break Sizes (EBS) of the core inlet pipe in the PHTS

EBS (mm)	Blowdown time
3	158 hr
4	91 hr
5	59 hr
6	41 hr
10	15 hr
30	1.8 hr
100	11 min
230	2 min
1000	12.3 sec

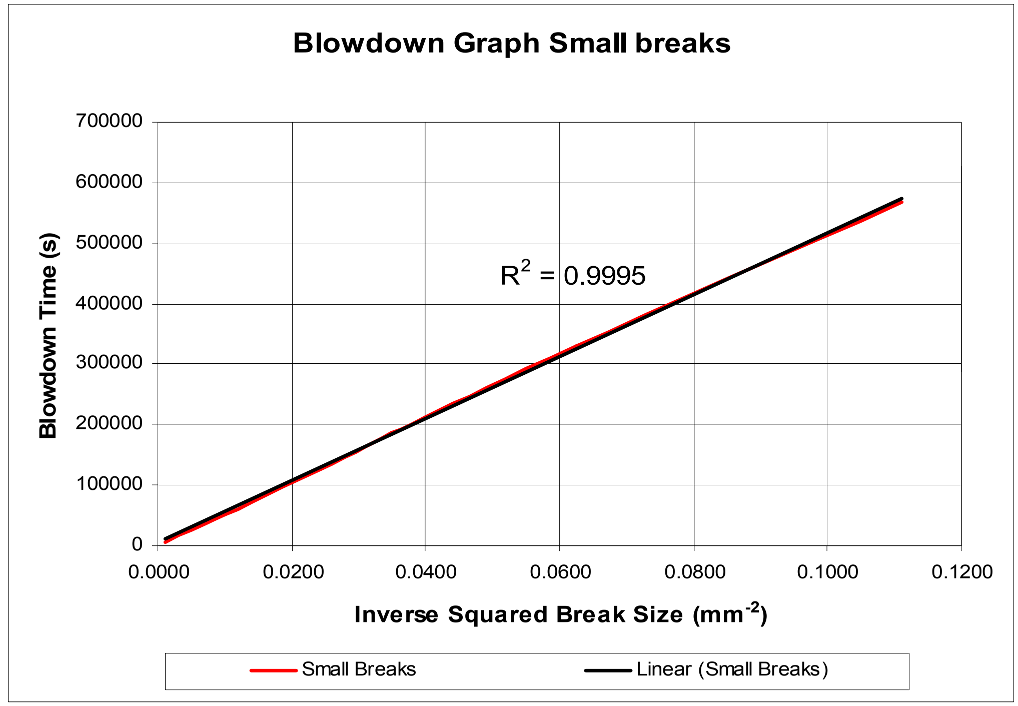

Shear Force Ratio Results

Results confirm 2008 Study results that breaks ≤100mm have SFR <1 and hence insignificant dust re-suspension and lift-off

	SFR vs. CIP Equivalent Break Size								
	3mm	**4mm**	**5mm**	**6mm**	**10mm**	**30mm**	**100mm**	**230mm**	**1000mm**
Reactor Inlet	0.0306	0.0306	0.0307	0.0308	0.0314	0.0390	0.8269	**2.3467**	**127.45**
Reactor Outlet	0.0195	0.0194	0.0195	0.0194	0.0194	0.0188	0.9879	**1.0002**	**1.5147**
Reactor Lower Volume	0.0685	0.0685	0.0687	0.0688	0.0695	0.0787	0.9953	**2.4003**	**84.30**
CCS Inlet Connection	0.0195	0.0194	0.0195	0.0194	0.0194	0.0188	0.9537	**1.0003**	**1.8534**
IHX Inlet	0.0083	0.0083	0.0083	0.0083	0.0083	0.0080	0.2333	0.9999	1.0000
Circulator Outlet	0.0062	0.0062	0.0062	0.0062	0.0062	0.0063	0.0251	1.0000	**1.1203**

Reactor Building Layout

Filter Inlet Plenum
(FIP)

Reactor Top Cavity
(RTC)

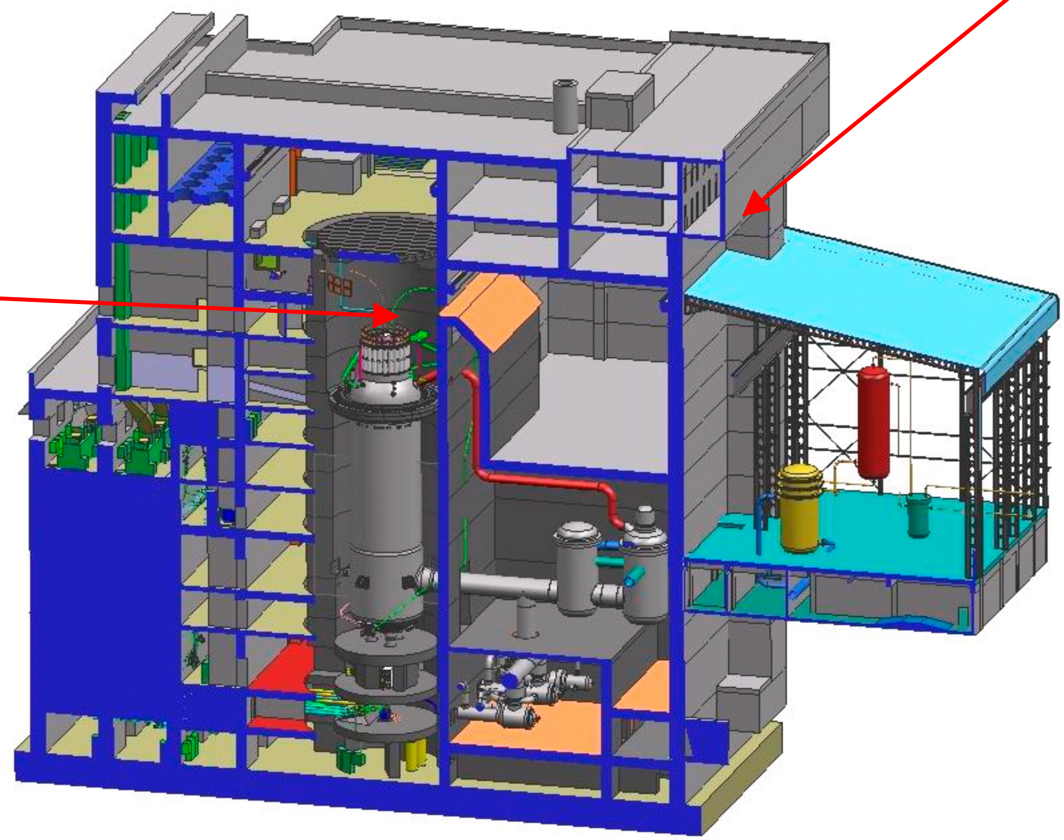

RB Gas Exchange for 100mm Break
PRS Relief Shaft Fails to Reclose Case

Helium mass fraction during the first hour in Reactor Top Cavity (RTC) and Filter Inlet Plenum (FIP) compartments of the Reactor Building after a 100 mm break of the core inlet pipe (break location inside RTC)

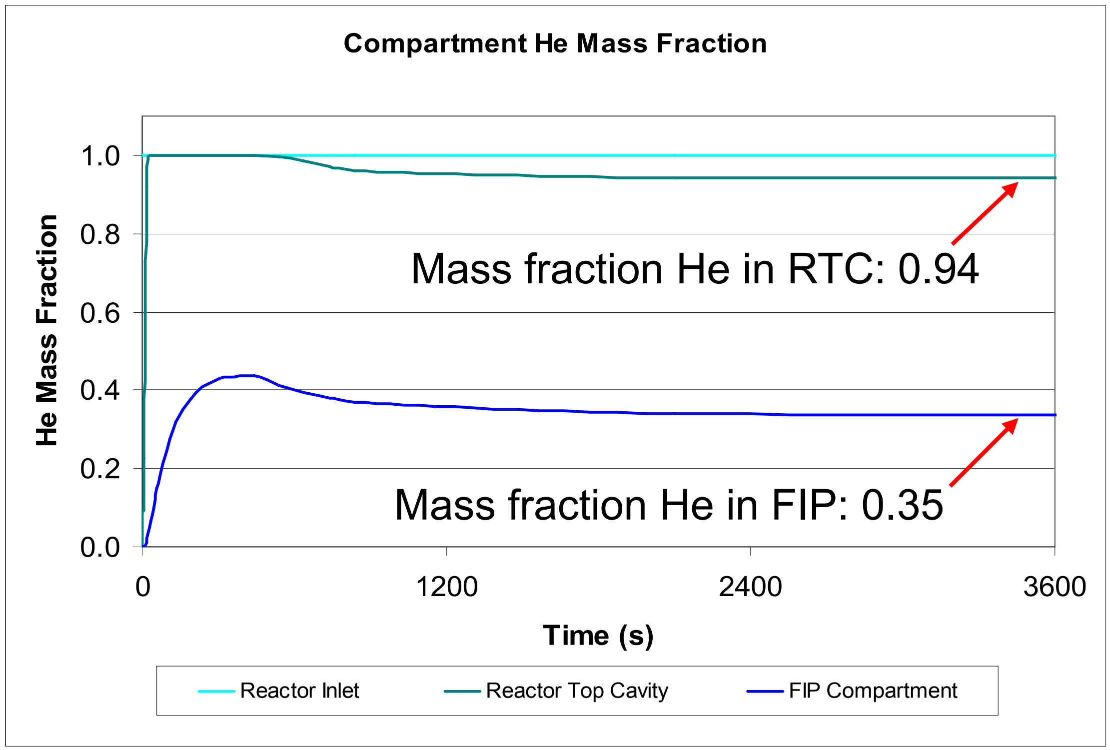

~0.9 mass fraction He (i.e.10% air content per mass) in RTC after 300 hrs

PHTS Gas Exchange for 100mm Break
PRS Relief Shaft Fail to Reclose Case

Air mass fraction in PHTS after a 100mm break of the core inlet pipe (break location: inside RTC)

Assumed failure to close DVS damper

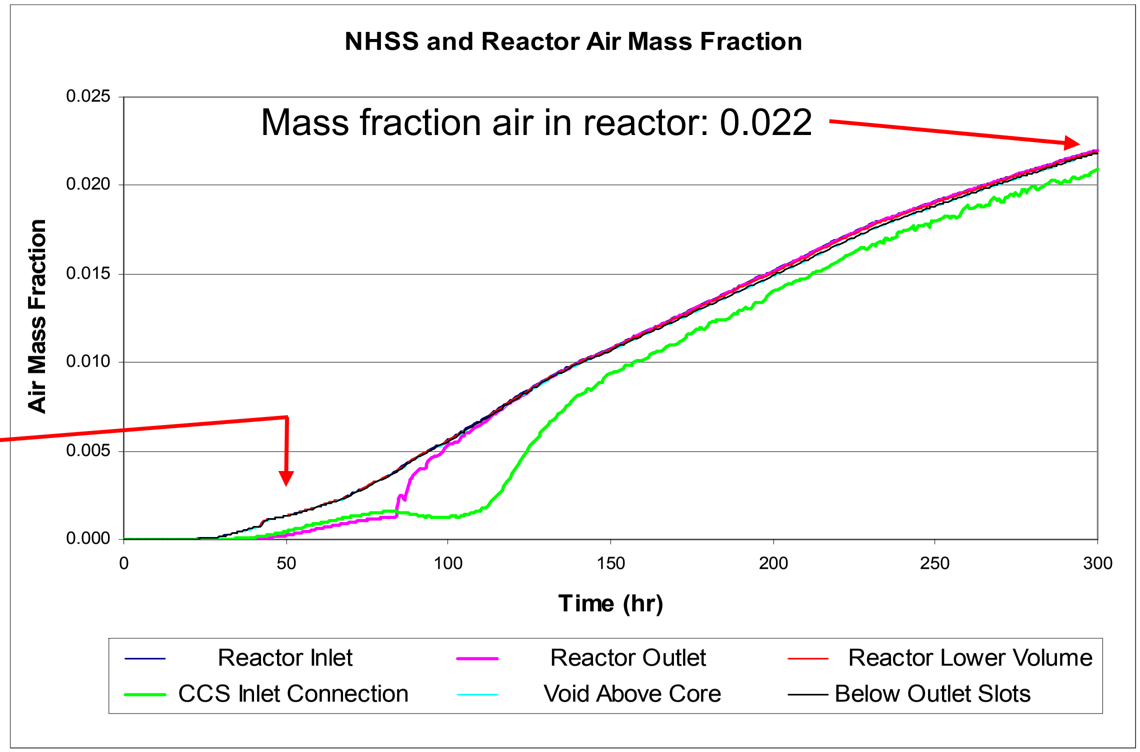

~0.022 mass fraction air (2.2% air content per mass) in PHTS after 300 hrs

Conclusions From Flownex Analyses

- Blowdown times vary from 158hr to 11min for the range of break sizes (3mm to 100mm break diameter)

- Results confirm 2008 study results that breaks ≤100mm have SFR <1 and hence insignificant dust re-suspension and lift-off

- For the 100mm break, thermal expansion of PHTS continues until about 50hr consistent with 2008 study

- RB gas exchange is dependent on break location, RB compartment layout, and response of the DVS damper

Lessons Learned and Future Work

- Lessons Learned
  - Small changes in NHSS He inventory and operation have a large influence on blow-down times
  - Flownex code capability at low mass flows: Care must be taken in using inventory mass results in cases where the flows are lower than the convergence criterion
- Future Work
  - This is a Best Estimate analysis – future sensitivity and uncertainty analyses should still be considered
  - CFD studies and possible experiments to evaluate PHTS-RB gas exchange phenomena not modelled in Flownex and to evaluate impact of oxidation reactions on flow associated phenomena
  - Expand spectrum of HPB leak and break cases
    - Different break sizes and locations
    - Impact of stuck open PHTS circulator check valve
    - Impact of actions to pump-down PHTS during slow depressurization

Current Topic

- Objectives and Scope
- *Plant Level Analyses I:* Normal Operation and Anticipated Transients
  - Requirements and Functional Analyses (Bullet 1 In SOW 6793)
  - Operating Range and Initial Transitions Analyses (Bullet 2)
- ***Plant Level Analyses II:* DLOFC for a Range of Primary HPB Leaks and Breaks**
  - Depressurization for Range of Leaks and Breaks (Bullet 3)
  - Coupled Thermo-fluid Analysis of PHTS and Reactor Building Response (Bullet 4)
  - **Radioactive Material Release Source Terms and Site Boundary Doses (Bullet 5)**
  - Retention Allocations and RN Retention DDNs (Bullet 5)
- Path Forward

Core Thermal Analysis

by

Gerhard Strydom

Core Thermal Analysis

DLOFC ACCIDENT ANALYSIS FLOW CHART

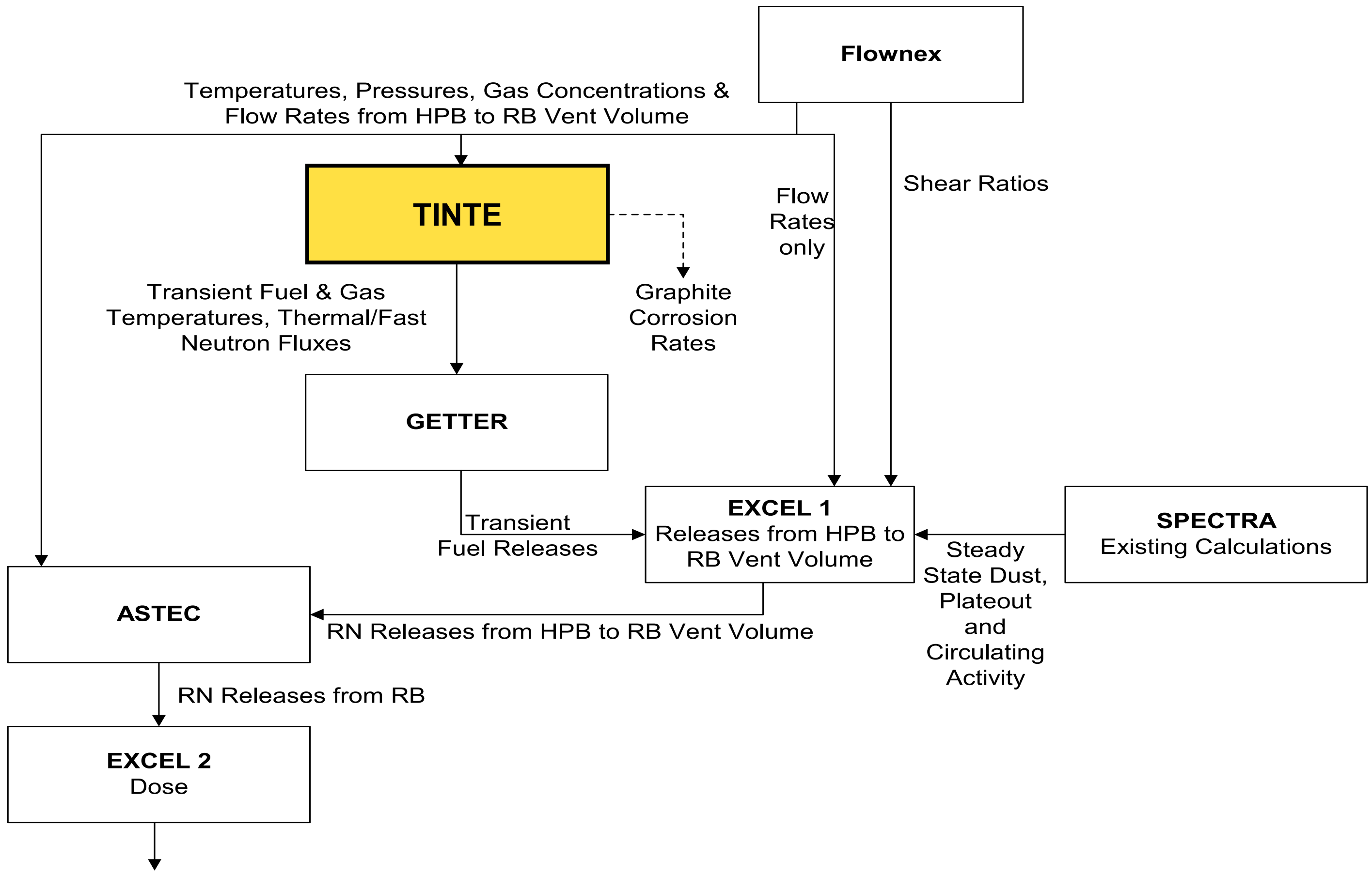

TINTE Model

- 5 DLOFC break sizes were modelled: 3, 4, 5, 10 and 100mm EBS
- Depressurisation data from FLOWNEX used as input flow conditions
- Modelling assumptions
  - Inlet forced mass flow rate decreased to 0.0 kg/s over first 60 s to simulate circulator coast down. (Note: Very small FLOWNEX mass flow rates were *not* used)
  - Reactor cavity cooling system (RCCS) ramped from 20°C to 135 ° C over first 14 hours to simulate water boil-off mode
  - All 24 rods SCRAM at 300s over 16s to simulate reactor trip
  - When atmospheric pressure was reached, all gas calculations were terminated for the duration of the 300h transients

Core Thermal Analysis Methodology and Definitions

- Definition of core average fuel temperature:
  - The volume-weighed average temperature of all the fuel in the core region. Note that this average is calculated over the fuel region in the spheres only (i.e. it is not the total sphere volume average), and it is averaged over all the fuel batch temperatures.
- Definition of Maximum Fuel Temperature (MFT):
  - TINTE calculates fuel sphere surface and centre temperatures for 260 spatial positions in the core (10 radial and 26 axial coarse meshes).
  - Temperatures are calculated for 6 “batches” of fuel for the 6 fuel passes through the core. Pass 1 represents the fresh fuel, and pass 6 the most-burnt fuel before final discharge.
  - Fresh fuel usually produces the highest temp.
  - MFT is defined as the spatial maximum of the highest fuel centre temperature. *This location changes over time.*
- Releases from fuel are primarily based on fraction of core at time and temperature and not directly correlated to instantaneous core temperatures.

Core Average Fuel Temperature

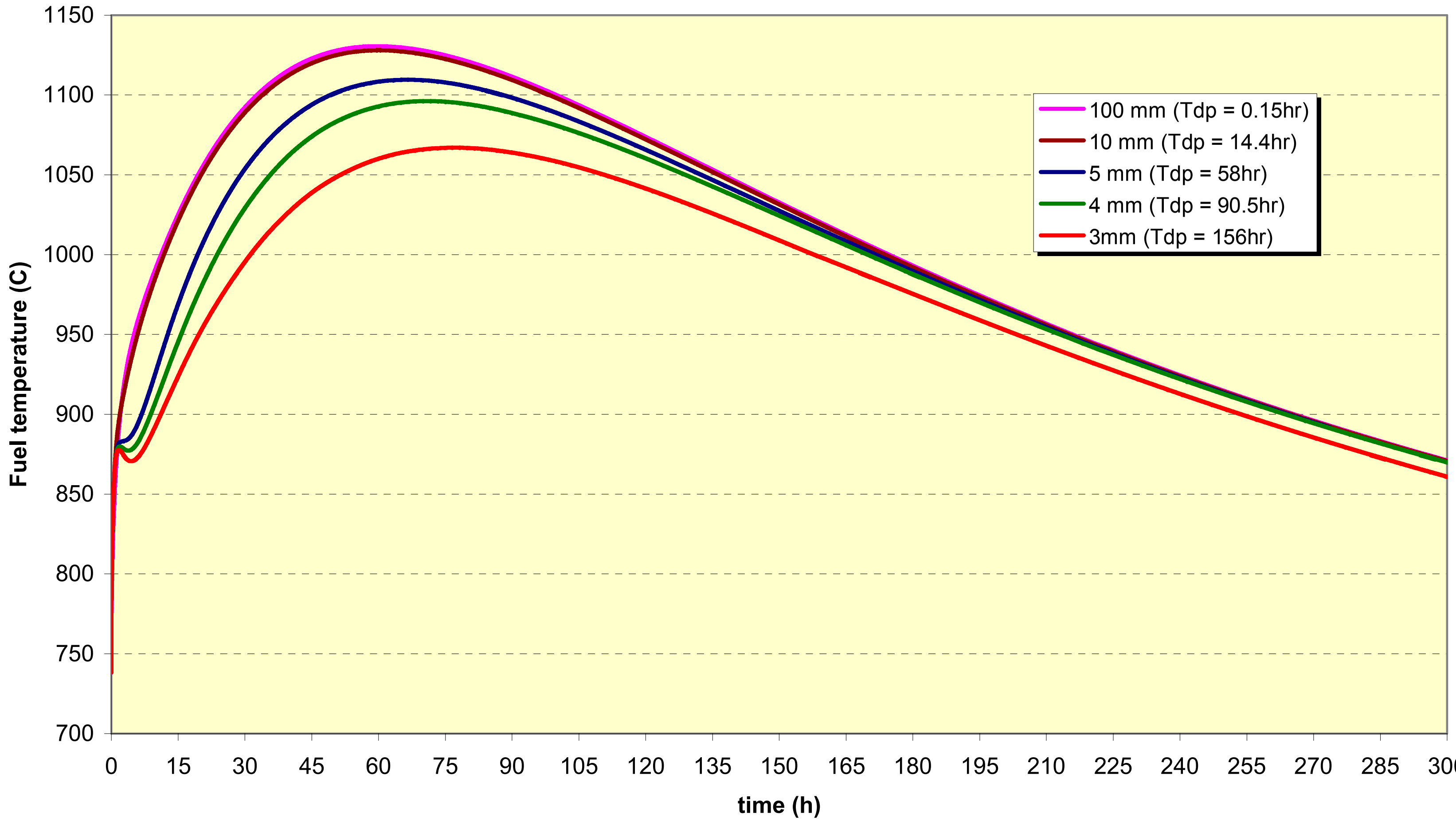

Maximum Fuel Temperature

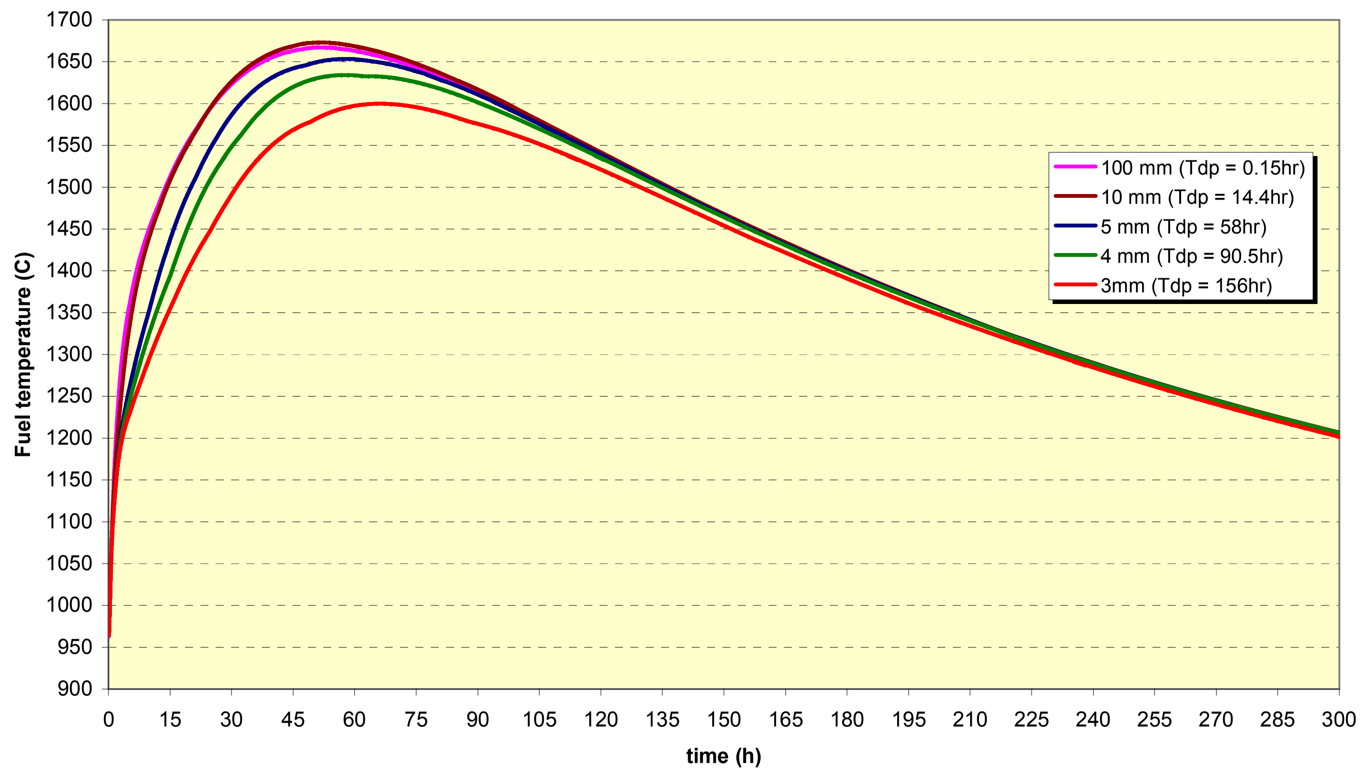

- MFTs converge after 150 hr; convective effects are significant only during first 120 hr
- MFT is lower and occurs later with smaller break sizes

MFT during the first hour

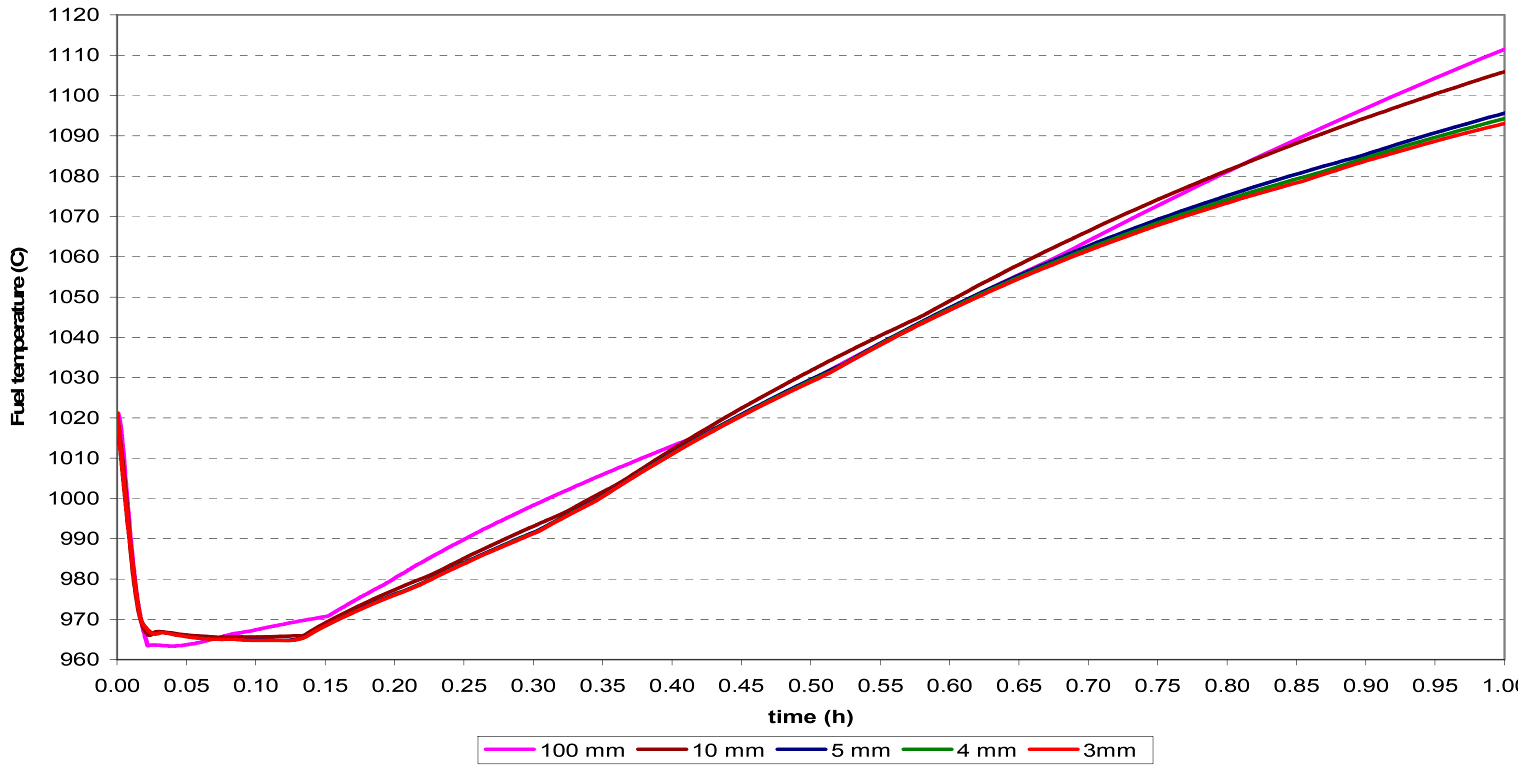

- It takes nearly 30 min for MFT to reach normal operation levels
- 10 mm and 100 mm cases separate from 3-5 mm breaks at 0.7 hr

MFT from 1-15 h

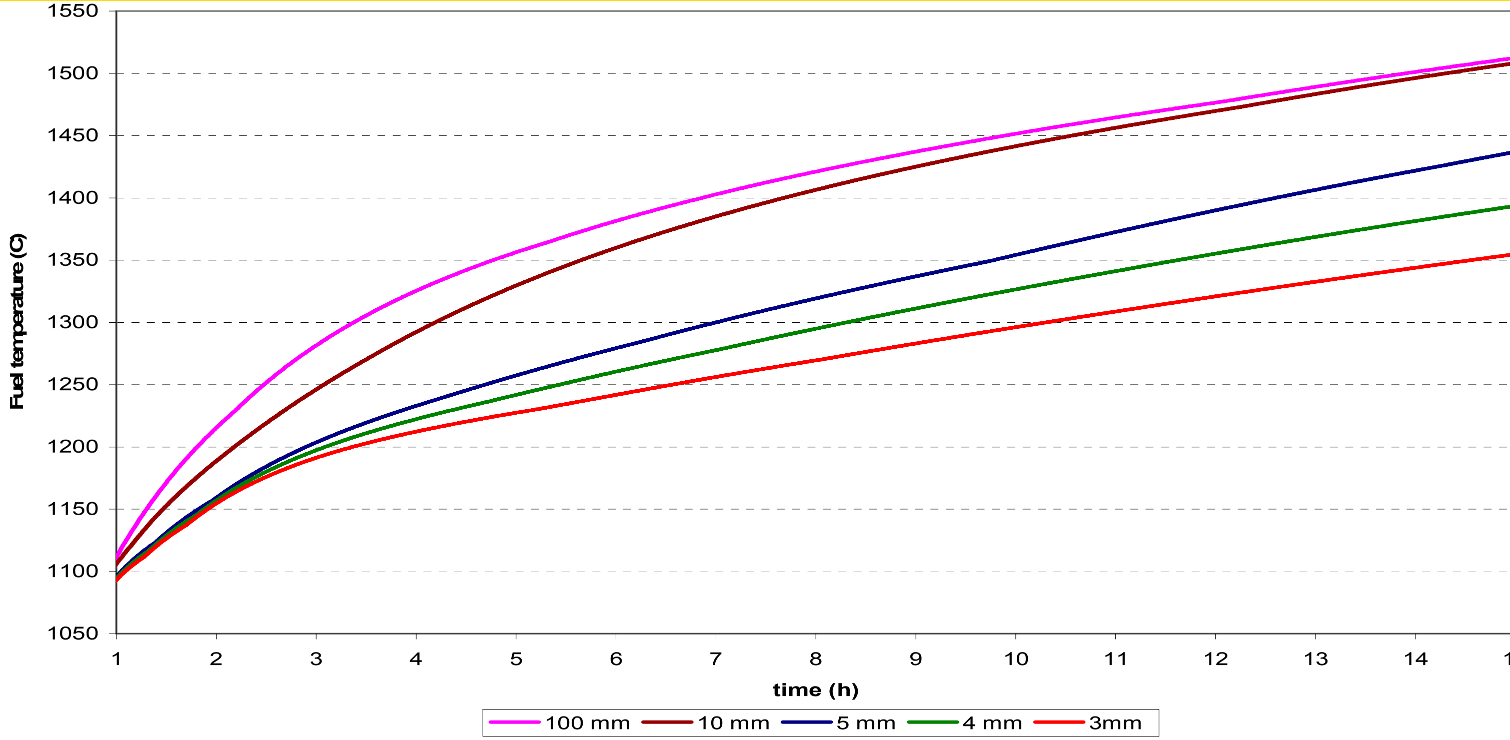

At t= 10 h, the MFT varies 154 °C between the 100 mm (1453 °C) and 3 mm (1299 °C) cases. The two larger breaks (10 and 100 mm) also lead to very similar MFT behaviour in this period, while the three smaller breaks are more evenly grouped together.

MFT from 40-80 h

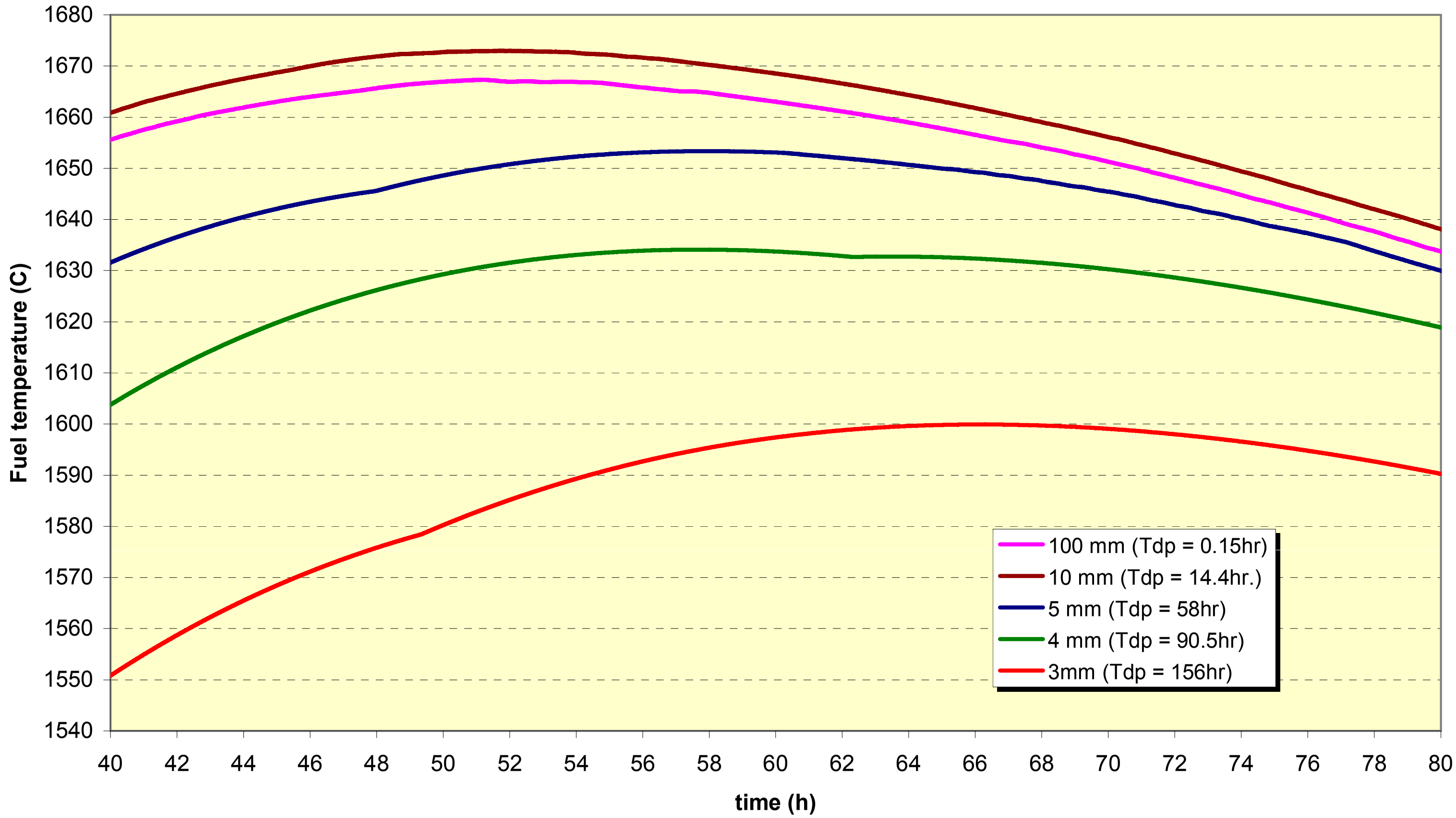

The spread between the 5 cases has decreased to less than 100 °C by the time the peak MFT values are reached. Note the time delay between the peak values.

Spatial MFT at t=53 h for the 100mm break

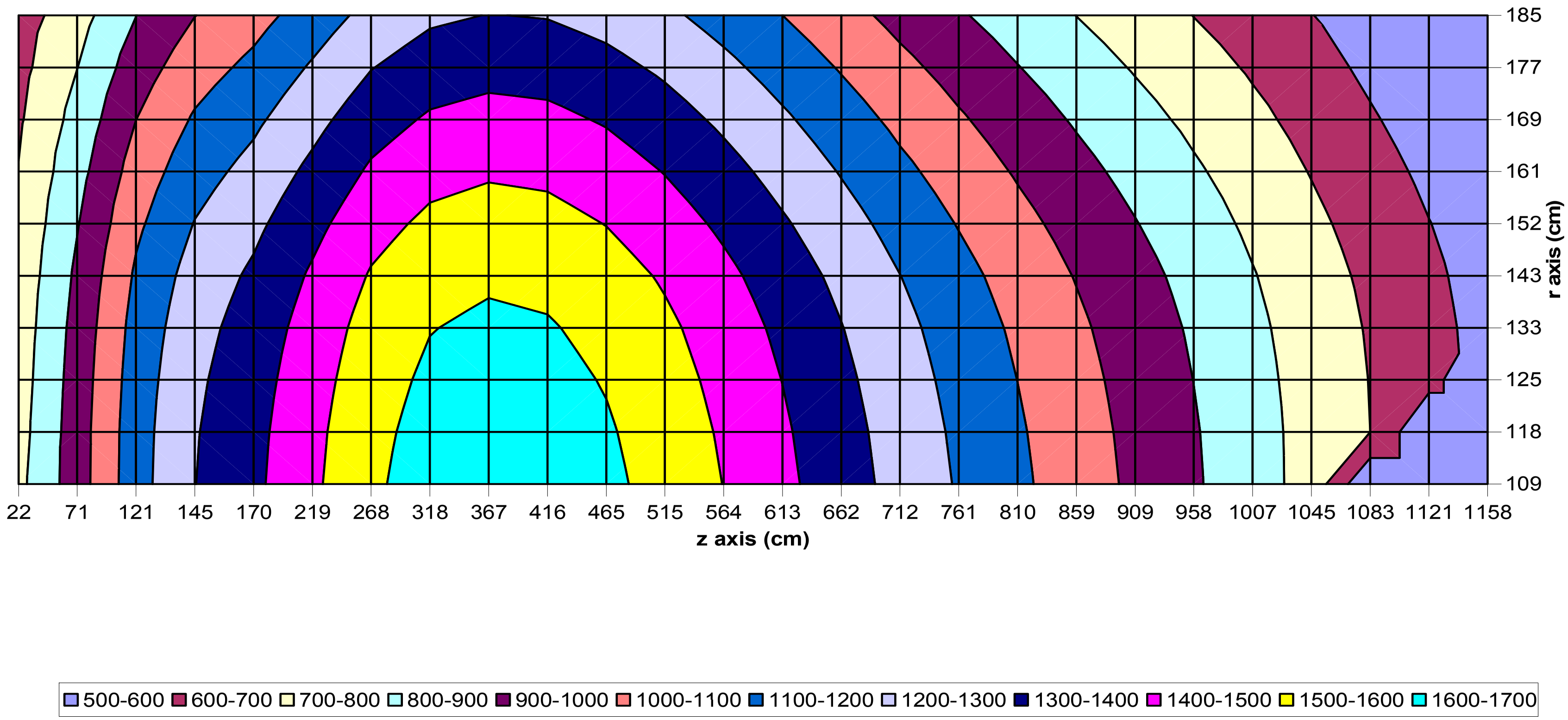

- Only a small volume of core exposed to MFT > 1600°C
- MFT peak located next to central reflector and ~360cm from the top of the core

Volumetric Temperature
% of Core Fuel Volume at 50 Hr

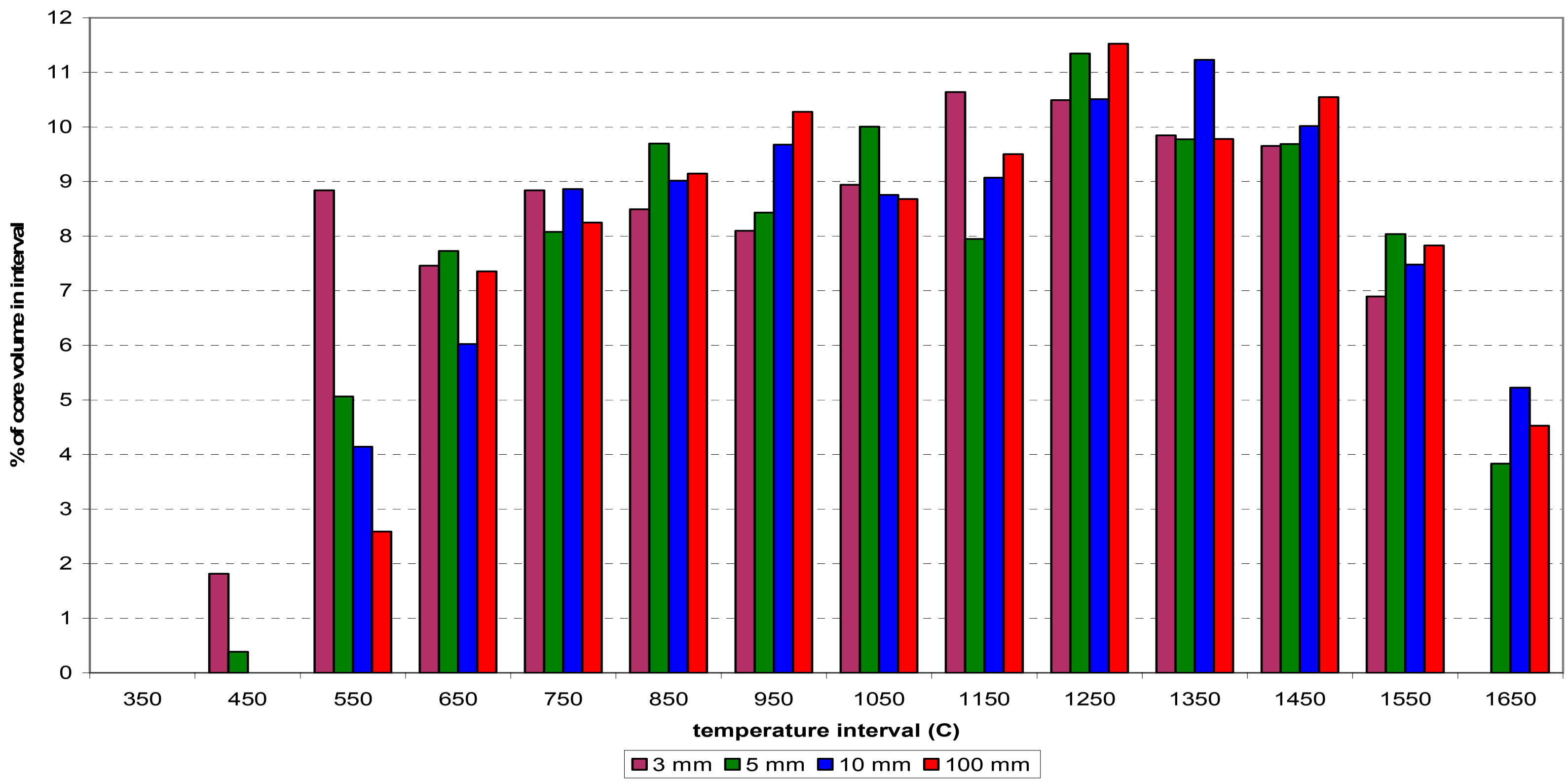

- 10mm case has 5.1% of core volume at a MFT >1600°C; 100mm case has 4.5% in same interval
- Between 1400-1600°C, this pattern is reversed
- Not easy to predict which case will lead to highest FP releases from fuel

100 mm Break RB to PHTS Gas Exchange Corrosion Sensitivity Study

- Two variations of the 100 mm breaks at the top of the inlet plenum were modelled, one with 1% air molar fraction, and one with 20%
- The following bounding assumptions were made
  - The FLOWNEX data predicted that the ingress of air would only start after ~40 hours. In this TINTE calculation RB He-air ingress assumed to start at 60 sec
  - The FLOWNEX He-air mass flow ingress rate varied between 0.1 and 4 gram/s. For the TINTE calculation, a constant mixture flow of 4 g/s was assumed from 60s onwards. Note that of the 4 g/s mixture ingress mass flow rate, only 0.02 g/s is air, of which 22% is O_2. Even the 1% air molar fraction modelled in TINTE is therefore more than the Flownex calculated amount.
  - The 20% air molar mass case is based on FLOWNEX calculations that indicated values in the region of 18% for the case where the break is located in the biggest RB cavity – the IHX.
  - The air ingress calculation is <u>extremely</u> time consuming (factor 5 slower than real time). This implies a real-time requirement of ~60 days to model a 300 hour air ingress case. Since the air ingress molar fraction and the air mass flow rate is very small for these cases, it was decided to only simulate this 100 mm break up to 40 hours for the 1% case, and up to 48 h for the 20% molar fraction case

Spatial Graphite Corrosion Concentration (mol/m3)
t=30h for the 1% molar fraction air ingress case

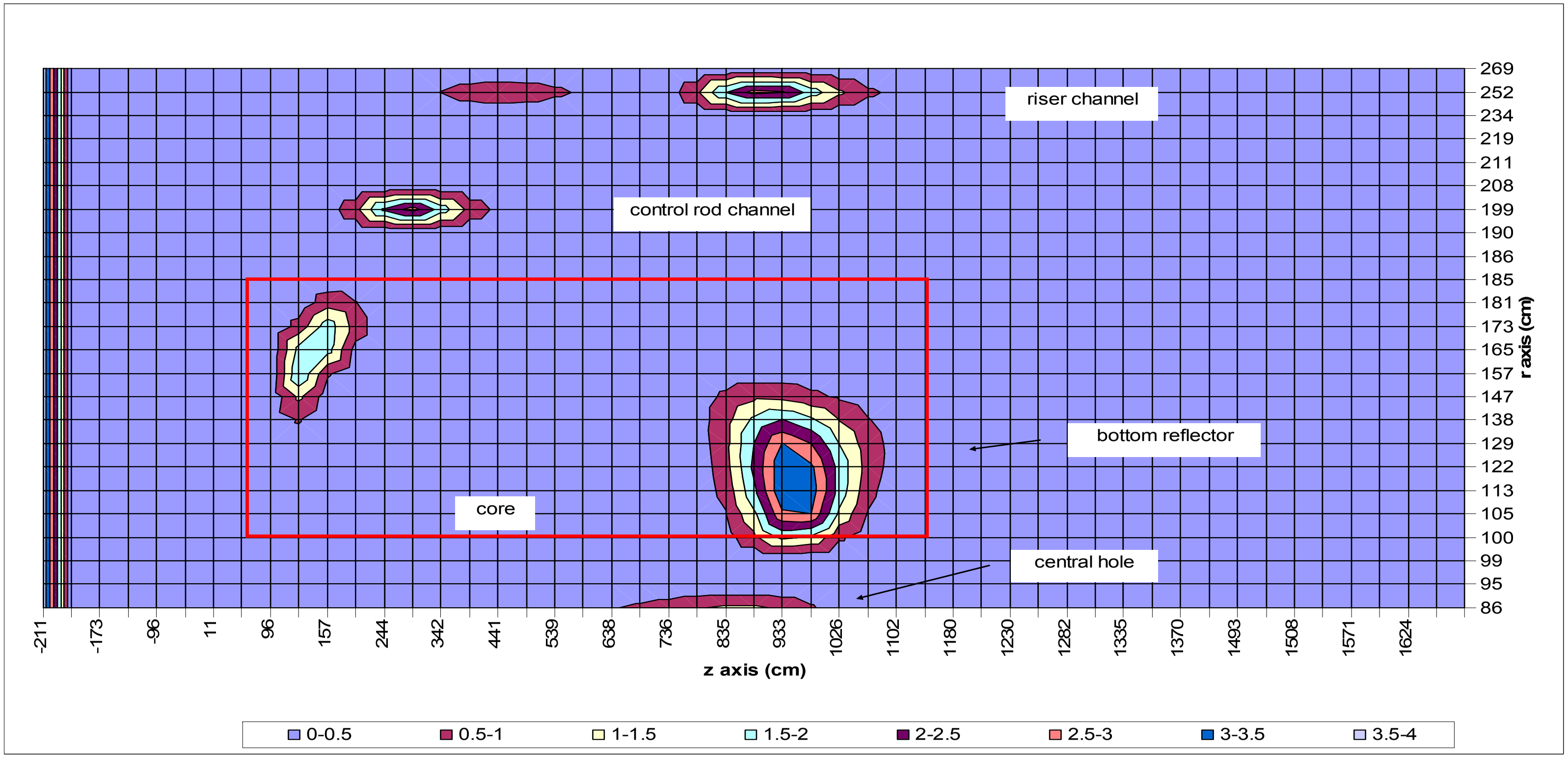

The major corrosion activity is concentrated in the bottom parts of the core and the riser channel, and the upper part of the control rod channel. Since gas flow paths are also modelled in the central hole, a small amount of corrosion is also visible here.

Spatial Graphite Corrosion Concentration (mol/m3)
t=30h for the 20% molar fraction air ingress case

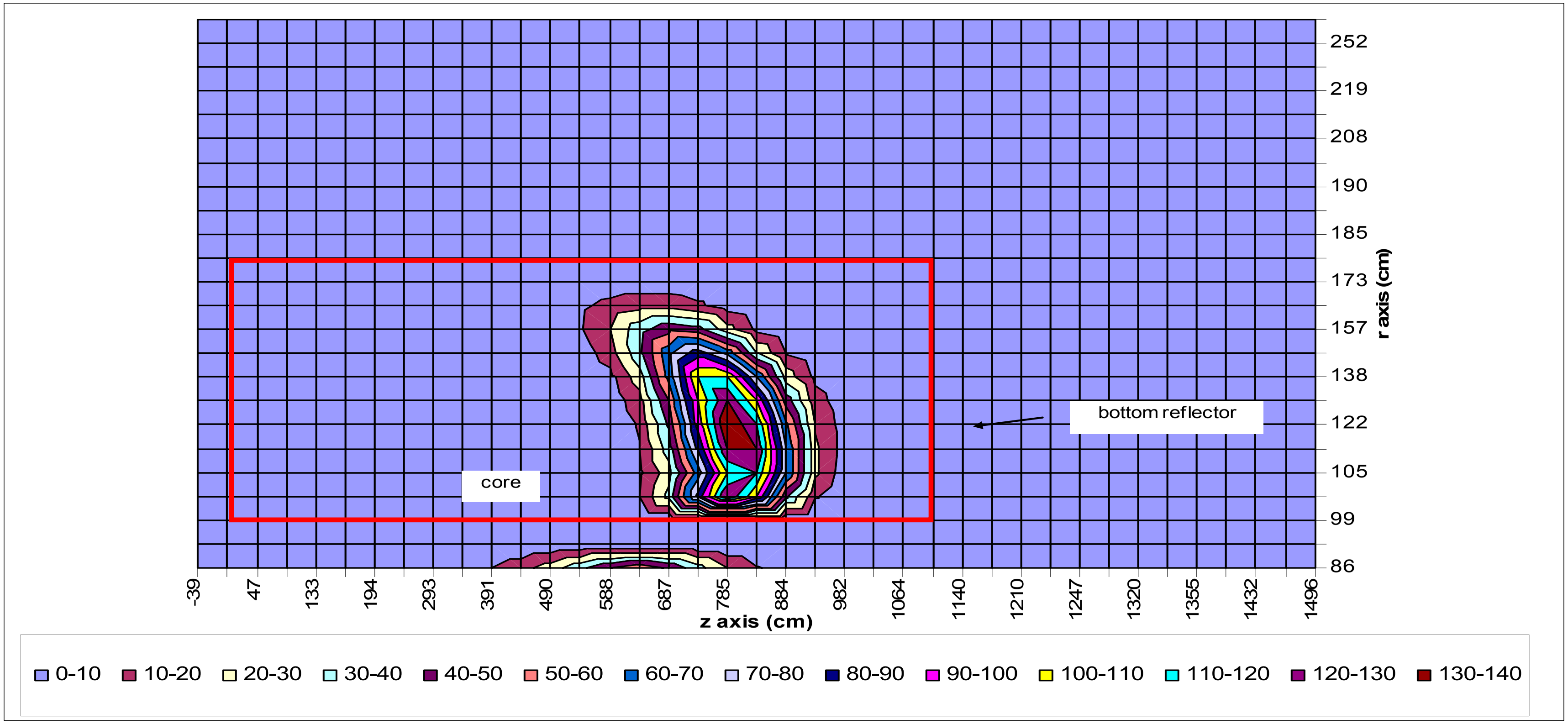

Corrosion in the bottom region of the core still dominates, but is 35 times larger than the 1% case. The smaller pockets of corrosion in the side reflector is not present here, but the corrosion still occurs in the central hole. Core corrosion dominates the 20% case, while reflector damage is more apparent for the 1% case.

Conclusions

- Core thermal response for various break sizes
  - The slightly higher 10 mm break MFT results compared with 100mm appear counter intuitive. However, detailed analysis traced the root cause back to increased convective heat mixing in the core during the 10 mm case, which distributes the high temperature region over a larger core volume than the 100 mm case
  - Apart from this insignificant anomaly, the 3 mm to 100 mm cases all confirmed the general trend of cooler fuel temperatures with an increase in gas inventory and blow down time
- Corrosion sensitivity study
  - The 100 mm air ingress sensitivity study was based on very low FLOWNEX-derived ingress rates and air fractions, assumed to occur during the PHTS thermal gas expansion starting at 60 sec
  - Over a period of 40-48 hours, the total corrosion in the core ranged from ~1 kg to ~10 kg for 1% to 20% air molar fractions, respectively. This represents an insignificant fraction of the core mass (~90 000 kg)

Lessons Learned and Future Work

- Lessons Learned
  - The spatial temperature distributions can have a effect on the MFT and can make results appear counter intuitive
- Future Work
  - The same analysis should be performed with a direct coupling between TINTE and Flownex
  - CFD analysis could be used to obtain a clearer understanding of the air ingress and the corrosion associated with such an event

Radionuclide Release from Fuel and from PHTS Circuit into Reactor Building

By

Hanno van der Merwe

Lori Mascaro

Fred Torri

Radionuclide Releases from the Fuel and from the PHTS circuit into the Reactor Building

DLOFC ACCIDENT ANALYSIS FLOW CHART

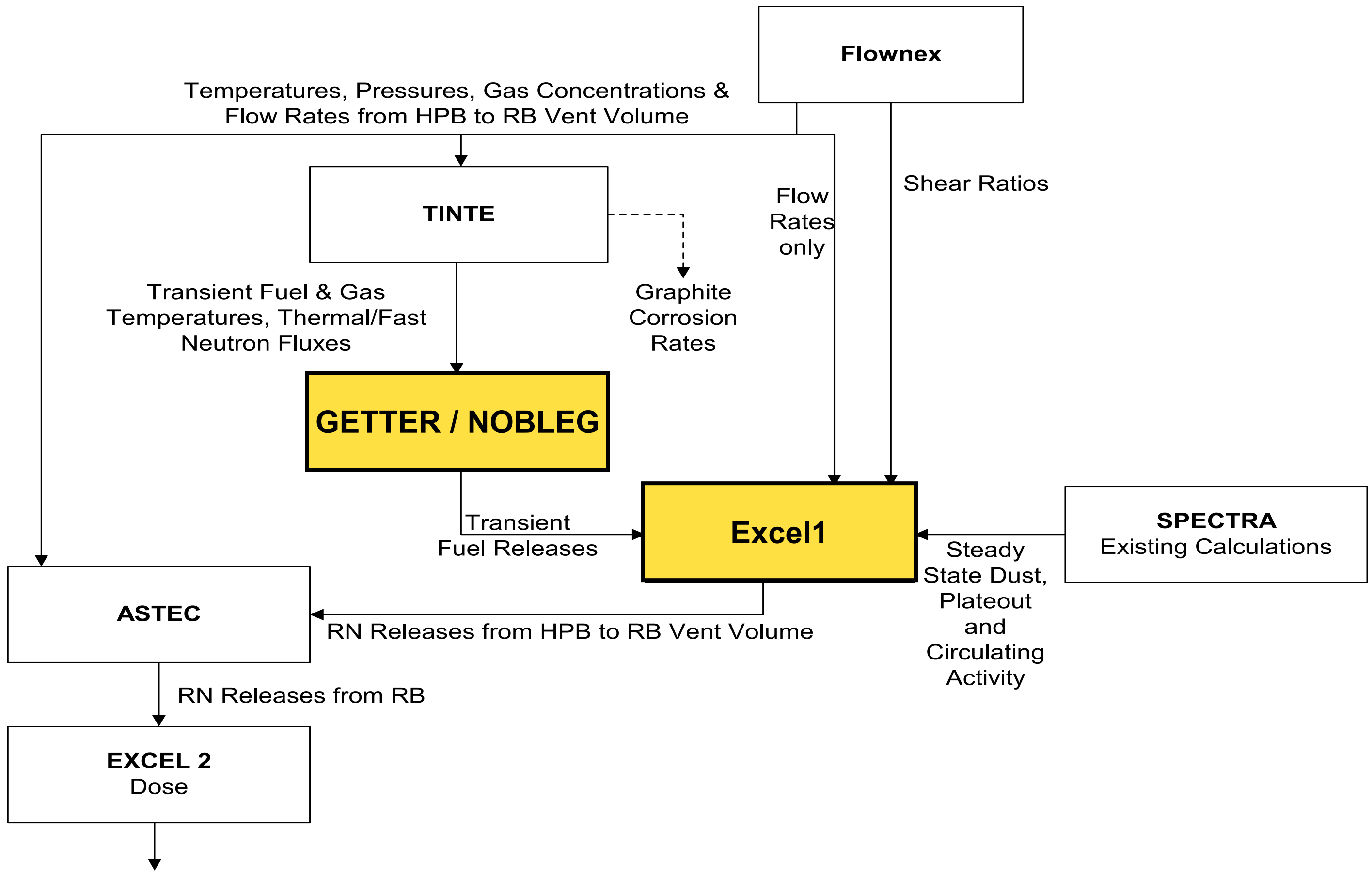

Radionuclide Releases from the Fuel Methodology

- Transport parameters are based on German reference fuel
- Based on German experience, it was conservatively assumed that tellurium and iodine behave similarly under transient conditions
- All five break events were calculated with the same verified model for all six fission products
- The only activation product Ag-110m, was calculated with a newly derived and unverified model. Ag-110m results may be over-conservative
- Calculated I-133, Te-132 and Ag-110m releases may be too high due to over conservative assumptions

Fission Product Release from the Fuel during DLOFC Transients

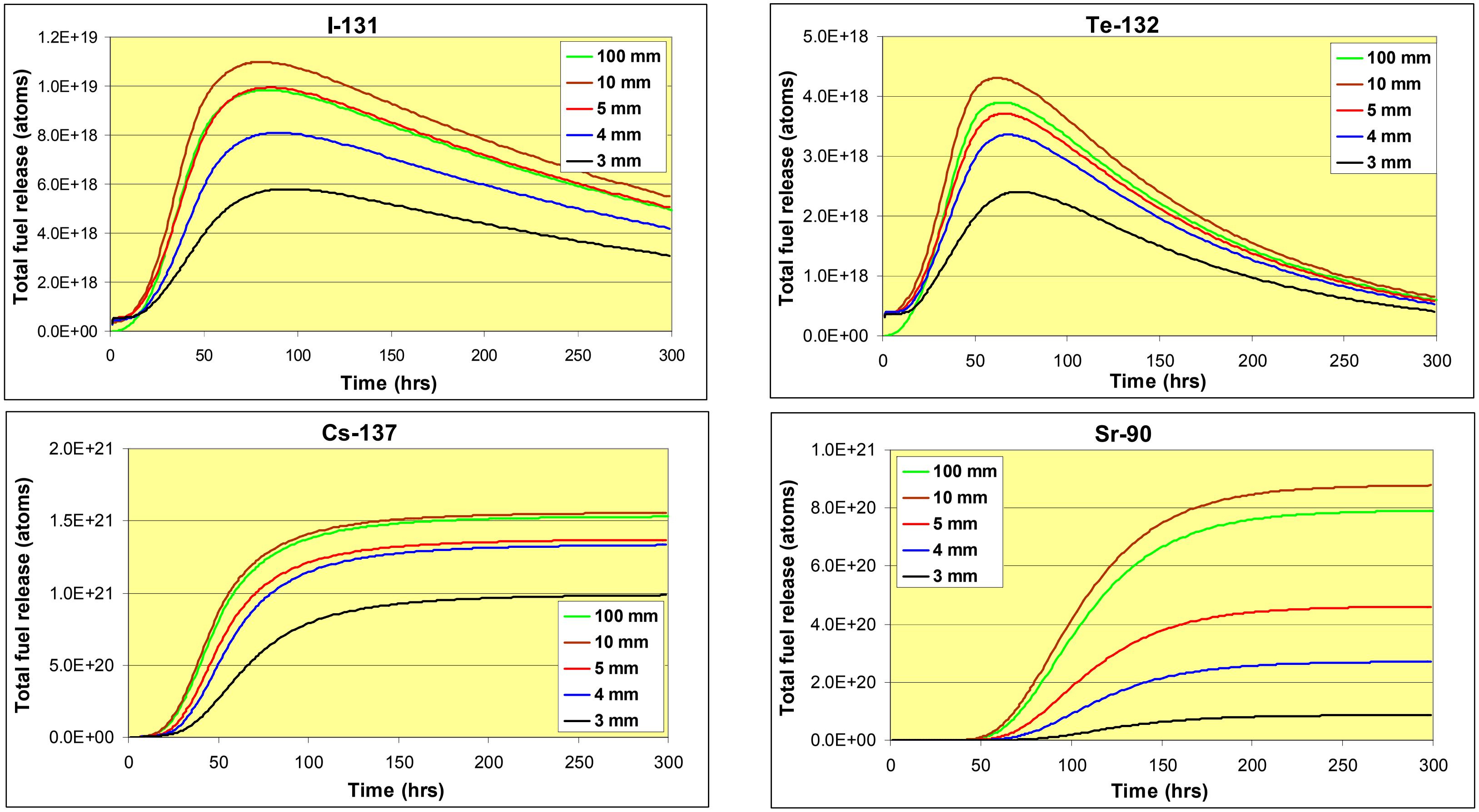

Release from fuel curves are dependent on transport behavior during transients and decay constants of each radionuclide

Radionuclide Releases from the Fuel Conclusions

- Release trends consistent with thermal response trends: 10mm break and larger provide the largest releases and have the highest MFT; smaller breaks have smaller releases due to lower temperatures
- Fuel releases are significantly lower than 2008 RB study, mainly due to lower TINTE temperatures.

Radionuclide Release from PHTS Circuit into RB

Comparison of RN Initial Inventories and DLOFC Transient Releases from the Fuel for 4mm break

RN	Initially Deposited (atoms)	Initially Re-suspended (.2%) (atoms)	Release from Fuel at 8hr (atoms)	Release from Fuel at 24hr (atoms)	Release from Fuel at 91hr* (atoms)	Release from Fuel at 300hr (atoms)
Ag-110m	1.7E+18	3.3E+15	3.0E+17	2.6E+18	7.3E+18	8.1E+18
Ag-111	1.4E+15	2.8E+12	1.5E+16	2.4E+17	8.5E+17	9.1E+17
Cs-137	6.9E+20	1.4E+18	2.0E+18	3.9E+19	1.1E+21	1.3E+21
I-131	7.6E+16	1.5E+14	4.1E+16	1.1E+18	9.2E+18	9.8E+18
I-133	1.0E+16	2.0E+13	5.8E+15	1.2E+17	5.6E+17	5.7E+17
Sr-90	5.8E+18	1.2E+16	3.9E+15	1.3E+17	6.2E+19	2.7E+20
Te-132	3.5E+16	7.0E+13	2.4E+16	7.1E+17	4.5E+18	4.7E+18

*End of release from PHTS

Radionuclide Release from PHTS Circuit into RB
Key Model Assumptions

- PHTS is considered one fully mixed volume
  - Initial inventories of circulating dust and RNs are assumed to be uniformly distributed in the one PHTS volume
  - Liftoff of deposited dust and RNs released from the fuel during the transient are assumed to instantaneously and uniformly mix in the PHTS volume
  - Transport of the RNs from the core to the break location is neglected
- Dust and RNs are proportionately released along with the helium from the PHTS to the RB
- RNs released from the fuel to the PHTS during the transient remain circulating and do not become attached to dust throughout the transient

Radionuclide Release from PHTS into RB Calculation Assumptions

- 4mm DLOFC
  - Zero release from the PHTS to RB post blowdown (after 91 hours)
  - He-air ingress due to thermal contraction into PHTS from RB starts once blowdown is complete
  - Release of helium/RNs due to buoyancy or convection driven mechanisms after blowdown is assumed to be zero
- 100mm DLOFC
  - Blowdown is complete in 11min and release from the PHTS to the RB continues until 50 hours due to thermal expansion of coolant as indicated by the Flownex results
  - Flownex PHTS helium mass results are used for the first 3 hours. From 3 – 50 hours the helium mass is calculated from fitted Flownex flow rates from the break to smooth out oscillations in the Flownex results
  - Zero release from the PHTS to RB after 50 hours as the start of He-air ingress is indicated by the Flownex results

Cumulative Release of I-131
4mm DLOFC

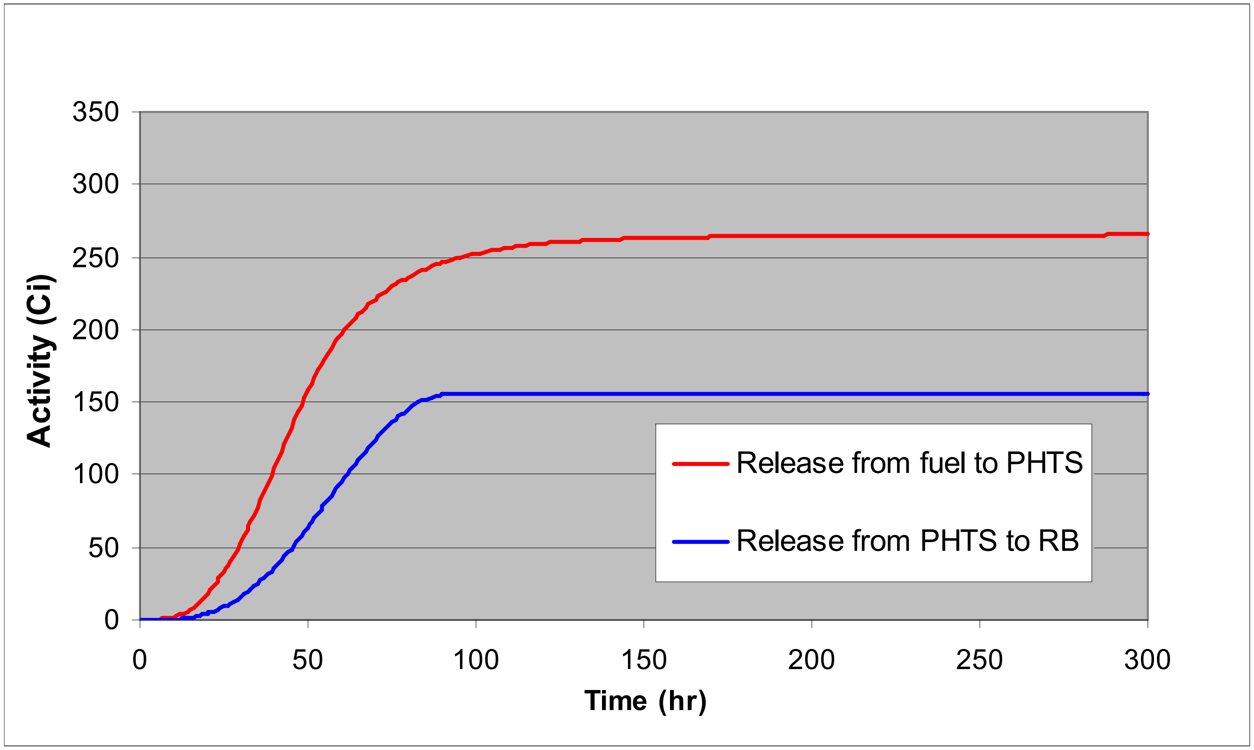

Cumulative Release of I-131
100mm DLOFC

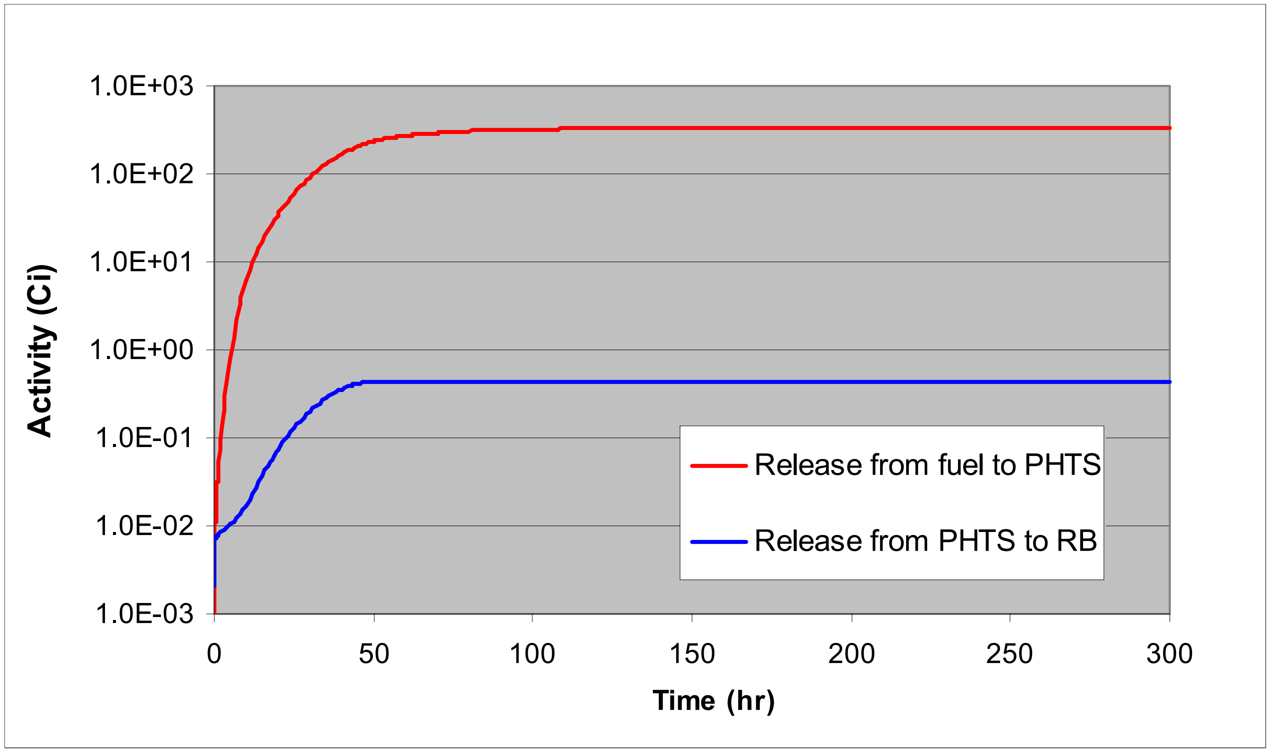

Cumulative 300 Hour Release 4mm DLOFC

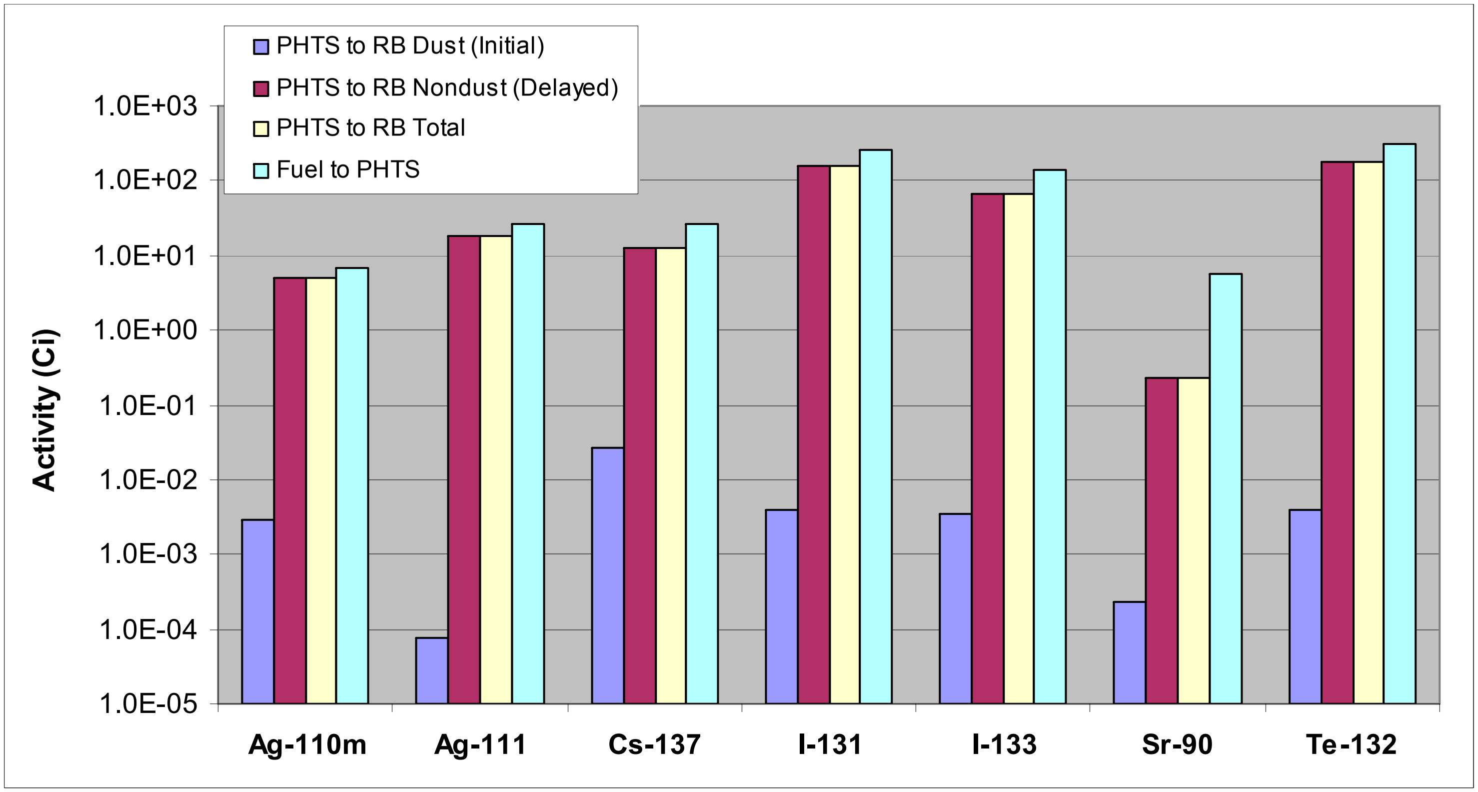

Cumulative 300 Hour Release
100mm DLOFC

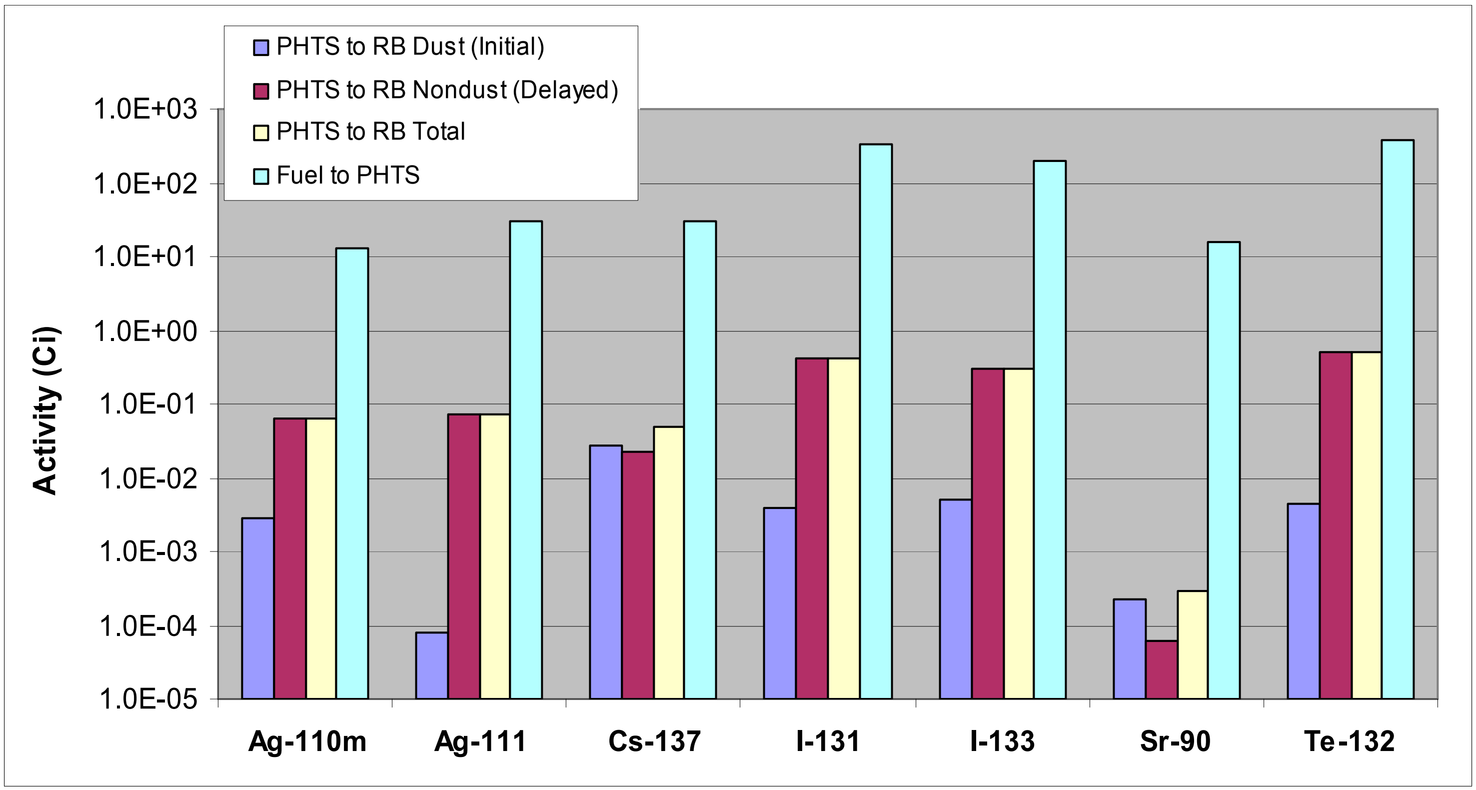

P B M R

Radionuclide Release from PHTS Circuit into RB Results Summary

- Results confirm 2008 study results that
  - longer blowdown time for the small break results in a significantly greater percentage of the delayed RN release from the fuel being transported to the RB
  - for breaks up to 100mm EBS the delayed fuel release dominates
- The 100mm break has 26% more I-131 release from the fuel to the PHTS than the 4mm break due to the higher temperatures during the transient (333Ci vs 265Ci); however because the release from the fuel occurs long after the blowdown is complete much less is released to the RB (0.43Ci vs 155Ci)

Radionuclides Released from Reactor Building

By

Alastair Ramlakan

Radionuclide Releases from the Reactor Building

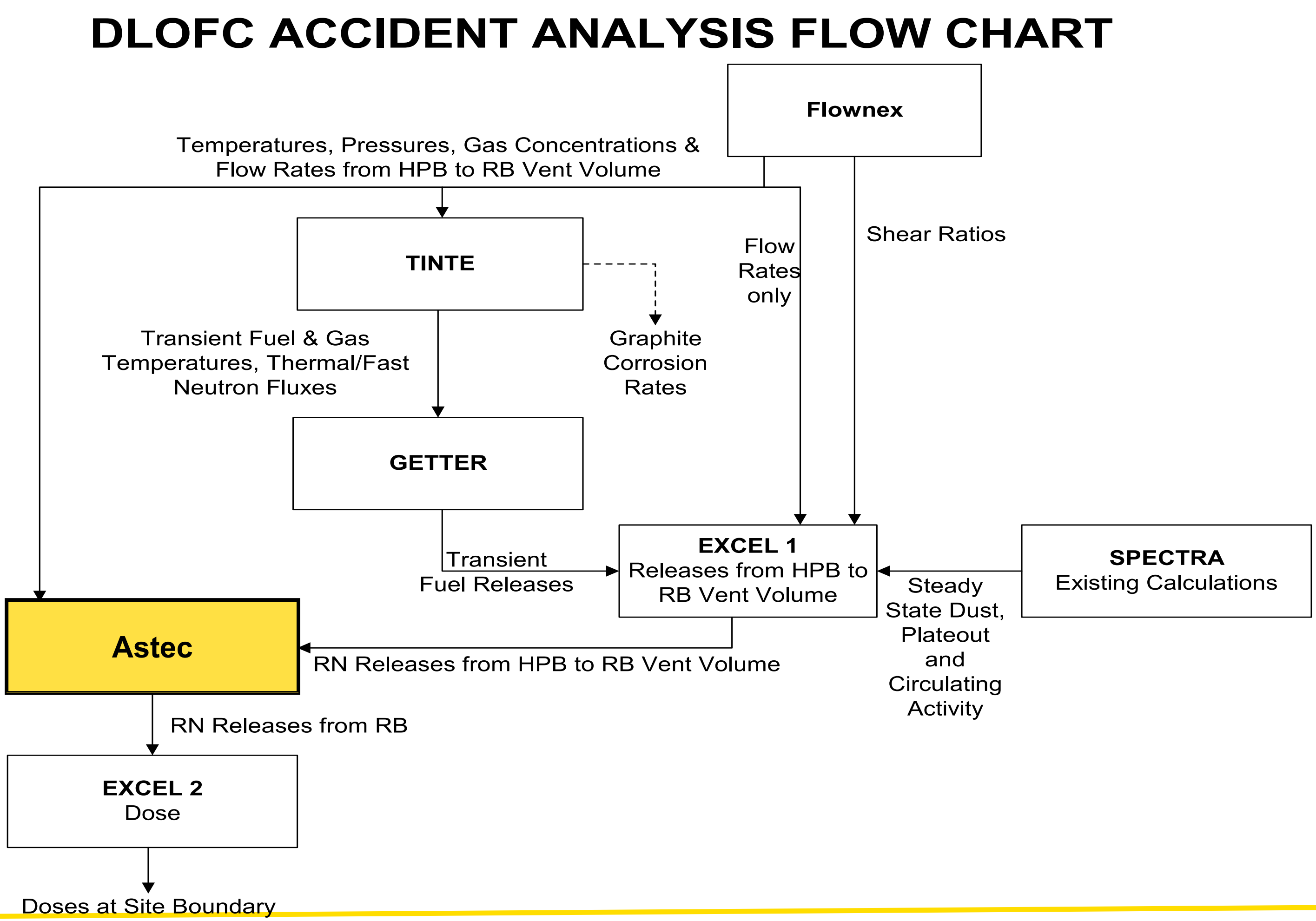

Reactor Building Mass and Radionuclide Transport Model

NGNP Block Flow Diagram

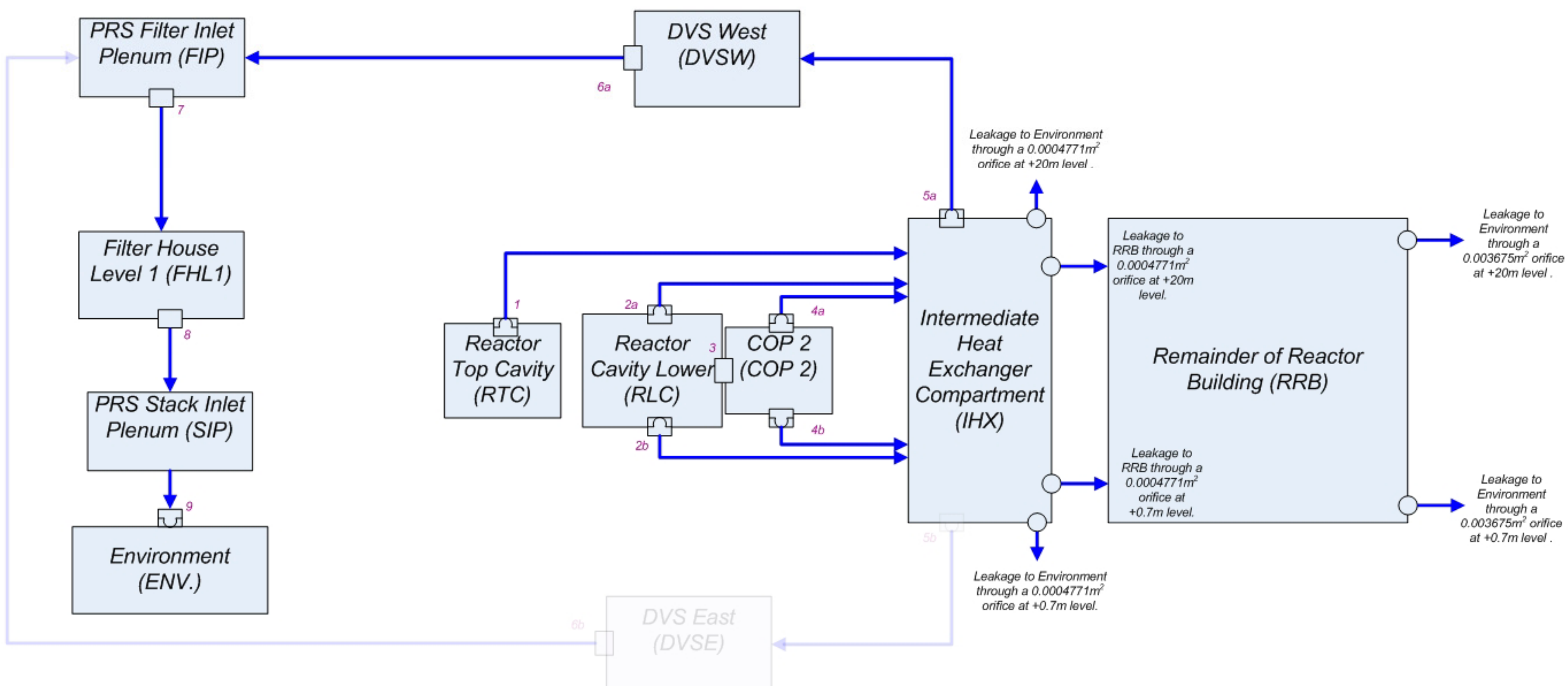

Model Overview

- NGNP Block Flow Diagram implemented in ASTEC model
- A 4mm and a 100 mm Single Ended Guillotine Break (SEGB) of the Core Inlet Pipe (CIP) was simulated to occur in the Reactor Top Cavity (RTC) compartment
- Dust size distribution based on AVR size distribution using 12 size classes
- Fission products not attached to dust are transported as gases in ASTEC

4mm Break Study

- Rupture panels between RTC and IHX compartments, IHX and DVSW compartments and SIP compartment and Environment break successively
- Temperature increase is relatively sharp in RTC (break compartment) compared to the remainder of the compartments

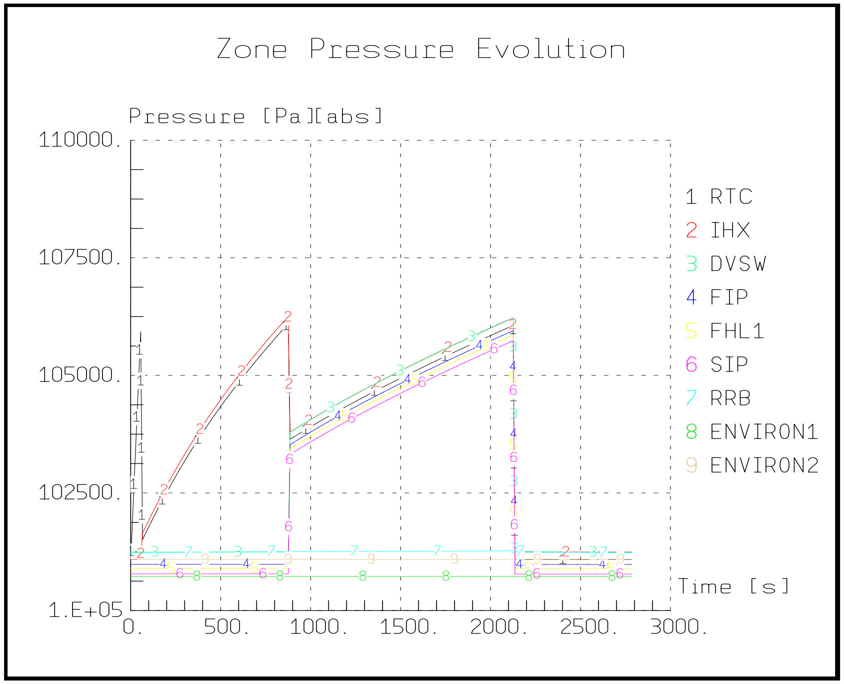

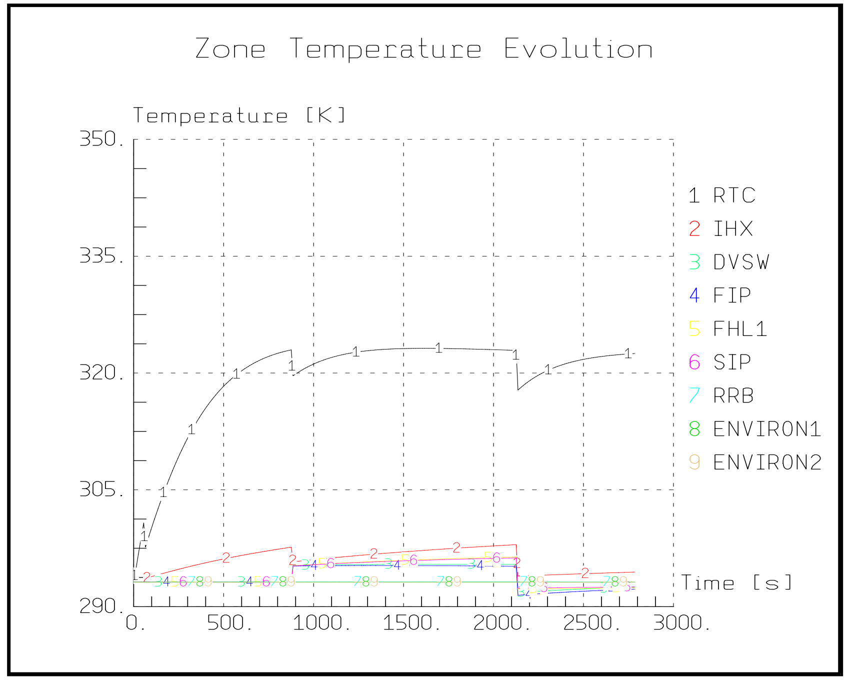

4mm Break Study

- Helium mass fraction in RTC and other compartments begin to increase with the RTC compartment approaching 100% He after 6 hours
- Due to the relatively higher gas temperature and larger surface to volume ratio the temperature in the RTC compartment decreases relatively faster than the IHX compartment temperature

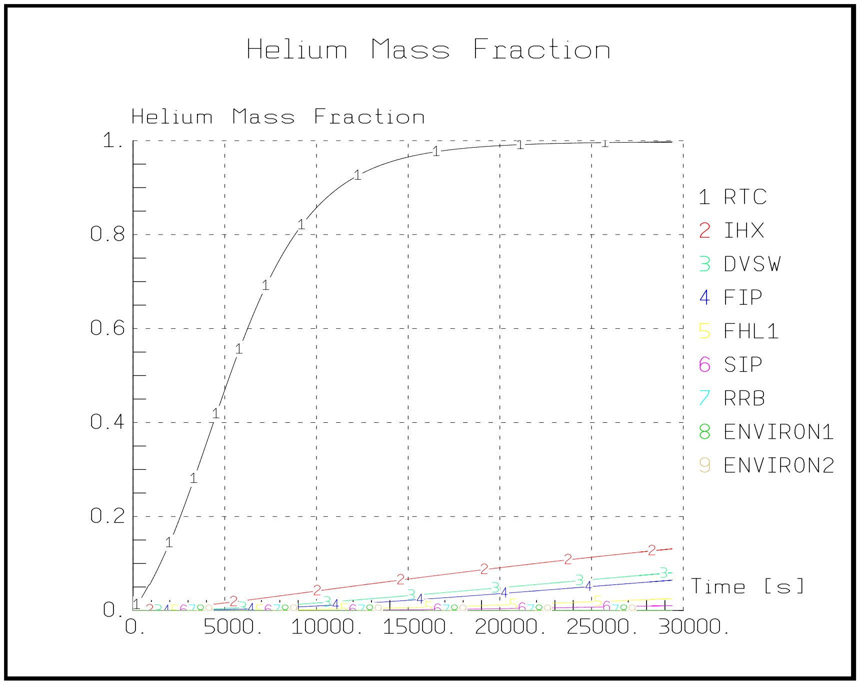

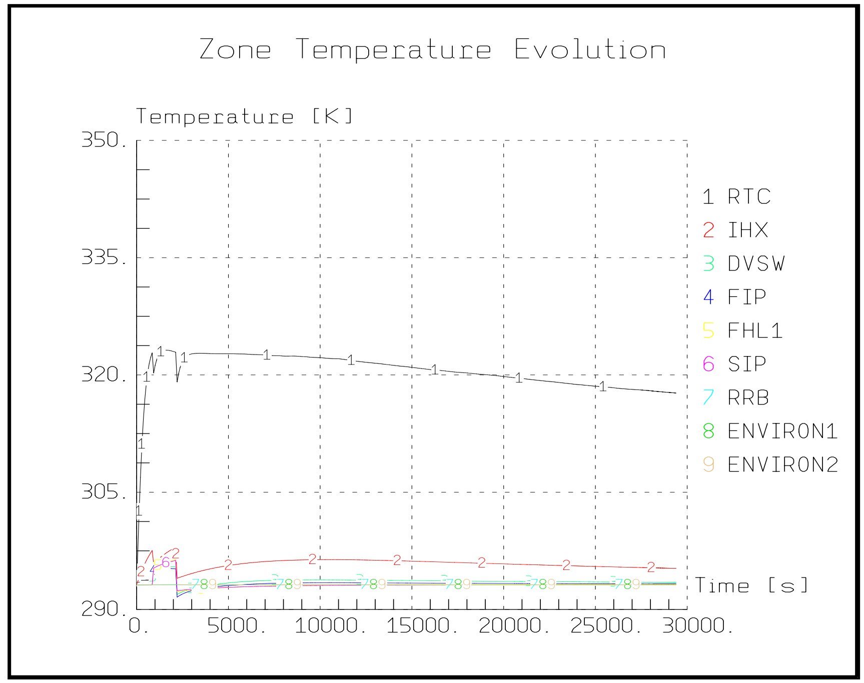

4mm Break Study

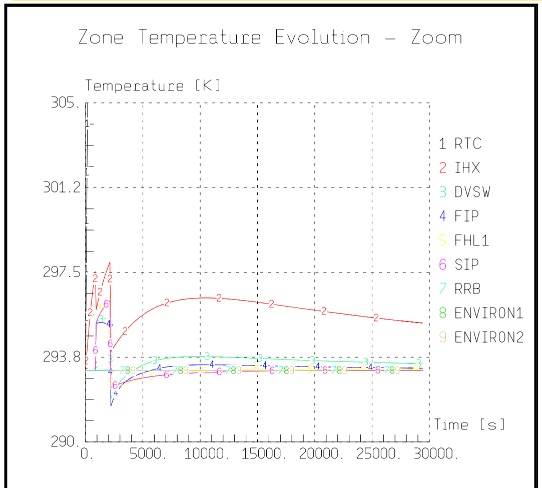

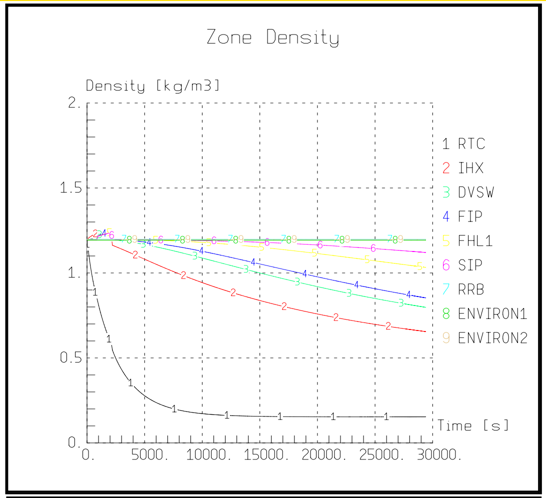

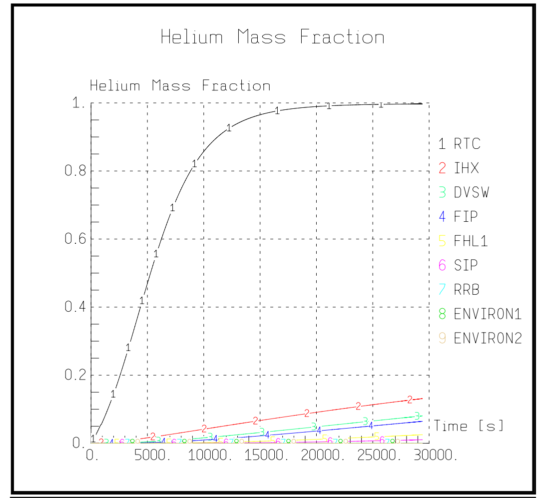

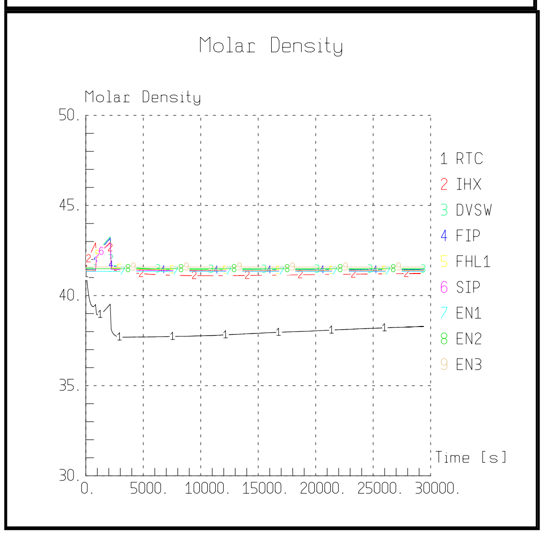

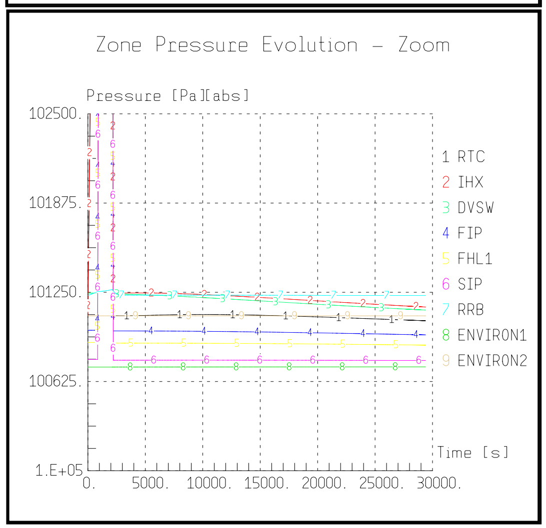

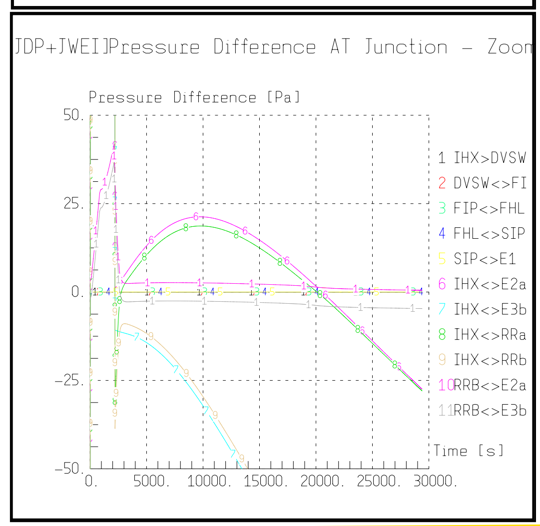

4mm Break
Further Effects

- Inflow of air through leakages results in a further driving force for flow through the stack
- Flow from the RTC to the IHX compartment reverses after blowdown is completed at 91 hours. This is due to the pressure drop in the RTC compartment as it is cooling at a faster rate than the IHX compartment

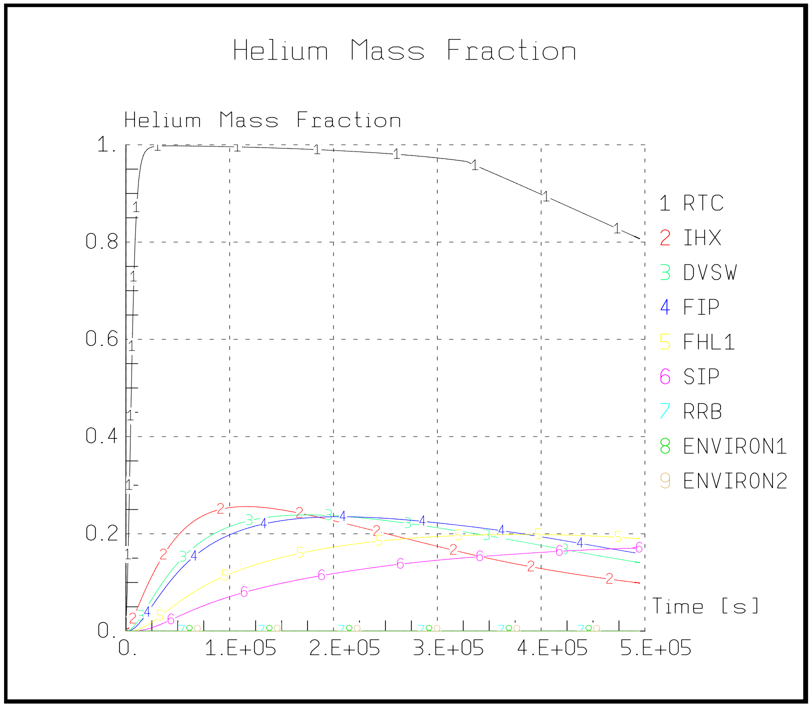

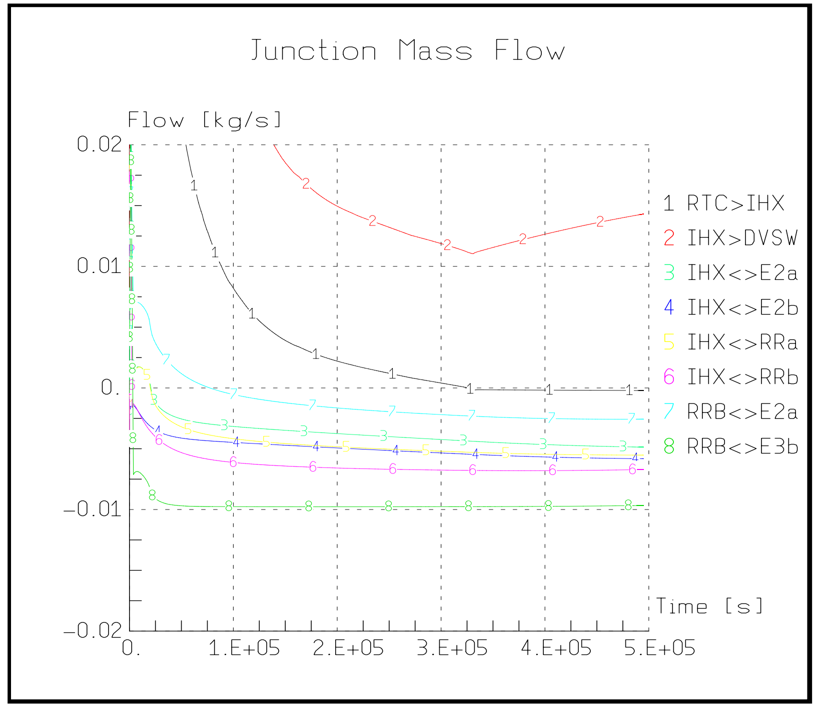

4mm Break
Damper Closure

- The option of damper closure at the stack at 91 hours results in a pressure buildup in the IHX compartment. Flow reverses for the upper IHX leakage path so that flow is now to the environment again. The lower IHX leakage path continues to intake air into the RB. The result is that a natural convection loop in the IHX and renewed release to the environment through the upper IHX leakage path.

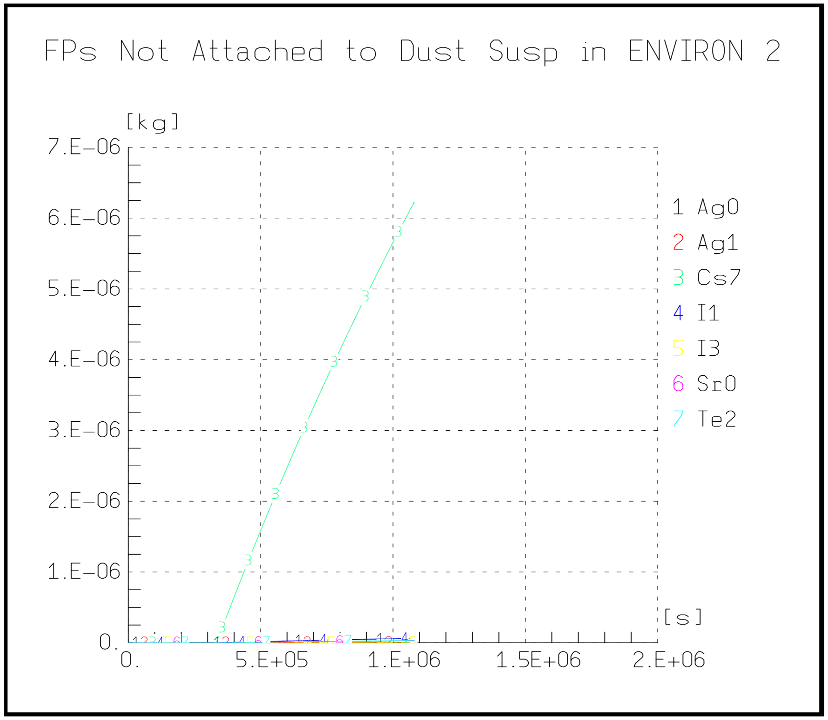

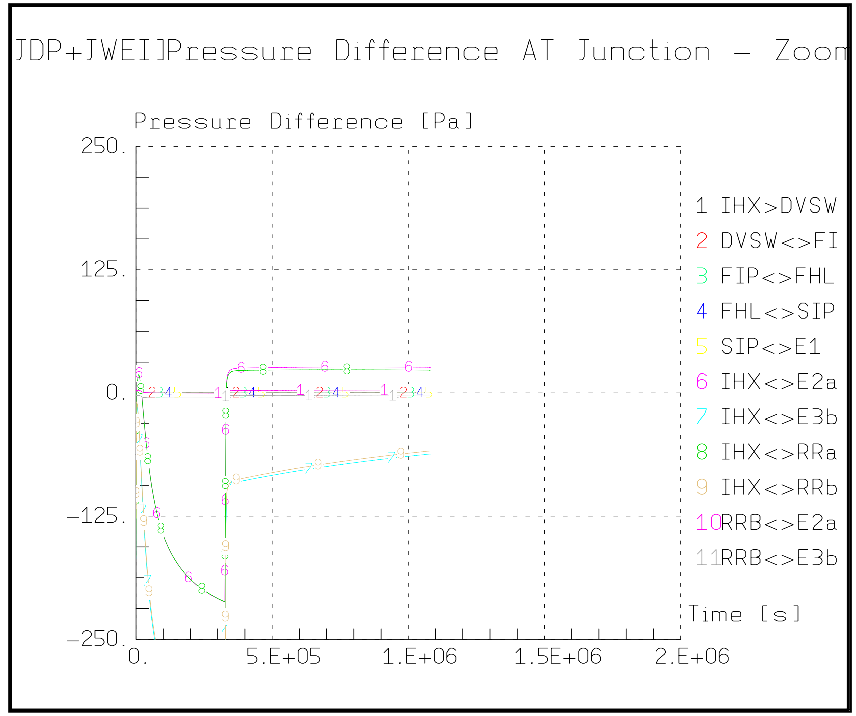

4 mm Break Study Dust Results

Dust Distribution in the Reactor Building and the Environment at 300 Hours
Case with no Damper (% of Total Dust Mass Injected)

	Dust Deposited on Walls	Dust Deposited on Ceiling	Dust Deposited on Floor	Total Dust Deposited in Zone	Dust Suspended in Zone
RTC Compartment	26.11	0.97	< 0.01	27.08	0.31
IHX Compartment	0.05	< 0.01	67.64	67.69	0.00
DVS Compartment	< 0.01	< 0.01	3.47	3.47	< 0.01
FIP Compartment	< 0.01	< 0.01	0.60	0.60	< 0.01
FHL1 Compartment	< 0.01	< 0.01	0.46	0.46	< 0.01
SIP Compartment	< 0.01	< 0.01	0.19	0.19	< 0.01
RRB Compartment	< 0.01	< 0.01	0.01	0.01	< 0.01
ENVIRON1 (Stack Release)	< 0.01	< 0.01	< 0.01	< 0.01	0.20
ENVIRON2 (Leakages at 20.0 m)	< 0.01	< 0.01	< 0.01	< 0.01	0.01
ENVIRON3 (Leakages at 0.7 m)	< 0.01	< 0.01	< 0.01	< 0.01	< 0.01

NOTE: No Filtration Modeled in ASTEC model

4 mm Break
I-131 Results

I-131 Distribution in the Reactor Building and the Environment at 300 Hours
(% of Total I-131 Mass Injected)

	I131 With No Damper	I131 With Damper	Sensitivity Case: I131 (I131 Not Attached to Dust - Modeled As 1E-7m Aerosol) With No Damper
RTC	49.39	49.47	88.24
IHX	10.86	25.94	9.34
DVSW	3.59	7.00	1.45
FIP	1.52	2.15	0.38
FHL1	8.38	3.42	0.35
SIP	7.27	1.11	0.15
RRB	< 0.01	5.12	< 0.01
ENVIRON1 (Stack Release)	19.03	0.69	0.13
ENVIRON2 (Leakage)	< 0.01	5.14	< 0.01
ENVIRON3 (Leakage)	< 0.01	< 0.01	< 0.01

NOTE: No Filtration Modeled in ASTEC model

100mm Break Study

- Rupture panels all break within the first 4s
- Temperature in the RTC compartment reaches a maximum of just over 500K after 11s

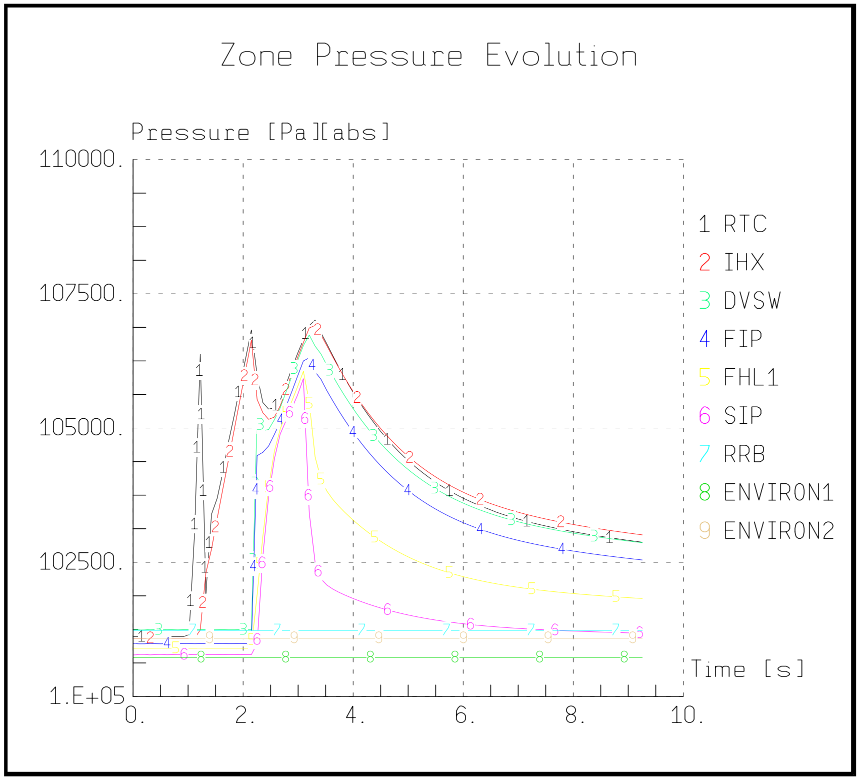

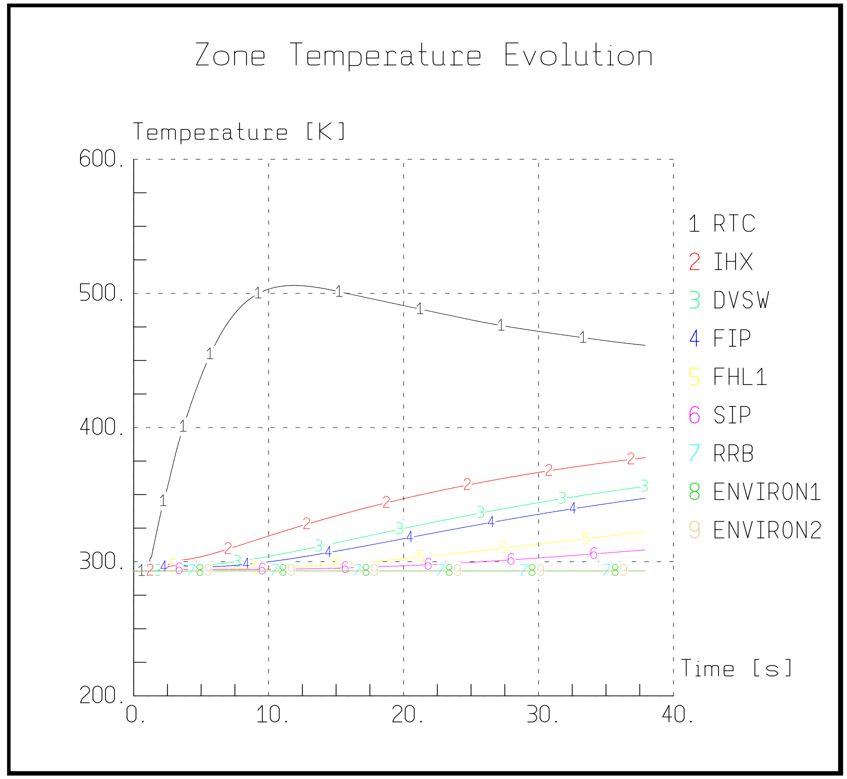

100mm Break Study

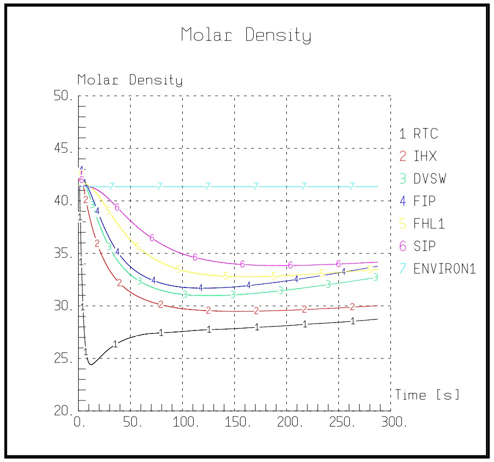

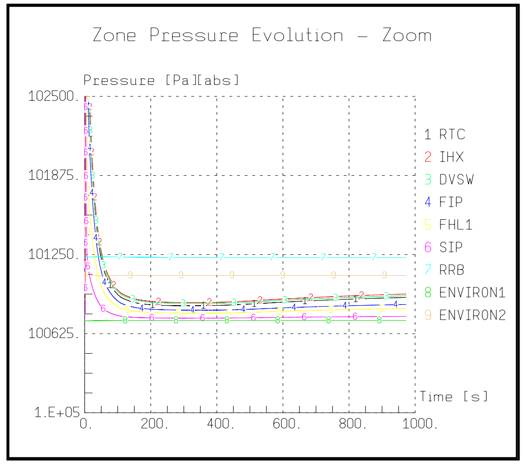

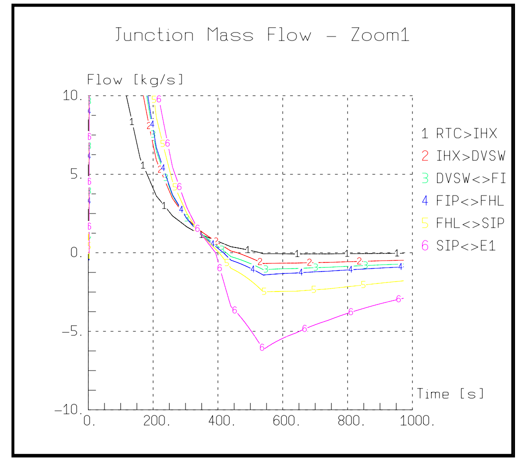

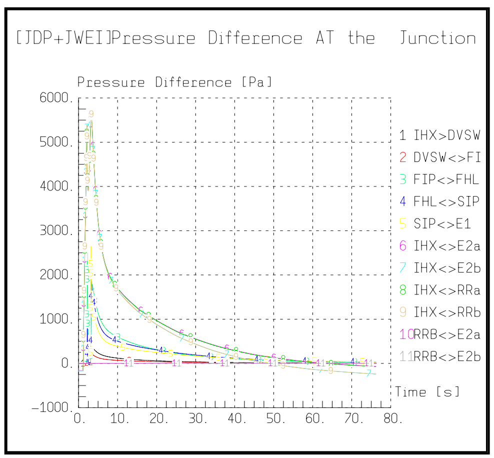

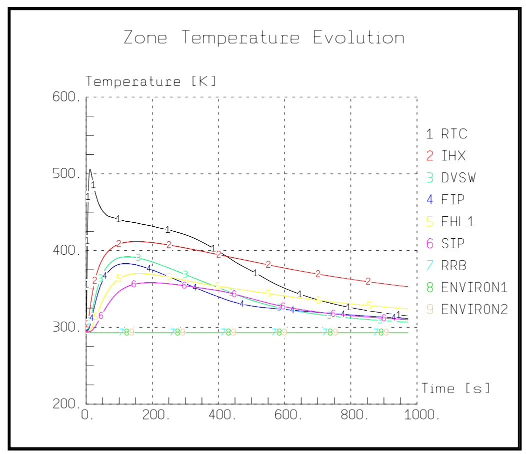

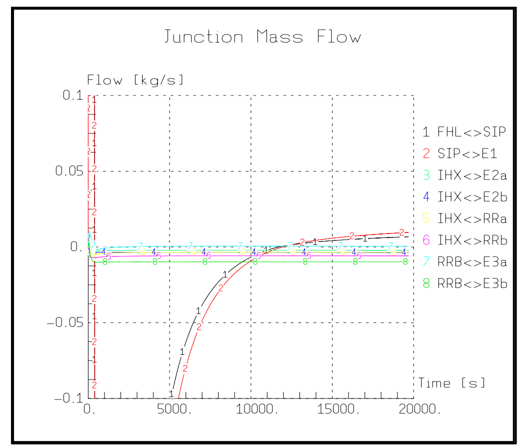

100 mm Break Study
Dust Results

Dust Distribution in Reactor Building and Environment at 300 Hours
Case With No Damper (% of Total Dust Mass Injected)

	Dust Deposited on Walls	Dust Deposited on Ceiling	Dust Deposited on Floor	Total Dust Deposited in Zone	Dust Suspended in Zone
RTC Compartment	0.87	1.80	0.00	2.67	0.49
IHX Compartment	0.13	0.03	41.75	41.91	<0.01
DVS Compartment	0.02	0.12	10.54	10.68	<0.01
FIP Compartment	<0.01	0.01	4.22	4.23	<0.01
FHL1 Compartment	<0.01	<0.01	10.65	10.66	<0.01
SIP Compartment	<0.01	<0.01	4.66	4.66	<0.01
RRB Compartment	<0.01	<0.01	<0.01	<0.01	<0.01
ENVIRON1 (Stack Release)	<0.01	<0.01	<0.01	<0.01	22.09
ENVIRON2 (Leakages at 20.0 m)	<0.01	<0.01	<0.01	<0.01	<0.01
ENVIRON3 (Leakages at 0.7 m)	<0.01	<0.01	<0.01	<0.01	<0.01

NOTE: No Filtration Modeled in ASTEC model

100 mm Break
I-131 Results

I-131 Distribution in Reactor Building and Environment at 300 Hours
(% of Total I-131 Mass Injected)

	I131 With No Damper Reclosing	I131 With Damper Reclosing	Sensitivity Case: I131 (I131 Not Attached to Dust Modeled As 1E-7m Aerosol) With No Damper Reclosing
RTC	98.71	98.71	98.72
IHX	0.44	0.56	0.70
DVSW	0.11	0.15	0.13
FIP	0.04	0.05	0.04
FHL1	0.14	0.11	0.10
SIP	0.09	0.04	0.04
RRB	0.00	0.05	< 0.01
ENVIRON1 (Stack Release)	0.33	0.15	0.14
ENVIRON2 (Leakage)	< 0.01	0.05	< 0.01
ENVIRON3 (Leakage)	< 0.01	< 0.01	< 0.01

NOTE: No Filtration Modeled in ASTEC model

Conclusions

- Significant retention of dust and fission products occurs in the RB especially in the RCT and IHX compartments
- Air intake to the RB through the leakage paths provides an additional driving force for release through the stack.
- Closure of the stack damper significantly reduces the stack release and increases the leakage release for the 4mm break. The reduction in stack release is less for the 100mm break because the contribution of the initial release that is attached to dust is more significant and unaffected by the damper closing.
- Releases from the RB are very sensitive to assumptions made regarding the form of the RNs entering the RB (aerosol or gas).
- The helium fraction in the RTC and IHX compartments increases to dominant levels reducing the density and thereby also the pressure in the compartments.
- The surface areas of the compartments within the RB play a significant role in the cooling of the gas which also influences the pressure in the compartments.

Lessons Learned and Future Work

- Lessons Learned
  - Temperature and density effects are important in the evolution of the flows in the reactor building.
  - Very small flows observed post-blowdown, thus important that the error bounds across junctions are kept very small in order for the code to obtain convergence.
  - Multi compartment RBVV will retain more RNs in the RBVV than a single compartment RBVV.
- Future Work
  - Further nodalization of the IHX and RRB compartments would be useful to investigate buoyancy effects.
  - Sensitivity studies with varying reactor building parameters.

Radiological Dose at Site Boundary

By

Lori Mascaro, Fred Torri, and

Karl Fleming

Radiological Dose at Site Boundary

DLOFC ACCIDENT ANALYSIS FLOW CHART

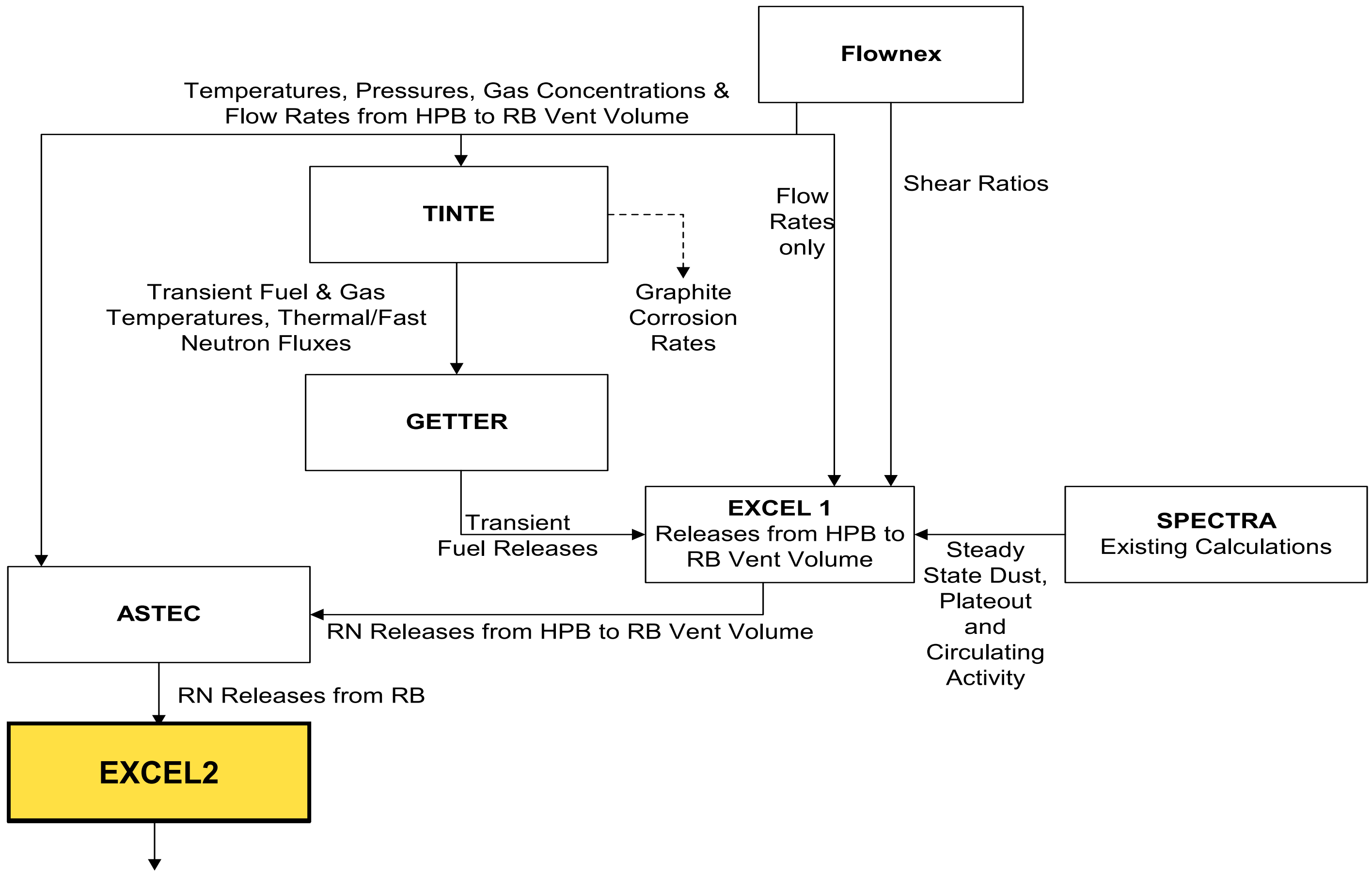

Model Overview

- The best estimate Total Effective Dose Equivalent (TEDE) and thyroid Committed Effective Dose Equivalent (CEDE) from inhalation are evaluated at the 400m site boundary in a Microsoft Excel spreadsheet (EXCEL2)
- TEDE is defined as the sum of the CEDE from inhalation and the EDE from external air submersion
- Doses calculated for seven RNs: Ag-110m, Ag-111, Cs-137, I-131, I-133, Sr-90 and Te-132
- Total doses from all RNs scaled based on "GT MHR Preliminary Safety Assessment Report (DOE-GT-MHR-100230, Rev. 0, September 1994)", Table 4.4.3-3
  - Thyroid CEDE calculated based on the seven RNs estimated to be 90% of the total dose from all RNs
  - TEDE calculated based on the seven RNs estimated to be 80% of the total dose from all RNs

Model Overview Continued

- Dose calculation assumptions were revised in response to questions raised at the 50% design review meeting
- Assumptions to calculate dose are selected to meet the objective of realistic assessment for a generic site to provide input to the next phase of the NGNP design
- Dose calculation methodology is based on NRC Reg. Guide 1.183 (2000) and MHTGR methods
- The cumulative dose is calculated for a 300hr (12.5 days) exposure time for an adult at the offsite boundary, after which relocation is assumed. The breathing rates and weather dispersion factors are constant for this period.

Model Overview Continued

- Dose conversion factors taken from Federal Guidance Report 13 CD (2002) adult values
- Daily average breathing rate of 2.32E-4m^3/s is based on NRC Reg. Guide 1.4, >1 day rate
- The weather conditions in NRC Reg. Guide 1.3 for the 1-4 day period are selected as generic weather conditions that yield conservative, 95th percentile weather X/Q values
  - The generic weather conditions for best estimate calculations are assumed to be such that the best estimate X/Q values are 10% of the conservative values
  - This approach is consistent with MHTGR PSID and PRA methods and Section 7.1 of Reg. Guide 4.2
  - Ground release weather X/Q of 2.60E-5s/m^3
  - Stack release weather X/Q of 1.90E-6s/m^3 for an assumed 50m stack
- No radioactive decay or deposition of the plume is assumed

Top Level Regulatory Criteria Used to Evaluate Site Boundary Doses

Regulation	Application	Offsite Dose Limits
NRC 10CFR50.34 and NRC 10CFR50.67	Offsite dose limits during design basis events (DBEs)	TEDE < 25rem/event
EPA Manual of Protective Action Guides and Protective Actions for Nuclear Incidents (1992)	Offsite dose limits during DBEs and beyond design basis events (BDBEs) at which sheltering is considered	TEDE < 1rem/event Thyroid CEDE < 5rem/event

Description of Dose Cases

- Description of cases for 4mm and 100mm breaks

  Case 1: No RB retention cases

  Case 2: RB retention with successful opening and failure to reclose the Depressurization Vent Shaft (DVS)

  Case 3: RB retention with successful opening and closing of the DVS

  Case 4: RB retention with successful opening and failure to reclose the DVS (Case 2) with no RB leakage pathways

- Description of options for RB retention cases

  Option a: No DVS filtration, non-dust RNs are vapor

  Option b: DVS filtration, non-dust RNs are vapor

  Option c: No DVS filtration, non-dust RNs are 10^{-7}m aerosols

  Option d: DVS filtration, non-dust RNs are 10^{-7}m aerosols

Specific Dose Analysis Cases

Case No.	PHTS HPB Break Size	RB Retention Modeled	RB Leakage Modeled	DVS Damper Reclosure	Form of Non-Dust RNs	DVS Filtration
1a(4)	**4mm**	**No**	**n/a**	**n/a**	**Vapor**	**n/a**
1c(4)	4mm	No	n/a	n/a	Aerosol	n/a
2a(4)	**4mm**	**Yes**	**Yes**	**No**	**Vapor**	**No**
2b(4)	4mm	Yes	Yes	No	Vapor	Yes
2c(4)	4mm	Yes	Yes	No	Aerosol	No
2d(4)	4mm	Yes	Yes	No	Aerosol	Yes
3a(4)	**4mm**	**Yes**	**Yes**	**Yes**	**Vapor**	**No**
3b(4)	4mm	Yes	Yes	Yes	Vapor	Yes
3c(4)	4mm	Yes	Yes	Yes	Aerosol	No
3d(4)	4mm	Yes	Yes	Yes	Aerosol	Yes
4a(4)	4mm	Yes	No	No	Vapor	No
1a(100)	100mm	No	n/a	n/a	Vapor	n/a
1c(100)	100mm	No	n/a	n/a	Aerosol	n/a
2a(100)	100mm	Yes	Yes	No	Vapor	No
2b(100)	100mm	Yes	Yes	No	Vapor	Yes
2c(100)	100mm	Yes	Yes	No	Aerosol	No
2d(100)	**100mm**	**Yes**	**Yes**	**No**	**Aerosol**	**Yes**
3a(100)	100mm	Yes	Yes	Yes	Vapor	No
3b(100)	100mm	Yes	Yes	Yes	Vapor	Yes

Assumptions for No RB Retention Cases

- No RB cases assume RN release from PHTS is directly to environment at ground level with no RB retention
- These cases selected to create a baseline to understand the importance of different RB retention characteristics defined in other cases
- Cumulative 300hr dose at 400m site boundary evaluated
- All non-dust RNs treated as either all vapor or all aerosol (10^{-7}m size) in different cases
- I and Te isotopes use vapor DCFs for nondust (delayed) releases which are about a factor of 3 greater than the DCFs used for the aerosols
- Metal RNs vapor DCFs assumed the same as the aerosol DCFs due to lack of metal vapor DCFs in FGR11 or FGR13
- Total of 4 dose analysis cases in this category

Results for No RB Retention Cases

Case No.	Break Size (mm)	Form of Non-Dust RNs	Total I-131 Release (Ci)	Thyroid CEDE (mrem)	Ratio of Thyroid PAG Limit to Thyroid CEDE	TEDE (mrem)	Ratio of NRC TEDE Limit to TEDE
1a(4)	4	Vapor	1.6E+02	2.0E+03	2.5E+00	1.4E+02	1.8E+02
1c(4)	4	Aerosol	1.6E+02	7.3E+02	6.9E+00	6.3E+01	4.0E+02
1a(100)	100	Vapor	4.3E-01	5.7E+00	8.7E+02	4.3E-01	5.8E+04
1c(100)	100	Aerosol	4.3E-01	2.1E+00	2.4E+03	2.2E-01	1.2E+05

- The highest no RB retention doses are obtained for the 4mm vapor case 1a(4). Vapor cases have higher doses due to higher DCFs.
- No RB retention needed to meet limits based on this best estimate analysis. Minimum ratio to Thyroid PAG limit is 2.5.
- 4mm breaks dominate due to delayed fuel release during blowdown
- 100mm breaks do not generate shear force ratios high enough to develop large contributions from lift-off and dust resuspension

Key RN Contributions to Offsite Dose
No RB Retention Case

- No RB case with the highest release rates and doses, 4mm vapor, case 1a(4)
- I-131 and Te-132 are key contributors to the offsite doses for this case

Radionuclide	Thyroid CEDE (mrem)	TEDE (mrem)	Contribution to Total Thyroid CEDE (%)	Contribution to Total TEDE (%)
Ag-110m	4.0E-01	1.4E+00	<.1	1.0
Ag-111	3.5E-02	7.0E-01	<.1	0.5
Cs-37	1.0E+00	1.1E+01	<.1	7.9
I-131	**1.4E+03**	**6.9E+01**	**68.7**	**50.3**
I-133	1.1E+02	6.1E+00	5.7	4.4
Sr-90	3.1E-03	8.2E-01	<.1	.6
Te-132	**3.1E+02**	**2.1E+01**	**15.5**	**15.3**
Subtotal	**1.8E+03**	**1.1E+02**	**90**	**80**
Other RNs Estimate	**2.0E+02**	**2.7E+01**	**10**	**20**
Total Estimate	**2.0E+03**	**1.4E+02**	**100**	**100**

Comparison to 2008 NGNP RB Report No RB Retention Case

- TEDE doses are a factor of 3 less and thyroid CEDE doses are a factor of 5 less than in the 2008 NGNP RB Report
- Many factors contribute to the dose differences and are listed on the following slide

Dose	3mm 2008 RB Report No RB Retention	4mm Current Case 1a(4)
TEDE, rem	0.4	.14
Thyroid CEDE, rem	10	2

Factors Contributing to Dose Differences No RB Retention Case

	3mm 2008 RB Report No RB Retention	4mm Current Case 1a(4)
Core inlet/outlet temperatures, °C	350 °C/950 °C	280 °C/750 °C
SS helium mass in PHTS, kg	3272	3920
Helium mass in PHTS at end of blowdown, kg	25	94
Blowdown time, hr	102	91
Maximum fuel temperature for fuel release calculations, °C	1741	1634
Cumulative I-131 release from fuel to PHTS at 300hr, Ci	1040	265
Cumulative I-131 release from PHTS to RB at 300hr, Ci	850 (82% of fuel release)	155 (58% of fuel release)
Weather X/Q, s/m^3	2.3E-5 (425 m EAB)	2.6E-5 (400 m EAB)
I-131 thyroid CEDE DCF for delayed releases, Sv/Bq	2.92E-7 (FGR11 particulate)	3.93E-7 (FGR13 vapor)
TEDE scaling factor	1/0.4 =2.5	1/0.8=1.25
Thyroid CEDE scaling factor	1/0.5=2.0	1/0.9=1.11

Assumptions for RB Retention Cases

- Cases in which the DVS damper opens at set pressure and recloses
  - 4mm: damper recloses post blowdown at 91hr
  - 100mm: damper recloses at end of PHTS thermal expansion, 50hr
- Filtration cases assume
  - 99% filtration of stack particulate and aerosol releases,
  - 0% filtration of ground level particulate and aerosol release and
  - 0% filtration of all vapor release.
  - Filtration resistance not included in RB model.
- Vapor cases assume
  - Delayed release from the fuel enters the RB as vapor.
  - No deposition in the RB for vapor RNs.
  - Vapor DCFs used for I and Te isotopes; default particulate DCFs are used for the metal RNs.
  - I and Te vapor DCFs are approximately a factor of 3 greater than the default particulate DCFs.
- Aerosol cases assume
  - delayed release from the fuel enters the RB as aerosols of size 10^{-7}m.
  - Deposition occurs in all compartments in the RB.
  - Default particulate DCFs are used for the aerosols.

Comparison of I-131 Effective DCFs RB Retention Cases

- Current dose model considers 4 contributions to the dose
  - Ground level vapor
  - Ground level aerosol
  - Stack level vapor
  - Stack level aerosol
- The differences in the eDCFs are important in understanding of the differences in doses for the various RB retention cases
- The thyroid CEDE effective DCF (eDCF) is equal to the BR * X/Q * DCF

	X/Q (s/m^3)	DCF (Sv/Bq)	eDCF (Sv/Bq)
Ground level vapor	2.6E-05	3.93E-07	2.4E-15
Ground level particulate/aerosol	2.6E-05	1.47E-07	8.9E-16
Stack level vapor	1.9E-06	3.93E-07	1.7E-16
Stack level particulate/aerosol	1.9E-06	1.47E-07	6.5E-17

Results for RB Retention Cases

Case No.	Break Size (mm)	RB Leakage	DVS Damper Reclosure	Form of Non-Dust RNs	DVS Filtration	Total I-131 Release (Ci)	Thyroid CEDE (mrem)	Ratio of Thyroid PAG Limit to Thyroid CEDE	TEDE (mrem)	Ratio of NRC TEDE Limit to TEDE
2a(4)	4	Yes	No	Vapor	No	**3.0E+01**	2.9E+01	1.7E+02	1.9E+00	1.3E+04
2b(4)	4	Yes	No	Vapor	Yes	3.0E+01	2.9E+01	1.7E+02	1.9E+00	1.3E+04
2c(4)	4	Yes	No	Aerosol	No	1.9E-01	7.2E-02	6.9E+04	6.0E-03	4.2E+06
2d(4)	4	Yes	No	Aerosol	Yes	2.0E-03	8.5E-04	5.9E+06	7.7E-05	3.2E+08
3a(4)	4	Yes	Yes	Vapor	No	9.1E+00	**1.1E+02**	4.7E+01	**7.2E+00**	3.5E+03
3b(4)	4	Yes	Yes	Vapor	Yes	9.1E+00	1.1E+02	4.7E+01	7.2E+00	3.5E+03
3c(4)	4	Yes	Yes	Aerosol	No	2.0E-01	3.9E-01	1.3E+04	3.4E-02	7.4E+05
3d(4)	4	Yes	Yes	Aerosol	Yes	7.6E-02	3.5E-01	1.4E+04	3.0E-02	8.3E+05
4a(4)	4	No	No	Vapor	No	1.4E-01	1.5E-01	3.3E+04	1.0E-02	2.4E+06
2a(100)	100	Yes	No	Vapor	No	1.4E-03	1.4E-03	3.5E+06	4.3E-04	5.9E+07
2b(100)	100	Yes	No	Vapor	Yes	8.5E-04	1.2E-03	4.3E+06	9.4E-05	2.7E+08
2c(100)	100	Yes	No	Aerosol	No	5.7E-04	2.5E-04	2.0E+07	3.4E-04	7.4E+07
2d(100)	100	Yes	No	Aerosol	Yes	5.8E-06	**2.6E-06**	1.9E+09	**3.6E-06**	7.0E+09
3a(100)	100	Yes	Yes	Vapor	No	8.3E-04	4.1E-03	1.2E+06	6.4E-04	3.9E+07
3b(100)	100	Yes	Yes	Vapor	Yes	2.7E-04	3.9E-03	1.3E+06	3.0E-04	8.2E+07

Summary of Key Dose Results for RB Retention Cases

Dose Analysis Case	I-131 Ground Release (Ci)	I-131 Stack Release (Ci)	I-131 Total Release (Ci)	Thyroid CEDE (mrem)	TEDE (mrem)
Case 1a(4) No RB Retention Max Dose Case 4 mm break, non-dust RNs are vapor	155	n/a	155	2000	140
Case 2a(4) RB Retention Max Release Case 4 mm break, DVS damper fails to reclose, no filtration, non-dust RNs are vapor	2.8E-5	30	30	29	1.9
Case 3a(4) RB Retention Max Dose Case 4 mm break, DVS damper recloses, no filtration, non-dust RNs are vapor	8.0	1.1	9.1	110	7.2
Case 2d(100) RB Retention Min Dose Case 100 mm break, DVS damper fails to reclose, 99% filtration of stack particulates/aerosols, non-dust RNs are aerosol	2.2E-8	5.7E-6	5.8E-6	2.6E-06	3.6E-06

Summary of Dose Results
RB Retention Cases

- RB retention maximum release case – case 2a(4)
  - 4mm break, DVS damper fails to reclose, no filtration, non-dust RNs are vapor
  - I-131 total release is 30Ci compared to 155Ci for similar no RB retention case, a reduction of a factor of 5
  - Release through the stack dominates, ground level release is negligible
  - Doses reduced by about factor of 70 relative to the no RB case because the release is mainly via the stack which has a X/Q that is an order of magnitude less than the X/Q for the ground level release in the no RB retention case
  - NO deposition for vapor in the RB, retention due only to volume to volume transport in the RB
  - RB natural circulation pattern develops that continues release through the stack post blowdown
- RB retention maximum dose case – case 3a(4)
  - 4mm break, DVS damper recloses, no filtration, non-dust RNs are vapor
  - I-131 total release is less than maximum dose case (9Ci vs. 30Ci) yet dose is a factor of 3 greater
  - Release through the ground level leakages dominates in this case (8 of the 9Ci)
  - Once the damper closes there is no further release from the stack but as pressure builds slightly in the RB more release exits through the ground level RB leakage paths relative to the open damper case.
  - Higher X/Q for ground level release results in higher dose compared to maximum release case

Summary of Dose Results
RB Retention Cases

- RB retention minimum dose case – case 2d(100)
  - 100mm break, DVS damper fails to reclose, DVS filtration, non-dust RNs are aerosols
  - The thyroid CEDE dose is 6 orders of magnitude less than the comparable no RB retention case, case 1c(100)
  - Larger break size has smaller doses for comparable cases (1 to 4 orders of magnitude)
  - Aerosol cases have smaller doses than vapor cases for comparable cases due to deposition in the RB (<2 orders of magnitude)
  - Filtration reduces the dust and aerosols stack release by 2 orders of magnitude

Effect of Break Size on Doses RB Retention Cases

- Cases 2a(4) and 2a(100): RB damper opens and never recloses, no filtration, RNs not attached to dust are vapor.
- Early in the transient, the cumulative dose is greater for the 100mm cases. The dose due to the prompt release of the RNs attached to dust is greater in the larger break due to the shorter blowdown and increased rate of transport to the RB during the blowdown.
- Conversely, the dose due to the delayed release is much less in the 100mm break as the blowdown is complete before any significant delayed release from the fuel occurs. This is consistent with 2008 study results

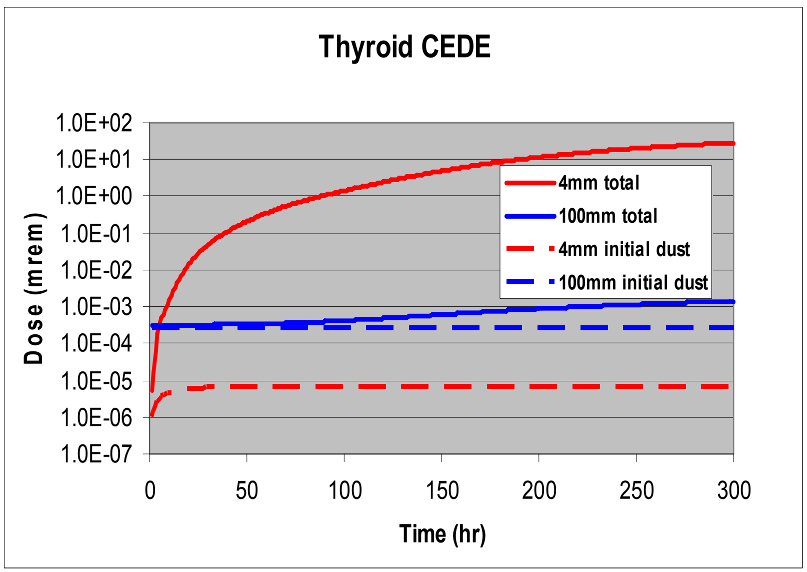

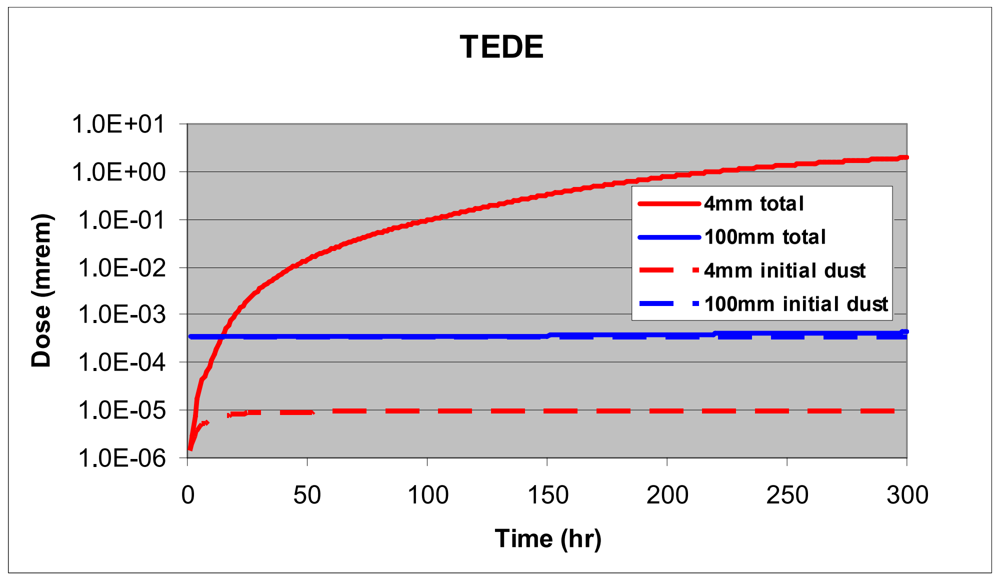

Effect of Filtration on Doses RB Retention Cases

- The effect of DVS filtration is different for the 4mm vs. 100mm cases and the vapor vs. aerosol cases
- 4mm cases
  - The total release is dominated by the contribution from the delayed non-dust RN release from the fuel. Therefore, for the 4mm cases in which the delayed non-dust release is assumed to be in vapor form, filtration has no effect on the 300hr cumulative doses since zero filtration of vapors is assumed.
  - For the 4mm aerosol cases when the DVS damper remains open, the effect of the filtration is to reduce the doses by 2 orders of magnitude consistent with the assumed DVS filtration efficiency.
  - For the 4 mm aerosol cases when the DVS damper recloses, the effect of the filtration is small since the majority of the release is ground level and not filtered.
- 100mm cases
  - For the vapor case a small reduction in doses from DVS filtration is evident since in the 100mm cases a larger percentage of the total release is from the initial release of the RNs that are attached to dust and are filtered.
  - Similar to the 4mm case, the 100mm aerosol cases with filtration also have doses that are 2 orders of magnitude less.

Effect of RN Form Assumption on Doses RB Retention Cases

- Case 2a(4) and Case 2c(4): 4mm RB damper opens and never recloses, no filtration, RNs not attached to dust are either vapor or aerosol
- Comparison of releases across barriers: Fuel 265Ci, PHTS 155Ci, RB 30Ci vapor case and 0.2Ci aerosol case
- Deposition of the aerosols in the RB reduces the releases from the RB by about 2 orders of magnitude for this case
- Doses for these two options differ more than the release difference because the aerosol DCFs are less than the vapor DCFs by a factor of about 3 for I and Te.

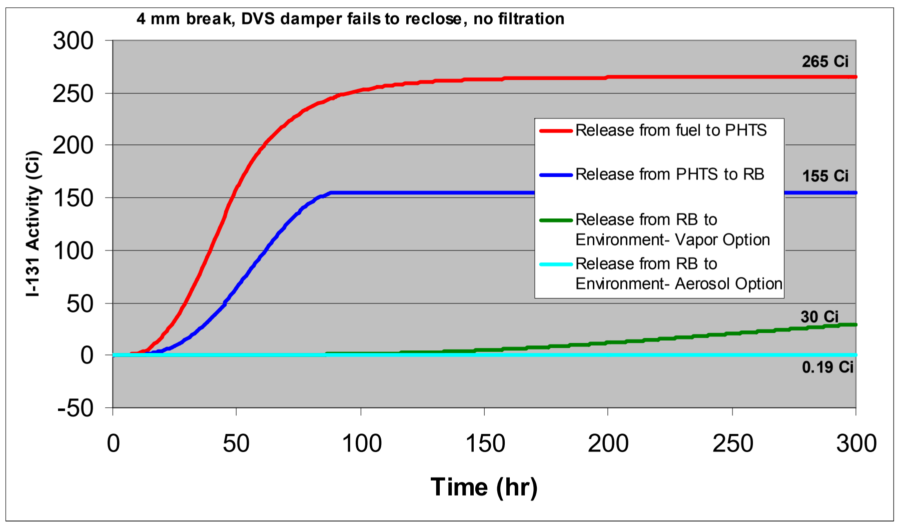

Effect of Leakage Pathways on Doses RB Retention Cases

- Case 4a(4) is a sensitivity case in which the RB leakage pathways are not included.
- This case is included to help understand the effect of the natural circulation that develops when the leakage pathways are included.
- Case 4a(4) is similar to Case 2a(4), 4 mm break with unsuccessful reclosure of the DVS damper without filtration vapor case, except that in Case4a(4) there are no RB leakage paths modeled.
- A comparison of the thyroid CEDE for these two cases shows that the dose is higher in the case with leakage paths by a factor of nearly 200.
- This increase in dose is primarily due to air intake to the RB through the leakage paths which provides an additional driving force for release through the stack. The release from the leakage paths is negligible compared to the stack release.
- The sensitivity of the doses to the modeling of the release paths in the RB ASTEC model requires additional investigation.
- More study is also needed to understand buoyancy driven helium-air exchange phenomena.

Comparison to 2008 NGNP RB Report RB Retention Case

- 2008 RB report case description: 3mm RB damper opens and never recloses, no filtration, RNs not attached to dust are aerosols, 20% vent volume
- Current case description: 4mm RB damper opens and never recloses, no filtration, RNs not attached to dust are aerosols, Case 2c(4)
- TEDE doses are a factor of 1400 less and thyroid CEDE doses are a factor of 2800 less than in the 2008 NGNP RB Report
- Many factors contribute to the dose differences and are listed on the following slide

Dose	3mm 2008 RB Report RB Retention	4mm Current Case 2c(4)
TEDE, mrem	8.5	.006
Thyroid CEDE, mrem	210	.073

Factors Contributing to Dose Differences RB Retention Case

	3mm 2008 RB Report RB Retention	4mm Current Case 2c(4)
Cumulative I-131 release from PHTS to RB at 300hr, Ci	850	155 (reduced fuel temperatures)
Cumulative I-131 release from from RB at 300hr, Ci	18 (2% of release to RB)	0.19 (0.1% of release to RB)
Ground level weather X/Q, s/m^3	2.3E-5 (425m EAB)	2.6E-5 (400m EAB)
Stack level weather X/Q, s/m^3	n/a (all ground level releases)	1.9E-6 (400m EAB)
I-131 thyroid CEDE DCF for aerosols, Sv/Bq	2.92E-7	1.47E-7
TEDE scaling factor	1/0.4 =2.5	1/0.8=1.25
Thyroid CEDE scaling factor	1/0.5=2.0	1/0.9=1.11
RB DVS compartments (More retention due to transport and larger size in multi volume model.)	single (20,000m^3)	multi (23,491m^3)
I-131 RB deposition/settling rate (1/hr)	0. 3	0.4-0.01
RB cooling, density and elevation differences effect on flow in and from RB considered.	no	yes (RB in flow from leakage paths increases stack releases)
Stack filtration for I-131 aerosols	95%	99%
RB radiactoive decay of RNs	yes	no

Dose Insights Relative to 2008 Study

- Lower initial core temperatures result in lower initial RN inventories and lower delayed fuel releases into PHTS for all break sizes
- Convection cooling for slow depressurization reduces delayed fuel releases into PHTS for break sizes less than 10mm due to lower time at temperature
- Cumulative release of I-131 to RB at 300hr for 4mm breaks are factor of 5 less due to the combined effects of reduced initial temperatures, convection cooling during blowdown, and model refinements
- Temperature and density effects are important in the evolution of the flows in the RB
- Multi-compartment ASTEC RB model indicates higher RB retention than single compartment 2008 model
- Modeling of multiple leakage paths from the RB to the environment allows for natural circulation into and out of the RB
- Assumptions made about the RB operation, RB features and characteristics of the source term greatly influence the offsite doses
- Differences in results from 2008 are all understood and are attributed to differences in the design, models, codes and assumptions.

Key Conclusions for Offsite Dose Results

- Minimum ratios of the PAG thyroid CEDE limit to dose:
  - 2.5 for the 4mm no RB retention cases, Case 1a(4)
  - 47 for the 4mm RB retention cases, Case 3a(4)

- Minimum ratios of the NRC TEDE limit to dose:
  - 180 for the 4mm no RB retention cases, Case 1a(4)
  - 3500 for the 4mm RB retention cases, Case 3a(4)

- No RB retention required to meet dose limits based on realistic assumptions used in this study; different conclusion than 2008 study
- The RB retention cases included in this study reduce the offsite doses by 1 – 6 orders of magnitude relative to the no RB case providing additional margin to limits
- Assumptions made about the RB response and characteristics of the source term greatly influence the offsite doses.
  - Cases in which the DVS damper recloses have higher doses than when it remains open due to the increase in ground level releases for these cases.
  - Cases with DVS filtration result in the same (for the 4mm vapor cases) or lower doses (for all other cases) especially for cases in which the non-dust RNs are assumed to be in aerosol form.
  - Cases in which the non-dust RNs are assumed to be in vapor form as opposed to aerosol form have higher doses. Significant RB deposition occurs for RNs assumed to be in aerosol form.

Key Conclusions for Offsite Dose Results

- Dose is more sensitive to ground level releases than DVS stack releases due to the 50m stack influence on X/Q.
- For each comparable case, the 100mm break dose is one to four orders of magnitude less than the 4mm break dose. Results confirm 2008 RB study results that longer blowdown time for the small break results in a significantly greater percentage of the delayed RN release from the fuel being transported to the RB and accordingly greater doses.
- Differences in trends for the 4mm and 100mm cases are a result of the larger contribution of the initial release that is attached to dust to the total dose in the 100mm cases. The RNs that are attached to dust do deposit in the RB and are filterable when released through the vent shaft
  - For the 100mm vapor case when the damper remains open, filtration reduces the doses, 20% for the thyroid CEDE and by a factor of 5 for the TEDE. For the 4mm vapor cases, filtration has no effect on the overall doses.
  - The reduction in doses is significantly larger between the RB vapor case with open damper and the no RB retention case for the 100mm case than for the4 mm case.
  - The opposite is true for the reduction in doses for the RB aerosol case with open damper, the 4mm shows a greater reduction in doses relative to the no RB retention case.

Future Considerations for Offsite Doses

- The PAG definition of TEDE includes the dose due to ground shine – consider the effect for comparison to the PAG TEDE limit
- The effect of a time variable breathing rate and weather dispersion needs to be considered
- Resolve the question as to why ruthenium is a major contributor in dose calculations performed at INEL
- The sensitivity of the doses to the modeling of the release paths in the RB ASTEC model requires additional investigation. More study is also needed to understand buoyancy driven helium-air exchange phenomena.
- Consider wider set of break sizes, locations, and plant response scenarios

Radionuclide Barrier Retention Allocations

Lori Mascaro
Fred Torri
Fred Silady

Current Topic

- Objectives and Scope
- *Plant Level Analyses I:* Normal Operation and Anticipated Transients
  - Requirements and Functional Analyses (Bullet 1 In SOW 6793)
  - Operating Range and Initial Transitions Analyses (Bullet 2)
- *Plant Level Analyses II:* DLOFC for a Range of Primary HPB Leaks and Breaks
  - Depressurization for Range of Leaks and Breaks (Bullet 3)
  - Coupled Thermo-fluid Analysis of PHTS and Reactor Building Response (Bullet 4)
  - Radioactive Material Release Source Terms and Site Boundary Doses (Bullet 5)
  - **Retention Allocations and RN Retention DDNs (Bullet 5)**
- Path Forward

Objectives

- To determine barrier retention allocations for each of the 3 main RN transport barriers based on the results obtained in this study
  - Fuel barrier
  - PHTS HPB barrier
  - RB barrier
- To evaluate uncertainties associated with these barrier retention allocations
- To define boundary conditions for the allocations
- Identify candidate Design Data Needs (DDNs) based on the evaluation performed

Technical Approach Applied

- Retention allocations supported by the 2009 and 2008 results were reviewed
  - 2009 results focused on 4mm and 100mm breaks expected to be limiting for design basis DLOFC
  - 2008 results provide some information for larger break sizes, albeit inconsistent assumptions and models relative to 2009
- The most suitable accident scenario and RN to analyze was identified
  - Focus on the 4mm case with Depressurization Vent Shaft (DVS) damper reclosing with no filtration of release
  - Focus on I-131 releases as dominant and limiting RN
- Engineering judgment was applied to identify and evaluate uncertainties associated with the point estimates of the doses
- Boundary conditions i.e. those conditions that need to be satisfied to meet the allocations, were identified
- Candidate DDNs that should be considered to reduce uncertainties were identified

Selection of Scenarios and RNs for Barrier Allocation

- Selected scenarios expected to be limiting DBEs; BDBEs also need to be considered
  - Breaks > 100mm expected to be BDBEs due to low initiating event frequency
  - Current and 2008 study results have shown small breaks less than 10mm as most likely limiting break size for DBEs
  - 4mm break in CIP selected as limiting break size for barrier allocation
- At this stage of design, barrier allocations focus on inherent and passive design capabilities with minimum reliance on active SSCs
  - No engineered filtration of releases from RB considered in allocations
  - Depressurization Vent Shaft (DVS) Damper closure case selected to minimize risks of gas-exchange between barriers
- Barrier allocations consider full spectrum of radio-nuclides expected to make significant dose contributions
  - I-131 is the dominant RN based on current and 2008 study and many previous HTGR safety evaluations
  - Iodine is volatile and relatively difficult to retain once released from fuel
  - Effectiveness of barriers to retain other RNs should be at least as good as for Iodine isotopes
  - Barrier allocations focus on I-131 retention with consideration on uncertainties in the ratio of total dose to I-131 dose
  - Future updates of barrier allocations to address additional RNs explicitly

Selected Scenario: 4mm DLOFC, Damper Re-closes, No Filtration
Selected RN: I-131

Barrier Retention Parameters

- Fuel Barrier Parameter
  - Fraction of fuel RN inventory that is released from fuel into the PHTS circuit during normal operation and during transient
- PHTS HPB Barrier
  - Fraction of RN initially present or released into the PHTS circuit that is released from the HPB into the RB
- RB Barrier
  - Fraction of RN released into the RB that is released to the environment
    - DVS releases
    - Ground level releases

Barrier Allocations Supported by Currently Available Best Estimate Results

- These cases assume DVS vent shaft closure and no engineered filtration of the release

I-131 Form	Analysis Case (Break Size mm)	Initial I-131 Inventory (Ci)		Fraction Released into PHTS	Fraction Released into RB	Fraction Released from RB ground level	Fraction Released from RB elevated	CEDE Thyroid (mrem)	Margin Factor to Limit
Vapor	3a(4)	Fuel	1.29E+07	2.05E-05	5.85E-01	5.14E-02	6.83E-03	1.1E+02	4.5E+01
		Circ.	0	1					
		Non-circ.	2.05E+00	2.00E-03					
Aerosol	3c(4)	Fuel	1.29E+07	2.05E-05	5.85E-01	4.81E-04	7.79E-04	3.9E-01	1.3E+04
		Circ.	0	1					
		Non-circ.	2.05E+00	2.00E-03					
Vapor	3a(100)	Fuel	1.29E+07	2.57E-05	1.29E-03	4.74E-04	1.46E-03	4.1E-03	1.2E+06
		Circ.	0	1					
		Non-circ.	2.05E+00	2.00E-03					
Aerosol	2008(3)	Fuel	1.29E+07	8.03E-05	8.17E-01	2.12E-02	n/a	2.1E+02	2.4E+01
		Circ.	0	1					
		Non-circ.	3.61E+00	2.00E-03					
Aerosol	2008(1000)	Fuel	1.29E+07	8.03E-05	8.33E-04	6.57E-01	n/a	6.5E+00	7.7E+02
		Circ.	0	1					
		Non-circ.	3.61E+00	2.50E-01					

Evaluation of Uncertainties

- Simplified model developed to represent key sources of uncertainty in current point estimate dose calculation
- Expert elicitation workshop performed at PBMR during week of August 24, 2009
  - Identified key sources of uncertainty in the capability of each barrier to retain RNs
  - Developed current best state-of-knowledge uncertainty distributions for each identified RN transport parameter
  - Evaluated and quantified uncertainties in each barrier retention factor, total release, and selected dose metrics using Microsoft Excel™ and Crystal Ball™
  - Defined the design and analysis boundary conditions that the uncertainty analysis is based on
  - Identified Candidate DDNs to reduce key contributors to uncertainty

Simplified Excel Model for RN Dose Calculation

- Series of equations that mimic the 2009 calculation flow sheet
- Variables defined to capture uncertainties in the dose calculation
- Most variables correspond to fractions of RNs released from the barrier that involved with uncertain RN transport phenomena
- Model benchmarked against 2009 result point estimates for selected cases
- Crystal Ball used to perform Monte Carlo uncertainty analysis

RN Barrier Retention Model Flow Chart

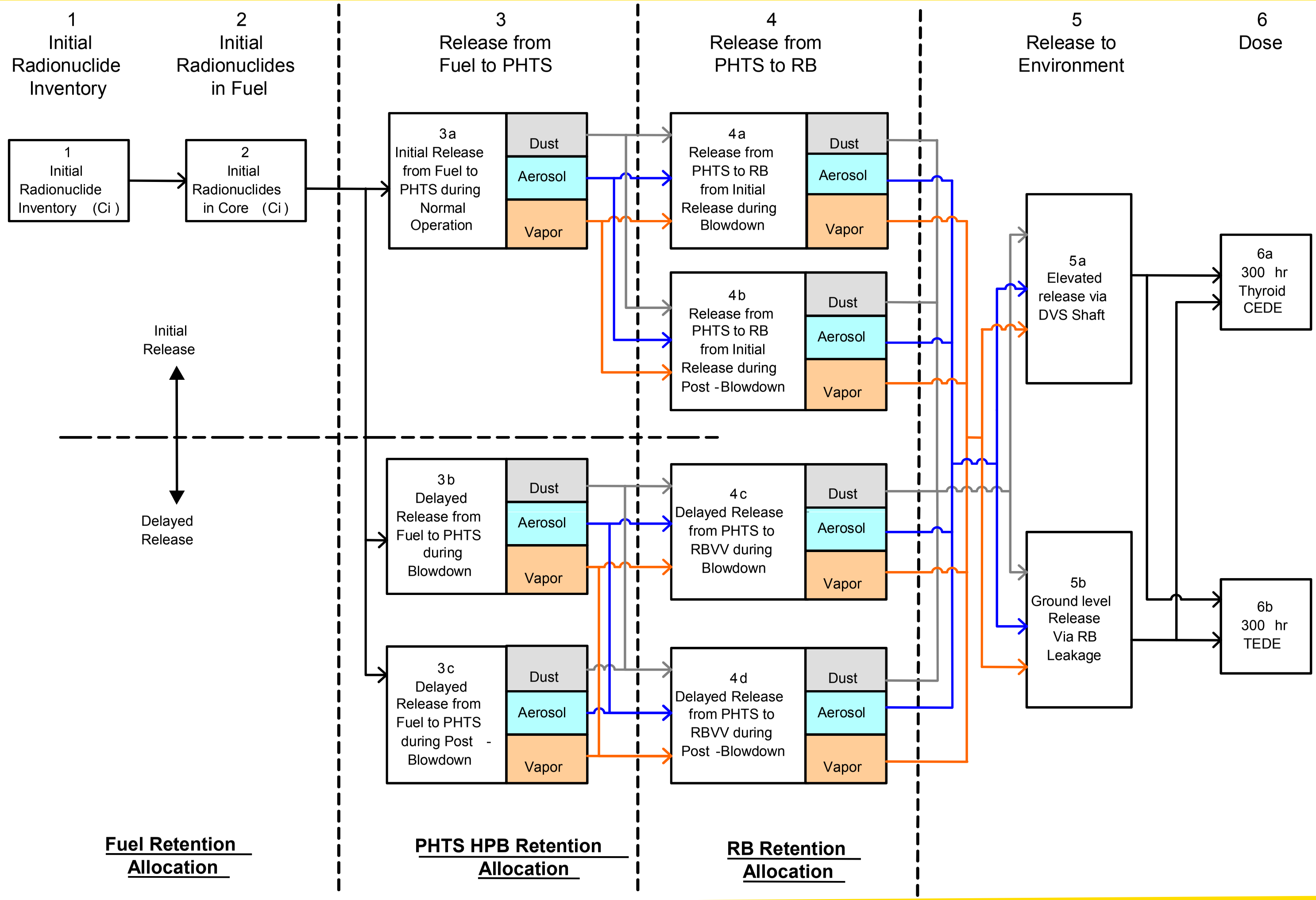

Flowchart converted to Excel Dose Quantification Tree

2009 RN Retention Allocation

Case: 4mm — Damper Reclose End of Blowdown, No DVS Filtration

RN Group: I-131

Net Retention at 300 h:

Barrier	Source in Bq	Retained in Barrier BQ	% Retai'd in Barrier Source in	Fraction Not Retained
Fuel	4.79E+17	4.79E+17	100.00%	2.07E-05
PHTS	9.91E+12	9.24E+12	93.25%	6.75E-02
RB	6.69E+11	6.52E+11	97.43%	2.57E-02

Release to Env. (Bq)	1.72E+10
Total Thyroid CEDE (Sv)	5.39E-05
Total TEDE (Sv)	3.63E-06
Fraction of Initial Inv Released to Env	3.59E-08

Net Retention at 300 h:

Barrier	Source in (Ci)	Retained Net (Ci)	% Retai'd of Source in
Fuel	1.29E+07	1.29E+07	100.00%
PHTS	2.68E+02	2.50E+02	93.25%
RB	1.81E+01	1.76E+01	97.43%

Release to Env. (Ci)	4.64E-01
Total Thyroid CEDE (mrem)	5.39E+00
Total TEDE (mrem)	3.63E-01

1	2	3	4	5	6	7	8
Total Initial Invent'ry (Bq)	Initially in Fuel (Bq)	Release to PHTS (Bq)	Release to RB (Bq)	Release to Environm't (Bq)	Release to Environm't (Bq)	I-131 300 h Dose (Sv)	Total 300 h Dose (Sv)
4.79E+17	4.79E+17	7.62E+10	3.68E+07	2.26E+05	2.21E+05	1.43E-11	2.15E-11
		In. Rel. BD	In. Rel. BD Dust	Att. To Dust	Elev-Filt	Thy CEDE 7.27E-13 TEDE	Thy CEDE 1.45E-12 TEDE
					5.49E+03	4.87E-12	7.30E-12
					Gd-Unfilt	Thy CEDE 2.47E-13 TEDE	Thy CEDE 4.94E-13 TEDE
			1.84E+07	1.13E+05	1.10E+05	7.16E-12	1.07E-11
			In. Rel. BD Aerosol	Aerosol	Elev-Filt	Thy CEDE 3.63E-13 TEDE	Thy CEDE 7.27E-13 TEDE
					2.74E+03	2.43E-12	3.65E-12
					Gd-Unfilt	Thy CEDE 1.24E-13 TEDE	Thy CEDE 2.47E-13 TEDE
			1.84E+07	1.13E+06	1.10E+06	1.91E-10	2.87E-10
			In. Rel BD. Vapor	Vapor	Elev-Filt	Thy CEDE 9.68E-12 TEDE	Thy CEDE 1.94E-11 TEDE
					2.60E+04	6.15E-11	9.23E-11
					Gd-Unfilt	Thy CEDE 3.11E-12 TEDE	Thy CEDE 6.22E-12 TEDE

Only part of tree shown - remaining part covers
Initial fuel releases during post blow-down and delayed fuel releases during blow-down and post blow-down phases

Uncertainty Distribution Considerations

- Basic approach is to define the best estimate, upper bound, and lower bound and to define distribution parameters to each
  - Best estimate candidates: mean, median, mode
  - Lower bound candidates: 1%tile, 5%tile
  - Upper bound candidates: 99%tile, 95%tile
- A distribution is then fit to the above or a probability distribution is estimated directly
- Examples used in similar elicitations:
  - Beta Distribution – good for fractions with high values between 0 and 1
  - Lognormal Distribution – good for small fractions with large uncertainties when upper tail
  - Triangle Distribution – most direct way to model a best estimate, upper bound and lower bound when good basis exists for the bounds
- If the distribution comes from data; curve fit the data
- Crystal Ball has a big library of distributions
- Monte Carlo results are not very sensitive to the assumed shape of the distribution; normally driven by the mean and the variance
- For sums and products of independent variables, the mean is the only parameter that propagates: (the mean of the monte carlo distribution equals the point estimate obtained using the mean inputs for these functions and independent variables)

Boundary Conditions

- Boundary conditions define a minimum set of plant capabilities that are necessary to make the barrier allocations valid
- Barrier allocations shall be consistent with PBMR safety design philosophy and the 2008 RB Technical and Functional Requirements
- Consider RB Functional Requirements from 2008 Study
  - Need to have a building and means of controlling releases during normal operation; this will likely lead to an HVAC with controlled pressure zones which may or may not have an accident mitigation role
  - Need to provide a pressure relief capability and structural features to protect RB and all the safety related SSCs for design and beyond design basis events
  - Will need to control leakage post blow-down to limit air ingress to building and post blow-down releases
  - Need for filtration should not be driven by the allocations and will be resolved in later stages of design

Retention Allocation Boundary Conditions

- All retention allocations are based on the current NGNP 500MW 750 ROT design, including the PHTS and RB layouts. Changes in these factors will lead to changes in the retention allocations
- 4mm break in CIP near RPV in reactor cavity of RB
- Plant response same as in current RN dose evaluation
  - Blowout panels open to relieve RB pressure and exhaust release out the depressurization vent shaft (DVS)
  - DVS damper is closed at end of PHTS blow-down
  - No filtration is assumed for the DVS release
  - RB HVAC is assumed to be switched off at time of break

Releases from Fuel to PHTS

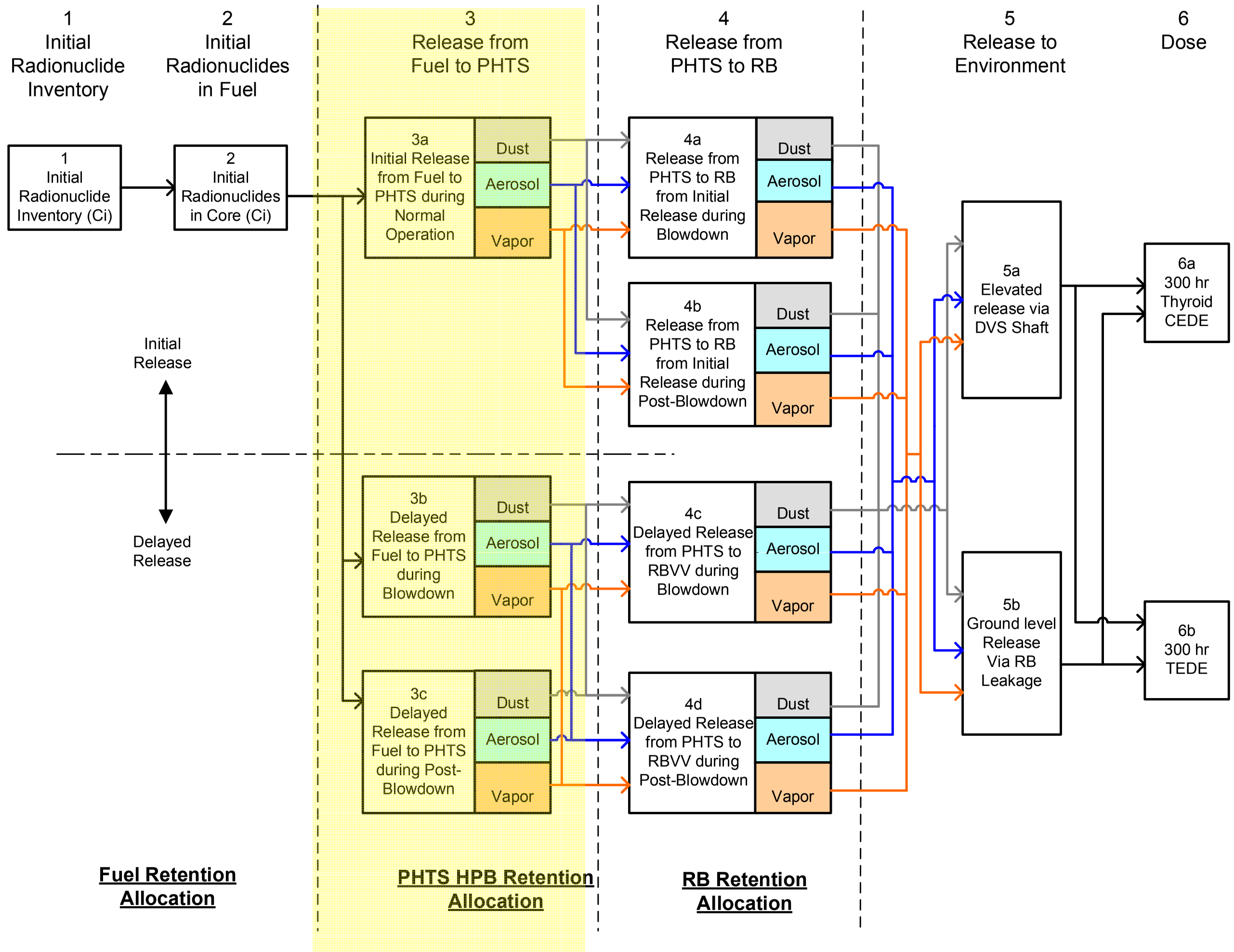

Release from Fuel to PHTS
Major Contributing Uncertainties

- When considering the RN releases from the fuel, both the uncertainties in the fuel temperature analysis during the transient as well as the uncertainties associated with the RN releases under those temperatures have to be considered
- Major Factors Leading to Fuel Temperature Uncertainties
  - Core Bypass and Leak Flows
  - Added Pressure Drops in By-pass Channels
  - Core Thermal Dispersion
  - Pebble Bed Heat Transfer Coefficients
  - Reflector and core graphite conductivity
- Major Factors Leading to RN Release Uncertainties
  - Transport Parameters (diffusion coefficients and sorption isotherms)
  - Heavy Metal Contamination
  - Fuel Failure Fractions

Release from Fuel to PHTS Uncertainty Model

- The uncertainties assigned to the release of I-131 during the transient are based on previous parametric Monte Carlo analysis performed on the VSOP-TINTE-GETTER chain
- The distribution was found to be of log-normal form
- For this analysis the DLOFC safety factors are used in the blow-down and post-blow-down phase

RN Release From Fuel Safety Factors

	^{137}Cs	^{111}Ag	^{131}I	^{90}Sr
Normal operation	6	14	**18**	280
DLOFC	12	16	**20**	1600

Release from Fuel to PHTS
Key Uncertainty Distributions

- Delayed fuel release fraction during blow-down and post blow-down are key sources of uncertainty

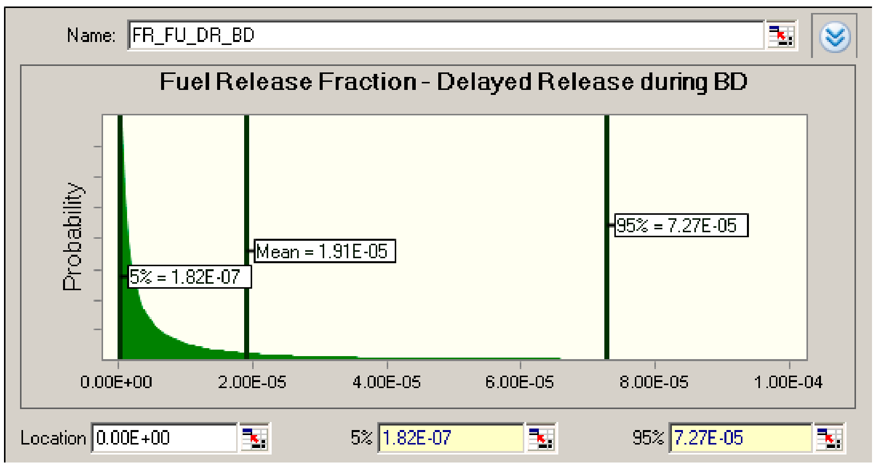

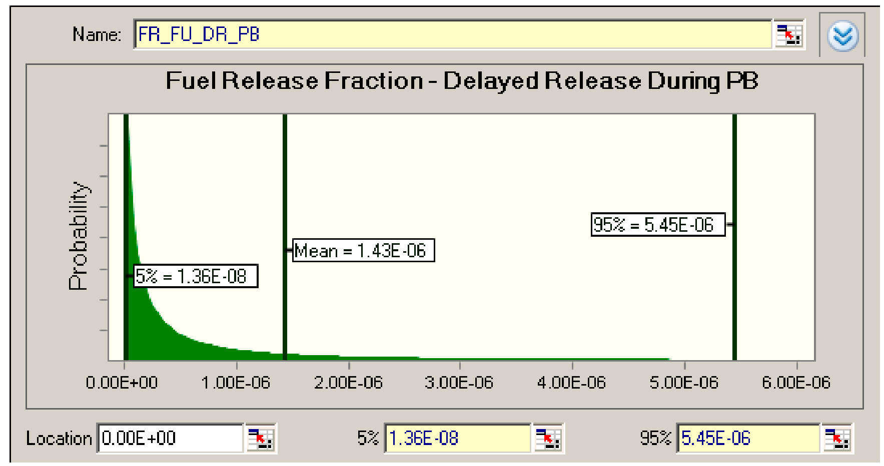

Releases from Fuel to PHTS Boundary Conditions

- Fuel quality must be equal or better than the current German qualified fuel
- Fuel temperatures during the transient do not exceed 1700 °C
- Burnup measurement and on-line refueling is sufficiently accurate that the limiting fuel burnup is not exceeded
- There is no water ingress during the event

Release from Fuel to PHTS Considerations

- In the 4mm break analysis the maximum temperature of the fuel does not exceed the temperature at which Sr^{90} release becomes dominant. This uncertainty is added as an uncertainty in the scaling of the 7 isotopes to the overall TEDE dose

Release from Fuel to PHTS Identified Candidate DDNs

- Fuel Qualification
- Core by-pass and leak flow analysis and measurements during hot conditions
- RN release from fuel physical phenomena investigation
- Graphite (including fuel sphere graphite) thermal conductivities under irradiation
- Fuel graphite impurities

Releases from PHTS to RB

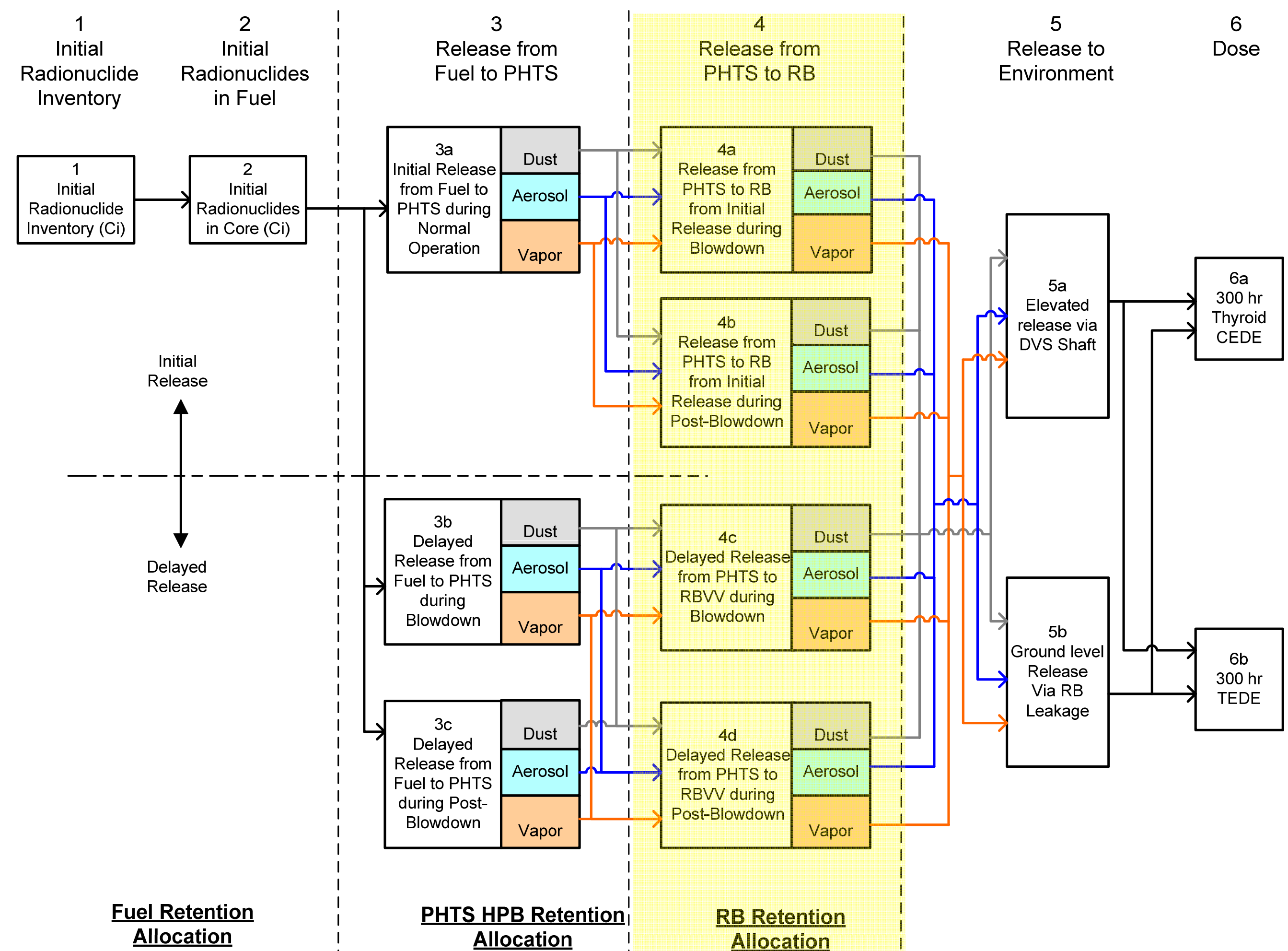

Release from PHTS to RB Phases

- Initial Inventory at time of break
  - Circulating and Non-circulating activity
  - Form of I-131 (dust / vapor / aerosol)
- Blow-down Phase
  - Re-suspension of normal operation plated-out or deposited I-131
  - Thermo-fluid behavior (blow-down and thermal expansion)
  - Retention of delayed release I-131 in the PHTS
  - Form of delayed release I-131 (dust / vapor / aerosol)
- Post-Blow-down Phase
  - Thermo-fluid behavior (thermal contraction, diffusion, natural circulation)
  - Not modeled in codes but considered in uncertainty analysis

Release from PHTS to RB – Initial Inventory at Time of Break Major Contributing Uncertainties

- Circulating vs. Non-circulating activity
  - Analysis of AVR data and experiments have indicated that most activity is either plated-out or deposited. Circulating activity within the PHTS during normal operation was found to be of the order of 1%
- Dust vs. Non-Dust
  - Significant uncertainties in sorption interaction between RNs and graphite
  - Previous experience (e.g. AVR data) has not been sufficiently analyzed to determine I-131 dust ratios
  - Assumption is that there is no knowledge on the dust vs. non-dust distribution of I-131 during normal operation (flat distribution)
- Vapor vs. Aerosol
  - Lack of knowledge of I-131 chemistry in a dry helium/air environment
  - Current analysis only considers vapor form
  - Flat distribution between 0 and 1 represents state of knowledge about fraction of initial and delayed releases of I-131 as vapor vs. aerosol

Release from PHTS to RB – Blow-down Phase Major Contributing Uncertainties

- Re-suspension of plated-out and deposited I-131
  - Flownex calculations indicate shear force ratios < 1 and hence insignificant liftoff. There is some uncertainty involved in this analysis, but it is seen as relatively small
- Thermal-fluid behavior
  - Low coolant flow rates close to the limit of the calculational model
  - Flow path reversal and directional changes
  - Buoyancy not modeled
  - Time of completion of blow-down
  - Transport of I-131 from the core to the break location
- Retention of delayed release I-131 in the PHTS
  - Low surface temperatures and its effect on the plate-out rate
  - Low flow velocities effect on both plate-out and deposition rates
  - Form of the I-131 effect on the plate-out and deposition
  - Reduction in effective surface area available as flow paths bypass certain components (e.g. IHX)
- Form of delayed release I-131
  - Less time available for I-131 sorption to the dust than in normal operation
  - Sorption is more likely on deposited dust than circulating dust
  - Most delayed release of I-131 is expected to reach the RB in non-dust form

Release from PHTS to RB – Post-blow-down Phase Major Contributing Uncertainties

- Thermal-fluid behavior
  - Time of blow-down exceeds the time of peak core temperatures; PHTS is in state of thermal contraction at end of blow-down
  - Low coolant flow rates close to the limit of the calculation model and hence estimates of the time to complete blow-down are uncertain
  - Buoyancy effects and diffusion not yet included in computer models
  - Transport path of I-131 from the core to the break location and extent of mixing in PHTS circuit is uncertain
  - Uncertainty distribution applied based on engineering judgment to bound the flow rates for gas-exchange
  - Plate-out and settling along release path if gas-exchange occurs is not modeled in computer models but is expected; magnitude of these phenomena is uncertain

Release from PHTS to RB
Key Uncertainty Distributions

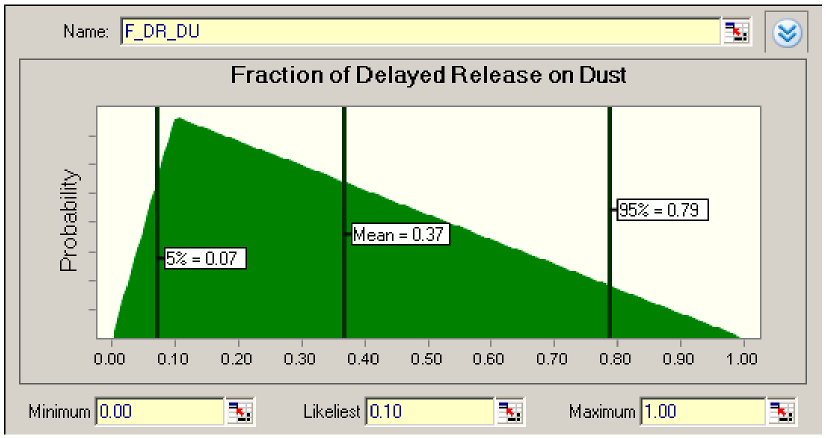

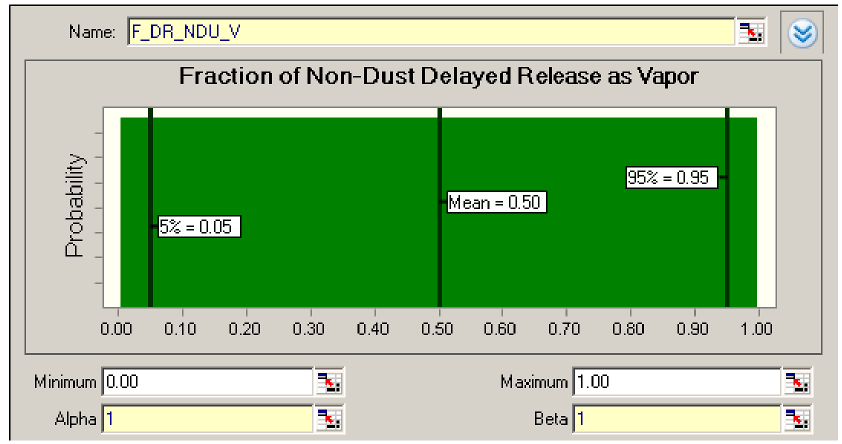

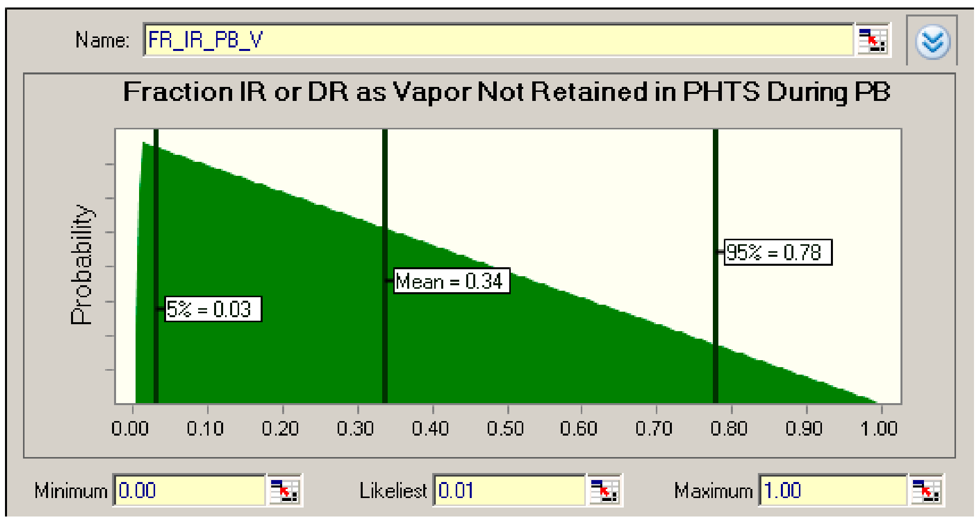

Releases from the PHTS to the RB Boundary Conditions

- The accident sequence, especially the function/non-function of certain equipment, must be similar to the one analyzed

Releases from the PHTS to the RB Identified Candidate DDNs

- Code validation
- Reduce uncertainty on distribution of I-131 and other radiologically significant RNs on dust, aerosol, and vapor as well as dust and aerosol size distributions
- Reduce uncertainty on plate-out, settling, and other retention phenomena
- Reduce uncertainty on PHTS-RB gas exchange phenomena
- Reduce uncertainty on the formation, size and chemical interaction of metallic dust
- Reduce uncertainty in heat transport coefficients of the pebble bed and other thermal-fluid factors, such as component flow restrictions

Releases from RB to Environment

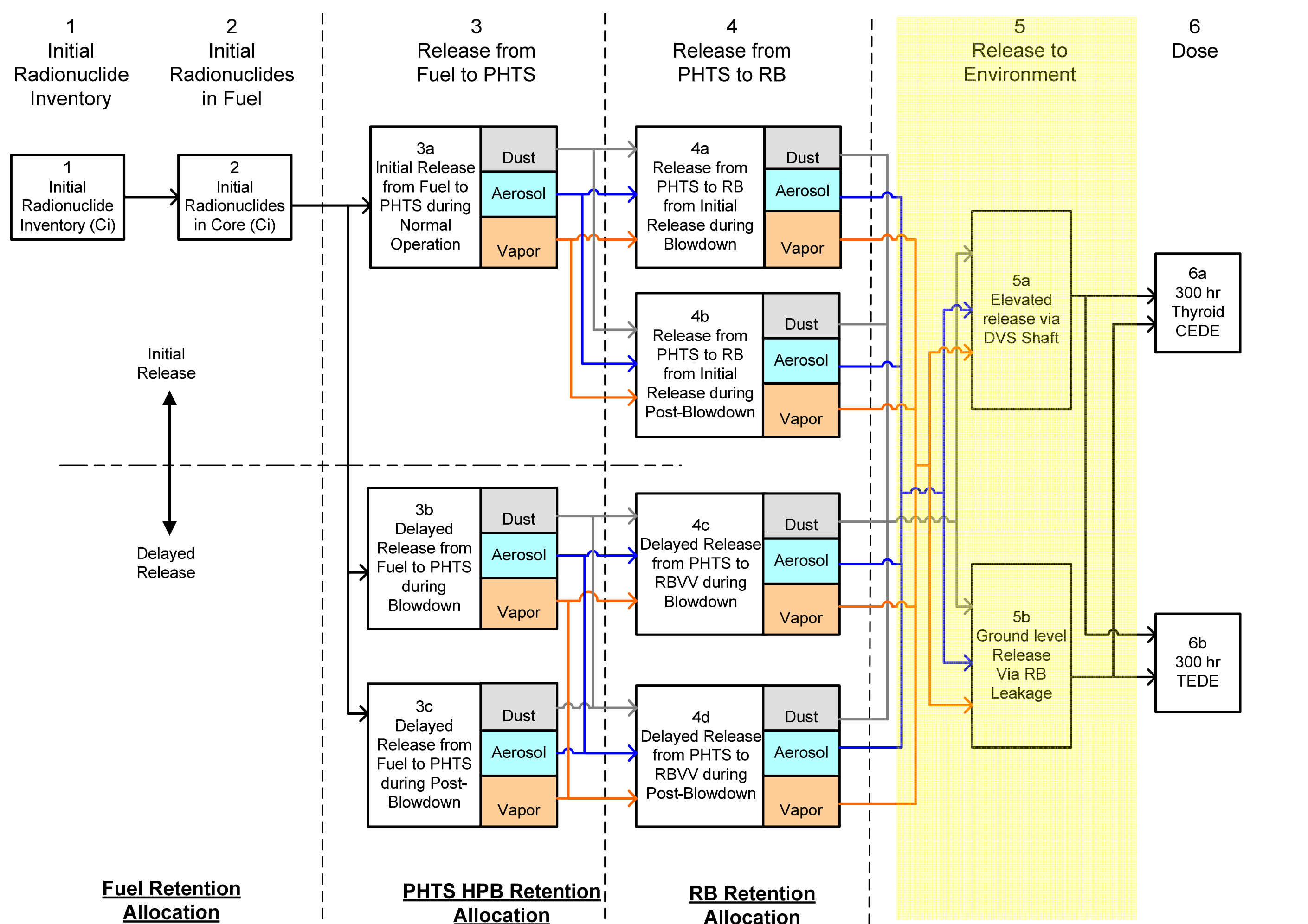

P B M R

Release from RB to the Environment Major Contributing Uncertainties

- Same uncertainties about distribution of RNs on dust, vapor, and aerosol as in PHTS plus changes to distribution inside RB
- Uncertainty in dust size distribution input leading to uncertainty in dust deposition rates
- Location and size of reactor building bypass leakage
  - Leaks from RBVV direct to environment
  - Leaks from RBVV into other RB compartments
  - Ingress of air into building and impact on gas mixtures
- Timing of DVS damper closure
- Uncertainties in RN retention phenomena for each form of RN (dust, vapor, aerosol)
- Model Uncertainties
- Limited validation of ASTEC for HTGR conditions

Release from RB to the Environment Key Uncertainty Distributions

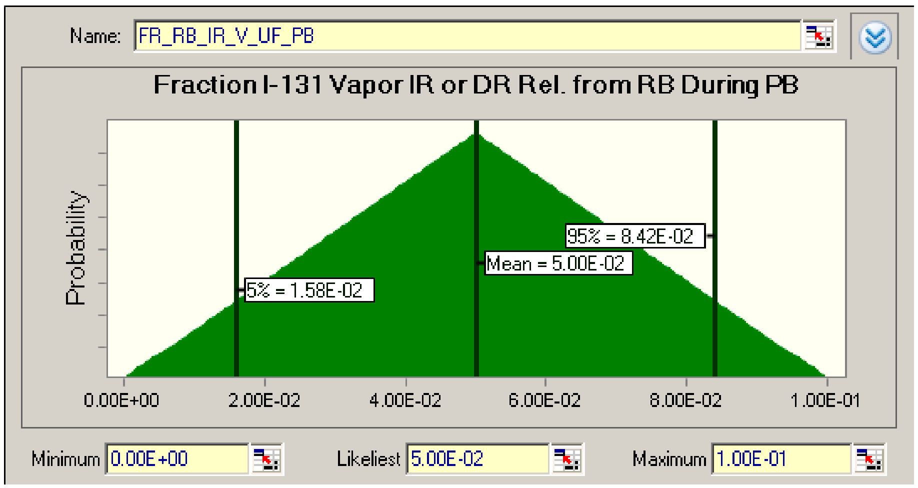

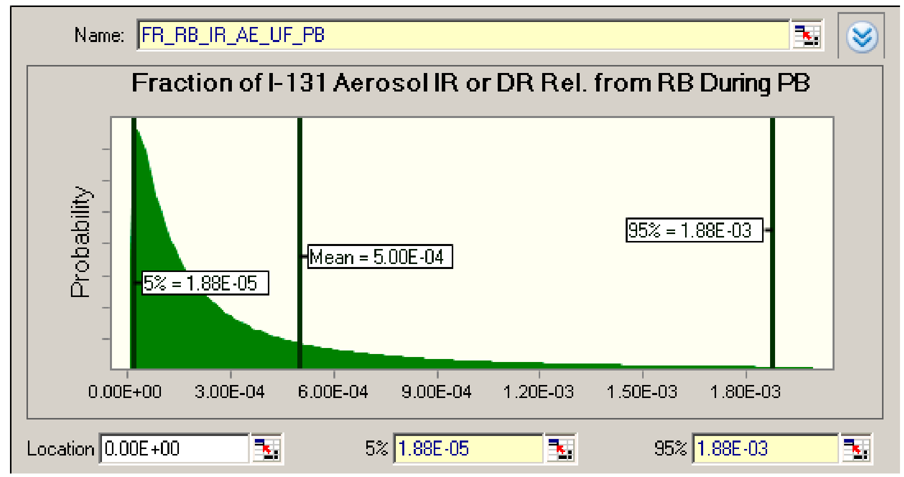

Release from RB to the Environment Boundary Conditions

- A multi-compartment building with blow-out panels must exist
- DVS has a tall (> 50m) stack and a closure mechanism
- The building leak rate is close to the assumed commercial grade leak rate
- The surface area to volume ratios of the building are comparable to what was modeled
- The HVAC system and systems injecting Helium into the PHTS shut down at the time of the break, i.e. these system does not negatively influence the releases
- The PHTS break does not adversely impact the RB an safety classified SSCs – no consequential second break scenario exists

Release from RB to the Environment Identified Candidate DDNs

- Code validation
- Reduce uncertainty on outside air-RB-PHTS gas exchange phenomena
- Reduce uncertainty on changes in the distribution of I-131 and other radiologically significant RNs on dust, aerosol, and vapor as well as dust and aerosol size distributions in the RB
- Reduce uncertainty on plate-out, settling, and other retention phenomena

Dose Calculations

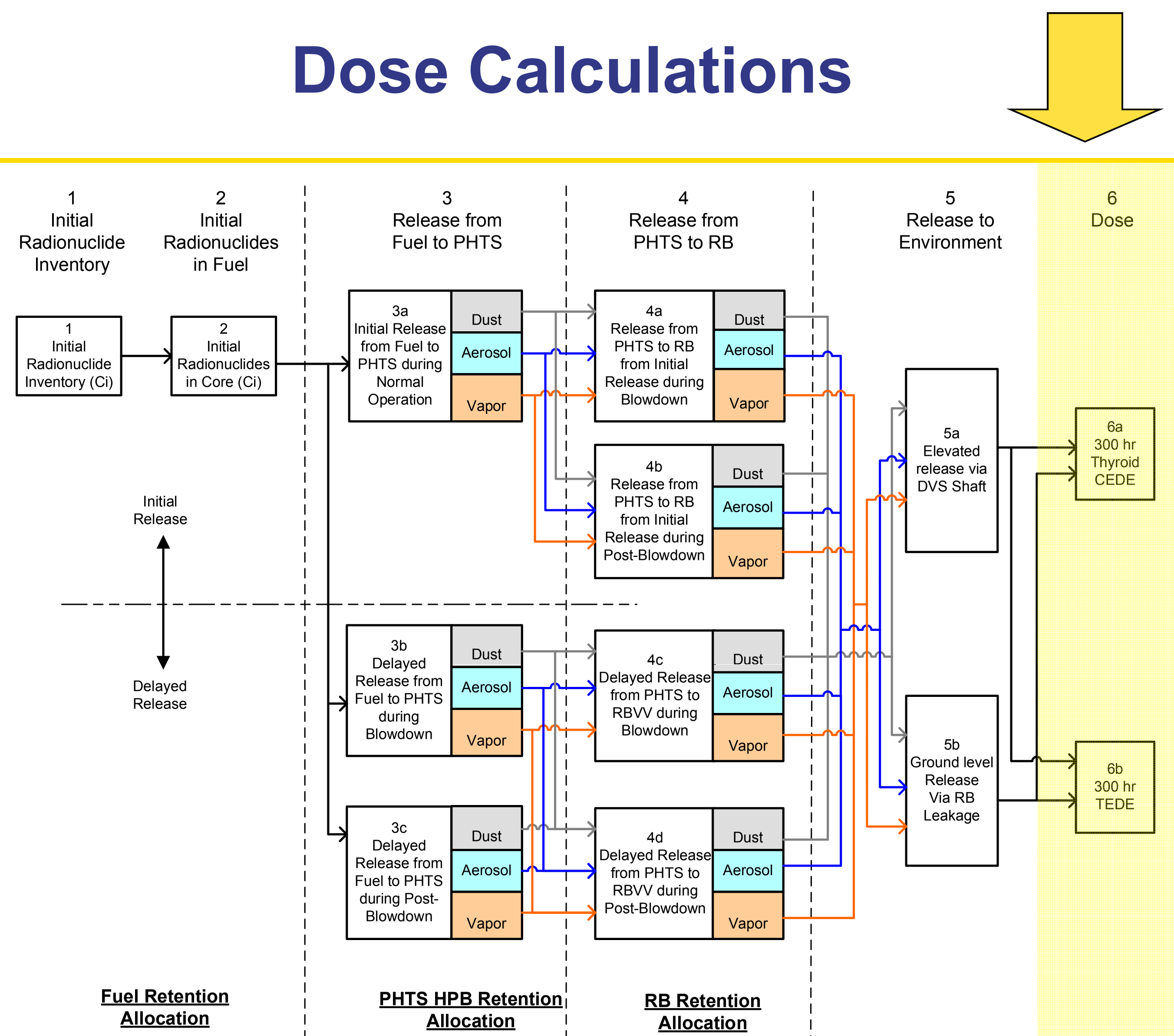

Dose Calculation Uncertainties

- Dose calculation based on Regulatory Guide rules and definitions of TEDE and CEDE PAG doses
- While there are considerable uncertainties in the dose calculation due to lack of defined site, weather variability, etc. these uncertainties can only be quantified for specific sites
- Decision made to treat dose parameters as fixed values
- Most significant uncertainty that can be influenced by the design is the extent to which I-131 is indicative of the total dose
  - Uncertainty assigned to scaling factor used to predict total dose from I-131 dose

Dose Calculation
Key Uncertainty Distributions

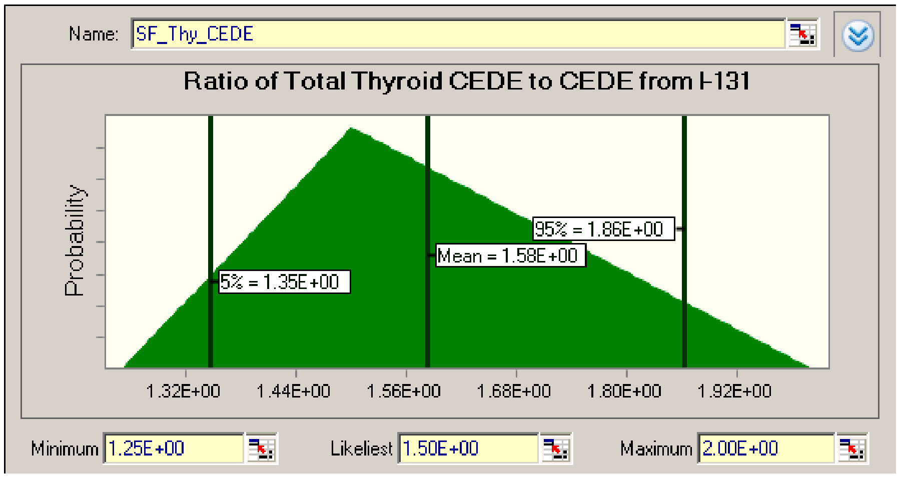

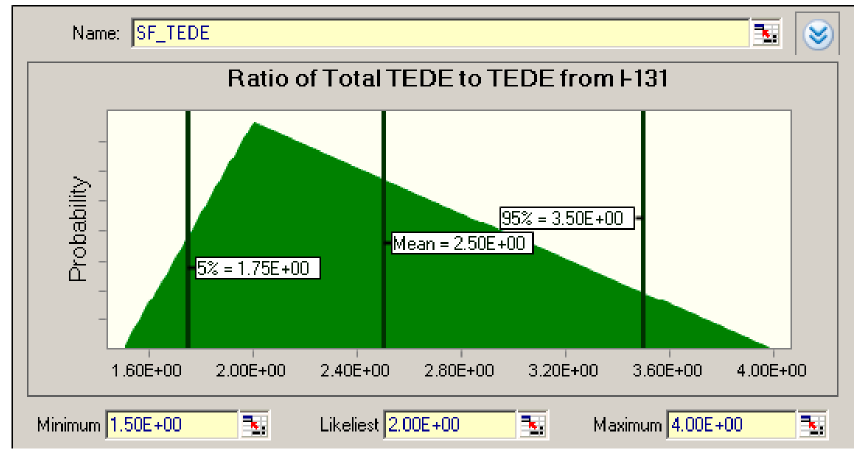

Candidate DDNs for Dose Calculations

- Need to confirm applicability of existing dose conversion factors for HTGR source terms including impact of:
  - Distribution of RNs as dust, aerosol, and vapor
  - Particle size distributions for dust and aerosol
  - Possible chemical reactions during transit to dose receptor

Results for Barrier Allocations

Approach to Barrier Allocations

- Barrier retention allocations assigned in terms of following parameters
  - Limits on fuel release fractions during normal operation and transient
  - Limits on PHTS HPB release fraction
  - Limits on RB release fraction
  - Limits on Composite release fraction across 3 barriers
  - Factor Margins to PAG and 10CFR50.34 dose limits
- Design targets given in terms of:
  - Best estimate based on mean and 50%tile values
  - Upper bounds based on 95%tile
  - Lower bounds based on 5%tiles
- Each barrier expected to meet or exceed targets in next phase of design
- Composite release fractions
  - used to assess integrated performance of all three barriers and to facilitate barrier performance trade-offs
  - Is given a higher priority than the individual barrier allocations as this parameter controls the margins to the dose limits
- Margins to dose limits used to provide allowance for risks due to
  - Evolution of design
  - Improvements and changes to analysis models and data
  - Licensing acceptance

RN Retention Barrier Design Target Allocations for NGNP Conceptual Design

Parameter	Mean	5%tile	50%tile	95%tile
Fuel Release Fraction	2.05E-05	2.68E-07	4.10E-06	7.87E-05
PHTS HPB Release Fraction	4.40E-01	1.47E-01	4.19E-01	8.00E-01
Reactor Building Release Fraction	1.73E-02	1.34E-03	1.31E-02	4.68E-02
Composite Three Barrier Release Fraction	1.64E-07	4.73E-10	1.86E-08	6.00E-07
I-131 Release to Environment - Curies	2.12E+00	6.05E-03	2.39E-01	7.81E+00
Margin Factor to 5rem Thyroid CEDE PAG Limit [Note 1]	1.85E+02	7.77E+04	1.67E+03	4.99E+01
Margin Factor to 25rem TEDE DBA Dose Limit [Note 1]	1.16E+04	4.99E+06	1.06E+05	3.14E+03

Note 1. These values obtained by dividing the dose limit by the corresponding percentile of the dose uncertainty distribution; Hence the higher doses have lower margins to the limit

Comparison of RN Barrier Release Fraction Allocations Based on Mean Values

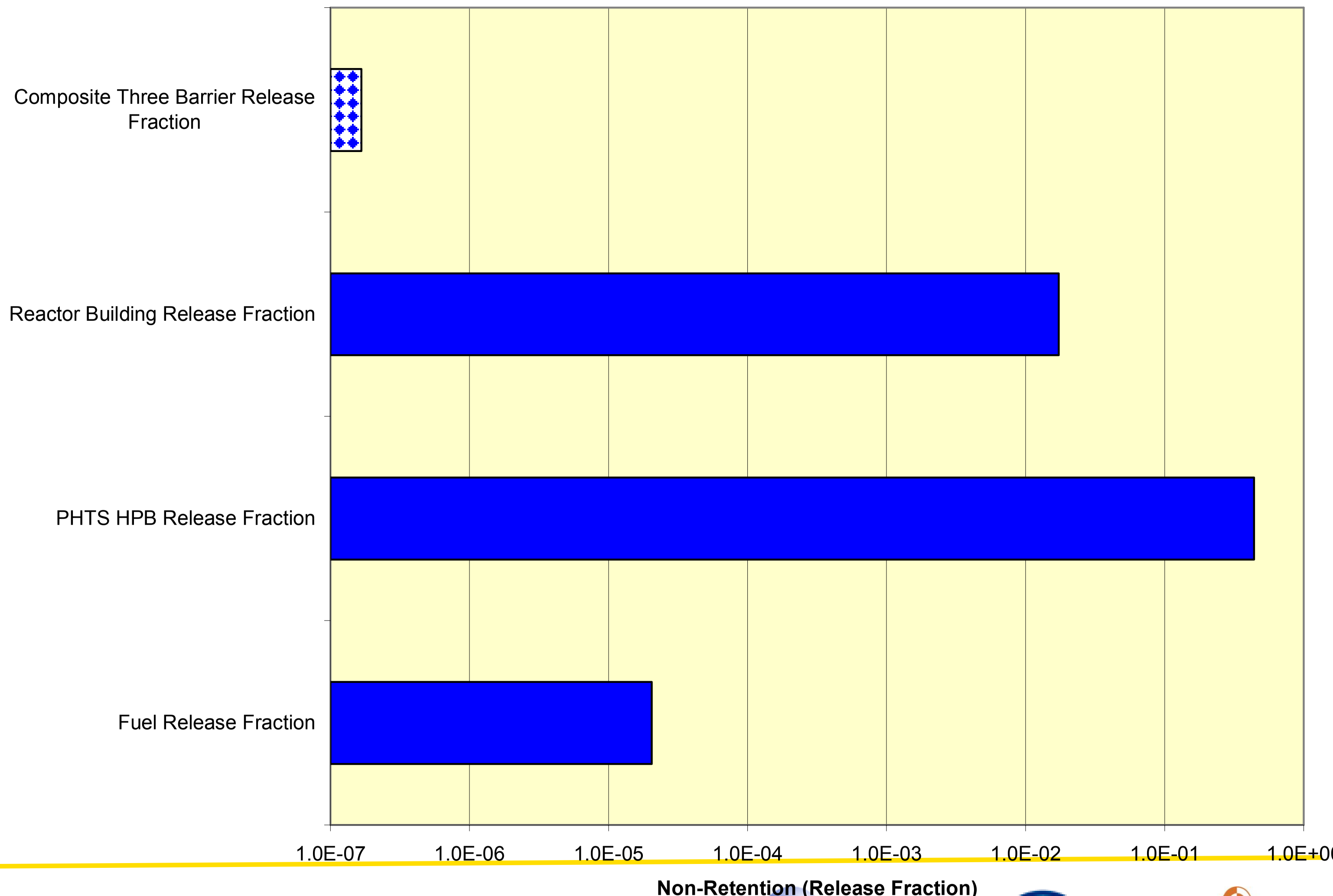

Uncertainty Distribution for Fuel Release Fraction

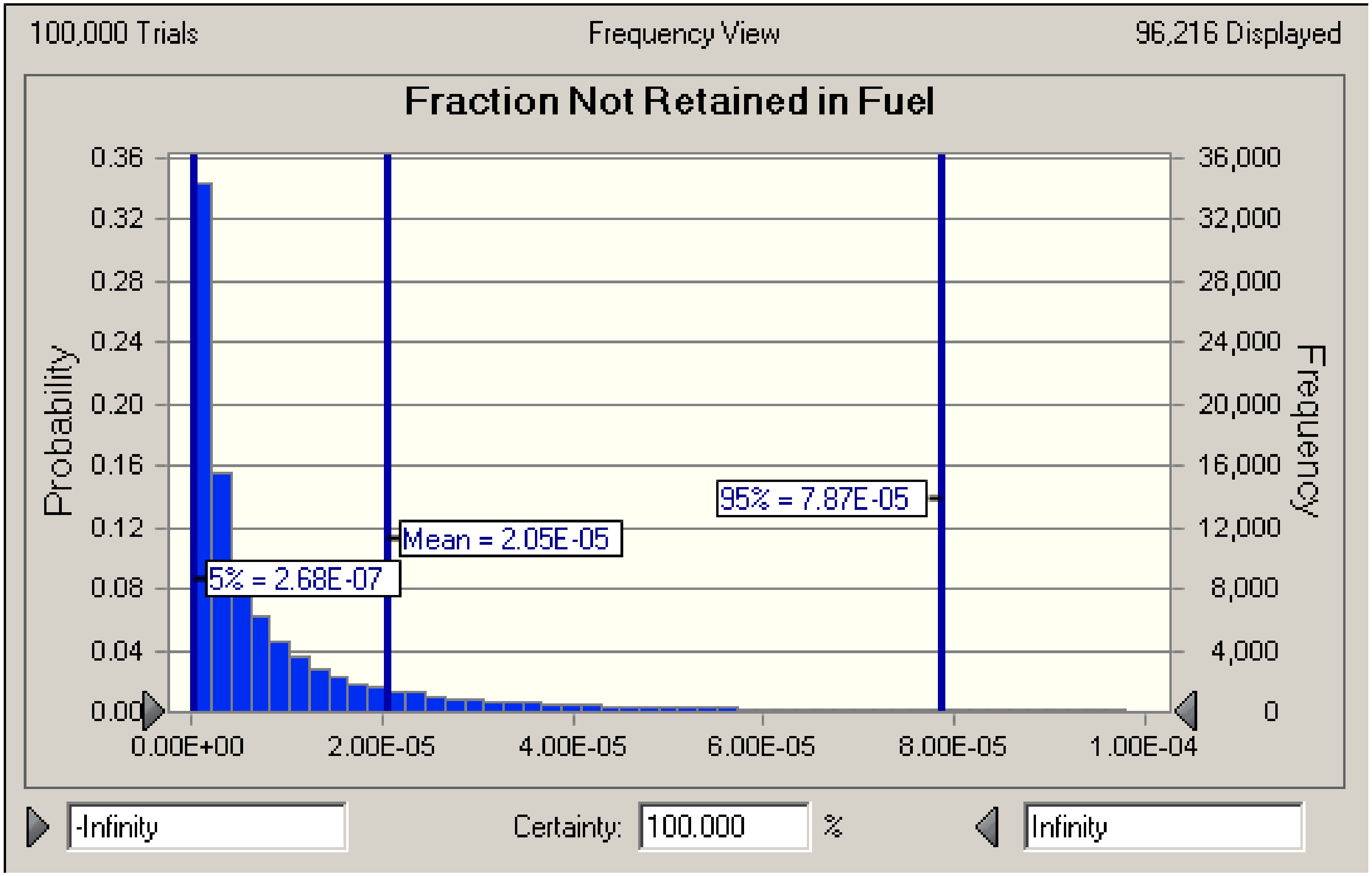

Uncertainty Distribution for PHTS HPB Release Fraction

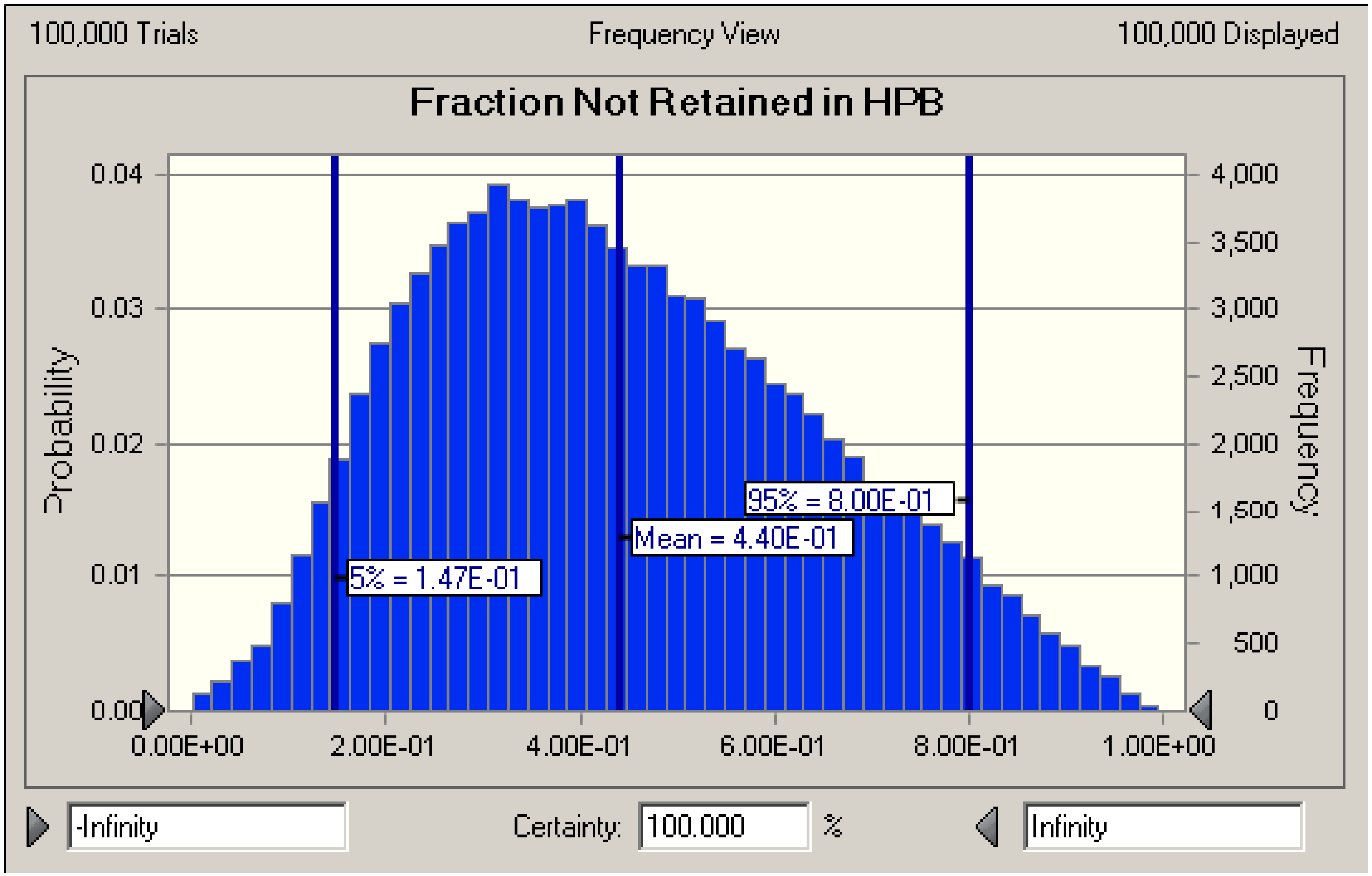

Uncertainty Distribution for Reactor Building Release Fraction

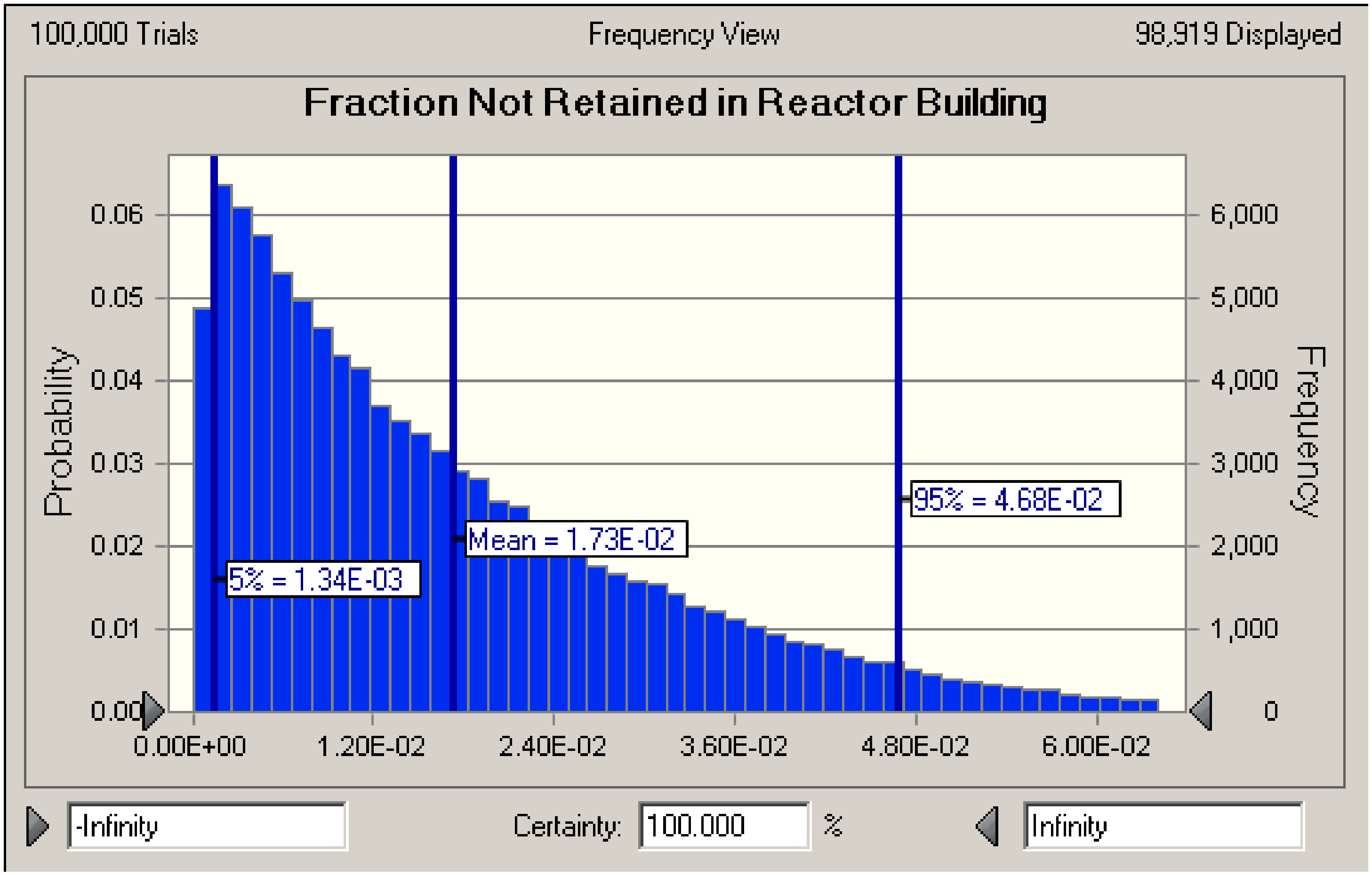

Uncertainty Distribution for Composite Three Barrier Release Fraction

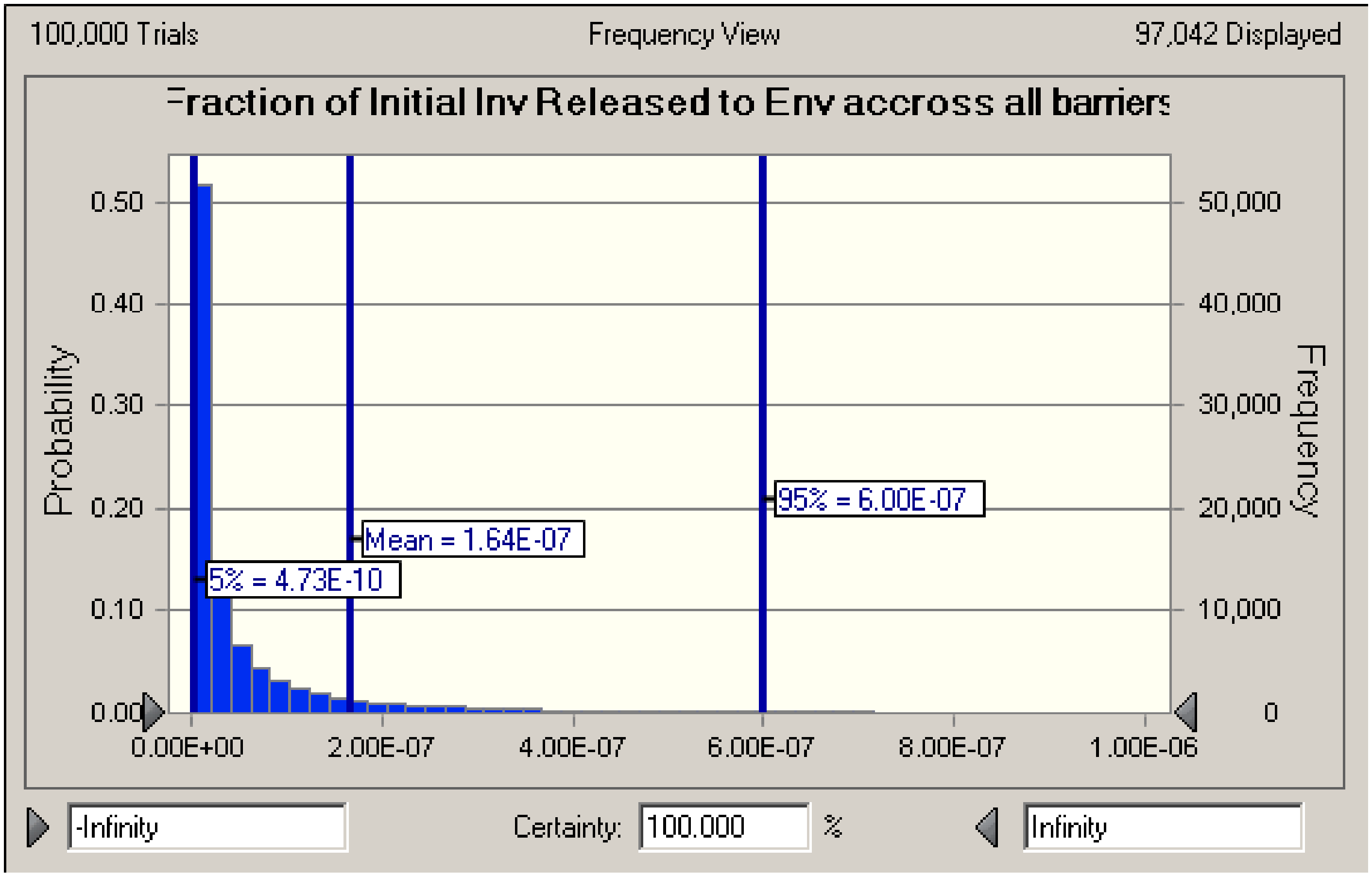

Uncertainty Distribution for Factor Margin to Thyroid PAG Limit (5 rem)

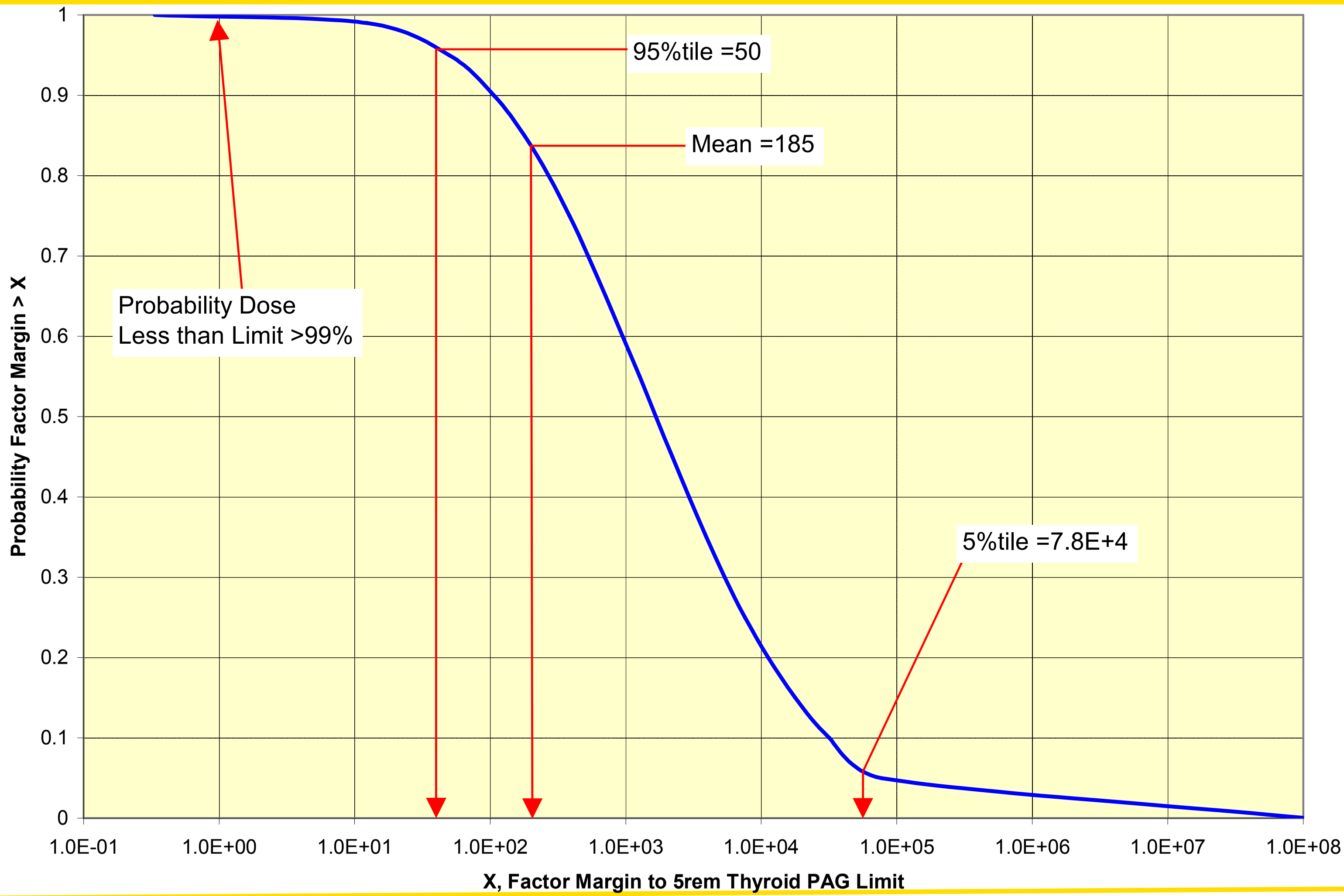

P B M R

RN Retention Allocation In Terms of Factor Reduction in Release Based on Mean Values

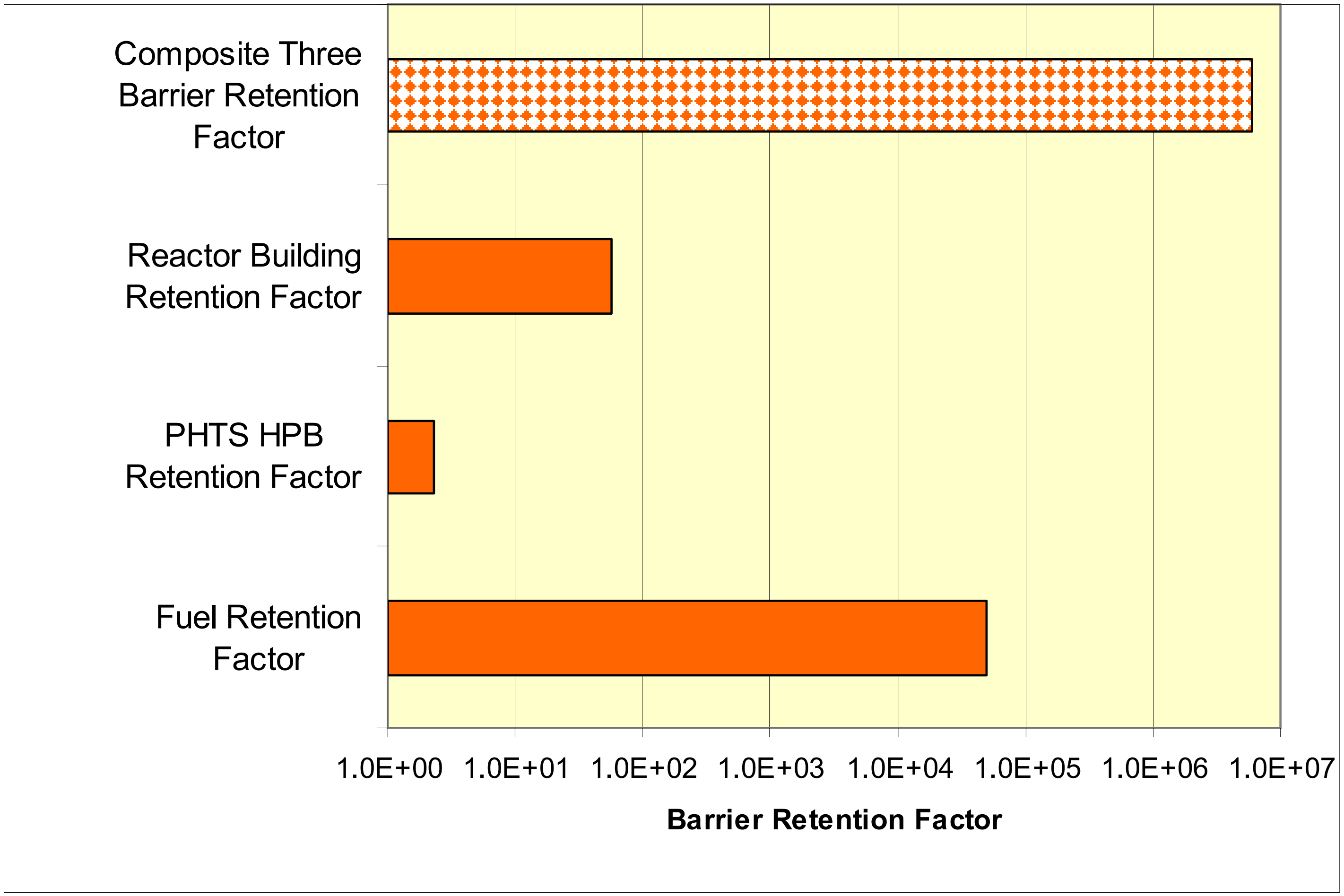

RN Barrier Retention Allocation Summary

- Barrier retention factors are design targets to guide next phase of NGNP design; not regulatory requirements
- Expectation that barrier retention capabilities are evaluated in next design phase and will expect changes due to:
  - Design changes and greater level of detail in design
  - Improvements in state of knowledge due to improved and more detailed models and data
  - More complete evaluation of HPB break sizes, locations, and plant response scenarios; treatment of more radio-nuclides; limiting scenarios to set allocations likely to change
- Barrier retention allocations may change as design is optimized to maintain margins against limits
- Margins to limits may be reduced if warranted by reduced uncertainties in performance

Barrier Allocation Conclusions

- Barrier allocations completed are based on HPB break size and location expected to be limiting for design basis events for an assumed set of boundary conditions
- RN retention allocation for reactor building enhanced by factor of 2 relative to 2008 study
- RN retention allocation for the HPB is limited for small breaks but it is important to include to demonstrate barrier defense-in-depth capability; HPB barrier retention is more significant for larger breaks due to lack of pressure driving force during delayed fuel release
- RN retention allocation targets for the fuel augments the fuel performance specification
- Thyroid PAG dose dominated by delayed fuel releases at ground level from RB that occur post-blow-down after DVS damper is closed
- Methodology for evaluating barrier performance and barrier allocations should be updated for each future design stage maintain adequate margins against dose limits

Current Topic

- Objectives and Scope
- *Plant Level Analyses I:* Normal Operation and Anticipated Transients
  - Requirements and Functional Analyses (Bullet 1 In SOW 6793)
  - Operating Range and Initial Transitions Analyses (Bullet 2)
- *Plant Level Analyses II:* DLOFC for a Range of Primary HPB Leaks and Breaks
  - Depressurization for Range of Leaks and Breaks (Bullet 3)
  - Coupled Thermo-fluid Analysis of PHTS and Reactor Building Response (Bullet 4)
  - Radioactive Material Release Source Terms and Site Boundary Doses (Bullet 5)
  - Retention Allocations and RN Retention DDNs (Bullet 5)
- **Path Forward**

FP Retention Task
Topics for Further Study

Topics for Further Study

- Analysis of buoyancy and natural circulation phenomena on gas exchange among the barriers and resulting impacts on core oxidation and RN releases from HPB and RB
- Improved understanding of the distribution of RNs between dust, vapor, and aerosol forms in the PHTS and in the RB
- Improved understanding of RN transport phenomena for dust, vapor, and aerosol in the PHTS and RB
- Expansion of leak and break locations and variations on plant response for a full spectrum of LBEs
- More realistic treatment of lift off and dust resuspension for beyond design basis larger HPB breaks (>100mm)
- Inclusion of filter resistance and aerosol formation in RB model
- Improved Coupling of Core, PHTS, and RB models
- Better characterization of Dose Conversion Factors for HTGR source terms

Summary of Most Important Uncertainties for Future DDN Development

- Fuel Barrier
  - Current fuel performance demonstration (currently covered by DDN NHSS-01-01, DDN NHSS-01-02)
- HPB Barrier
  - Computer code validation
  - Reduce uncertainty on distribution of I-131 and other radiologically significant RNs on dust, aerosol, and vapor as well as dust and aerosol size distributions
  - Reduce uncertainty on PHTS-RB gas exchange phenomena
  - Reduce uncertainty on plate-out, settling, and other retention phenomena
- RB Barrier
  - Computer code validation
  - Reduce uncertainty on outside air-RB-PHTS gas exchange phenomena
  - Reduce uncertainty on changes in I-131 distribution in RB
  - Reduce uncertainty on plate-out, settling and other retention phenomena
- Radiological Dose
  - Confirm applicability of DCFs for HTGR releases for dust, aerosol, and vapor

Final determination and definition of necessary DDNs will be undertaken as part of forthcoming conceptual design studies

Additional Slides

Code Overviews

Flownex

FLOWNEX is a thermal-fluid network analysis code. It is based on the numerical solution of flow, pressure and temperature distribution in any unstructured collection of one-dimensional elements with connecting nodes by implementing the conservation laws of mass, momentum and energy. It can calculate the gas mixture as the helium breaks into the reactor building and determines how the helium/air mixture moves back into the NHSS and the reactor.

It is an integrated systems-CFD code used for the design, simulation and optimization of thermal-fluid systems such as:

- Gas, steam or combined cycle power plants
- High temperature gas-cooled nuclear power plants
- Aircraft air conditioning systems
- Heat exchanger networks
- Ventilation systems

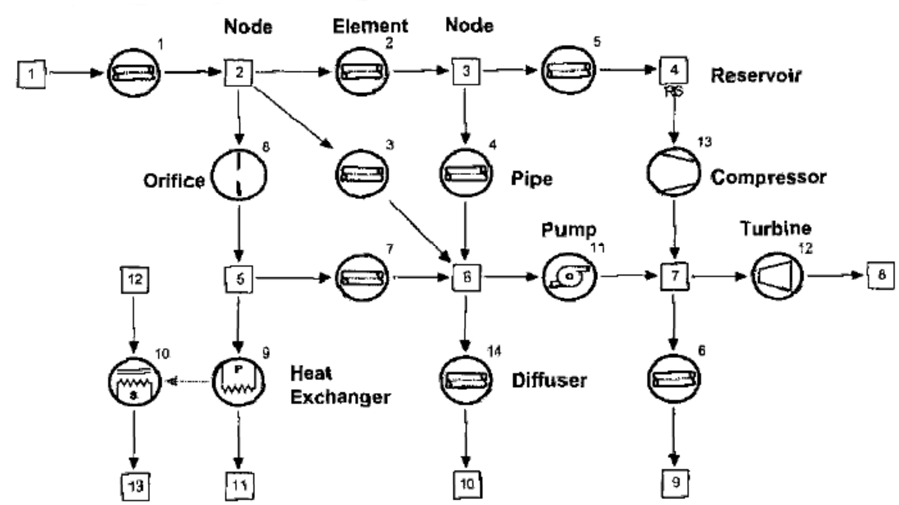

TINTE

- TINTE (**<u>Ti</u>**me Dependent **<u>N</u>**eutronics and **<u>Te</u>**mperatures) is mainly used to model time-dependent transients in HTGRs
- These events can be slow (DLOFC over 24 hours, Xenon oscillations over a few days), or fast (Control Rod ejection)
- TINTE provides transient temperature data for core component design and design limits (fuel, reflectors, CR, SAS, etc), as well as fission/total power indicators
- SAR analyses performed at PBMR with TINTE include: DLOFC & PLOFC, Total Control Rod Withdrawal, Safe Shutdown Earthquake, Helium overcooling events.

TINTE - neutronics

- 2-D r-z, time-dependent neutron diffusion equations, with coarse mesh finite difference solver
- 1-D leakage iteration method on fine mesh: transverse leakage coupling of radial and axial fluxes and currents
- 2 Neutron energy groups (3.07 eV thermal cut-off) and neutron XS data, created from MUPO XS library and coupling with VSOP
- Fuel element burn-up history (for calculation of decay heat) and spatial isotopic distribution are supplied by VSOP. Coupling with VSOP is via interface codes that also prepare the Tinte XS polynomials and reference XS sets
- 6 Groups of delayed neutrons
- Local and non-local heat deposition
- Time-dependent Iodine-Xenon dynamics

TINTE – thermal hydraulics

- 2-D r-z heat transport
- Gas and solid temperatures calculated seperately from neutronic power in subroutines
- FE surface temperatures from the effective heat conductivity in pebble-bed and convective heat transport
- Fuel element burn-up history (for calculation of isotopic decay heat) supplied by VSOP
- Conduction heat transfer from solid to cooling gas
- Convective heat transport of cooling gas

FIPREX-GETTER

- GETTER is a dynamic fission product release code used to predict long-lived metallic fission product behavior under normal conditions and metallic and halogen fission product release during temperature transients.
- GETTER contains neutronic, thermal hydraulic and mass transfer subroutines to determine fuel burn-up, fuel temperatures and fission product production and transport in spherical fuel.
- FIPREX automates GETTER calculations to perform full core best estimate and design analyses for normal operation and accident conditions.
- The FIPREX-GETTER calculation model has been extensively verified and validated with German irradiation test data.

NOBLEG

- NOBLEG is a steady state fission product release code using Booth equations to solve short lived gaseous fission product diffusion behavior under normal operating conditions.
- NOBLEG contains thermal hydraulic and mass transfer subroutines to determine fuel temperatures and fission gas production and transport in spherical fuel.
- NOBLEG calculates all radiological important short-lived gaseous fission products (including bromine and iodine which is based on krypton and xenon measured parameters respectively).
- The NOBLEG calculation model has been extensively verified and validated with German irradiation test data.

Astec

ASTEC[1]

Accident Source Term Evaluation Code

The Purpose is to simulate all the phenomena that occur during a severe accident in a light water reactor, from the initiating event to the possible release of radioactive products (the 'source term') outside the reactor building.

- Multi-module code for LWRs.
- Integral code similar to MELCOR.
- European reference software within the European Commission SARNET network.
- Developed jointly by IRSN (France) and GRS (Germany) since 1996.

1. http://net-science.irsn.org/scripts/net-science/publigen/content/templates/show.asp?P=2949&L=EN

Astec
Main Physical Phenomena Modelled

- Thermal hydraulics :
  - Mass and energy balance of gaseous components
  - 1D heat equation in wall
  - Heat / mass transfer between gas and structures
  - Water Mass and energy balance in sump (liquid water).
  - Heat / mass transfer between gas and sump.
  - H2-combustion and recombination.
  - Spray interaction with containment atmosphere.

- Aerosols and Fission products behaviour :
  - Coagulation, Thermophoresis and diffusiophoresis
  - Filters
  - Steam condensation onto aerosols.
  - Washing.
  - Aerosols removal by spray.

Used in HTR Modeling

- Currently Used
- Not Currently Used